Molecular mapping of rust resistance and genome-wide association study for grain mineral concentration in wheat

Deepak Kumar Baranwal

A thesis submitted in fulfilment of the requirements for the degree of

Doctor of Philosophy

Plant Breeding Institute, Cobbitty
Faculty of Science
The University of Sydney
February 2021

Author Attribution Statement

Chapter 3 of this thesis is published as "Nsabiyera V[#], Baranwal D[#], Qureshi N, Kay P, Forrest K, Valárik M, Doležel J, Hayden MJ, Bariana H, Bansal U (2020). Fine Mapping of *Lr49* using 90K SNP chip array and flow-sorted chromosome sequencing in Wheat. Frontiers in Plant Science 10(1787) DOI 10.3389/fpls.2019.01787. 1-11".

Author contributions:

VN	Vallence Nsabiyera
DB	Deepak Baranwal
NQ	Naeela Qureshi
PK	Pippa Kay
KF	Kerrie Forrest
MV	Miroslav Valárik
JD	Jaroslav Doležel
MH	Matthew Hayden
HB	Harbans Bariana
UB	Urmil Bansal
#	Joint first author

VN conducted initial mapping of KASP markers and drafted the manuscript. DB developed high resolution population, survey of flanking markers to identify recombinants and progeny testing of these recombinants. MV and JD sorted chromosome 4B from parental lines and conducted sequencing. NQ mapped markers developed from the flow sorted chromosomes. PK, KF, and MH aligned flow sorted chromosome sequences with the reference sequence. UB developed KASP and *sunKASP* markers. PK, MH, UB, and HB edited the manuscript. UB and HB provided overall supervision.

Urmil Bansal — Supervisor

Harbans Bariana — Supervisor

Attestation of Authorship Attribution Statement

In addition to the statements above where I am not the corresponding author of a published item, permission to include the published material has been granted by the corresponding author.

Deepak Kumar Baranwal

As supervisor and corresponding author for the candidature upon which the thesis is based, I can confirm that the authorship attribution statements above are correct.

Urmil Bansal

Supervisor

Statement of Originality

This is to certify that the content of this PhD thesis is my own work. To the best of my knowledge, this thesis or part of it has not been submitted for any other degree or diploma in any university.

I certify that the intellectual content of this thesis is the outcome of my own work, and assistance received in preparing this thesis and sources have been acknowledged.

Deepak Kumar Baranwal
(SID: 460114442)

Acknowledgements

I would like to express my sincere gratitude to primary supervisor Associate Professor Urmil K. Bansal. Her supervision, encouragement and constructive remarks throughout the PhD journey were highly commendable. I extend my sincere thanks to auxiliary supervisor Professor Harbans S. Bariana, for his guidance in planning greenhouse and field experiments and improvement of writing skills. I would like to express the heartiest gratitude to auxiliary supervisor Professor Richard M. Trethowan for his support and encouragement to complete this study.

I thank Lyndon Palmer, Analytical Chemist, Flinders University Plant Nutrition, for estimating the mineral concentration of wheat grain through Inductively Coupled Plasma Mass Spectrometry (ICPMS). I highly appreciate the guidance of Prof James Stangoulis and Dr Soung Cu, College of Science and Engineering, Flinders University on analysis of micronutrient content in wheat.

Financial support provided by the Australian government through the Australian Centre for International Agricultural Research (ACIAR) John Allwright Fellowship and the Australian Research Council (ARC) funded postgraduate supplementary fellowship is greatly acknowledged. Grants provided through Postgraduate Research Supplementary Support University of Sydney, Irvine Armstrong Watson Fellowship, Sydney Institute of Agriculture and a bursary from the Australian Society of Plant Scientists are also duly acknowledged. I sincerely thank my employer Bihar Agricultural University, Sabour, India for granting me study leave for four years.

I would like to thank Dr Hanif Miah, Ms Annette Treadea, Dr Bashir Gill, Mr Matthew Williams, Ms Kate Rudd, Ms Jill Azmi and Dr James Hull for their help in administrative and

technical aspects of my project. I also acknowledge Information and Communication Technology (ICT) staff of the University of Sydney in providing desk service, rebuilding the desktop and provision of statistical analysis resources. I am overwhelmed with the kind support offered by Dr Prashanth Babu (Indo-Australia Career Boosting Post-doctoral Fellow) and PhD students Naeela Qureshi, Usman Ijaz, Huma Saffdar, Mehwish Kanwal, Hoan Dinh, Raghvendra Sharma, Kamal Uddin, Laura Ivonne Ruiz Espinosa, Gurpreet Singh, Mehnaz, Michelle Demers, Guy Coleman, and Shemil Macelline during my study.

I am highly indebted to my beloved mother Mrs Aruna Baranwal and elder brother Mr Ashish Baranwal for their patience, dedication, and encouragement to complete my PhD project.

Abbreviations

APR	Adult plant resistance
ASR	All stage resistance
BARC	Beltsville Agricultural Research Center
ANOVA	Analysis of variance
bp	Base pairs
B	Boron
CIMMYT	International Maize and Wheat Improvement Center
Ca	Calcium
cm	Centimeter
cM	centi-Morgan
CRM	Certified reference material
χ^2	Chi-square
CAPS	Cleaved amplified polymorphic sequences
Cu	Copper
°C	Degrees celsius
DNA	Deoxyribonucleic acid
dNTP	Deoxyribonucleotidetriphosphate
dH2O	Distilled water
DArT	Diversity Arrays Technology
EDTA	Ethylene di-amine tetra acetic acid
F_1, F_2 and F_3	Filial 1, 2 and 3 generations
f. sp.	forma specialis
Gb	Gigabite
GBS	Genotyping by sequencing
gm	Gram
GWAS	Genome-wide association study

gwm	Gatersleben wheat microsatellite
HRU	Horse research unit
h	Hours
HPAMP	HarvestPlus association mapping panel
IBS	Identity by state
ICPMS	Inductively coupled plasma mass spectrometry
Fe	Iron
KASP	Kompetitive allele specific PCR
LDN	Lansdowne
LSD	Least significant difference
L	Litre
LOD	Logarithm of the odds
MTA	Marker-trait association
Mg	Magnesium
Mn	Manganese
MgCl2	Magnesium chloride
mg	Milligram
µl	Microlitre
µM	MicroMolar
min	Minutes
mM	MilliMolar
MLM	Mixed linear model
ng	Nanogram
CTAB	N-Cetyl-N, N, N-trimethyl Ammonium Bromide
%	Percent
P	Phosphorous
PBI	Plant Breeding Institute
PCR	Polymerase chain reaction
P3D	Population parameter previously determined

PC	Principal component
K	Potassium
Pgt	*Puccinia graminis* f. sp. *tritici*
Pst	*Puccinia striiformis* f. sp. *tritici*
Pt	*Puccinia triticina*
QTL	Quantitative trait loci
RILs	Recombinant inbred lines
®	Registered trademark symbol
RFLP	Restriction fragment length polymorphism
SCAR	Sequence-characterised amplified region
STS	Sequence-tagged site
SSR	Simple sequence repeat
SNP	Single nucleotide polymorphism
S	Sulphur
TASSEL	Trait analysis by association, evolution and linkage
™	Trade mark symbol
U	Unit
sun	Sydney University
WHO	World Health Organisation
wmc	Wheat microsatellite consortium
Zn	Zinc

Thesis abstract

This investigation included characterisation of diverse sources for rust resistance, identification of genomic regions underpinning rust resistance and fine mapping of an adult plant leaf rust resistance gene in wheat. Genome-wide association mapping in a HarvestPlus panel was also undertaken to identify genomic regions conferring rust resistance and mineral concentration.

Markers linked to the adult plant leaf rust resistance gene *Lr49* were identified using the 90K SNP (single nucleotide polymorphisms) array genotyping of the VL404/WL711 RIL population and alignment of flow-sorted chromosome sequences of chromosome 4B of parents VL404 and WL711. The *Lr49*-linked markers *sunKASP_21, sunKASP_24, sunKASP_26* and *KASP_8082* were tested on a large VL404/Avocet 'S' F_2 population for fine mapping of the region.

A RIL population of VL404/Avocet 'S' was evaluated against *Puccinia striiformis* f. sp. *triticii* (Pst) pathotypes in the greenhouse and monogenic segregation for seedling stripe response was observed and the underlying locus was named *YrVL*. Molecular mapping using the 40K Illumina XT SNP array placed *YrVL* on the long arm of chromosome 2B. Comparative analysis with known ASR genes on chromosome 2BL indicated that *YrVL* is likely to be a new locus.

A stripe rust resistant Tunisian landrace Aus26670 was crossed with the susceptible parent Avocet 'S' (AvS) to develop the Aus26670/AvS RIL population. Seedling tests on this population indicated the presence of a single seedling stripe rust resistance gene and this locus was named *YrAW12*. Targeted genotyping-by-sequencing (tGBS) assay mapped *YrAW12* in the 754.9-763.9 Mb region of chromosome 2BL. Composite interval mapping of adult plant stripe rust response variation suggested the involvement of four Quantitative trait loci (QTL)

for stripe rust resistance in chromosomes 1BL, 5AL, 5BL and 6DS. Two QTL, *QYr.sun-5AL* (654.5Mb) and *QYr.sun-6DS* (1.4Mb), appear to be new.

A HarvestPlus panel comprising synthetic hexaploid wheat, *T. spelta* L., emmer wheat and progenies derived from landraces was evaluated for resistance to rust diseases and accumulation of 10 minerals in the grains. This panel was genotyped using the 90K Infinium SNP array and 13 markers linked with rust resistance genes. Genome-wide association mapping identified six new QTL for rust resistance in addition to 27 known genes/QTL. Forty-one known and 76 new QTL were identified for mineral content. Accessions carrying alien translocations (1B:1R and 2NS) displayed higher accumulation of some minerals.

Table of Contents

Contents	Pages
Author attribution statement	i
Attestation of authorship attribution statement	ii
Statement of originality	iii
Acknowledgements	iv
Abbreviations	vi
Thesis abstract	ix
Table of contents	xi
List of tables	xiv
List of figures	xv
List of appendices	xvi
Chapter 1	1
Introduction	1
Chapter 2	4
Review of literature	4
2.1 Introduction	4
2.2 Identification of rust resistance genes	5
2.2.1 Multi-pathotype tests	5
2.2.2 Genetic analysis of rust resistance	6
2.3 Mapping of rust resistance genes	8
2.3.1 Bi-parental mapping	8
2.3.2 Consensus maps and their application in fine mapping and cloning of rust resistance genes	10
2.3.3 Application of mutational genomics in isolating rust resistance genes	13
2.4 Association mapping for gene discovery	16
2.4.1 Bi-parental Mapping (BM) versus Association Mapping (AM)	19
2.5 Biofortification	21
2.5.1 Genetic biofortification	22
2.5.2 Association among grain zinc, iron and protein content	24
2.5.3 Genomic regions controlling grain mineral concentration	26
Chapter 3	28
Fine mapping of *Lr49* using 90K SNP chip array and flow-sorted chromosome sequencing in wheat	28
3.1 Introduction	30
3.2 Materials and methods	30
3.2.1 Plant and pathogen materials	30
3.2.2 Greenhouse tests	30
3.2.3 Sorting and sequencing of chromosome 4B	31
3.2.4 SNP detection using flow sorted chromosome 4B sequence	31

Contents		Pages
	3.2.5 DNA genotyping	31
	3.2.6 High resolution mapping	31
	3.2.7 Data analyses and genetic mapping	31
3.3 Results		32
	3.3.1 Genetic analysis	32
	3.3.2 Chromosome sorting and sequencing	32
	3.3.3 Molecular mapping	32
	3.3.4 Construction of high resolution map	33
	3.3.5 Assessing marker linkage using unrelated materials	33
	3.3.6 Identification of closely linked markers	33
	3.3.7 Genomic Structure of the *Lr49* region	35
3.4 Discussion		36
3.5 Acknowledgements		38
3.6 References		38
Chapter 4		40
Molecular mapping of all stage stripe rust resistance in Indian wheat cultivar VL404		40
4.1 Introduction		40
4.2 Materials and methods		41
	4.2.1 Development of mapping population	41
	4.2.2 Greenhouse screening	42
	4.2.3 DNA extraction	42
	4.2.4 Genotyping using 40K XT-chips technology	43
	4.2.5 Statistical analysis	43
4.3 Results		43
	4.3.1 Assessment of seedling stripe rust response	43
	4.3.2 Construction of the genetic map	44
	4.3.3 Molecular mapping of *YrVL*	44
4.4 Discussion		45
Chapter 5		48
Genetic dissection of stripe rust resistance in a Tunisian wheat landrace Aus26670		48
5.1 Introduction		48
5.2 Materials and methods		49
	5.2.1 Development of mapping population	49
	5.2.2 Greenhouse screening for seedling stripe rust resistance	50
	5.2.3 Field screening for adult plant stripe rust resistance	50
	5.2.4 Correlation analysis	51
	5.2.5 Genotyping using targeted genotyping by sequencing (tGBS)	51
	5.2.6 Genotyping with markers linked with rust resistance	51
	5.2.7 Statistical analysis	52
5.3 Results		53

Contents		Pages
	5.3.1 Seedling screening	53
	5.3.2 Adult plant screening	53
	5.3.3 Genotyping with gene-linked markers	53
	5.3.4 Construction of the genetic map	54
	5.3.5 Molecular mapping of seedling stripe rust resistance gene *YrAW12*	55
	5.3.6 Quantitative trait loci (QTL) mapping	56
5.4 Discussion		60
Chapter 6		65
Identification of genomic regions conferring rust resistance and mineral accumulation in a diverse wheat panel		65
6.1 Introduction		65
6.2 Materials and methods		67
	6.2.1 Plant materials	67
	6.2.2 Rust response assessments under field conditions	67
	6.2.3 Measurement of grain mineral concentration in 2018 and 2019	68
	6.2.4 Sampling and nutrient analysis	70
	6.2.5 Statistical analysis	70
	6.2.6 Genotypic data, population structure and linkage disequilibrium	71
	6.2.7 Identification of known rust resistance genes	72
	6.2.8 Genome-wide association study (GWAS)	72
6.3 Results		74
	6.3.1 Adult plant rust response variation	74
	6.3.2 Detection of known rust resistance genes using linked markers	76
	6.3.3 Phenotypic variation for grain mineral accumulation and agronomical traits	77
	6.3.4 Marker Distribution	78
	6.3.5 Population structure, kinship and linkage disequilibrium	78
	6.3.6 GWAS of rust resistance	83
	6.3.7 Genome-wide association study for grain mineral concentration	84
	6.3.8 Identification of biofortified rust resistance donor sources	95
6.4 Discussion		95
	6.4.1 New sources of rust resistance	98
	6.4.2 New sources of grain mineral accumulation	100
Chapter 7		103
Conclusions		103
References		107
Appendices		142

List of Tables

Table no.	Title	Pages
Table 2.1	Identification of new rust resistance alleles in some GWAS studies	20
Table 3.1	Primer sequences for kompetitive allele-specific PCR (KASP) markers designed from SNP sequences that showed association with Lr49 on chromosome 4BL and SNPs discovered from the sequences of flow sorted chromosome 4B of parental genotypes.	32
Table 3.2	Validation of closely linked kompetitive allele-specific PCR (KASP) marker on Australian and European wheat cultivars	34
Table 3.3	High confidence genes annotated in the IWGSC v1.0 genome sequence between flanking markers *sunKASP_21* and markers co-segregating with *sunKASP_24*.	36
Table 5.1	Details of stripe rust resistance QTL detected in Aus26670/AvS RIL population	57
Table 6.1	Virulence and avirulence pattern of rust pathotypes used in present study based on Australian differential set	69
Table 6.2	List of gene-linked markers used in this study	73
Table 6.3	Nutrients' profile (mg/kg) of association mapping panel across 2018 and 2019	77
Table 6.4	List of significant marker-trait association (MTA) conferring triple rust resistance at field level	85
Table 6.5	List of significant marker-trait association (MTA) conferring grain mineral concentration	87
Table 6.6	List of rust resistance and biofortified lines for stripe (YR), leaf (LR) and stem (SR) rust resistance on a 1-9 disease scale and corresponding favourable alleles	96

List of Figures

Figure No.	Title	Pages
Fig. 3.1	Genetic linkage map of chromosome 4BL for the VL404/WL711 RIL population	33
Fig. 3.2	Exome SNP genotypes for 890 globally diverse accessions across the *Lr49* region	34
Fig. 3.3	Comparison of *Lr49* genetic linkage map with the 585 to 617 Mbp interval of Chinese Spring chromosome 4B physcial map using Pretzel	35
Fig. 3.4	Diagrammatic representation of the *Lr49* interval and flanking region on chromosome 4B	36
Fig. 4.1	Distribution of 40K SNPs across 21 wheat chromosomes of wheat genome	44
Fig. 4.2	Genetic linkage map of chromosome 2BL: (A) *YrVL*, of VL404/AvS RIL population (B) comparative location of *YrVL* and other known genes in the physical map	46
Fig. 5.1	Adult plant stripe rust response variation among Aus26670/AvS RILs when tested under field conditions in different crop seasons	54
Fig. 5.2	Distribution of targeted genotyping by sequencing (tGBS) markers across the wheat genome	55
Fig. 5.3	Partial linkage map of Aus26670/AvS chromosome 2BL showing location of *YrAW12*	56
Fig. 5.4	Contours showing stripe rust resistance QTL on chromosomes A) 1B (*QYr.sun-1BL/Yr29*), B) 5A (*QYr.sun-5AL*), C) 5B (*QYr.sun-5BL*) and D) 6D (*QYr.sun-6DS*) in Aus26670/AvS RIL population	58
Fig. 5.5	Comparison of common SSR and wPt markers across genetic linkage maps in Pretzel; a genetic map viewing software (http://plantinformatics.io) showing positions of different QTL A) *QYr.sun-5AL* (peak marker of this QTL was placed at 654.5 Mb and nearest known gene *Yr34/Yr48* was placed at 697.9-698.6 Mb; Qureshi et al. 2018) and B) *QYr.sun-5BL*	62
Fig. 6.1	Frequency distribution of the diversity panel against a mixture of pathotypes (field study)	75
Fig. 6.2	Marker survey: Distribution of known rust resistance genes among the diversity panel	76
Fig. 6.3	Distribution of SNPs across the chromosomes and length of individual chromosome	78
Fig. 6.4	Representation of population structure using first two major principal components	79
Fig. 6.5.1	Representation of 929 relationships among the association mapping panel using pedigree visualisation tool HELIUM	80
Fig. 6.5.2	Visualisation of wheat pedigree derived using *T. dicoccon* PI94625 (A), *T. dicoccon* CI9309 (B), Kukuna (C) and Francolin#1 (D)	81
Fig. 6.5.3	Visualisation of wheat pedigree derived using Quaiu#2(A), Chonte*2 (B), Brambling (C), Mutus (D), Solala (E) and Waxwing*2/Tukuru*2 (F)	82
Fig. 6.6	Heat map presenting kinship among the diversity panel (Red blocks indicate closely related accessions)	83
Fig. 6.7	Boxplot analysis depicting contribution of significant markers in grain mineral accumulation	93
Fig. 6.8	Boxplot analysis depicting contribution of significant markers including markers linked with rust resistance in grain mineral accumulation	94

List of Appendices

Appendix	Chapter	Title	Pages
Appendix I	Chapter 3	Supplementary Figure 1. Pretzel (http://plantinformatics.io) visualisation of synteny between (a) *Ae. tauschii* chromosome 4D, (b) Chinese Spring chromosome 4D, (c) emmer chromosome 4B, (d) Chinese Spring chromosome 4B, and (e) the *Lr49* genetic map, based on physical mapping of high confidence genes across the *Lr49* region (a to d) and corresponding physical map position (d) and genetic map position (e) of markers across the *Lr49* region	142
Appendix II	Chapter 3	Supplementary Figure 2. Log2 ratio plot (VL404:WL711) of average paired-end sequence read coverage across (a) chromosome 4B, and (b) *Lr49* region. Blue and black lines represent sequence coverage based on 10 and 500 kb sliding windows, respectively. Physical mapping position of microsatellite markers and the *Lr49* interval in chromosome 4B are shown in (a). The position of the putative deletion in VL404, relative to WL711, along with physical mapping position for markers that validated (*sunKASP_21* and *KASP_8082*) and did not validate (*KASP_20289, KASP_20288, KASP_35049, KASP_21440, KASP_39484* and *sunKASP_24*) are shown in (b)	143
Appendix III	Chapter 6	List of genotypes of HarvestPlus AM panel (HPAMP) and their pedigree	144
Appendix IV	Chapter 6	Representation of decay of linkage disequilibrium over distance. Each dot shows a pair of distances between two markers and their squared correlation coefficient (r^2). The red line indicates the moving average of the 10 adjacent markers	156
Appendix V	Chapter 6	Manhattan plots depicts significant SNPs detected against mixture of stripe rust (YR) pathotypes in field environments. Chromosome name on x-axis and the -log10 (p-value) on the y-axis have been plotted. Site (Horse research unit- HRU and Lansdowne research unit-LDN) is suffixed with the rust type and year e.g. HRU-YR2018	157
Appendix VI	Chapter 6	Manhattan plots depicts significant SNPs detected against mixture of leaf rust (LR) pathotypes in field environments. Chromosome name on x-axis and the -log10 (p-value) on the y-axis have been plotted. Site (Horse research unit- HRU and Lansdowne experimental unit-LDN) is suffixed with the rust type and year e.g. HRU-LR2018	161
Appendix VII	Chapter 6	Manhattan plots depicts significant SNPs detected against mixture of stem rust (SR) pathotypes in field environments. Chromosome name on x-axis and the -log10 (p-value) on the y-axis have been plotted. Site (Horse research unit- HRU and Lansdowne experimental unit-LDN) is suffixed with the rust type and year e.g. HRU-SR2018	165
Appendix VIII	Chapter 6	Manhattan plots depicts significant grain Zn MTAs detected in field environments. Chromosome name on x axis and the -log10 (p-value) on the y-axis have been plotted. Narr-I, Narr-II, HRU and LDN represent 2018-Narr-I, 2018-Narr-II, 2019-Horse research unit and 2019-Lansdowne experimental unit, respectively	169
Appendix IX	Chapter 6	Manhattan plots depicts significant grain Fe MTAs detected in field environments. Chromosome name on x axis and the -log10 (p-value) on the y-axis have been plotted. Narr-I, Narr-II, HRU and LDN represent 2018-Narr-I, 2018-Narr-II, 2019-Horse research unit and 2019-Lansdowne experimental unit, respectively	173
Appendix X	Chapter 6	List of significant markers and their alleles displaying their effects in accumulating higher grain minerals	177

Appendix XI	Chapter 6	Boxplot analysis depicting contribution of significant markers in grain S, K, Ca, Cu, Fe and P accumulation. X- and Y-axis represent alleles and mineral concentration (mg/kg) in wheat grain, respectively	179
Appendix XII	Chapter 6	Boxplot analysis depicting contribution of *Sr31/Lr26/Y9* linked marker *iag95* in grain mineral accumulation. X- and Y-axis represent alleles and mineral concentration (mg/kg) in wheat grain, respectively	180

Chapter 1

Introduction

Wheat is the most widely cultivated cereal crop and it provides one-fifth of the total dietary and calorific source to the current population (WHO 2017). A recent study estimated the world's population to reach 10 billion by 2050 (Ranganathan et al. 2019). A 60% increase in global wheat production will be required to achieve food security (Ray et al. 2013). Developing high yielding rust resistant wheat cultivars can minimise the gap between the global wheat production and requirement.

Three different species of the genus *Puccinia* cause rust diseases. Stem rust is caused by *P. graminis* f. sp. *tritici* (*Pgt*), leaf rust by*P. triticina*; (*Pt*) and stripe rust (*P. striiformis* f. sp. *tritici* (*Pst*) (McIntosh et al. 1995). Exotic incursions and evolution among rust pathogen populations can render resistance genes deployed in wheat cultivars ineffective (McIntosh 2007). These pathogens can migrate long-distances (Brown and Hovmøller 2002), undergo mutational changes from avirulence to virulence (Hovmøller and Justesen 2007), acclimatise to fluctuating climatic conditions (Milus et al. 2009) and create new variants through sexual and somatic hybridization (Ali et al. 2017).

The Mendelian inheritance of stripe rust resistance was first demonstrated by Biffen in 1905. A pioneering book, 'The Rusts of Australia' written by McAlpine (1906), highlighted the serious concerns about stem rust and leaf rust in Australia. Stripe rust was detected in eastern Australia in 1979 and the pathotype was designated 104 E137A- (O'Brien et al. 1980). This pathotype evolved to render stripe rust resistance genes *YrA*, *Yr6* and *Yr7* individually and in all combinations ineffective (Wellings 2007). Another exotic incursion of pathotype 134 E16A+ (with virulence on *Yr8* and *Yr9*) appeared in Western Australia in 2002 (Wellings et al. 2003). Variants of pathotype 134 E16A+ acquired virulence on *Yr10, Yr17, Yr24, YrJ, YrT* and *Yr27* (Wellings 2007). Two *Pst*

pathotypes 239 E237A-Yr17+Yr33+ and 198 E16A+YrJ+YrT+Yr17+ were detected recently in eastern Australia (Park et al. 2020), the former possessed virulence for *Yr33* and the latter showed increased severity on durum wheat cultivars.

Two classes of genes namely, all stage resistance (effective at all stages of plant growth against avirulent pathotypes; ASR) and adult plant resistance (effective at the post seedling stages; APR), condition rust resistance in wheat. The modern wheat breeding programs aim to deploy combinations of ASR and APR genes to attain long-term rust resistance (Bariana et al. 2007a).

The World Health Organisation (WHO) estimated over two-billion people relying on wheat as their primary diet and people living in the Indian sub-continent preferentially eat wheat and show essential micronutrient deficiency (WHO 2017). Essential micronutrients including Zn and Fe play a significant role in overall body development and metabolic activities (Bouis et al. 2011). Although essential micronutrients are available in form of tablets, most people living in developing countries cannot afford the cost. Promotion of nutrient-dense wheat is an important step to alleviate malnutrition (Bouis et al. 2011). HarvestPlus is a global effort initiated during the last decade of 20th century to enhance Zn levels in wheat cultivars (Rawat et al. 2009). This program identified and used the germplasm that had the inherent ability to accumulate higher levels of micronutrients and delivered five biofortified cultivars in the Indian subcontinent (Velu et al. 2019). These cultivars carry 30% additional Zn content and yield comparable to local checks.

Wheat progenitors like landraces, spelta, emmer, durum, rye, einkorn and *Aegilops* species were characterised to discover rust resistance genes (McIntosh et al. 1995; McIntosh et al. 2017). Some studies found that spelta and emmer wheat accumulate up to four-times higher micronutrients than modern wheat cultivars (Cakmak et al. 2004; Peleg et al. 2008). Advances in genomic resources including the availability of reference genome assemblies of hexaploid, tetraploid (wild emmer accession Zaviton and durum wheat Svevo) and the diploid progenitor *Aegilops tauschii* L. (https://www.10wheatgenomes.com) and high throughput genotyping

platforms such as 90K SNP array helped in precise mapping and identification of rust resistance genes and discovery of genomic regions underpinning nutrient accumulation (Bariana and Bansal 2017; Gupta et al. 2020).

Over 200 rust resistance genes have been formally named and several others have been temporarily designated (McIntosh et al. 2017; Joukhadar et al. 2020). Many commercially deployed rust resistance genes have been defeated by matching virulence of continuously evolving rust pathogens. On the other hand, identification of genomic regions conditioning higher mineral loading in wheat grain is still in its infancy. This highlights the need to accelerate discovery of genes that control economic and nutritional quality traits to ensure continued wheat improvement. In the current study, bi-parental mapping populations were screened in greenhouse and field conditions to discover rust resistance genes. Advanced genotyping platforms 90K, flow-sorting based chromosomal sequencing, tGBS and 40K SNP array were explored to precisely position these targeted genes. A Harvestplus association mapping panel (HPAMP) was evaluated for rust resistance and 10 grain minerals to identify new genomic regions conferring disease resistance and enhanced accumulation of grain minerals. The four research chapters cover:

1. Fine mapping of the adult plant leaf rust resistance gene *Lr49.*
2. Molecular mapping of seedling stripe rust resistance in VL404/AvS RIL population.
3. Genetic dissection of stripe rust resistance in a Tunisian wheat landrace Aus26670.
4. Identification of genomic regions conferring rust resistance and mineral accumulation in a diverse wheat panel.

Chapter 2

Review of literature

2.1 Introduction

Common wheat is an allohexaploid plant with a vast genome size (~15.8 Gb). It constitutes 85 per cent of highly repetitive sequences (Wicker et al. 2018). The wheat genome evolved through two continuous polyploidisation events accommodating three diploid progenitors' genomes (AA, BB, DD). About a million years ago, wild tetraploid emmer wheat (AABB genome; *Triticum turgidum ssp. dicocc*oides L.) originated after a primary hybridisation between two diploid AA (*T. urartu* L.) and BB (closely related to *Aegilops speltoides, Ae. longissima, Ae. sharonensis, Ae. searsii* and *Ae. bicornis*) genome progenitors (Jordan et al. 2015; Avni et al. 2017). The derived emmer wheat (AABB) faced a secondary hybridisation around 10,000 years ago with the D genome donor (*Ae. taushii).* The origin of agriculture led the intense changes in wheat biology (Preece et al. 2017) and this resulted in the cultivation of domesticated wheat in the Fertile Crescent (Nevo et al. 2013) and led the evolution of common wheat (Salamini et al. 2002).

Wheat production reached 759 million tons and supplies one-fifth of the total protein and calorific requirements of mankind (USDA 2020). Global wheat production should be increased by 60 to 70 per cent to feed 10 billion people by 2050 (Ray et al. 2013; Ranganathan et al. 2019). To meet this requirement, wheat production in the developing countries need to be doubled (Ray et al. 2013). Wheat encounters numerous biotic and abiotic stresses that continuously challenge its sustainable production. Fungal diseases are considered as one of the most serious threats. Rust diseases of wheat are of major concern due to the highly evolutionary nature of fungal pathogens that cause these diseases to result in up to 30% of yield loss (Juliana et al. 2018). Potential losses from a *Pgt* (causal agent of stem rust) pathotype Ug99 are three billion USD per year (Pardey et al. 2013) and annual yield losses due to stripe rust are estimated 5.47 million tonnes globally that

equates to USD 979 million (Beddow et al. 2015). Deployment of stripe rust resistant varieties in Australia alone has been estimated to save around AUD one billion annually (Murray and Brennan 2009).

The outbreak incurred by the *Pgt* race Ug99, with virulence on *Sr31* in Uganda has challenged the rating of stem rust resistance of commercial wheat cultivars across the world (Singh et al. 2011). Later, faster spreading nature of the race resulted in its migration in other African nations and the Middle East and chances to cover Asian wheat-growing belt as well (Ayliffe et al. 2008). In 2006-07, two mutant versions of race Ug99 were noticed in Kenya, with added virulence on *Sr24* and *Sr36*, respectively. In Australia, the epidemic of race Ug99 could cost up to $140 million per year (Ayliffe et al. 2008). Therefore, it is imperative to eradicate the likelihood of invasion of the race Ug99 derivatives through deploying wheat varieties with resistance to Ug99, surveillance of the pathogen populations over the time and fostering pre-breeding efforts for rust resistance (Ayliffe et al. 2008). Race Ug99 was avirulent on stem rust resistance genes *Sr13, Sr14, Sr22, Sr25, Sr26, Sr27, Sr28, Sr35, Sr45, Sr46, Sr48* and *Sr50*. These effective genes are available in modern wheat backgrounds. The defeated genes should not be used singly in wheat breeding programs (Singh et al. 2011).

2.2 Identification of rust resistance genes

2.2.1 Multi-pathotype tests

Comparison of infection types (ITs) produced by test entries against an array of pathotypes of the target rust pathogen on a set of genotypes carrying known genes (differentials) facilitates gene postulation (McIntosh et al. 1995). Several studies reported results on postulation of rust resistance genes in different sets of wheat genotypes. For example, Singh et al. (2008) reported the presence of *Sr5, Sr8a, Sr9g, Sr12, Sr30, Sr31, Sr36* and *Sr38* in British wheat cultivars. Stem rust resistance genes *Sr7b, Sr8a, Sr8b, Sr9b, Sr9g, Sr11, Sr15, Sr17, Sr29, Sr31, Sr31, Sr36* and *Sr38* were

reported in European wheat cultivars (Pathan and Park 2007). Similarly, *Sr5, Sr7a, Sr7b, Sr8a, Sr9e, Sr11, Sr21, Sr27, Sr29, Sr30* and *Sr37* have been postulated in Ethiopian durum and common wheat cultivars (Admassu et al. 2012). Randhawa et al. (2016) postulated the presence of *Sr7b, Sr8a, Sr12, Sr15, Sr17, Sr23, Sr30, Lr1, Lr3a, Lr13, Lr14a, Lr16* and *Lr20* either in combinations or singly among 87 Nordic spring wheat genotypes. DNA markers confirmed the presence of *Sr2, Lr34/Yr18/Sr57, Lr68* and *Yr48* in this collection (Randhawa et al. 2016). Singh and Rajaram (1992) postulated the presence of *Lr3, Lr10, Lr13, Lr26* and *Lr34* in CIMMYT wheat genotypes. A collection of European winter wheat carried *Lr1, Lr3a, Lr3ka, Lr10, Lr14a, Lr17b, Lr20, Lr26* and *Lr37* (Winzeler et al. 2000). Chinese wheat lines are likely to carry *Yr2, Yr3a, Yr4a, Yr6, Yr7, Yr9, Yr26, Yr27* and *YrSD* genes based on rust tests (Li et al. 2006). Two CIMMYT and one Australian wheat nurseries including 153 entries were screened against *Pst* pathotypes to postulate major and minor genes (Singh et al. 2014) and around half of the entries did not carry any effective ASR against Australian *Pst* pathotypes and *Yr6, Yr7, Yr9, Yr17* and *Yr27* were detected either singly or in combinations. Based on their resistance level, some entries were postulated to carry uncharacterised resistance genes and known APR genes *Yr18, Yr29* and *Yr30* (Singh et al. 2014).

2.2.2 Genetic analysis of rust resistance

Host resistance has been categorised into two broad classes: ASR/qualitative resistance and APR/field resistance/quantitative resistance (Bariana 2003; Bariana et al. 2007a). ASR is conditioned by major genes (R) effective from seedling to adult plant stage and this type of resistance is often matched by virulence in the corresponding pathogen. In contrast, APR is governed by minor genes effective at the post-seedling stages and it generally retards pathogen development and hence referred to as partial resistance/slow rusting. It is assumed to be race non-specific (Bariana et al. 2007a). However, some APR genes express hypersensitive responses at adult plant stages and show pathotypic specificity, for example, *Lr22b* (McIntosh et al. 1995).

The resistant parent (carrying ASR and/or APR) is crossed with a susceptible parent to develop a bi-parental population to understand inheritance of resistance and to determine genomic location(s) of underlying resistance gene(s). Although several studies involved tests on individual F_2 plants, tests on F_3 families are preferred for its amenability for checking reproducibility of results (Bariana 2003). Population advancement to the F_6 generation can be conducted through single seed/head method to create recombinant inbred lines (RILs) and alternatively the doubled haploid approach (Ahmed and Trethowan 2020). F_3 populations carrying ASR gene(s) are classified into three categories using phenotypic responses: 1. homozygous resistant (HR), 2. segregating (Seg) and 3. homozygous susceptible (HS) and phenotypic data are subjected to Chi-squared analysis to determine the number of resistance loci controlling the target trait. An F_3 population can be used for preliminary genetic analysis, however, a good number of seeds is required to study the segregation pattern. A RIL population has an advantage over an F_3 generation as RILs are fixed after many recombination events and few seeds are needed for genetic analysis and it allows endless screening for different traits segregating among the target population. The segregation ratios for the involvement of a different number of genes are listed in Bariana (2003). Wright's formula is used to estimate the number of loci governing rust resistance based on phenotypic evaluation under field conditions (Wright 1968).

The presence of more than one gene in a bi-parental population requires development of single gene segregating populations to precisely locate genes conferring resistance. For example, an F_3 family of Aus27858/Westonia showed segregation of two seedling stripe rust resistance genes (Randhawa et al. 2014; Randhawa et al. 2015). Families showing single gene segregation for different ITs were advanced separately to generate F_6 RIL populations. Molecular mapping of two F_6 RILs revealed two new ASRs; *Yr51* (;n–;1-nn) on chromosome arm 4AL (Randhawa et al. 2014) and *Yr57* (0;) on 3BS (Randhawa et al. 2015). Australian wheat cultivars Sunco and Kukri expressed high level of stripe rust resistance (Bariana et al. 2001). Two BC_1F_2 populations derived

from each cultivar and a common susceptible parent Avocet 'S' confirmed the presence of three independent loci each (1HR:6Seg:1HS) in Sunco and Kukri. The wheat cultivar Sunco was reported to carry *Yr18* (Kolmer et al. 2008) and *YrCK* (Bariana et al. 2001) on chromosome 2D. To map the third gene, a Sunco/2*Avocet S-derived BC_1F_2 line SA65 (a resistant line) was crossed with a susceptible sib (SA67) and 123 RILs of cross SA65/SA67 was generated (Bariana et al. 2016). Monogenic segregation among derived RILs was demonstrated and the resistance locus was named *YrSA3*. Further selective genotyping using a 90K SNP array and SSRs placed the *YrSA3* gene on chromosome 3D and catalogued as *Yr71* (Bariana et al. 2016).

2.3 Mapping of rust resistance genes

2.3.1 Bi-parental mapping

Precise mapping of rust resistance loci became more convenient with the availability of high throughput genotyping platforms including DArTseq (www.diversityarrays.com), genotyping-by-sequencing (Poland and Rife 2012) and SNP arrays including 90K (Wang et al. 2014), 820K (Winfield et al. 2015), 660K (Cui et al. 2017) and 35K chips (Allen et al. 2017). These platforms are frequently used for bulked segregant analysis (BSA; Michelmore et al. 1991), selective genotyping (SG; Lebowitz et al. 1987) and whole population genotyping. For BSA, equal amounts of genomic DNA from 20 resistant and 20 susceptible RILs is pooled separately to constitute resistant and susceptible bulks, respectively. DNA samples from up-to forty randomly selected RILs should also be pooled to prepare an artificial F_1 sample. One µg DNA samples of both parents, the constituted resistant and susceptible bulks and artificial F_1 sample are being used for genotyping using the 90K SNP array to detect linkage of resistance loci and their position in the wheat genome. GenomeStudio software (Illumina Ltd) is being used in detecting putatively linked SNPs using their normalised theta value (Wang et al. 2014). Associated SNPs can be converted into kompetitive allele-specific PCR (KASP) assays using the bioinformatics pipeline, PolyMarker (https://www.polymarker.info). The KASP assay includes two allele-specific forward primers that

are labelled with specific sequences that correspond to two universal fluorescence resonant energy transfer (FRET) cassettes labelled with FAM™ and HEX™ dye and a common reverse primer (www.lgcgroup.com). It allows accurate bi-allelic discrimination of known SNPs. BSA was used to map major genes, for example *Sr49* (Bansal et al. 2015), *Yr47* (Bansal et al. 2011), *Yr51* (Randhawa et al. 2014) and *Yr57* (Randhawa et al. 2015). It was also used in saturating the *Lr79*-region (Qureshi et al. 2018) and SG to map the APR gene *Yr71* (Bariana et al. 2016). Polymorphic markers can be recommended to deploy targeted genes in the wheat background.

Several software programs namely QTL IciMapping (Meng et al. 2015), Map Manager QTX20 (Manly et al. 2001) is routinely being used in gene mapping using putatively linked markers and phenotypic responses using the Kosambi and Haldane mapping function (Haldane 1919; Kosambi 1943). Map chart was used to draw the genetic map (Voorrips 2002).

Sixty genes for stem rust, 79 for leaf rust and 83 for stripe rust resistance has been catalogued using bi-parental populations (McIntosh et al. 2017; Li et al. 2020). In a recent study, a Portugees landrace Aus27969 expressed a high level of stripe rust resistance at seedling and adult plant stage in the field. Kandiah et al. (2019) observed monogenic segregation at the seedling stage against three *Pst* pathotypes in the Aus27969/AvS RIL population. BSA using the 90K SNP Infinium array placed this locus on chromosome arm 3BL. The seedling gene was catalogued as *Yr82* and linked markers identified.

Many methods namely Single-Marker Analysis (SMA), Composite Interval Mapping (CIM) and Multiple Interval Mapping (MIM) have been reported for QTL mapping (Bernardo 2020). However, the CIM function of QTL Cartographer was frequently used and offered a platform to align genome-wide markers and phenotypic data together to detect resistance gene loci using default parameters (Wang et al. 2012).

Several studies focussed mapping QTL underpinning rust resistance (Rosewarne et al. 2013; Maccaferri et al. 2015). A RIL population derived from a cross of the CIMMYT line Arableu#1 (source of APR) and Apav#1 (susceptible line) to identify QTL for leaf rust and stripe rust (Yuan et al. 2020) and QTL analysis identified four and six genomic regions that controlled leaf rust resistance and stripe rust resistance, respectively. A new pleiotropic locus *QLr.cim-1BL.2/QYr.cim-1BL.2* was reported that is 37 cM (~6 Mb) far from the known pleiotropic APR locus *Lr46/Yr29*. They found *QLr.cim-3DS, QYr.cim-2AL, QYr.cim-4BL, QYr.cim-5AL,* and *QYr.cim-7DS* as putatively new loci after comparing them with the published literature (Yuan et al. 2020).

2.3.2 Consensus maps and their application in fine mapping and cloning of rust resistance genes

Integration of known stripe rust resistance loci resulted in two consensus maps (Rosewarne et al. 2013; Maccaferri et al. 2015). The first map included 49 chromosomal regions covering 140 stripe rust resistance QTL from thirty bi-parental mapping studies (Rosewarne et al. 2013). The second map incorporated 56 stripe rust resistance genes and 169 QTL from ten Genome wide association study (GWAS; Maccaferri et al. 2015). Similarly, a consensus map of stem rust resistance loci was drafted that included 24 bi-parental populations, two backcross populations and three association mapping panels (Yu et al. 2014). This study identified 141 stem rust resistance loci effective against Ug99 and reported linked markers. In more than 50 publications, 80 QTL for leaf rust and 119 QTL for powdery mildew were reported on 16 and 21 chromosomes, respectively (Li et al. 2014). Eleven loci on 10 chromosome arms (1BS, 1BL, 2AL, 2BS, 2DL, 4DL, 5BL, 6AL 7BL and 7DS) showed potential pleiotropic effects including known multi-pathogenic resistance genes *Lr34/Yr18/Sr57*, *Lr46/Yr29/Sr58*, *Lr67/Yr46/Sr55* and *Lr27/Yr30/Sr2* (Li et al. 2014). Genetic mapping of an individual gene is usually carried out in low-resolution populations. To delimit the gene-region, a high-resolution family (HRF) is the pre-requisite. HRF can help to develop closely

linked markers (<0.1 cM) (Singh and Singh 2015). Flanking markers from the low-resolution mapping are tested for initial screening of a large population, preferably F_2 or backcross population. Progeny testing of these individuals helps in confirming marker positions. Screening of recombinants with additional markers specific to underlying candidate genes can offer a platform to initiate cloning work (Periyannan et al. 2013; Klymiuk et al. 2018; Zhang et al. 2019a). High level of sequence similarity between homoeologous genomes (95-99% in coding sequences) and over 80% of repetitive DNA had posed challenges to clone rust resistance genes in wheat (Borrill et al. 2015). To fine map and clone a gene, several modern genomic approaches have been undertaken and these include sequence similarity and repetitiveness in the wheat genome (Keller et al. 2018; Steuernagel et al. 2020).

A comparative study of DNA markers in related taxa originated from a similar ancestor and their arrangement in different maps is known as comparative mapping (Singh and Singh 2015). An orthologous and conserved marker, especially complementary DNA sequences (cDNA) across the taxa, are more useful in a comparative mapping. This can reveal genome organisations of diploid progenitors and common wheat. The orthologous genes and conserved marker sequences located in the same chromosome is referred to as synteny. However, the arrangement of DNA markers in the same linear order in two different chromosomes of the same or different species is termed as collinearity (Singh and Singh 2015).

The orthologous region of *Brachypodium distachyon* L. was used in developing a high-resolution map of *Lr52/Yr47* (Qureshi et al. 2017). *B. distachyon* and related genera *Oryza sativa* L. and *Sorghum bicolor* L. were explored in a collinearity study to saturate the *Yr15*-region flanked by markers *uhw264* and *uhw258* (Klymiuk et al. 2018). Gene annotation studies using *Ae. tauschii* genomic resources inferred *NLR1* as *Lr22a* (Thind et al. 2017). To saturate the pleiotropic APR *Lr67*-region, additional markers were designed using conserved orthologs and its collinear sequences in *B. distachyon* and *O. sativa* (Moore et al. 2015). A high-density map of *Yr36* was

drafted using collinear gene regions in *O. sativa* that confirmed the gene to be in a 0.14 cM interval spanned by markers *ucw113* and *ucw111* (Fu et al. 2009). Similarly, collinear region sequences of *B. distachyon* were used to narrow down the *Sr35*-region with markers *AK331487* (0.02 cM proximal) and *AK332451* (0.98 cM distal) (Saintenac et al. 2013).

To reduce genome complexity, the chromosome flow-sorting technology (Vrána et al. 2012) was employed to dissect individual chromosomes based on their relative DNA content followed by their sequencing individually. A high-resolution map of *Lr49* was prepared using this approach (Nsabiyera et al. 2020). The largest wheat chromosome 3B was separated easily with this approach, however isolation of the remaining chromosomes was challenging due to similar sizes (Shatalina et al. 2013). Wide application of chromosomes specific labelled repetitive DNA as a probe assisted in isolation of 21 bread wheat and seven barley chromosomes, individually (Giorgi et al. 2013). Sánchez-Martín et al. (2016) demonstrated the importance of flow cytometry-based chromosome sorting of derived mutants followed by alignment of their sequences as a robust and unbiased approach for reduction of genome complexity.

The whole-genome shotgun (WGS) approach has assembled 'long' sequence reads using 454 technology and published the first draft sequence of wheat genome in 2012 (Brenchley et al. 2012). However, this approach failed to overcome the sequence similarity issues between homoeologous genomes and their mis-assembly. Another WGS approach using large-insert sequencing libraries was undertaken to draft assemblies of each of the three homoeologous genomes of synthetic hexaploid wheat 'Synthetic W7984' (Chapman et al. 2015). This large insert genomic libraries or Bacterial Artificial Chromosome (BAC) libraries represented in-depth genome coverage and have been used in the cloning of *Yr36* (Fu et al. 2009), *Sr33* (Periyannam et al. 2013), *Sr35* (Saintenac et al. 2013), *Sr50* (Mago et al. 2015) and *Yr15* (Klymiuk et al. 2018). Mascher et al. (2013) have anchored both CSS and W7984 scaffolds into a high-density genetic map using population sequencing (POPSEQ). In POPSEQ, several individuals from a bi-parental

population were sequenced to low coverage (c.1.5x) followed by SNP calling to parental lines and *in silico* mapping of the sequenced contigs associated with the identified SNPs. Through the POPSEQ analysis, 80-90 doubled haploid individuals of synthetic W7984 x Opata M85 (Sorrells et al. 2011) were anchored on a high-density genetic map covering 4.5 Gb (CSS) and 7.1 Gb (W7984) of the wheat genome. POPSEQ relies on meiotic recombination that occurs frequently in the distal ends of wheat chromosomes (Anderson et al. 2006; Saintenac et al. 2009). Due to uneven recombination, POPSEQ generates a distorted assignment of scaffolds concentrated in centromeric regions with much lower resolution than in the more recombinogenic distal regions of the chromosome. Over 600,000 SNPs from 820K Axiom and 90K iSelect SNP platforms have been integrated into the Chinese Spring survey sequence assembly. However, most of the SNPs were mapped *in silico* by genome browser Ensembl (https://www.cerealsdb.uk.net/; https://plants.ensembl.org).

2.3.3 Application of mutational genomics in isolating rust resistance genes

The fine mapping approach in wheat delimits the target gene region with the closely linked markers and the delimited gene-region can be annotated to reveal underlying candidate genes using bioinformatic approaches (Appels et al. 2018). However, this approach seeks specific expertise, state of the art resources, cutting-edge technologies, and obviously biosafety approval. In general, a candidate gene can be used to transform the susceptible wheat variety like Fielder or Bobwhite to confirm the role of candidate genes in conditioning resistance to the target pathogen (Chen et al. 2020). It is a time consuming and laborious method. Therefore, the mutational genomics approach is preferred to detect the target gene via induced loss-of-function in the parental stock.

Ethyl methane sulfonate (EMS; CH3SO3C2H5) is a chemical mutagen that is frequently used in wheat for generating mutants (Acquaah 2009). EMS produces C/G to T/A transitions (Ashburner 1989). It results in impaired complementary base-pairing followed by a series of allelic mutations that are required for comprehensive structural and functional studies (Silme and

Cagirgan 2007). A low concentration (0.2 to 0.6%) of EMS has been used to knock-out the target gene in rust research; however, kill curve using LD-50 threshold is the most recommended protocol (Acquaah 2009; Periyannan et al. 2013; Thind et al. 2017). The detailed procedure of mutagenesis has been described by Mago et al. (2017).

Rust resistance genes *Lr1* (Qiu et al. 2007), *Lr10* (Feuillet et al. 2003), *Lr21* (Huang et al. 2003), *Lr22a* (Thind et al. 2017), *Sr13* (Zhang et al. 2017), *Sr22*, *Sr45* (Steuernagel et al. 2016), *Sr33* (Periyannan et al. 2013), *Sr35* (Saintenac et al. 2013), *Sr50* (Mago et al. 2015), *Yr5*, *Yr7*, *YrSP*, (Marchal et al. 2018), *Yr10* (Liu et al. 2014) and *YrAS2388R* (Zhang et al. 2019a) have been cloned successfully and belong to nucleotide-binding and leucine-rich repeat protein (NLR) or its variants. Of them, *Lr1*, *Lr10* and *Lr21* were cloned a decade ago using a conventional map-based cloning approach. Isolation of *Lr34* (encodes an ATP binding cassette transporter), *Lr67* (encodes a Hexose transporter), *Yr15* (encodes a wheat tandem kinase 1), *Yr36* (encodes a Kinase-START gene) and *Sr60* (encodes a wheat tandem kinase 2) were successfully executed by map-based cloning (Fu et al. 2009; Krattinger et al. 2009; Moore et al. 2015; Klymiuk et al. 2018; Chen et al. 2020).

Steuernagel et al. (2016) demonstrated a rapid gene isolation approach called MutRenSeq. It combines chemical mutagenesis followed by capturing NLRs via exome capture to explore pan-genome variation that existed in wild diploid wheat relatives (*Ae. tauschii*, *T. boeoticum* L. and *T. monococcum* L.). Arora et al. (2019a) developed the AgRenSeq approach using a diversity panel of *Ae. tauschii* ssp. *strangulata* L. It is based on R-gene enrichment followed by extraction of NLR k-mers from each accession and k-mers based association mapping to report resistance gene. *Sr46* and *SrTA1662* (both encode NLR) were cloned via the AgRenSeq approach. To validate this approach, they used *Sr33* and *Sr45* (previously cloned) as positive controls, fine map of *Sr46* and three *Sr46* mutants (Arora et al. 2019a). It indicates that the success of both technologies depends directly or indirectly on the mutational genomics approach. MutRenSeq and AgRenSeq can be

used to isolate only NLR-class of genes and probability of missing NLR during R-gene enrichment, alignment and annotation are the limitations of both technologies. Steuernagel et al. (2020) compared and aligned NLR loci identified via NLR annotator with automated gene annotation used in IWGSC RefSeq v1.0. Of 3,400 loci predicted by NLR annotator, 2,955 NLRs match with genes annotated in IWGSC RefSeq v1.0. Of these NLRs, 578 correspond to two or more genes annotated in IWGSC RefSeq v1.0. They hypothesized three major factors for these poor gene calling and false annotations: 1. gaps (stretches of unassigned nucleotides) in the wheat genome assembly, 2. a potential overextension of the NLR locus carrying at least three consecutive NB-ARC motifs and 3. a stop-codon in the coding sequence interrupting the open reading frame in the transcript. One of the possible hypotheses was verified after cloning of *Pm2* from wheat cultivar Ulka (Sánchez-Martín et al. 2016). *Pm2* confers resistance to powdery mildew caused by *Blumeria graminis* L. This encodes a full-length NLR, and the corresponding allele in IWGSC RefSeq v 1.0 substitutes five bases with a stretch of twelve bases resulting in a premature stop codon.

Complex genome and suppressed recombinogenic regions challenge identification of point mutations in wheat and barley. To overcome these obstacles, a complexity reduction approach MutChromSeq was developed that relies on flow sorting, sequencing of mutant chromosomes and referencing this with a parental chromosome (Sánchez-Martín et al. 2016). This technique is equally applicable to all classes of genes. Single candidate genes of barley *Eceriferum-q* gene and wheat *Pm2* were identified using six mutants and verified by Sanger sequencing of additional mutants (Sánchez-Martín et al. 2016).

The presence of introns or repetitive regions hindered the progress to clone underlying genes. Therefore, the targeted chromosome-based long-range assembly (TACCA) approach was used to clone *Lr22a* (Thind et al. 2017). These genes were isolated and validated either by developing loss-of-function mutants or transgenesis and/or gene silencing. These studies

demonstrated the importance of mutational genomics approach in the positional cloning. However, *Yr10* was cloned using a transgenesis and gene silencing approach (Liu et al. 2014) and *Sr60* was isolated using a transgenesis approach (Chen et al. 2020).

2.4 Association mapping for gene discovery

Linkage disequilibrium (LD) is the non-random co-occurrence of two or more gametes/alleles in a mapping population. LD occurs between loci placed in proximity, and recombination can break it down (Korte and Farlow 2013). Population structure and selection can maintain higher than expected LD across the different chromosomes. LD is estimated by the observed frequency of an allele in a population deducted by the product of the frequencies of the corresponding alleles (Bernardo 2020). Linkage helps in restoring parental allelic combinations.

The GWAS offer high-resolution mapping due to exploitation of higher levels of allelic diversity at a locus coupled with ancestral/historical recombination events that are represented in a diversity panel (Yu and Buckler 2006). Rust resistance genes/alleles are reported in various germplasm collections including old and modern wheat cultivars, synthetic hexaploid wheat, diploid and tetraploid wheat progenitors/relatives and wild relatives (Yu et al. 2014; Maccaferri et al. 2015; Pinto da Silva et al. 2018). GWAS has played a key role to dissect various complex traits in wheat (Yu et al. 2011; Juliana et al. 2015). Five GWAS (Maccaferri et al. 2015; Gao et al. 2016; Jighly et al. 2016; Pasam et al. 2017; Turner et al. 2017) based on high throughput marker platforms have uncovered novel rust resistance alleles (Table 2.1). The success of GWAS in uncovering new genetic variation relies on diversity of genotypic and resultant phenotypic differences between individuals (Korte and Farlow 2013). It can detect marker-trait associations for the phenotype of interest. Although, several major QTL identified through GWAS have not been functionally characterised and validated for their application in wheat breeding programs, IWGSC RefSeq v1.0 can be used to investigate precise locations of QTL identified using high throughput genotyping platforms (Appels et al. 2018).

The LD decay usually drops at 2-8 cM across the three (A, B and D) genomes (Gao et al. 2016; Riaz et al. 2018). GWAS studies can consider the marker trait associations (MTAs) corresponding to a 5 cM region as an independent QTL. Identified MTAs deviating from known genes/QTLs by more than 5 cM interval could be treated as new in the case of ASRs/APRs. However, further validation using bi-parental populations and physical positions of underlying rust resistance alleles is essential to catalogue candidate genes. Zhang et al. (2014) developed a customized scale to linearised the 0-4 IT scale into a 0-9 scale for GWAS analysis. This customised scale accommodates complex infection types like ";13+" and calculate the weighted arithmetical mean. It is available in R packages (https://github.com/umngao/rust_scores_conversion).

Statistical software like TASSEL, and a few R based programs like GAPIT and rrBLUP are used in GWAS (Yu and Buckler 2006; Endelman 2011; Yang et al. 2014a). The GWAS highlights the significant MTAs using $-\log_{10}$ (p) that can result in four possible outcomes while considering the null hypothesis (H_0) that the marker under investigation is unlinked to a single QTL; 1. False positive, when a QTL is incorrectly reported, 2. True positive, when a QTL is correctly reported, 3. False negative, when a QTL is incorrectly unreported and 4. True negative, when a QTL is correctly unreported (Bernardo 2020). Type I error rate or significance level (α) is the probability of rejecting the null hypothesis in case H_0 is true. However, the type II error rate (β) equates to the probability that a false H_0 is not rejected. High precision mapping experiments can lower the values of α and β. To specify experiment-wise control rate (α_E) and comparison wise significance level (α_C), Bonferroni correction, permutation testing and false discovery rate (FDR, Benjamini and Hochberg 1995) have been used to attain higher stringency. For instance, 5,000 (n) unlinked markers, α_E of 0.05 resulted in α_C of $1x10^{-5}$, where $\alpha_C = \alpha_E/n$. In addition to controlling false positives, it can reduce the power of QTL detection and may not be more robust criteria to detect true QTL (Bernardo 2020). To minimise the level of stringency, a threshold of 1/n, where n (5,000) is the number of markers used in the study, would be $2x10^{-4}$ to qualify putative linkage

into a significant association (Yang et al. 2014b). One may prefer a high FDR threshold when aiming to discover the genetic architecture of a trait and a low FDR to identify candidate loci for subsequent studies and validation (Korte and Farlow 2013).

Several GWAS studies have been conducted to detect significant MTAs for rust resistance using mixed linear model (MLM-Q+K) accounting principal component (Q) and kinship matrix (K) and compressed MLM that cluster individuals into a subset to minimise the effective sample size (Table 2.1; Zhang et al. 2010; Pasam et al. 2017; Juliana et al. 2018; Bhatta et al. 2018; Cu et al. 2020). A complementary approach, 'population parameters previously determined' (P3D) was preferably used in some studies to circumvent re-computing variance components (Zhang et al. 2010). Juliana et al. (2018) applied a GWAS approach to identify leaf rust and stripe rust resistance alleles in International Bread Wheat Screening nurseries. In this study, the POPSEQ map and Ensembl plants were used to report candidate genes associated with significant MTAs. Genomic regions conferring rust resistance on chromosomes 1DS, 2AS, 2BL, 2DL, 3B, 4AL, 6AS, 6AL and 7DS were identified. Maccaferri et al. (2015) performed GWAS using a worldwide collection of 1,000 spring wheat accessions and 9K SNP Infinium assay. A greater level of *Pst* resistance was observed in a subpopulation from southern Asia. Ten significant MTAs explained 15% of the phenotypic variation (PVE) individually for stripe rust resistance, however, the PVE increased up to 45% when combining the effect of all QTL. Kankwatsa et al. (2017) evaluated 159 old wheat cultivars and landraces against 35 Australian rust pathotypes and postulated several known ASRs, APRs and few uncharacterised APRs. Similarly, Bansal et al. (2013) screened 205 wheat land pathotypes against rust isolates and high-throughput DArT genotyping using a single marker scan and identified 68 significant MTAs. They reported linked stripe rust-leaf rust resistance loci on chromosome arms 1AL, 2BS, 2BL, 3DL, 5BS, 6BS and 7DL and linked stripe rust-stem rust resistance loci on chromosome arms 4BL and 6AS.

2.4.1 Bi-parental mapping (BM) versus association mapping (AM)

QTL can be identified using BM and AM approaches. It raises the question about the choice of one of these methods (Bernardo 2020). When the population development is challenging, AM is the obvious choice. For instance, developing segregating progeny from a clonal selection of tuber crops is tedious due to their mode of propagation and AM can be chosen in this instance. The probability of detecting rare variants using AM is however lesser than BM. For example, among a diverse wheat collection of 300 accessions, only three lines carried the same resistance allele for pathotype Ug99, while remaining lines of the panel carried the susceptible allele. The AM approach is less likely to detect the rare variants due to lower frequency (1%). In BM, out of three lines, one accession with a good agronomical background (resistant parent) crossed with the susceptible parent and 200 RILs are developed. In this case, the frequency of resistance allele would be 50% in the population that increases the power of QTL detection.

If an AM panel has 30 resistant lines and 270 susceptible lines that means the frequency of the resistance allele is 10% and QTL can be detected using GWAS. However, a challenge for the breeder would be to determine a resistant line with better agronomical performance as well as a linked marker to expedite the deployment of QTL in the elite cultivars (Bernardo 2020).

Table 2.1 Identification of new rust resistance alleles in different GWAS studies

Reference	**Maccaferri et al. (2015)**	**Gao et al. (2016)**	**Jighly et al. 2016**	**Pasam et al. (2017)**	**Turner et al. 2017**
Genotyping platforms	9K SNP array *(4585)	90K SNP array *(18924)	DArT and DArT-Seq *(6176)	90K SNP array *(51208)	9K SNP array *(5732)
Materials	Spring wheat accessions	Elite wheat Lines	Synthetic wheat	Watkin's collection	Spring wheat
No. of entries	1000	338	173	676	1032
Novel	**Stripe rust**	**Leaf rust**	**Stem rust**	**Stem rust**	**Leaf rust**
alleles	1B-*IWA3892*	3B-*IWB74350*	2D-*1101415*	3A-*IWB8720*	2BS-*IWA8221*
	1D-*IWA980*	4A-*IWB40915*	2D-*1102301*	3B-*IWA1196*	2BS-*IWA4894*
	2A-*IWA422*	4A-*IWB7998*	**Stripe rust**	4B-*IWB59588*	2BL-*IWA5177*
	2A-*IWA424*	6A-*IWA7764*	2B-*wPt-8776*	5A-*IWB46277*	2DL-*IWA5637*
	3B-*IWA5202*	6A-*IWB40242*	3D-100136169	6A-*IWA5781*	4AS-*IWA1900*
	4A-*IWA1034*	6B-*IWB65148*	3D-1267912	**Leaf rust**	4DS-*IWA5375*
	4D-*IWA5375*			1B-*IWA5474*	5DS-*IWA6289*
	5A-*IWA6988*			2B-*IWB35072*	5DL-*IWA1429*
	6B-*IWA7257*			5A-*IWB34703*	7AS-*IWA1277*
	6D-*IWA167*			**Stripe rust**	
				1A-*IWB766*	
				1B-*IWB44883*	
				3A-*IWA7440*	
				5B-*IWB10356*	
				5D-*IWB73687*	
				6A-*IWB48922*	
				6B-*IWB 68655*	
				7A-*IWB60768*	
				7B-*IWA1971*	

*Number of polymorphic markers; SNP = Single nucleotide polymorphism; DArT = Diversity Array Technology

2.5 Biofortification

Nutrients including carbohydrates, fat, protein and minerals are chemical compounds essential for living organisms for their survival, growth and development. Some minerals required in relatively large quantity are called macronutrients, for example, Ca, K, Mg, P and S and those needed in relatively smaller quantities are known as micronutrients (B, Fe, Cu, Mn and Zn). Inadequate intake of these minerals in the daily diet results in malnutrition problems in one of three persons in the world. This deficiency is termed as 'Hidden hunger' and results in stunted growth in children, poor immunity, and reduced work efficiency. One-fourth of the world's population suffers from anaemia due to Fe deficiency and substantial numbers of children encounter impaired mental development due to Zn deficiency (WHO 2008). A balanced diet containing adequate Zn content can boost immunity, control diabetes, trigger healing and digestion process as well as advance reproduction and physical growth. A report on risk factors associated with illness ranked Zn and Fe deficiencies at 5^{th} and 6^{th} place, respectively, in the undeveloped world (WHO 2002; Kumar et al. 2019). Severe health complications including osteoporosis, impaired bone growth, inadequate bone mineralisation and hypertension have been noticed among human populations due to dietary deficiency of Ca, Mg and P (Broadley and Hartl 2009; Rude et al. 2009). Increasing the intake of these deficit nutrients in human body is possible with the multi-nutrient pills. However, it may not be feasible for major portion of the world population. Groups of low-income people prefer to have staple diet like wheat, rice, maize, millets, and sweet potato. This situation drew the attention of policymakers towards genetic biofortification as a cost-effective approach to combat malnutrition. This approach was promoted as a sustainable option to alleviate malnutrition worldwide during the Copenhagen consensus 2008 (Gomez-Becerra et al. 2010).

The CGIAR (Consultative Group of International Agricultural Research) approved a "CGIAR Micronutrients Program for eight years (1995-2002)". Later, the organisation launched the "Biofortification Challenge Program" and renamed it as "HarvestPlus" (Rawat et al. 2009). It attempts to improve nutrition and public health by favouring biofortified food crops. These approaches require a continuous investment, cutting-edge laboratory, and other resources. During last two decades, HarvestPlus collaborates with multiple partner organisations worldwide and primarily partners from south Asian and African countries to increase intake of micronutrients and Vitamin A (www.harvestplus.org). Genetic biofortification includes exploitation of high mineral accumulating progenitors in breeding programs to deliver nutritious crops. Other approaches addressing the problem are nutrient supplementation, dietary diversification, agronomic fortification, and fortification via gene editing/transgenes. Genetic biofortification in wheat resulted in the release of biofortified varieties in South Asia such as Zinc Shakti (Chitra), HPBW-01, WB-02, Zincol-2016, and BARI-Gom33 that possess above 30% grain Zn concentration and at least equivalent yield to local checks (Velu et al. 2018).

2.5.1 Genetic biofortification

Biofortification is the process of enhancing the bioavailability of essential nutrients in the edible part of a crop plant (Welch and Graham 2004). It includes agronomic biofortification through foliar application of nutrients on crop plants, genetic biofortification relying on high nutrient accumulating progenitors in a breeding program and fortification via genetic modification in crop plants (White and Broadley 2005). Genetic biofortification is a cost-effective and affordable breeding strategy to tackle the malnutrition issues of the developing countries through developing mineral-dense crops (Gomez-Becerra et al. 2010). Reducing levels of anti-nutritional factors like saponins, tannins and phytic acid of crop plants and

promoting nutrient absorption in the human diet are also key concerns of biofortification (Bouis 2003; Samtiya et al. 2020). Wheat, being a major staple crop, is ideally suited for genetic biofortification. Increasing Zn and Fe concentration in the wheat grain is the major objective of the genetic biofortification program (Cakmak 2008). It includes characterisation and exploitation of genetic variation present in wheat gene pools in terms of grain ionic content followed by genomics-assisted breeding to enhance mineral content of grain.

Continuous selection events have narrowed down the genetic variation for micronutrients (Zn and Fe) concentration among cultivated wheat. Diploid progenitors, wild tetraploid and hexaploid wheat have higher micronutrient levels. Incorporation of the DD genome progenitor "*Ae. tauschii*" as a donor in wheat breeding led into the constitution of synthetic wheat (SW). These derivatives carry rare alleles for high Zn and Fe content in the cultivated wheat background (Calderini and Ortiz-Monasterio 2003; Velu et al. 2014). Cakmak (2008) highlighted "concentration effects" that indicated high grain mineral concentration can jeopardise yield by reducing the grain size. Negative correlations were evident in further studies on emmer, durum and spelta wheat (Monasterio and Graham 2000; Gomez-Becerra et al. 2010). In contrast, zero concentration effect of Zn content on grain size was recorded by Velu et al. (2012) in cultivated wheat. However, primitive wheat showed poor grain size due to higher concentration of Zn (Morgounov et al. 2007). Spelt wheat accessions carried high grain Zn (~70 ppm), Fe (~ 60 ppm) Ca (~ 880 ppm) and Mg (~2400 ppm) concentrations and yield equal to cultivated wheat across environments (Calderini and Ortiz-Monasterio 2003; Troccoli and Codianni 2005; Oury et al. 2006). A set of wild emmer wheat *T. turgidum* ssp. *dicoccoides* expressed outstanding genetic variation for Zn (~190 ppm), Fe (~ 109 ppm) and grain size (Cakmak et al. 2004; Peleg et al. 2008); *T. aestivum* ssp. *spelta* and *T. turgidum*-based synthetics have demonstrated their potential in terms of higher micronutrient content and at least parallel yield to local checks (Srinivasa

et al. 2014). A significant and positive correlation was observed between Zn and Fe content in the flag leaves and matured grain in *Aegilops* species (Rawat et al. 2009). Testing of grain mineral content at flag leaf stage can aid in selecting promising entries. However, mineral loading in wheat grain happens during the grain filling period (GFP) and it varies from five to eight weeks depending upon genotype and environmental factors. Further extensive studies can demonstrate a particular stage of GFP predominating in mineral loading in wheat grain, and this finding would be helpful for early-stage prediction of mineral content (Cu et al. 2020).

2.5.2 Association among grain zinc, iron and protein content

A significant positive correlation among grain Zn, Fe and protein content were evident in spelt wheat, wild emmer and other diverse wheat accessions (Uauy et al. 2006; Distelfeld et al. 2007; Morgounov et al. 2007). These studies demonstrated the presence of co-segregating or pleiotropic alleles conferring accumulation of grain Zn, Fe and protein. McDonald and Mousavvi (2009) demonstrated the role of sulphur in increasing the concentration of grain Zn and Fe. The hypothesis believes that there is interaction of grain Zn and Fe with S-containing amino acids like methionine followed by binding with sulphydryl ligands (Cakmak et al. 2000). This hypothesis was confirmed by Takahashi et al. (2003) and Cakmak et al. (2010). These studies revealed that methionine is an essential precursor of nicotianamine biosynthesis that plays a role in the synthesis of soil-based Fe and Zn-chelating compound phytosiderohores and transport of Zn and Fe via phloem into cereal seeds and flowers. Foliar application of nitrogenous fertilisers can also stimulate the accumulation of grain Zn, Fe and protein content in wheat (Kutman et al. 2011). Additional soil or foliar application of N in wheat upregulated root absorption and accumulation of Zn and Fe in shoots and grain. Kutman et al. (2011) reported that under excessive N application,

~60% of total shoot Fe was translocated into seeds, whilst under low N supply, this figure was around 38%. Both N and S can act jointly to accelerate high grain accumulation of Zn and Fe during key physiological steps: 1) root uptake, 2) root-to-shoot transport, 3) re-translocation from the senescing leaf tissue and 4) seed deposition of Fe and Zn (Cakmak et al. 2010; Aciksoz et al. 2011; Erenoglu et al. 2011).

Presence of anti-nutritional factors (ANFs) can hinder the nutrient bioavailability in cereals and legumes (Nadeem et al. 2010). Pallauf et al. (1998) found adverse effects of phytate (an ANF) in controlling the bioavailability of Fe, Zn and Mg in human diet suggesting strong associations between P and other essential minerals. Similarly, monoferric phytate reduces the bioavailability of Fe up to 60% in wheat bran (Morris and Ellis 1976). Ruibal-Mendieta et al. (2005) highlighted that higher P concentrations in spelt bran than normal wheat bran due to 40% lower phytic acid concentration. This could be either due to higher endogenous phytate activity or a reduced phytic acid level in spelt wheat. These findings confirmed that spelt wheat is a promising source to enrich protein content and minerals including Zn, Fe, Ca, Mg and P of cultivated wheat due to its wide adaptation, compatibility at ploidy level and high heritability (Troccoli and Codianni 2005; Gomez-Becerra et al. 2010).

2.5.3 Genomic regions controlling grain mineral concentration

A comprehensive screening of the wheat gene pool has demonstrated diploid progenitors, wild emmer, durum, spelt and landraces as promising sources of higher concentrations of Zn and Fe (Peleg et al. 2009; Velu et al. 2014). Various studies identified loci elevating Zn and Fe concentrations using bi-parental (Peleg et al. 2009; Tiwari et al. 2009; Srinivasa et al. 2014; Tiwari et al. 2016) and association mapping populations (Alomari et al. 2018; Bhatta et al. 2018; Velu et al. 2018; Cu et al. 2020). Few studies focused on minerals other

than Zn and Fe (Peleg et al. 2009; Bhatta et al. 2018; Cu et al. 2020). Peleg et al. (2009) targeted wild emmer derived RILs to study the genetic basis of micronutrient (Zn, Fe, Mn and Cu) and macronutrient (Ca, Mg, P, K and S) concentrations and grain protein content. In this study, a considerable transgressive segregation for grain protein and minerals was observed and 82 QTL with LOD scores >3, were identified. Four QTL for grain P concentration were co-located with protein content (Peleg et al. 2009). Fourteen QTL were co-located at homoeologous positions in AA and BB genomes for mineral concentration. Few genomic regions on chromosomes 2A, 5A, 6B and 7A harboured clusters of QTL for higher protein and mineral content (Peleg et al. 2009). Bhatta et al. (2018) detected 60 new loci for grain minerals namely Ca, Cd, Cu, Co, Fe, Li, Mg, Mn, Ni and Zn among a synthetic wheat panel. Cu et al. (2020) reported QTL controlling Zn, Fe, Mn, Cu and P concentration in a diverse association mapping panel.

A major locus *GPC-B1* (250 kb-locus) was associated with increased protein, Zn and Fe in wild emmer encoding a NAC (NAM-No apical meristem, ATAF-Arabidopsis transcription activation factor and CUC-cup shaped cotyledon) transcription factor gene NAM-B1 (Uauy et al. 2006; Distelfeld et al. 2007). This locus triggers senescence and nutrient re-mobilisation from leaves to grain. A major QTL linked with higher grain Zn, Fe, Cu and Mn concentration was identified on chromosome 5B (Ozkan et al. 2007). Four QTL for grain Zn and one for Fe concentration were identified in a DH population (Genc et al. 2009). A majority (~90%) of the genetic variation controlling grain Zn concentration was governed by major QTL located on chromosomes 3D, 4B, 6B, and 7A (Velu et al. 2014). Velu et al. (2018) identified 37 grain Zn MTAs and two major QTL on chromosomes 2A and 7B. Forty MTAs including three major effect QTL on chromosomes 3B and 5A were detected for higher grain Zn content among a European wheat collection (Alomari et al. 2018). Among *Ae. tauschii* accessions, nine MTAs for grain Fe and Zn concentrations were

reported using GBS markers (Arora et al. 2019b). QTL for grain Zn and Fe content were reported on chromosomes 2A and 7A among crosses of diploid wheat relatives *T. boeoticum* /*T. monococcum* (Tiwari et al. 2009). Similar regions were reported in *Ae. kotschyi* and *Ae. peregrina* (Singh et al. 2010). Velu et al. (2019) evaluated the effects of translocated segments of rye and *Ae.* species in accumulating higher Zn and Fe in a "Pavon76" wheat background. Elite translocation stocks 1) Pavon76+1Rr(1D), PAVON10, 2) Pavon76+MA1S.1RLe(1D), 3) Pavon76+2D(s)+4" and 4) Pavon76, 1RS.1AL" 1RS.1DL conferred significantly higher Zn content than the parental wheat line "Pavon76" and local varieties. This study also confirmed a significant positive association between grain Zn and Fe content and the possibility to target both micronutrients simultaneously (Velu et al. 2019). While many MTAs/QTL for grain mineral concentration were reported using wheat genetic resources, there is a little consensus among studies on the location of QTL.

Chapter 3

Fine mapping of *Lr49* using 90K SNP chip array and Flow-sorted chromosome sequencing in wheat

(This chapter has been published in a peer-reviewed journal)

"Nsabiyera V[#], Baranwal D[#], Qureshi N, Kay P, Forrest K, Valárik M, Doležel J, Hayden MJ, Bariana H, Bansal U (2020). Fine Mapping of *Lr49* using 90K SNP chip array and flow-sorted chromosome sequencing in wheat. Frontiers in Plant Science 10: DOI 10.3389/fpls.2019.01787. 1-11".

Joint first author

frontiers in Plant Science

ORIGINAL RESEARCH
published: 04 February 2020
doi: 10.3389/fpls.2019.01787

Fine Mapping of *Lr49* Using 90K SNP Chip Array and Flow-Sorted Chromosome Sequencing in Wheat

Vallence Nsabiyera[1†], Deepak Baranwal[1†], Naeela Qureshi[1,2], Pippa Kay[2], Kerrie Forrest[2], Miroslav Valárik[3], Jaroslav Doležel[3], Matthew J. Hayden[2,4], Harbans S. Bariana[1] and Urmil K. Bansal[1*]*

[1] Faculty of Science, School of Life Sciences and Environment, The University of Sydney Plant Breeding Institute, Cobbitty, NSW, Australia, [2] Agriculture Victoria Research, AgriBio, Bundoora, VIC, Australia, [3] Institute of Experimental Botany of the Czech Academy of Sciences, Centre of the Region Haná for Biotechnological and Agricultural Research, Olomouc, Czechia, [4] School of Applied Systems Biology, La Trobe University, Bundoora, VIC, Australia

OPEN ACCESS

Edited by:
Marion S. Röder, Leibniz Institute of Plant Genetics and Crop Plant Research (IPK), Germany

Reviewed by:
Pasqualina Colasuonno, University of Bari Aldo Moro, Italy
Jian Ma, Sichuan Agricultural University, China

***Correspondence:**
Matthew J. Hayden
matthew.hayden@agriculture.vic.gov.au
Urmil K. Bansal
urmil.bansal@sydney.edu.au

†These authors have contributed equally to this work

Specialty section:
This article was submitted to Plant Breeding, a section of the journal Frontiers in Plant Science

Received: 07 October 2019
Accepted: 20 December 2019
Published: 04 February 2020

Citation:
Nsabiyera V, Baranwal D, Qureshi N, Kay P, Forrest K, Valárik M, Doležel J, Hayden MJ, Bariana HS and Bansal UK (2020) Fine Mapping of Lr49 Using 90K SNP Chip Array and Flow-Sorted Chromosome Sequencing in Wheat. Front. Plant Sci. 10:1787. doi: 10.3389/fpls.2019.01787

Leaf rust, caused by *Puccinia triticina*, threatens global wheat production due to the constant evolution of virulent pathotypes that defeat commercially deployed all stage-resistance (ASR) genes in modern cultivars. Hence, the deployment of combinations of adult plant resistance (APR) and ASR genes in new wheat cultivars is desirable. Adult plant resistance gene *Lr49* was previously mapped on the long arm of chromosome 4B of cultivar VL404 and flanked by microsatellite markers *barc163* (8.1 cM) and *wmc349* (10.1 cM), neither of which was sufficiently closely linked for efficient marker assisted selection. This study used high-density SNP genotyping and flow sorted chromosome sequencing to fine-map the *Lr49* locus as a starting point to develop a diagnostic marker for use in breeding and to clone this gene. Marker *sunKASP_21* was mapped 0.4 cM proximal to *Lr49*, whereas a group of markers including *sunKASP_24* were placed 0.6 cM distal to this gene. Testing of the linked markers on 75 Australian and 90 European cultivars with diverse genetic backgrounds showed that *sunKASP_21* was most strongly associated with *Lr49*. Our results also show that the *Lr49* genomic region contains structural variation relative to the reference stock Chinese Spring, possibly an inverted genomic duplication, which introduces a new set of challenges for the *Lr49* cloning.

Keywords: adult plant resistance, chromosome sorting, Infinium iSelect 90K SNP array, leaf rust, marker assisted breeding

HIGHLIGHTS

High-density SNP genotyping and flow-sorted chromosome sequencing were used to fine map adult plant leaf rust resistance gene *Lr49*.

INTRODUCTION

Leaf rust, caused by *Puccinia triticina* (Pt), is one of the most important diseases of wheat worldwide and can result in yield losses of up to 70% (Kolmer, 2005). While wheat has inherent defense mechanisms to resist diseases, an emphasis on selection for high yield and other desirable traits has resulted in a narrow genetic base for disease resistance (Borlaug, 2007). The release of resistant cultivars is the best strategy to control leaf rust, and to reduce production costs and risk of environmental pollution resulting from fungicide usage (Bariana, 2003; Bariana et al., 2007; Bariana and Bansal, 2017).

Many leaf rust resistance genes have been identified and named in wheat (McIntosh et al., 1995; McIntosh et al., 2013; Bariana and Bansal, 2017). Resistance genes include two categories; all stage resistance (ASR) and adult plant resistance (APR). The ASR genes are effective throughout the life of the plant, whereas adult plant resistance genes are effective only at adult plant stage. A majority of the formally named genes confer ASR (McIntosh et al., 1995; McIntosh et al., 2013). ASR genes exhibit hypersensitive reaction to condition a high level of resistance against avirulent pathogen isolates. However, they are prone to breakdown when the pathogen evolves to acquire virulence. The ASR genes can be identified at the seedling stage under greenhouse conditions. In contrast, APR genes express at the postseedling stages and retard pathogen growth. They are considered durable due to their race nonspecific nature. Examples of pleiotropic APR genes include *Lr34/Yr18* (Singh, 1992), *Lr46/Yr29* (Singh et al., 1998), *Lr67/Yr46/Sr55* (Hiebert et al., 2010; Herrera-Fossel et al., 2011), *Lr68* (Herrera-Foessel et al., 2012) and *Lr75* (Singla et al., 2017). Some APR genes show race-specific responses, and these include *Lr12* (McIntosh et al., 1995) and *Lr22b* (Dyck, 1979). While *Lr48* and *Lr49* were assigned by Saini et al. (2002) to the hypersensitive category based on monocyclic flag leaf tests, Bariana and Bansal (unpublished results) observed these genes to be slow rusting under polycyclic infection conditions in the field.

Traditionally, the development of new wheat cultivars has followed conventional phenotypic selection of desirable traits. Although this approach remains effective, it faces significant challenges due to the length of time taken to release a new cultivar (Forster et al., 2015). Recent advances in wheat genomics have led to the development of more efficient and precise approaches for wheat improvement (Dubcovsky and Dvorak, 2007; Bariana et al., 2013). For example, the identification of DNA markers linked with rust resistance genes has largely overcome the limitations of phenotypic selection for pyramiding two or more genes in breeding programs (Bariana et al., 2007; Bariana and Bansal, 2017). Similarly, the availability of high-density genotyping platforms such as DArTseq (Diversity Arrays Technology, Bruce, Australia; Cruz et al., 2013) and Infinium iSelect 90K SNP bead chip array (Wang et al., 2014) have expedited the mapping of economic traits (Bariana and Bansal, 2017). The development of simple gel-free marker genotyping systems such as kompetitive allele-specific PCR (KASP; LGC Genomics, UK) have encouraged marker assisted selection in breeding programs.

The rate for development of trait-linked DNA markers has also been accelerated by the increasing availability of genomic resources and tools supporting high throughput genomics. For example, methods have been developed to isolate specific chromosomes using flow cytometry (Vrána et al., 2000; Giorgi et al., 2013), which can then be sequenced to interrogate individual chromosome DNA code. Such approaches are particularly useful in polyploid species such as wheat, because they not only reduce the genome complexity to a single chromosome but also eliminate problems associated with presence of homoeologous genomes for sequence assembly (Doležel et al., 2007). The ability to sequence individual chromosomes adds a new dimension to marker development and gene cloning in allopolyploids including wheat (Doležel et al., 2012; International Wheat Genome Sequencing Consortium (IWGSC), 2014).

An Indian cultivar VL404 (Kentana/Bungulla//Frontana/General-Urquiza/3/ST464/PI-74106) was released in 1973 by Vivekananda Parvatiya Krishi Anusandhan Sansthan, Almora. This cultivar was susceptible at the two-leaf stage but showed resistance at the flag-leaf stage against Indian Pt pathotypes in monocyclic inoculations and the underlying resistance locus was formally named *Lr49* (Saini et al., 2002). *Lr49* was mapped on the long arm of chromosome 4B (Bansal et al., 2008) using the VL404/WL711 RIL population, however, the flanking markers were not sufficiently close for efficient marker assisted selection. The aim of this study was to fine map the gene *Lr49* using recently published assembled reference genome sequence for variety Chinese Spring (Appels et al., 2018) and flow sorted chromosome 4B sequence for VL404 and WL711. This is a first step towards cloning the causal gene for *Lr49* and developing a diagnostic marker for use in marker assisted selection.

MATERIALS AND METHODS

Plant and Pathogen Materials

The VL404/WL711 $F_{6:8}$ derived recombinant inbred line (RIL) population used in this study comprised 181 lines. Pedigree information for both parents is described in the earlier study (Saini et al., 2002). A diverse set of Australian (75) and European (90) wheat cultivars was used to test the strength of linkage between markers developed in this study and *Lr49*. DNA was extracted from each wheat line using the method described in Bansal et al. (2014a).

Greenhouse Tests

Eight to 10 seeds of each RIL and parents were sown in 9-cm diameter pots as four lines per pot. Twenty grams of complete fertilizer Aquasol dissolved in 10L of tap water was applied to pots filled with potting mix before sowing. Plants were grown to the 4th leaf stage at 20°C in a rust-free microclimate room prior to inoculation. Urea was applied every week prior to inoculation with *Lr49*-avirulent Pt pathotype 76-1,3,5,10,12 (culture no 539). The inoculation procedure described in Bansal et al. (2008) was followed. Rust response assessments were made 18 to 20 days post-inoculation using the infection type (IT) scale detailed in

McIntosh et al. (1995). Briefly 0-4 infection type scale was used and RILs classified <3 were considered resistant and >3 susceptible.

Sorting and Sequencing of Chromosome 4B

Suspensions of intact mitotic chromosomes were prepared from synchronised root meristems of parental lines VL404 and WL711 (Vrána et al., 2000; Vrána et al., 2012) and GAA microsatellites on the chromosomes were labeled in suspension by fluorescein isothiocyanate (FITC) using the protocol for Fluorescence In Situ Hybridization In Suspension (FISHIS) (Giorgi et al., 2013). Genomic DNA was stained by 4',6-diamidino2-phenylindole (DAPI) and chromosomes were analyzed on a FACSAria II SORP high speed flow sorter (BD Biosciences, San José, USA) as described in Kubaláková et al. (2002). One thousand chromosomes from each cluster were sorted onto a microscopic slide into a drop of 10 µl of PRINS buffer supplemented with 5% sucrose (Kubaláková et al., 1997). To assign chromosomes to an individual cluster on a dot plot, FISH with probes for GAA and Afa repeats was used to identify flow-sorted chromosomes and to assess purity. Chromosomal DNA of 4B was amplified by the Multiple Displacement Amplified (MDA) approach using the Illustra GenomiPhi V2 DNA amplification kit (GE Healthcare, http://www.gehealthcare.com) as described in Šimková et al. (2008). Sequencing libraries were generated using the Nextera DNA sample preparation kit (Illumina Inc, San Diego, CA, USA) and 50 ng of DNA was amplified (according to the manufacturer's instructions, with the exception for usage of 3 µl of TDE1 for DNA fragmentation). Libraries with insert sizes of 600–800 bp were selected for sequencing. The insert sizes were verified using the Agilent DNA 1000 Kit (Agilent Technologies, Inc.) and concentrations were assessed by the KAPA Library Quantification Kit (Kapa Biosystems, Woburn, USA). The libraries were sequenced as paired-end reads using the HiSeq Rapid SBS Kit v2 (2x250 bp) (Illumina Inc, San Diego, CA, USA).

SNP Detection Using Flow Sorted Chromosome 4B Sequence

GYDLE software (Gydle Inc. Bioinformatics Service, Quebec City, Canada; http://www.gydle.com) was used to quality filter the raw sequence reads (minimum phred score 20; minimum read length 50 bp) derived from flow-sorted 4B chromosome sequences of VL404 and WL711 and to align the filtered reads to the International Wheat Genome Sequencing Consortium (IWGSC) reference genome sequence assembly for cultivar Chinese Spring (RefSeq assembly v1.0; Appels et al., 2018). Gydle software performs an exhaustive alignment search to guarantee each paired-end read is aligned at its best mapping position, providing the alignment score that exceeds 80% sequence homology. Paired-end reads that align to multiple positions with equal scores are randomly distributed across those positions to ensure that all alignment positions are fully and correctly reflected. The SNP variant discovery and genotype calling was performed using the aligned paired-end sequence reads for WL711 and VL404 and GYDLE "findsnp" function.

DNA Genotyping

Microsatellite markers previously reported to be linked with *Lr49* (Bansal et al., 2008) were genotyped on the entire RIL population and parents following the amplification conditions described in Bansal et al. (2014b). Infinium iSelect 90K SNP genotyping was performed on 12 resistant and 12 susceptible RILs, as reported in Wang et al. (2014). Genotype calling was performed using GenomeStudio (Illumina) and a custom perl script to assign genotype calls. Closely linked 90K SNPs and those identified from the flow-sorted chromosome sequences were converted into kompetitive allele-specific PCR (KASP) assays (LGC Genomics) following the manufacturers guidelines. For each KASP marker, two allele-specific forward primers and one common reverse primer were designed using BatchPrimer3 v1.0 (https://wheat.pw.usda.gov/demos/BatchPrimer3/) software. The PCR reaction contained 3 µl of DNA (30ng/µl), 5 µl KASP mix (LGC Biosearch Technologies), and 0.11 µl of primer mix (12 µM of each allele specific primer and 30 µM of reverse primer). Reaction was performed in CFX96 real time PCR machine (Biorad, USA) with the following cycling conditions: 15 min at 94°C; 10 touchdown cycles of 20 s at 94°C, 60 s at 65–57°C (dropping 0.8°C per cycle); and 26–35 cycles of 20 s at 94°C, 60 s at 57°C. Flourescence reading was taken at 40°C for 30 s and were analysed using allelic discrimination function. The KASP markers derived from 90K SNPs were named with the prefix KASP, followed by a number corresponding to the SNP index on the Infinium bead chip. The KASP markers derived from flow-sorted chromosome sequence variants were designated by the prefix *sunKASP* (sun = Sydney University) followed by a consecutive number.

High Resolution Mapping

VL404 was crossed with Avocet S to develop a high-resolution mapping population consisting of 2560 F_2 plants. DNA was extracted from each F_2 plant and tested with the *Lr49* flanking markers. Plants showing recombination between the flanking markers were transplanted and the high resolution F_3 family was generated and phenotyped with Pt pathotype 76-1,3,5,10,12 at the 4th leaf stage.

Data Analyses and Genetic Mapping

The RIL population was categorized as homozygous resistant (HR) or homozygous susceptible (HS) based on the phenotypic scores of parents. Chi-squared (χ^2) test was used to determine the goodness of fit of the observed segregation to the expected genetic ratios. Alleles for SNP and SSR markers were scored as A and B for parents VL404 and WL711, respectively.

A genetic map was generated using MapManager Version QTXb20 (Manly et al., 2001) and the Kosambi map function (Kosambi, 1943). The linkage map was drawn according to Voorrips (2002). A likelihood of odds (LOD) score of 3.0 was used as the threshold for declaring linkage among loci.

The genetic-physical map viewer Pretzel (Keeble-Gagnère et al., 2019) was used to identify and visualize structural variation in the genomic region containing the *Lr49* locus.

RESULTS

Genetic Analysis

VL404 (*Lr49*) and WL711 exhibited infection type (IT) X (mesothetic response which includes more than two infection types on the same leaf) and IT3+, respectively, when inoculated with Pt pathotype 76-1,3,5,10,12 at the 4th leaf stage under greenhouse conditions. Leaf rust test on VL404/WL711 RIL population revealed clear segregation of *Lr49* (99 resistant: 82 susceptible; $\chi^2_{1:1} = 1.59$, nonsignificant at $P = 0.05$ and *1d.f.*).

Chromosome Sorting and Sequencing

Thirty-five thousand copies of chromosome 4B from each of VL404 and WL711 were sorted with 97% and 98% purity, respectively, and amplified by MDA. To minimize the risk of representation bias, the products from three independent MDA reactions were pooled. The amplification and pooling of 4B chromosomal DNA from VL404 and WL711 yielded 7.88 and 8.36 µg DNA, respectively, and paired-end sequencing provided 70,519,221 and 70,685,036 reads. Following quality filtering, the filtered reads were aligned to the reference genome sequence assembly of cultivar Chinese Spring. This resulted in 68.8 and 64.7% of the filtered reads uniquely mapping to chromosome 4B, representing 16.5 and 17.3 fold coverage for VL404 and WL711, respectively.

Molecular Mapping

Forty-five SNPs from the iSelect 90K Infinium array showed linkage with *Lr49* and were converted into single-locus KASP assays. Twenty-one KASP markers that clearly discriminated the parents (**Table 1**) were genotyped on the entire RIL population and integrated into the previously reported microsatellite marker-based genetic linkage map carrying *Lr49* (**Figure 1**). The closest proximal marker *KASP_54629* mapped 2.7 cM from *Lr49*, whereas the closest distal markers at 0.6 cM and included several co-segregating KASP markers.

To further increase marker density for the *Lr49* region, SNP discovery was performed using the flow-sorted chromosome sequences for VL404 and WL711. Twenty-eight SNPs with approximately even physical spacing were selected to span the *Lr49* region and converted into KASP assays. Seven of these markers (**Table 1**) produced clear parental clusters and could be unambiguously scored on the RIL population. Integration of these KASP markers into the genetic map for the *Lr49* region, resulted in *sunKASP_21* mapping at 0.4 cM proximal and *sunKASP_24* (clustered with five additional KASP markers derived from 90K SNPs) at 0.6 cM distal to *Lr49* (**Figure 1B**).

TABLE 1 | Primer sequences for kompetitive allele-specific PCR (KASP) markers designed from SNP sequences that showed association with *Lr49* on chromosome 4BL and SNPs discovered from the sequences of flow sorted chromosome 4B of parental genotypes.

KASP marker	SNP ID	Forward (Allele 1) primer	Forward (Allele 2) primer	Common/reverse primer
KASP_5827	*IWB5827*	gaagcagctggcagcactca	gaagcagctggcagcactcg	gctcagcctcaaggtggtgtt
KASP_7042	*IWB7042*	tccaagttgactcaagagacgaga	ccaagttgactcaagagacgagg	cctcctacgcaaacaacgacacaa
KASP_7783	*IWB7783*	agtaagaggcactacogttcagatt	aagaggcactacogttcagatc	agagggcgtgctttccaagtgaat
KASP_8082	*IWB8082*	ttgctggtctttagaaatcoctc	gctttgctggtctttagaaatccccta	cttgcactaacatcacaacccccat
KASP_8302	*IWB8302*	acoctttacaacaacttcattcgc	ctaccttttacaacaacttcattcgt	gggaataatcagggattgacccccta
KASP_8708	*IWB8708*	ggtcgtggtgacgcacgcaa	gtcgtggtgacgcacgcag	ttcacatgacoatggccaggagat
KASP_8980	*IWB8980*	agagcagaattgattgctgcaact	agagcagaattgattgctgcaacc	ctccactttcctccatgtcatctgtt
KASP_12434	*IWB12434*	cgcaogacgagtgctgcca	gcacgacgagtgctgccc	gtcaaggtogaccaccccctgaa
KASP_20268	*IWB20268*	gtcctcaattggagatgogctt	gtcctcaattggagatgogctg	atcaagatgtaatttctgattcagcaagcaa
KASP_20269	*IWB20269*	tcttttatactcacattctgaatcaggat	cttttatactcacattctgaatcaggac	ctcogagagtcaaaatacaagcaagtgttt
KASP_21440	*IWB21440*	gtccccagctaatcctgtggaa	ccccagctaatcctgtggag	tagttctgtagcttoggttgatacctt
KASP_26845	*IWB26845*	cagtttaaatatgcagcagcactta	ctcagtttaatatgcagcagcactic	gacgcagatccatctcagaaggtaa
KASP_35049	*IWB35049*	aagcgaaagagaaactatttacagt	ctaagcgaaagagaaactatttacagc	tttagacacagcgatacgttgtacatgtt
KASP_36379	*IWB36379*	gtgaoctatgactggtagaag	cctgtgaoctatgactggtagaaa	aaatogcaattttaaacatgaattcagttctt
KASP_39484	*IWB39484*	agtcaatgcaaggaggagaaa	ctagtcaatgcaaggaggagaag	gcogcttgttaggctttggctt
KASP_53740	*IWB53740*	tgtcatcttcatttcagcatctgca	gtcatcttcatttcagcatctgcg	gatccagaggagaaggtttctgcta
KASP_54629	*IWB54629*	gtgtctccaagtgacagttgaatgt	gtctccaagtgacagttgaatgc	atccagcttctttgtacagcggagaa
KASP_54728	*IWB54728*	gatgacatogacggcgaactga	atgacatogacggcgaactgg	acaccggctggtatgccaccaa
KASP_59160	*IWB59160*	aagattttgcttttogatccgtacttca	agattttgcttttogatccgtacttcg	gtaacaacgatttcaaatgtggcaccgaaa
KASP_72709	*IWB72709*	cgatcctaatgaaccgacgtattgt	gatcctaatgaaccgacgtattgc	acogtagctgacttggttgcagaa
KASP_1109	*IWB1109*	tattcatcttacgattcttaaatacttccaat	catcttacgattcttaaatacttccaac	ccaggtgtgtgtgcttcctttatt
sunKASP_21	–	gattcgaatgttttgtaggattic	ttcagatctaaaatcacggcact	ctattaacgtagagcccagtgc
sunKASP_24	–	ttcgattaccogggagc	ttcgattaccogggagt	tgggtaaggccaagaaaca
sunKASP_26	–	agtaccaaatgcagcaaaaaaa	cagtaccaaatgcagcaaaaaat	ctttggcccaagtgtgtct
sunKASP_31	–	tcaatcatttacttttcatgcgag	aatgtaatttattttgttttgcttgc	caccgaccaccatttgttcta
sunKASP_33	–	catgtcaatagttatgcactcaaattg	aatcttttgctagcctticatctc	tggtccaagtacagtctaacca
sunKASP_35	–	caaatcctaaaagccaagatgc	ttcatttcggggactggga	cggagctatttttggaccag
sunKASP_39	–	caccatctcctcctcattatca	catcctctagaacaatggtggtc	ctcttcccgttgcaagaaat

Allele 1 primer labeled with FAM: GAAGGTGACCAAGTTCATGCT;
Allele 2 primer labeled with HEX: GAAGGTCGGAGTCAACGGATT.

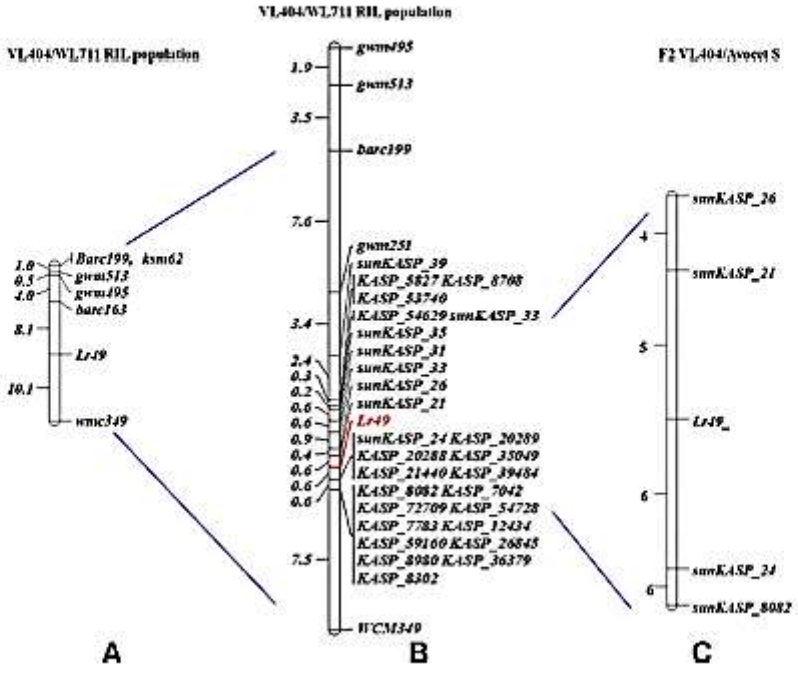

FIGURE 1 | Genetic linkage map of chromosome 4BL for the VL404/WL711 RIL population **(A)** Bansal et al. (2008), **(B)** present study (resistance gene is shown in red text), and **(C)** high resolution map of VL404/Avocet S (number of recombinants is given on the left).

Construction of High-Resolution Map

Markers *sunKASP_21*, *sunKASP_26*, *sunKASP_24* and *KASP_8082* that flanked *Lr49* were genotyped on 2560 VL404/Avocet S F_2 plants to identify recombinants for the construction of a high-resolution map. Twenty-one recombinants were observed. The recombinant F_3 families were scored as homozygous resistant, homozygous susceptible and segregating. Five and six recombinants were observed between *Lr49* and markers *sunKASP_21* and *sunKASP_24*, respectively (**Figure 1C**).

Assessing Marker Linkage Using Unrelated Materials

Flanking markers *sunKASP_21*, *sunKASP_24*, *KASP_20289*, *KASP_20288*, *KASP_35049*, *KASP_21440* and *KASP_39484* were genotyped on a diverse set of 75 Australian and 90 European cultivars, unlikely to carry *Lr49*, to test the marker linkage with *Lr49*. Across the diverse germplasm, the proximal marker *sunKASP_21* showed the strongest linkage, amplifying the susceptible WL711 (T:T) allele in all cultivars, except Gazelle, Safir and JO 8023, which amplified the resistance VL404 allele (C:C) (Table 2). In contrast, the distal markers (*sunKASP_24*, *KASP_20289*, *KASP_20288*, *KASP_35049*, *KASP_21440* and *KASP_39484*) showed poor linkage, amplifying both the resistant and susceptible alleles (data not shown).

Identification Closely Linked Markers

Exome SNPs from 890 globally diverse accessions (He et al., 2019) located within the *Lr49* region were used to identify recombination hot spots distal to marker *sunKASP_21*. The physical order of SNPs across the *Lr49* region were used to identify five major haplotypes. VL404 belonged to one of these haplotypes and WL711 to another. Across the five haplotypes, two recombination sites were observed distal to the physical mapping position of *sunKASP_21* and proximal to those of the co-segregating markers (*sunKASP_24*, *KASP_20289*, *KASP_20288*, *KASP_35049*, *KASP_21440* and *KASP_39484*) in the RIL population (**Figure 2**). The recombination sites explain the breakdown in linkage (many false positives) observed in the diverse panel of Australian and European cultivars for markers distal to *Lr49*.

To develop markers between the two recombination sites and *sunKASP_21*, 35 exome SNPs proximal to the recombination sites and distal to *sunKASP_21* were converted into KASP markers. However, only two of the KASP markers (*sunKASP_261* and *sunKASP_282*) were polymorphic between VL404 and WL711 and produced a scorable pattern. When genotyped on the RIL population and integrated into the genetic map, neither marker was closely linked to *Lr49*. Further, based on the physical position of *sunKASP_282* in the reference genome assembly of cultivar Chinese Spring, the marker fell within a putative deletion in the haplotype corresponding to VL404 (**Figure 2**). No additional SNP from the

TABLE 2 | Validation of closely linked kompetitive allele-specific PCR (KASP) marker on Australian and European wheat cultivars.

Cultivars/lines	*sunKASP_21*
VL404 (*Lr49*)	C:C
WL711	T:T
AGT Katana, Axe, Baxter, Beaufort, Bolac, Calingiri, Carnamah, Catalina, Chara, Cobra, Corack, Correll, Crusader, Dart, Denimut, Diamondbird, EGA Bonnie Rock, EGA Bounty, EGA Burke, EGA Gregory, EGA Wedgetail, EGA Wylie, Elmore CL Plus, Emu Rock, Envoy, Espada, Estoc, Forrest, Fortune, Gauntlet, GBA Sapphire, Giles, Gladius, Grenade CL Plus, Impala, Impose CL Plus, Janz, Justica CL Plus, King Rock, Kord CL Plus, Kunjin, Lang, Lincoln, Livingston, Mace, MacKellar, Magenta, Merinda, Merlin, Naparoo, Orion, Phantom, Preston, Scout, Sentinel, Shield, Spitfire, SQP Revenue, Strzelecki, Sunco, Sunguard, Suntop, Sunvale, Sunvex, Sunzell, Ventura, Waagan, Wallup, Wedin, Westonia, Wyalkatchem, Wylah, Yandanooka, Yitpi, Young	T:T
Gazelle, JO 8023, Safir	C:C
Apu, Aros, Arson, Avle, Bastian, Bjarne, Blanka, Bersum, Boru, Canon, Dala, Dalama, Diamant, Diamant II, Drabant, Dragon, ELS 6404 - 102 - 3, Ergo, Eroica, Extra Kolben, Fagott, Fram I, Fram II, Fylgia I, Fylgia II, Haarajärvi ME102 Apu, Halland, Horsmanaho ME201 Timantti, J-03, Järvenkylä ME0302 Timantti, JO 3524, Jokikylä ME0505 Apu, Kadett, Kärn II, Kenya Farmer, Kimmo, Kuru, Kota, Latsla AP0103, Landvärkvete, Lantvete från Dalarna, Lantvete från Halland, Lavett, Manu, Monola ME1301, Mayestad, MS273-150, Naxos, Nemares, Nora, Norrena, ostby, Polka, Pompe, Pondus, Prins, Progress, Rang, Reno, Ring, Rival, Rollo, Rubin, Runar, Ruso, Safran, Sappo, Sibirian, Skirre, Snegg II, Snegg I, Sober, Sopu, Sport, Svenno, Timantti, Timantti Paavo, Tjalve, Touko, Troll, Trym, Ulla, Vinjett, Vitus, Walter, William, WW 20299, Zebra,	T:T

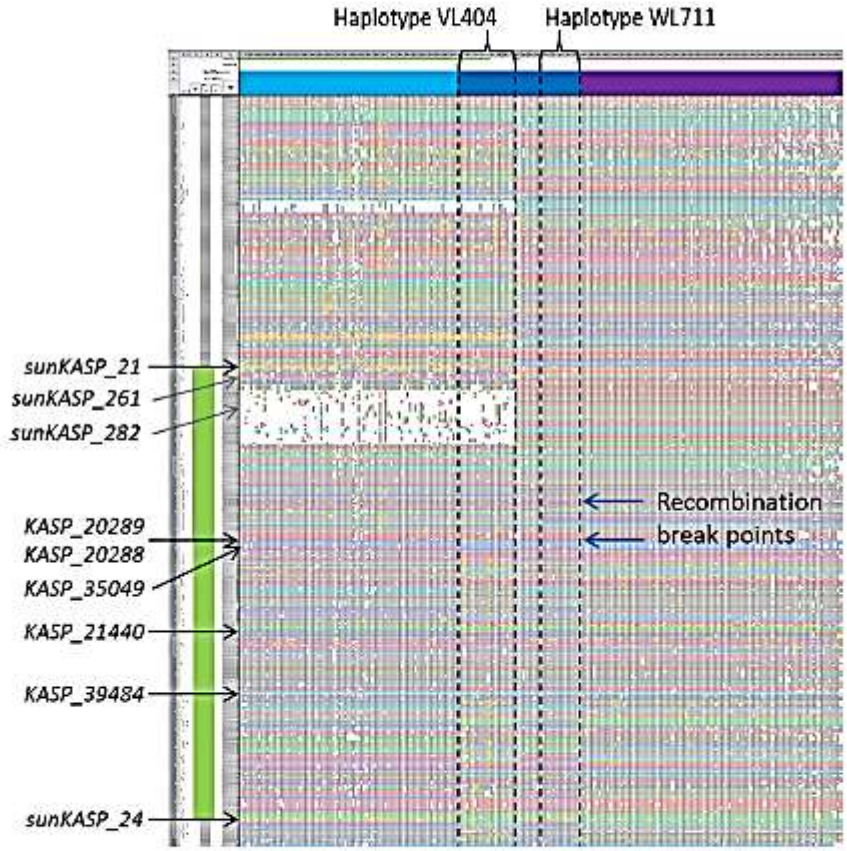

FIGURE 2 | Exome SNP genotypes for 890 globally diverse accessions across the *Lr49* region (green box). The *sunKASP_21* maps proximal to *Lr49*, while *KASP_20289*, *KASP_20288*, *KASP_35049*, *KASP_21440*, *KASP_39484*, and *sunKASP_24* cosegregate and map distally to *Lr49* in the RIL mapping population. Physical mapping positions for the flanking markers are indicated by black arrows. Two recombination breakpoints present between *sunKASP_21* and *KASP_20289* are shown by blue arrows. Two additional markers, *sunKASP_261* and *sunKASP_282*, developed from parental SNPs proximal to the recombination break points and mapped in the RIL population were not linked to *Lr49*. The physical mapping position for these two markers is denoted by grey arrows.

parental flow-sorted chromosome sequences could be identified for the region between *sunKASP_21* and the two recombination sites.

Genomic Structure of the *Lr49* Region

Comparison of marker loci order in the genetic linkage map for the VL404/WL711 RIL population with the physical positions of the same marker loci in the reference genome assembly for Chinese Spring revealed a complex pattern (**Figure 3**). It showed that the marker loci order distal to *sunKASP_21* in the RIL population was colinear with Chinese Spring, while the marker loci order proximal to *sunKASP_26* was inverted. The inversion was contained within the genomic region of Chinese Spring that appeared to be colinear with the RIL population distal to marker *sunKASP_26*. As repeated genotyping of the RIL population with the KASP markers produced the same result, the complex pattern suggested the presence of structural variation between one or both parents of the RIL population and Chinese Spring. Comparison of the physical map order of high confidence genes across the orthologous region in *Ae. tauschii* chromosome 4D, and homoeologous regions in Chinese Spring chromosome 4D (IWGSCv1.0), emmer chromosome 4B (Avni et al., 2017) and Chinese Spring chromosome 4B (IWGSCv1.0) showed no evidence for structural rearrangements (**Supplementary Figure 1**), indicating that the structural variation was present in one or both parents and not Chinese Spring.

The genomic region between *sunKASP_21* and the markers cosegregating with *sunKASP_24* in the Chinese Spring reference genome assembly sequence contained 13 high confidence genes annotated in the IWGSC v1.0 genome release (**Table 3**). A gene containing a putative LRR motif (TraesCS4B01G301300) could be the likely candidate for *Lr49*. However, despite having good sequence read coverage in both VL404 and WL711, no nucleotide variation was identified in the coding sequence of the gene that would result in an asynonymous mutation or premature stop codon. This finding suggests that this gene is an unlikely candidate for *Lr49*, although differences in gene expression caused by a noncoding variant between the parent lines cannot be ruled out.

The alignment of the flow-sorted chromosome paired-end sequence reads from each parent to the reference genome

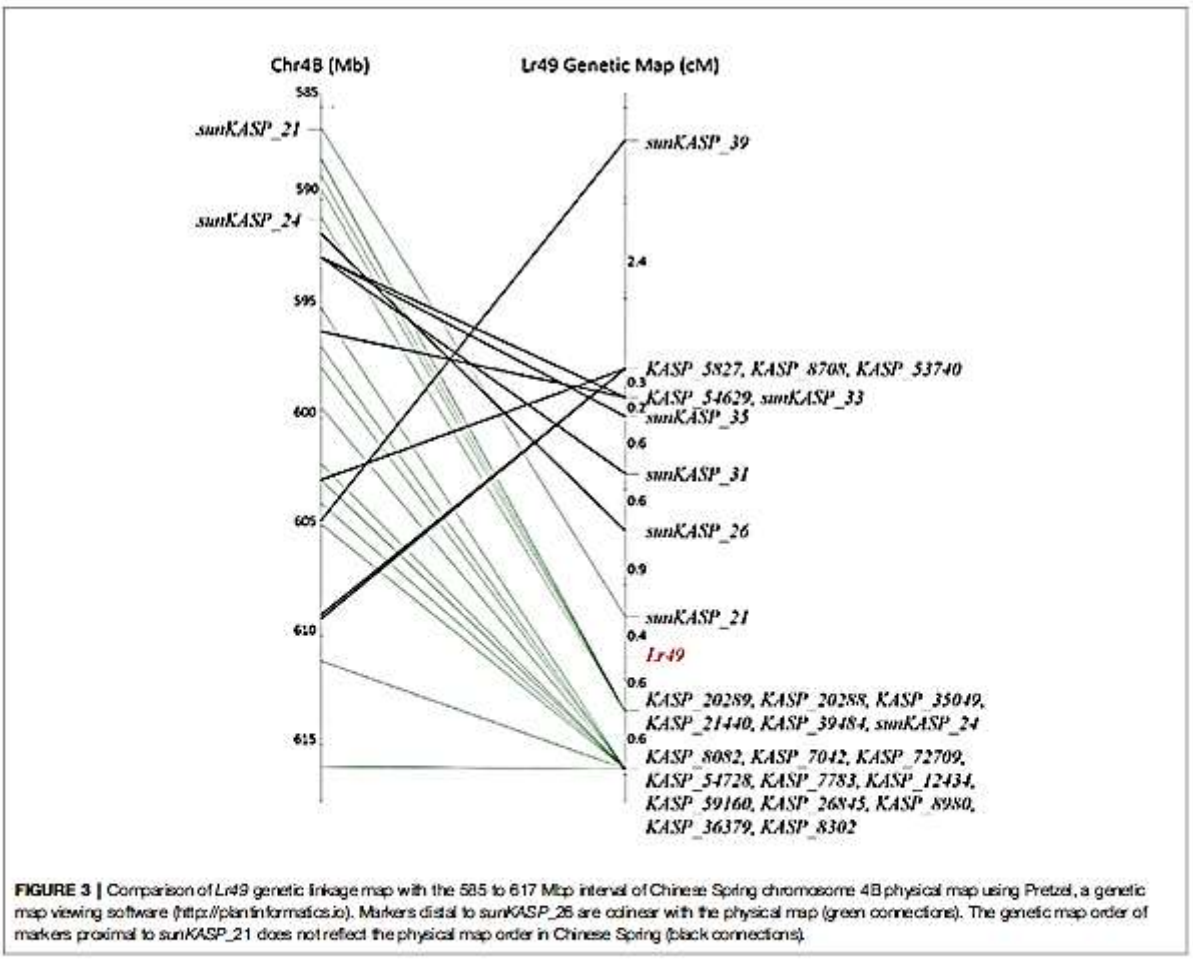

FIGURE 3 | Comparison of *Lr49* genetic linkage map with the 585 to 617 Mbp interval of Chinese Spring chromosome 4B physical map using Pretzel, a genetic map viewing software (http://plantinformatics.io). Markers distal to *sunKASP_26* are colinear with the physical map (green connections). The genetic map order of markers proximal to *sunKASP_21* does not reflect the physical map order in Chinese Spring (black connections).

TABLE 3 | High confidence genes annotated in the IWGSC v1.0 genome sequence between flanking markers *sunKASP_21* and markers cosegregating with *sunKASP_24*.

IWGSC v1.0 Gene ID	IWGSC v1.0 human readable gene annotation
TraesCS4B01G300700	Carotenoid cleavage dioxygenase
TraesCS4B01G300800	Tryptophan synthase beta chain
TraesCS4B01G300900	Peptide chain release factor 1
TraesCS4B01G301000	DNA-directed RNA polymerase subunit beta
TraesCS4B01G301100	Receptor-like protein kinase
TraesCS4B01G301200	Hexosyltransferase
TraesCS4B01G301300	Leucine-rich repeat receptor-like protein kinase
TraesCS4B01G301400	B3 domain-containing protein
TraesCS4B01G301500	NAD(P)-binding Rossmann-fold superfamily protein
TraesCS4B01G301600	Origin recognition complex subunit 2
TraesCS4B01G301700	Transmembrane protein, putative
TraesCS4B01G301800	Alpha/beta-Hydrolases superfamily protein
TraesCS4B01G301900	Thionin-like protein
TraesCS4B01G302000	Agmatine coumaroyltransferase-2
TraesCS4B01G302100	Agmatine coumaroyltransferase-2
TraesCS4B01G302200	Agmatine coumaroyltransferase-2
TraesCS4B01G302300	Agmatine coumaroyltransferase-2
TraesCS4B01G302400	Uroporphyrinogen ■ synthase
TraesCS4B01G302500	Transmembrane protein 131
TraesCS4B01G302600	MADS box transcription factor
TraesCS4B01G302700	Vacuolar-sorting-associated protein 37-like protein
TraesCS4B01G302800	Aspartic proteinase nepenthesin-1
TraesCS4B01G302900	DNA-directed RNA polymerase subunit
TraesCS4B01G303000	Dentin sialophosphoprotein-related, putative isoform 1
TraesCS4B01G303100	WD and tetratricopeptide repeat protein, putative
TraesCS4B01G303200	Zinc finger protein
TraesCS4B01G303300	Ubiquitin carboxyl-terminal hydrolase 2

assembly of Chinese Spring using GYDLE software revealed the presence of two distinct sequence haplotypes in the susceptible parent WL711 that spanned the entire *Lr49* region delineated by markers *sunKASP_21* and *sunKASP_36379*. Indeed, these sequence haplotypes extended well beyond the *Lr49* region both distally and proximally (**Figure 4**). In contrast, a single but different sequence haplotype was observed in the resistant parent VL404 within the *Lr49* region delineated by markers *sunKASP_21* and *sunKASP_36379*. Outside this region, VL404 possessed two distinct sequence haplotypes, one of which was identical to one of those observed in WL711 and the single sequence haplotype present in Chinese Spring, which was observed when Chinese Spring flow-sorted chromosome paired-end sequence reads were aligned to pseudomolecule 4B (IWGSCv1.0) (**Figure 4**). The presence of only a single sequence haplotype within the *Lr49* region delineated by markers *sunKASP_21* and *sunKASP_36379* in VL404, relative to WL711, was further supported by paired-end sequence read coverage across the interval (**Supplementary Figure 2**). These observations indicate the presence of structural chromosomal differences between VL404, WL711 and Chinese Spring.

DISCUSSION

Cultivars carrying long-lasting resistance to diseases have been released through conventional phenotypic screening; however, the genetic basis of resistance has been largely unknown. It is

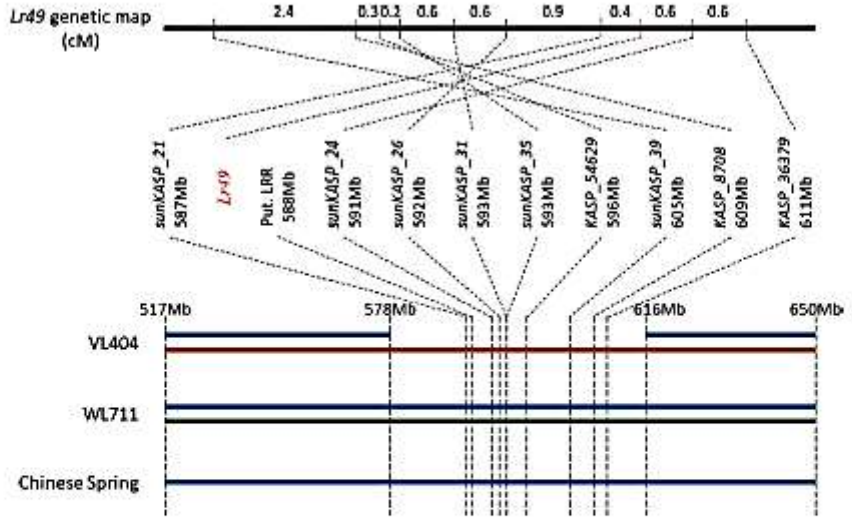

FIGURE 4 | Diagrammatic representation of the *Lr49* interval and flanking region on chromosome 4B. Both VL404 (resistant parent) and WL711 (susceptible parent) have two sequence haplotypes outside the *Lr49* region, while VL404 has only one sequence haplotype within the *Lr49* interval. Chinese Spring has only one sequence haplotype across entire region. Each unique sequence haplotype is represented by a different color. Markers mapping within the *Lr49* interval are ordered based on their physical mapping location. The *Lr49* genetic map does not reflect the physical mapping order as illustrated by comparison of genetic and physical map order across the *Lr49* interval. Differences in sequence haplotype structure and physical-genetic map order in VL404 and WL711, relative to Chinese Spring, suggests structural rearrangement or copy number variation (CNV) relative to Chinese Spring.

challenging to combine ASR and APR genes with confidence into a single genotype using phenotypic assays, as the high level of resistance conditioned by effective ASR genes masks the detection of APR loci. Molecular markers linked with rust resistance genes developed through fine mapping can be used to pyramid resistance genes into a single genotype efficiently and reliably.

We used high-density genotyping and flow-sorted chromosome sequencing to fine-map the genomic region on chromosome 4B containing *Lr49* as a first step towards developing a diagnostic marker for use in marker assisted selection and for cloning of this gene. Genetic mapping of VL404/WL711 RIL population using the iSelect 90K wheat SNP bead chip array localized *Lr49* to a 3.3-cM interval. Subsequent mapping using KASP markers targeting nucleotide variation identified from flow-sorted chromosome sequences of the parental lines VL404 and WL711 that was expected to tile across the physical region corresponding to *Lr49* in the Chinese Spring chromosome 4B pseudomolecule, further reduced the *Lr49* interval to 1.0 cM (**Figure 1**).

While the availability of flow-sorted chromosome sequences for the parental lines VL404 and WL711 allowed the rapid identification of nucleotide variation to further fine map the *Lr49* interval and to largely preclude a high-confidence gene containing a LRR motif as a candidate for *Lr49*, many of the KASP markers targeting this polymorphism could not be reliably scored in the mapping population. Indeed only seven of 28 KASP assays developed for this purpose could be genetically mapped. Comparison of the *Lr49* genetic linkage map with the Chinese Spring chromosome 4B physical map (**Figure 3**), followed by visualization of the alignment of the flow-sorted chromosome paired-end sequence reads from each parent to the reference genome assembly of Chinese Spring (**Figure 4**), suggested structural variations in VL404 and WL711 compared to Chinese Spring. This was supported by observed collinearity of high confidence genes across the orthologous region in *Ae. tauschii* chromosome 4D, and homoeologous regions in Chinese Spring chromosome 4D, emmer chromosome 4B, and Chinese Spring chromosome 4B (**Supplementary Figure 1**). These observations suggested that the linkage map appeared inverted and overlapping when compared to the physical position of the markers in the Chinese Spring 4B pseudomolecule (**Figure 3**), and the presence of two sequence haplotypes in WL711 across the *Lr49* region and beyond the *Lr49* interval in VL404 (**Figure 4**). These results implied the presence of an inverted local duplication in each of the parental lines relative to Chinese Spring. The presence of two distinct sequence haplotypes across the *Lr49* region in the susceptible parent W711 and only one in the resistant parent VL404 suggested further localized structural variation between the parental lines (**Figure 4**). This structural variation is likely to explain the difficulty encountered for developing scorable KASP markers for polymorphism identified from the parental flow sorted chromosome sequence. KASP markers that assay multiple loci exhibit cluster compression due to the increase in allele dosage, and therefore are more difficult to score compared to a KASP marker that assays only a single locus. Cluster compression is expected for KASP markers that assay a duplicated genomic region. The presence of extensive local structural variation between wheat cultivars has been previously reported (Montenegro et al., 2017; Clavijo et al., 2017).

It is unclear whether the presence of only one haplotype for the *Lr49* region in VL404 represents a structural deletion, or the presence of a chromosomal segment that is sufficiently diverged at the nucleotide level such that paired-end reads from this region in VL404 could not be aligned to the assembled genome sequence of Chinese Spring. As Chinese Spring does not carry *Lr49*, it is likely that VL404 carries a resistance gene absent in Chinese Spring. This scenario is possible since VL404 was derived through crosses involving durum wheat. We are currently using various sequencing technologies including Nextera mate-pair sequencing and Dovetail Genomics scaffolding technology (Thind et al., 2017) to *de novo* assemble the *Lr49* region for VL404 and WL711, which will elucidate the physical structure and help to clone *Lr49* and develop a diagnostic marker for use in breeding.

Marker *sunKASP_21* showed the strongest association with *Lr49* when tested on a diverse set of 75 Australian and 90 European cultivars, which were unlikely to carry *Lr49*. The marker amplified the VL404 allele in only three genotypes (Gazelle, JO 8023 and Safir) and the non-*Lr49* associated alleles in the remaining 162 genotypes. This result was supported by the major SNP haplotypes for the *Lr49* region revealed by the 890 globally diverse exome sequenced accessions, which showed evidence for two historical recombination sites distal to *sunKASP_21* (**Figure 2**). The combination of these two pieces of evidence suggests that *sunKASP_21* can be used for marker assisted deployment of *Lr49* in breeding programs.

In conclusion, our study has demonstrated application of the assembled reference genome sequence for cultivar Chinese Spring and the flow-sorted chromosome sequences of the parental lines to accelerate fine-mapping of trait loci in common wheat. Our results also highlight the challenge for cloning *Lr49* caused by the presence of structural variation in the parental lines of the mapping population, relative to Chinese Spring, and the importance of being able to assemble such regions to enable the cloning of causal genes and development of diagnostic markers for use in breeding.

DATA AVAILABILITY STATEMENT

The SNP data used in the study were previously generated and can be found in the European Nucleotide Archive using accession number ERZ805275 (https://www.ebi.ac.uk/ena/data/view/ERZ805275).

AUTHOR CONTRIBUTIONS

VN conducted initial mapping of KASP markers and drafted the manuscript. DB developed high resolution population and tested

flanking markers on it. MV and JD sorted chromosome 4B from parental lines and conducted sequencing. NQ mapped markers developed from the flow sorted chromosomes. PK, KF, and MH aligned flow sorted chromosome sequences with the reference sequence. UB developed KASP and *sunKASP* markers. PK, MH, UB, and HB edited the manuscript. UB and HB provided overall supervision. All authors read the manuscript.

FUNDING

VN was funded by Australia Awards and the Ugandan Government. UB, HB, PK, KF and MH were funded through research grants from the Grains Research & Development Corporation (GRDC) Australia. MV and JD were supported by the ERDF project "Plants as a tool for sustainable global development" (No. CZ.02.1.01/0.0/0.0/16_019/0000827).

ACKNOWLEDGMENTS

The authors thank Dr. Jan Vrána for chromosome sorting and Zdeňka Dubská and Romana Šperková for technical assistance.

SUPPLEMENTARY MATERIAL

The Supplementary Material for this article can be found online at: https://www.frontiersin.org/articles/10.3389/fpls.2019.01787/full#supplementary-material

REFERENCES

Appels, R., Eversole, K., Feuillet, C., Keller, B., Rogers, J., Stein, N., et al. (2018). Shifting the limits in wheat research and breeding using a fully annotated reference genome. *Science* 361, 661. doi: 10.1126/science.aar7191

Avni, R., Nave, M., Barad, O., Baruch, K., Twardziok, S. O., Gundlach, H., et al. (2017). Wild emmer genome architecture and diversity elucidate wheat evolution and domestication. *Science* 357, 93–97. doi: 10.1126/science.aan0032

Bansal, U. K., Hayden, M. J., Venkata, B. P., Khanna, R., Saini, R. G., and Bariana, H. S. (2008). Genetic mapping of adult plant leaf rust resistance genes *Lr48* and *Lr49* in common wheat. *Theor. Appl. Genet.* 117, 307–312. doi: 10.1007/s00122-008-0775-6

Bansal, U. K., Kazi, A. G., Singh, B., Hare, R. A., and Bariana, H. S. (2014a). Mapping of durable stripe rust resistance in a durum wheat cultivar Wollaroi. *Mol. Breed* 33, 51 – 59. doi: 10.1007/s11032-013-9933-x

Bansal, U. K., Wicker, T., Keller, B., Hayden, M., and Bariana, H. S. (2014b). Molecular mapping of an adult plant stem rust resistance gene *Sr56* in winter wheat cultivar Arina. *Theor. Appl. Genet.* 127, 1441–1448. doi: 10.1007/s00122-014-2311-1

Bariana, H. S., and Bansal, U. K. (2017). "Breeding for disease Resistance," in *Encyclopedia of applied plant sciences*, vol. 3 . Eds. B. Kole, G. B. Murray and J. D. Murphy (Waltham, MA: Academic Press), 69–76.

Bariana, H. S., Brown, G. N., Bansal, U. K., Miah, H., Standen, G. E., and Lu, M. (2007). Breeding for triple rust resistance wheat cultivars for Australia using conventional and marker assisted selection technologies. *Aust. J. Agric. Res.* 58, 576–587. doi: 10.1071/AR07124

Bariana, H., Bansal, U., Basandrai, D., and Chhetri, M. (2013). "Disease Resistance," in *Genomics and breeding for climate-resilient crops Vol. 2 Target Traits*. Ed. C. Kole (Berlin, Germany: Springer-Verlag), 291–314.

Bariana, H. S. (2003). "Breeding for disease resistance," in Encyclopedia of applied plant sciences. Eds. B. Thomas, D. J. Murphy and B. G. Murray (UK: AcademicPress, Harcourt), 244–253.

Borlaug, N. E. (2007). Sixty-two years of fighting hunger: personal recollections. *Euphytica* 157, 287–297. doi: 10.1007/s10681-007-9480-9

Clavijo, B. J., Venturini, L., Schudoma, C., Accinelli, G. G., Kaithakottil, G., Wright, J., et al. (2017). An improved assembly and annotation of the allohexaploid wheat genome identifies complete families of agronomic genes and provides genomic evidence for chromosomal translocations. *Genome Res.* 27, 885–896. doi: 10.1101/gr.217117.116

Cruz, V. M., Kilian, A., and Dierig, D. A. (2013). Development of DArT marker platforms and genetic diversity assessment of the US collection of the new oilseed crop lesquerella and related species. *PLoS ONE* 8, e64062. doi: 10.1371/journal.pone.0064062

Doležel J, Kubaláková M, Paux, E., Bartoš, J., and Feuillet, C. (2007). Chromosome-based genomics in the cereals. *Chromosome Res.* 15, 51–66. doi: 10.1007/s10577-006-1106-x

Doležel J, Vrána J, Šafář, J., Bartoš, J., Kubaláková, M., and Šimková, H. (2012). Chromosomes in the flow to simplify genome analysis. *Funct. Integr. Genomics* 12, 397–416. doi: 10.1007/s10142-012-0293-0

Dubcovsky, J., and Dvorak, J. (2007). Genome plasticity a key factor in the success of polyploid wheat under domestication. *Science* 316, 1862–1866. doi: 10.1126/science.1143986

Dyck, P. L. (1979). Identification of the gene for adult-plant leaf rust resistance in Thatcher. *Can J. Plant Sci.* 59, 499–501.

Forster, B. P., Till, B. J., Gharim, A. M. A., Huynh, H. O. A., Burstmayr, H., and Caligari, P. D. S. (2015). Accelerated plant breeding. *CAB Rev.* 43, 1749–8848. doi: 10.1079/PAVSNNR20149043

Giorgi, D., Farina, A., Grosso, V., Gennaro, A., Ceoloni, C., and Lucretti, S. (2013). FISHIS: fluorescence *in situ* hybridization in suspension and chromosome flow sorting made easy. *PLoS One* 8, e57994. doi: 10.1371/journal.pone.0057994

He, F., Pasam, R., Shi, F., Kant, S., Keeble-Gagnere, G., Kay, P., et al. (2019). Exome sequencing highlights the role of wild-relative introgression in shaping the adaptive landscape of the wheat genome. *Nat. Genet.* 51, 896–904. doi: 10.1038/s41588-019-0382-2

Herrera-Foessel, S. A., Singh, R. P., Huerta-Espino, J., Rosewarne, G. M., Periyannan, S. K., Viccars, L., et al. (2012). *Lr68*: a new gene conferring slow rusting resistance to leaf rust in wheat. *Theor. Appl. Genet.* 124, 1475–1486. doi: 10.1007/s00122-012-1802-1

Herrera-Fossel, S. A., Lagudah, E. S., Huerta-Espino, J., Hayden, M. J., Bariana, H. S., Singh, D., et al. (2011). New slow-rusting leaf rust and stripe rust resistance genes *Lr67* and *Yr46* in wheat are pleiotropic or closely linked. *Theor. Appl. Genet.* 122, 239–249. doi: 10.1007/s00122-010-1439-x

Hiebert, C. W., Thomas, J. B., McCallum, B. D., Humphreys, D. G., DePauw, R. M., Hayden, M. J., et al. (2010). An introgression on wheat chromosome 4DL in RL6077 (Thatcher*6 / PI 250413) confers adult plant resistance to stripe rust and leaf rust (Lr67). *Theor. Appl. Genet.* 121, 1083–1091. doi: 10.1007/s00122-010-1373-y

International Wheat Genome Sequencing Consortium (IWGSC). (2014). A chromosome-based draft sequence of the hexaploid bread wheat (*Triticum aestivum*). *Science* 345, 6194. doi: 10.1126/science.1251788

Keeble-Gagnère, G., Isdale, D., Suchecki, R., Kruger, A., Lomas, K., Carroll, D., et al. (2019). Integrating past, present and future wheat research with Pretzel. *bioRxiv*. 4. doi: 10.1101/517953

Kolmer, J. A. (2005). Tracking wheat rust on a continental scale. *Curr. Opin. Plant Biol.* 8, 441–449. doi: 10.1016/j.pbi.2005.05.001

Kosambi, D. D. (1943). The estimation of map distances from recombination values. *Ann Eugen.* 12, 172–175. doi: 10.1111/j.1469-1809.1943.tb02321.x

Kubaláková, M., Macas, J., and Doležel, J. (1997). Mapping of repeated DNA sequences in plant chromosomes by PRINS and C-PRINS. *Theor. Appl. Genet.* 94, 758–763. doi: 10.1007/s001220050475

Kubaláková, M., Vrána, J., Čihalíková, J., Šimková, H., and Doležel, J. (2002). Flow Karyotyping and chromosome sorting in bread wheat (*Triticum aestivum* L.). *Theor. Appl. Genet.* 104, 1362–1372. doi: 10.1007/s00122-002-0888-2

Manly, K. F., Cudmore, RHJr, and Meer, J. M. (2001). Map Manager QTX, cross-platform software for genetic mapping. *Mamm. Genome* 12, 930–932. doi: 10.1007/s00335-001-1016-3

McIntosh, R. A., Park, R. F., and Wellings, C. R. (1995). *Wheat Rusts: An Atlas of Resistance Genes* (East Melbourne, Australia: CSIRO Publications).

McIntosh, R. A., Dubcovsky, J., Rogers, J. W., Morris, C., Appels, R., and Xia, C. X. (2013). Catalogue of gene symbols for wheat: 2013-2014 supplement. *KOMUGI Integr. Wheat Sci. Database*. Available online at http://www.shigen.nig.ac.jp/wheat/komugi/genes/symbolClassList.jsp (Accessed on 15 August 2015).

Montenegro, J. D., Golicz, A. A., Bayer, P. E., Hurgobin, B., Lee, H., Chan, C. K., et al. (2017). The pangenome of hexaploid bread wheat. *Plant J.* 90, 1007–1013. doi: 10.1111/tpj.13515

Saini, R. G., Kaur, M., Singh, B., Sharma, S., Nanda, G. S., Nayar, S. K., et al. (2002). Lr48 and Lr49, novel hypersensitive adult plant leaf rust resistance genes in wheat (Triticum aestivum L.). *Euphytica* 124, 365–370. doi: 10.1023/A:1015762812907

Singh, R. P., Mujeebkazi, A., and Huerta-Espino, J. (1998). Lr46: a gene conferring slow rusting resistance to leaf rust in wheat. *Phytopathology* 88, 890–894. doi: 10.1094/PHYTO.1998.88.9.890

Singh, R. P. (1992). Association between gene *Lr34* for leaf rust resistance and leaf tip necrosis in wheat. *Crop Sci.* 32, 874–878. doi: 10.2135/cropsci1992.0011183X003200040008x

Singla, J., Lüthi, L., Wicker, T., Bansal, U., Krattinger, S. G., and Keller, B. (2017). Characterization of Lr75: a partial, broad-spectrum leaf rust resistance gene in wheat. *Theor. Appl. Genet.* 130, 1–12. doi: 10.1007/s00122-016-2784-1

Šimková, H., Svensson, J. T., Condamine, P., Hřibová, E., Suchánková, P., Bhat, P. R., et al. (2008). Coupling amplified DNA from flow-sorted chromosomes to high-density SNP mapping in barley. *BMC Genomics* 9, 294. doi: 10.1186/1471-2164-9-294

Thind, A. K., Wicker, T., Šimková, H., Fossati, D., Moullet, O., Brabant, C., et al. (2017). Rapid cloning of genes in hexaploid wheat using cultivar-specific long-range chromosome assembly. *Nat. Biotechnol.* 35, 793–796. doi: 10.1038/nbt.3877

Voorrips, R. E. (2002). MapChart: software for the graphical presentation of linkage maps and QTLs. *J. Hered* 93, 77–78. doi: 10.1093/jhered/93.1.77

Vrána, J., Kubaláková, M., Šimková, H., Číhalíková, J., Lysák, M. A., and Doležel, J. (2000). Flow-sorting of mitotic chromosomes in common wheat (*Triticum aestivum* L.). *Genetics* 156, 2033–2041.

Vrána, J., Šimková, H., Kubaláková, M., Číhalíková, J., and Doležel, J. (2012). Flow cytometric chromosome sorting in plants: the next generation. *Methods* 57, 331–337. doi: 10.1016/j.ymeth.2012.03.006

Wang, S., Wong, D., Forrest, K., Allen, A., Chao, S., Huang, B. E., et al. (2014). Characterization of polyploid wheat genomic diversity using a high-density 90,000 single nucleotide polymorphism array. *Plant Biotechnol J.* 12, 787–796. doi: 10.1111/pbi.12183

Conflict of Interest: The authors declare that the research was conducted in the absence of any commercial or financial relationships that could be construed as a potential conflict of interest.

Chapter 4

Molecular mapping of all stage stripe rust resistance in Indian wheat cultivar VL404

4.1 Introduction

Wheat stripe rust caused by *P. striiformis* f. sp. *tritici* Erikss. (*Pst*) can incur serious production losses under favourable weather conditions (Chen 2014; Juliana et al. 2018). Cultivation of stripe rust resistant wheat cultivars and application of fungicides are two common means of control of this disease. Continued fungicidal application has the potential risk of build-up of chemical tolerance in pathogens and hazardous effects on living organisms (Bariana et al. 2007a; Chen 2014). Growing of rust resistant cultivars has demonstrated its advantages in terms of reduced cost of disease control and environmental safety. Two types of rust resistance genes namely, seedling resistance or all-stage resistance (ASR) and adult plant resistance (APR), have been characterised from modern cultivars, landraces, synthetic wheats and tetraploid wheats (Bariana and Bansal 2017).

Evolution in pathogen populations has historically been known to render ASR genes ineffective (Bariana et al. 2007a). Cuddy and Hollaway (2018) confirmed the prevalence of *Pst* pathotypes virulent on *YrA*, *Yr2*, *Yr6*, *Yr7*, *Yr8*, *Yr9*, *Yr17*, and *Yr25* using 19 single-gene stripe rust differentials. A new *Pst* pathotype, 239 E237A-Yr17+Yr33+, carrying virulence for stripe rust resistance gene *Yr33* was identified (Park et al. 2020). This pathotype is also virulent on *Yr57*, *Yr63*, *Yr72* and *Yr75* (Bariana and Bansal unpublished results). Wan and Chen (2014) confirmed the presence of 41 *Pst* pathotypes among 348 *Pst* samples collected across the United States. A high frequency of virulence was observed for *YrTr1*, *YrExp2*, *Yr6*, *Yr7*, *Yr8*, *Yr9*, *Yr17*, *Yr27*, *Yr43*, and *Yr44*. The prevalence of virulence on *Yr10*, *Yr24*, *Yr32* and *YrSP* was rare (Wan and Chen 2014).

Eighty-three stripe rust resistance genes have been permanently named from common wheat and its relatives and 47 are temporarily named (Maccaferri et al. 2015; McIntosh et al. 2017; Li et al. 2020). Genotyping platforms DArTseq (www.diversityarrays.com), genotyping by sequencing (Poland and Rife 2012) and SNP arrays including 90K (Wang et al. 2014), 820K (Winfield et al. 2015), 35K (Allen et al. 2017) and 660K (Cui et al. 2017) have been used for selective genotyping (Lebowitz et al. 1987), Bulked segregant analysis (Michelmore et al. 1991) and whole population genotyping to determine genomic locations of economic traits including rust resistance (Kandiah et al. 2019). Molecular mapping of ASR genes *Yr47* (Bansal et al. 2011), *Yr51* (Randhawa et al. 2014), *Yr57* (Randhawa et al. 2015) and *Yr82* (Kandiah et al. 2019) was performed using these genomic technologies. A new Illumina 40K XT-chip was designed using exon-based SNPs from a 90K array and named targeted genotyping by sequencing (tGBS) (www.latrobe.edu.au/agribio). It also includes gene-linked markers.

An Indian wheat cultivar VL404 [Kentana/Bungulla//Frontana/General-Urquiza/3/ST464 (durum)/PI74106 (durum)] expressed high levels of stripe rust resistance against all Australian pathotypes at seedling and adult plant stages. The present study was aimed to understand the genetic basis of all stage stripe rust resistance in VL404.

4.2 Materials and methods

4.2.1 Development of mapping population

A cross was made between cultivar VL404 and stripe rust susceptible line Avocet 'S' (AvS). One hundred F_2 seeds form a single VL404/AvS F_1 plant progeny were grown and harvested individually to produce the F_3 population. This population was enhanced to the F_6 generation of 94 recombinant inbred lines (RILs) following the single seed descent (SSD) method (Allard 1999).

4.2.2 Greenhouse screening

Ninety-four VL404/AvS F_6 RILs along with parents were tested against three *Pst* pathotypes 134 E16A+Yr17+Yr27+ (virulent on *Yr2, Yr6, Yr7, Yr8, Yr9, Yr17, Yr27*), 110 E+143A+ (virulent on *Yr2, Yr3, Yr4, Yr6, Yr7, Yr34, YrA*) and 239 E237A-Yr17+Yr33+ (virulent on *Yr1, Yr2, Yr3, Yr4, Yr6, Yr7, Yr9, Yr17, Yr25, Yr32, Yr33, Yr57, Yr63, Yr72, Yr75, YrND, YrS92/O, YrSP*). Eight to 10 seeds of each RIL along with parents were sown in 9 cm diameter plastic pots as four lines per pot in a clockwise manner. Twenty grams of aquasol, fertiliser, was dissolved in 10 l of tap water and applied to 100 pots before sowing. Pots were kept at 17°C in a microclimate room ideal for seedling growth under dark condition. Urea was applied at 20 gm per 10 l of water at a weekly interval. The rust screening procedure and 0-4 disease scale outlined in McIntosh et al. (1995) was used. After 14 days of inoculation, RILs expressing infection types (ITs) below 3+ were considered resistant and RILs showing IT 3+ or above were considered susceptible (McIntosh et al. 1995).

4.2.3 DNA extraction

The genomic DNA of the RILs and parents (VL404 and AvS) was extracted from young leaf tissue (10-day old seedlings) following the modified cetyl trimethyl ammonium bromide (CTAB) method (Doyle and Doyle 1987; Bansal et al. 2014a). The quality of DNA samples was checked on 1% agarose gel. The quantity of the DNA samples was measured using a NanoDrop ND-1000 spectrophotometer (Nanodrop Technologies, Wilmington, USA) considering A260/A280 ratio between 1.8-2.0.

4.2.4 Genotyping using 40K XT-chip technology

Genomic DNA of the VL404/AvS RIL population and parents were diluted to 300 ng/µl and genotyped using the 40K XT-chip technology at AgriBio, Bundoora, Australia. A preliminary genetic linkage map aligning 40K SNPs using pairwise LOD (Logarithm of odds) score 6 was generated using ASMap package and Kosambi mapping function in the R program (Taylor and Butler 2017). Genetic map was constructed after removal of SNPs expressing segregation distortion, high crossover and low call rate. SNP markers showing Mendelian inheritance among the RIL population were integrated into the genetic map.

4.2.5 Statistical analysis

Chi-squared test was performed to check the goodness of fit of observed segregation versus expected genetic ratios among RILs for stripe rust response variation. A linkage map for seedling stripe rust resistance gene was constructed using Map Manager QTX version 20 and Kosambi mapping function at $P = 0.05$ (Kosambi 1943; Manly et al. 2001). The genetic and physical maps were drawn using MapChart version 2.3 (Voorrips 2002) and Pretzel (https://plantinformatics.io; Keeble-Gagnère et al. 2019), respectively.

4.3 Results

4.3.1 Assessment of seedling stripe rust response

VL404 produced a low infection type (IT 0;) and AvS was scored susceptible (IT 3+) against *Pst* pathotypes 239 E237A-Yr17+Yr33+, 134 E16A+Yr17+Yr27+ and 110 E+143A+. The response of homozygous resistant lines against these pathotypes varied from IT 0C to 2C and homozygous susceptible lines expressed ITs 33+ to 3+. Single gene segregation was evident among the VL404/AvS RIL population [54*YrVL YrVL*: 40 *yrVL yrVL*; $\chi^2_{(1:1)} = 0.14$, non-significant at $P = 0.05$ and 1 *d. f.*]. This locus was temporarily named *YrVL*.

4.3.2 Construction of the genetic linkage map

The preliminary genetic linkage map of 40K tGBS assay included 5,491 SNPs. A set of 2,148 markers that showed Mendelian inheritance and had high call rates were used for construction of the final map. The average number of markers per chromosome was 102.2. In term of marker coverage, the 'B' genome was a major contributor (51.5%) followed by the 'A' genome (43.5%). The contribution of 'D' genome was comparatively low (6.01%) (Fig. 4.1). The largest chromosome was 7A (252.2 cM) and smallest chromosome was 4D (14.23 cM). The average distance of markers per cM across the wheat genome was 0.74.

4.3.3 Molecular mapping of *YrVL*

The resistant and susceptible phenotypes of RILs were converted into genotypes A and B,

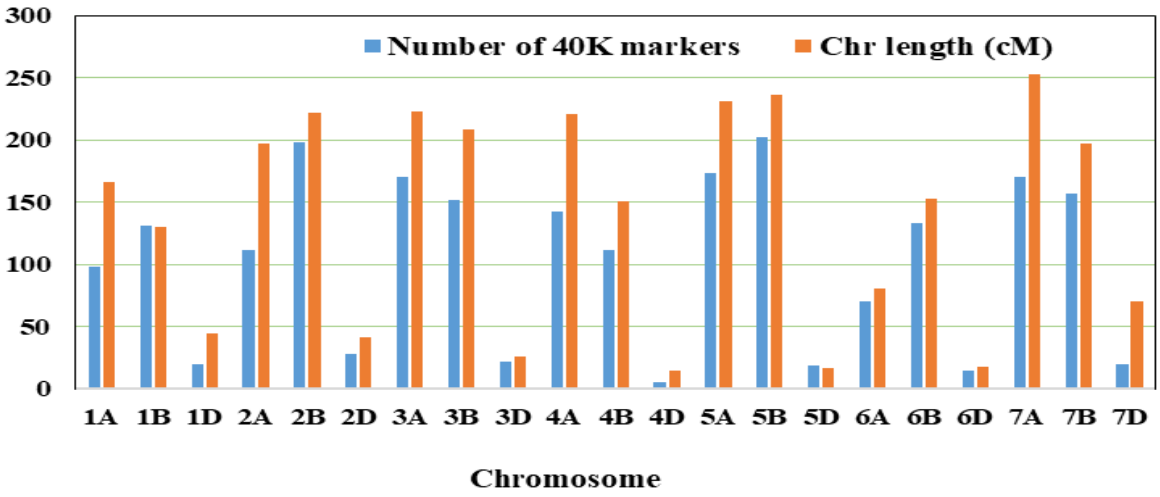

Fig. 4.1 Distribution of 40K SNPs across 21 chromosomes of wheat genome

respectively, and data were incorporated into the 40K genetic map. *YrVL* was mapped to the long arm of chromosome 2B and was flanked by co-segregating markers *AVRIG20667* and *AVRIG36406* on the proximal end (8.6 cM) and *AVRIG36280* at the distal end (3.8 cM). (Fig. 4.2A).

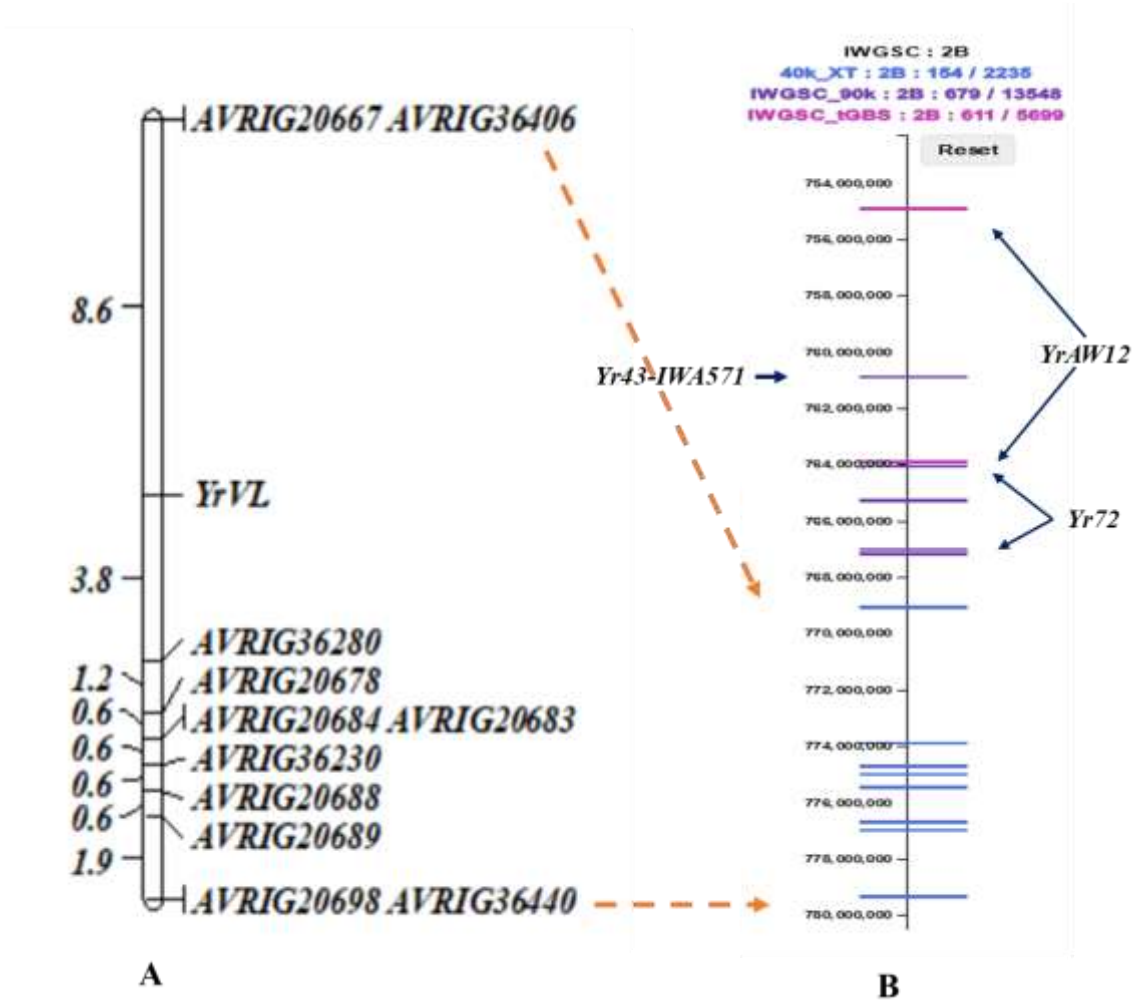

Fig. 4.2 Genetic linkage map of chromosome 2BL: A) *YrVL* of VL404/AvS RIL population B) comparative location of *YrVL* and other known genes in the physical map

4.4 Discussion

Deployment of effective ASR and APR genes in wheat cultivars is a logical breeding approach to sustain global wheat production (Randhawa et al. 2015). The present study identified an ASR gene *YrVL* in wheat cultivar VL404. Flanking markers, *AVRIG20667* and *AVRIG36280*, placed this ASR on the long arm of chromosome 2B in the 769.08-779.3 Mb region (Fig. 4.2B; IWGSC RefSeq v 1.0). *Yr43* (Cheng and Chen 2010), *Yr44* (Cheng and Chen 2010), *Yr53* (Xu et al. 2013), *YrAW12* (a major gene presented in the next chapter that

maps in the 754.9–763.9 Mb region) and *Yr72* (Chhetri 2015) are located on chromosome 2BL. To confirm the uniqueness of identified ASR, locations of markers linked with *YrVL* and other genes located on 2BL were compared using a physical map in Pretzel (Fig. 4.2B). Linked markers for *Yr44* and *Yr53* (simple sequence repeat marker *wmc441*-598.1 Mb; Xu et al. 2013), *Yr5* (754.9 Mb; Marchal et al. 2018), *YrAW12* (754.9-763.9 Mb; reported in chapter 5), *Yr43 (IWA571*-760.8 Mb; www.wheat.pw.usda.gov) and *Yr72* (765.0-767.1 Mb; Chhetri 2015) were mapped in the 598.1-767.1 Mb region (Fig. 4.2B). Comparative data indicated that *Yr5*, *Yr43*, *Yr44*, *Yr53*, *YrAW12* and *Yr72* are located proximal to *YrVL*. *YrVL* appears to map closer to *Yr43*, *YrAW12* and *Yr72*. *YrAW12* and *Yr72* express similar resistance responses (ITs 23C to 3C) against *Pst* pathotypes 134 E16A+Yr17+Yr27+ and 110 E+143A, and susceptible reaction against pathotype 239 E237A-Yr17+Yr33+, whereas *YrVL* showed low IT (0;-2C) against all these pathotypes

Yr43 expresses consistent seedling response IT 2 on a 0-9 scale (1 on 0-4 scale) against 13 US *Pst* pathotypes (Cheng and Chen 2010). In contrast, seedling response of *YrVL* varies from 0; to 2C and is presumably due to the interaction with APR genes *Yr18* and *Yr29* present in VL404. Based on the pathogenicity, resistance reaction and physical position, *YrVL* appears to be a new locus.

In majority of cases, effective adult plant stripe rust resistance genes express additive gene action, and associated DNA marker data are equally effective as traditional field selection (McIntosh 2007). In addition to *YrVL*, VL404 also carries adult plant leaf rust resistance genes *Lr49* (discussed in Chapter 3), *Lr34*/*Yr18*/*Sr57* and *Lr46*/*Yr29*/*Sr58*. Incorporating this variety in the hybridisation program can accelerate the deployment of multiple rust resistance genes simultaneously in future wheat lines. This work is in progress

under the Australian Cereal Rust Control Program, Plant Breeding Institute, the University of Sydney.

Chapter 5

Genetic dissection of stripe rust resistance in a Tunisian wheat landrace Aus26670

5.1 Introduction

Puccinia striiformis Westend. f. sp. *tritici* Erikss. (*Pst*), the causal agent of wheat stripe rust, was listed among the top 10 fungal pathogens of plants (Dean et al. 2012). It is still prevalent in several wheat-producing countries and causes substantial production losses (Juliana et al. 2018). Yield losses vary with the initiation of infection at different developmental stages of the crop. The occurrence of stripe rust at the seedling stage can reduce wheat yield more than 60% (Juliana et al. 2018). Cultivation of stripe rust resistant cultivars have the potential to save around one billion AUD per annum in Australia (Murray and Brennan 2009).

Many studies reported QTL for stripe rust resistance; however, the uniqueness of these loci has often not been proved. Rosewarne et al. (2013) developed a consensus map that included 140 stripe rust resistance loci from 30 bi-parental mapping populations and these QTL represented 49 genomic regions of the wheat genome. A similar report by Maccaferri et al. (2015) developed an integrated map by incorporating 56 previously reported stripe rust resistance genes and 169 QTL from 10 association mapping studies. A physical map of Chinese Spring (a landrace) was released by the International Wheat Genomic Sequencing Consortium (IWGSC RefSeq v1.0; Appels et al. 2018) and the map viewing software, Pretzel was developed by Keeble-Gagnère et al. (2019) to align different classes of markers namely: SSRs, DArT-Seq, DArT-GBS, t-GBS and SNPs (https://plantinformatics.io). It enables comparisons of genomic locations of new rust resistance genes/marker trait associations (MTAs) identified in different studies.

Eighty-three loci conferring stripe rust resistance have been genetically characterised and catalogued using bi-parental mapping populations (McIntosh et al. 2017; Li et al. 2020). Unfortunately, several commercially deployed genes have succumbed to matching virulence against *Pst* pathotypes (Wellings 2007; Cuddy and Hollaway 2018). These events stress the need to identify new sources of stripe rust resistance. Landrace collections (Watkins and Vavilov) have been demonstrated as the reservoirs of uncharacterised rust resistance genes (Bansal et al. 2010; Daetwyler et al. 2014; Riaz et al. 2018). Several ASR genes for stripe rust resistance; *Yr47* (Qureshi et al. 2017), *Yr51* (Randhawa et al. 2014), *Yr57* (Randhawa et al. 2015), *Yr63* (Bariana and Bansal 2017), *Yr72* (Chhetri 2015), *Yr81* (Gessese et al. 2019), *Yr82* (Kandiah et al. 2019) and an APR gene *Yr80* (Nsabiyera et al. 2018) have been identified and formally named from the Watkins Collection. A Tunisian wheat landrace Aus26670 from the Watkins Collection showed moderately resistant adult plant stripe rust resistance in the field across several years. This study was planned to determine the genetic basis of stripe rust resistance in Aus26670.

5.2 Materials and methods

5.2.1 Development of mapping population

Aus26670 was procured from the Australian Winter Cereal Collection, Tamworth (currently Australian Grains Genebank, Horsham). A cross was made between Aus26670 and stripe rust susceptible line Avocet 'S' (AvS) and three F_1 plants were grown and individually harvested to produce F_2 populations. One hundred and fifty F_2 seeds from a single F_1 plant were planted 10 cm apart and harvested individually to generate a F_3 population. The population was advanced from the F_3 to F_7 generation through single seed descent (SSD) method (Allard 1999).

5.2.2 Greenhouse screening for seedling stripe rust resistance

One hundred twenty-three Aus26670/AvS F_7 recombinant inbred lines (RILs) and parents were tested against three *Pst* pathotypes 134 E16A+Yr17+Yr27+, 110 E+143A+ and 239 E237A-Yr17+Yr33+. Ten seeds of each RIL and parents were sown as four lines per pot in 9 cm diameter plastic pots filled with potting mixture that contained composted pine bark and coarse sand in 2:1 ratio. Twenty grams of Aquasol was dissolved in 10 L of tap water and applied to a set of 100 pots before sowing. Pots were kept at 17°C in a microclimate room for ideal seedling growth. Urea (20gm/10 L) was applied twice, one week after sowing and immediately after inoculation. Ten to 12-day old seedlings were inoculated with 2 mg of urediniospores of individual *Pst* pathotypes suspended in 10 mL of light mineral oil (IsoparL, Univar) using a hydrocarbon propellant atomizer. Inoculated seedlings were incubated in enclosed hoods filled with lukewarm water (to create humidity) at 9-11°C for 24 hours under dark condition. After incubation, seedlings were moved to a microclimate room maintained at 16-18°C. Seedling stripe rust response variation as infection type (IT) was assessed 14 to 16 days after inoculation using the 0 to 4 scale (McIntosh et al. 1995). The RILs expressing ITs below 3+ were considered resistant and those showing ITs 3+ or above were considered susceptible.

5.2.3 Field screening for adult plant stripe rust resistance

The Aus26670/AvS RIL population was sown in two replications as 30 cm rows during the first week of June (timely-sown; TS) in three consecutive years (2018 to 2020) and the first week of July (late-sown; LS) in 2019 at the Horse research unit (HRU), an experimental site of the University of Sydney Plant Breeding Institute, Cobbitty. A mixture of susceptible genotypes was sown as a border row covering the whole experimental area and as hill plots after a block of four experimental rows to facilitate epidemic development. The

experimental site was inoculated three times fortnightly starting from the 30-day old seedling stage using a mixture of *Pst* pathotypes 134 E16A+Yr17+Yr27+, 110 E+143A+ and 239 E237A-Yr17+Yr33+. Irrigation was performed twice a week to support good plant growth and rust development. Adult plant stripe rust response variation among RILs was scored on a 1-9 scale (Bariana et al. 2007b).

5.2.4 Correlation analysis

Pearson's correlation coefficients were calculated among mean stripe rust responses of Aus26670/AvS RILs tested across four environments (2018-TS, 2019-TS, 2019-LS and 2020-TS) using Genstat (version 18, VSN International, Hemel Hempstead, UK, 2015).

5.2.5 Genotyping using targeted genotyping by sequencing (tGBS)

Genomic DNA samples from the entire RIL population and parents (Aus26670 and AvS) were extracted from young (12 days old) leaf tissues according to Bansal et al. (2014a). The quality of DNA was checked on 1% agarose gels and quantified using the NanoDrop ND-1000 spectrophotometer (Nanodrop Technologies, Wilmington, USA). Genomic DNA (300 ng/µl) of all RILs and parents was genotyped using the tGBS assay at AgriBio, Bundoora, Australia. The tGBS assay reported co-dominant markers covering seven groups of the wheat chromosomes.

5.2.6 Genotyping with markers linked with rust resistance

KASP primers linked to *Yr29* (*SNP1Lr46G22*; Lagudah unpublished), *Yr18* linked marker *csLV34* (Lagudah et al. 2006), *Yr46* (*TM4*; Moore et al. 2015) and *Yr72* (*KASP12294, KASP1770, KASP11101* and *KASP6107*; Chhetri 2015) were used to determine the presence/absence of these loci.

KASP assays were performed following the protocol given in Nsabiyera et al. (2016). The end-point fluorescent images were detected with the CFX96 Touch™ real-time PCR detection system and allelic discrimination was analysed using Bio-rad CFX Manager Software (Bio-Rad Laboratories Pty. Ltd., USA).

5.2.7 Statistical analysis

Chi-squared tests were performed to check the goodness of fit of the observed seedling stripe rust response variation among RILs with the expected genetic ratio(s). The Wright's formula [$n = (GR)^2 / (4.27 \times \sigma 2g$] was used to estimate the number of loci governing stripe rust resistance in Aus26670/AvS RIL population at the adult plant stage, where n is the number of loci, GR is the genotypic range and $\sigma^2 g$ is the genetic variance (Wright 1968).

A linkage map was constructed using tGBS marker with ASMap function in R software (Taylor and Butler 2017). Genotypic data of known gene-linked markers were incorporated into the Aus26670/AvS linkage map. This linkage map was used to find the location of ASR genes using the Map Manager QTX version 20 (Manly et al. 2001) and Kosambi mapping function at $P = 0.05$ (Kosambi 1943). The map was drawn using MapChart version 2.3 (Voorrips 2002). Genotypic data from the tGBS linkage map and phenotypic data collected at the adult plant stage across years were exported to QTL Cartographer version 2.5 to detect marker-trait associations using composite interval mapping (CIM) function with 1,000 permutations and 2 cM walk speed (Wang et al. 2012). A physical map viewing software Pretzel (https://plantinformatics.io) was used to align markers linked with QTL identified in this study with previously reported QTL.

5.3 Results

5.3.1 Seedling screening

Aus26670 produced low infection types (IT 2C to 23C) and AvS was scored susceptible (IT 3+) against *Pst* pathotypes 134 E16A+Yr17+Yr27+ and 110 E+143A+. The responses of 123 RILs against both pathotypes varied from IT 23C to 3+. The involvement of a single ASR gene was observed [63 homozygous resistant: 60 homozygous susceptible; $\chi^2_{(1:1)}$ = 0.07, non-significant at $P = 0.05$ and 1 *d. f.*]. This locus was tentatively named *YrAW12*. Parents and RIL population showed susceptible responses against a recently identified *Pst* pathotype 239 E237A-Yr17+Yr33+.

5.3.2 Adult plant screening

Aus26670 showed moderately resistant response (4) and AvS produced susceptible response (8-9) on a 1-9 disease scale. Adult plant stripe rust responses of Aus26670/AvS RILs ranged from 3 to 9 across 2018 and 2019 experiments, whereas none of the RIL was scored 3 in 2020 (Fig. 5.1). A skewness towards resistance response was evident in 2018. The 2018 rust response data showed a significant positive correlation with 2019-TS (0.92**), 2019-LS (0.91**) and 2020-TS (0.88**). Similarly, 2019-TS data showed a strong correlation with 2019-LS (0.94**) and 2020-TS (0.91**) scores. Segregation at three to four stripe rust resistance loci among the Aus26670/AvS RIL population was estimated using the Wright's formula.

5.3.3 Genotyping with gene-linked markers

Stripe rust resistance gene *Yr72* that produced seedling stripe rust response similar to Aus26670 against three *Pst* pathotypes was mapped to chromosome 2BL in Aus27507/Aus27894-derived RIL populations (Chhetri 2015). Therefore, *Yr72*-linked

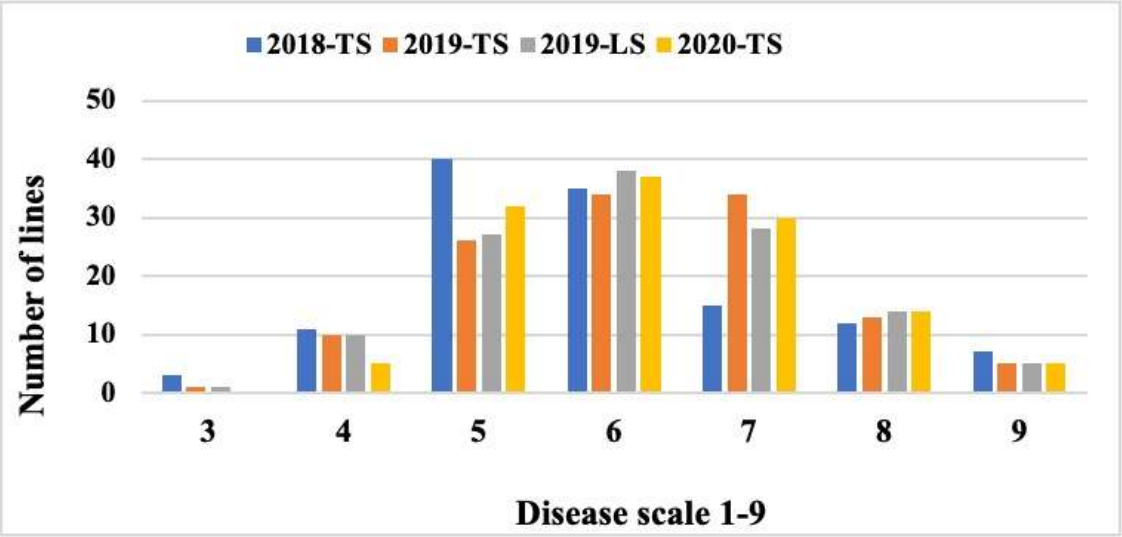

Fig. 5.1 Adult plant stripe rust response variation among Aus26670/AvS RILs when tested under field conditions in different crop seasons (TS: Timely sown and LS: Late sown)

markers (*KASP_1770*, *KASP_12294*, *KASP*_6107 and *KASP_11101*) were assayed on parents to test for polymorphism. Only one marker, *KASP_1770*, was polymorphic between parents. Seventy RILs carried the Aus266770 allele and 53 amplified the AvS allele [$\chi^2_{(1:1)}$ = 1.66, non-significant at *P = 0.05* and 1 *d.f.*].

The *Yr29*-linked allele (*SNP1Lr46G22*; A:A) was amplified when DNA template of Aus26670 was used, whereas AvS carried the alternate allele (G:G). These results indicated the presence of APR gene *Yr29* in Aus26670. Sixty RILs amplified the A:A allele and 63 RILs carried the G:G allele [$\chi^2_{(1:1)}$ = 0.07, non-significant at *P = 0.05* and 1 *d.f.*]. Genotyping with markers linked to APR genes *Yr18* and *Yr46* indicated the absence of these loci in Aus26670.

5.3.4 Construction of the genetic map

In total, 2,447 co-dominant tGBS markers were used to generate a genetic map of the Aus26670/AvS population. Distribution of tGBS markers among the A, B and D genomes

is given in Fig. 5.2. The average number of tGBS markers per chromosome was 116.52. The 'A' (~47%) and 'B' genomes (~43.4%) had a higher marker density compared to the 'D' genome (~10%). A uniform coverage of tGBS markers across telomeric ends and centromere regions was found on genome A and B. The genome D has comparatively big gaps between tGBS markers. The average distance of markers per cM across the wheat genome was 0.696. Genotypic data among Aus26670/AvS RILs for markers linked to *Yr29* and *Yr72* were also incorporated into the Aus26670/AvS genetic map.

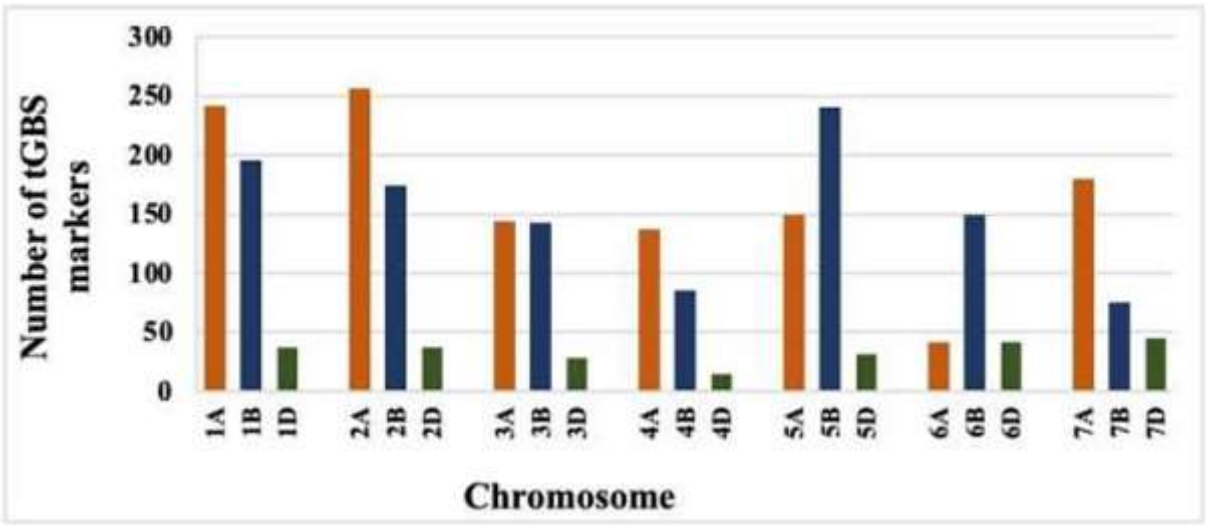

Fig. 5.2 Distribution of targeted genotyping by sequencing (tGBS) markers across the wheat genome

5.3.5 Molecular mapping of seedling stripe rust resistance gene *YrAW12*

The resistant and susceptible phenotypes of RILs were converted into genotypes A and B, respectively, and integrated into the Aus26670/AvS linkage map. *YrAW12* was flanked by tGBS markers *scaffold62231-5(TaGBSv2-1641_1443403)* (8.2 cM proximal) and *scaffold31324(TaGBSv2-1654_1377177)* (3.5cM distal) on the long arm of chromosome 2B and the *Yr72*-linked marker *KASP_1770* mapped 7.8 cM distal to *YrAW12* (Fig. 5.3).

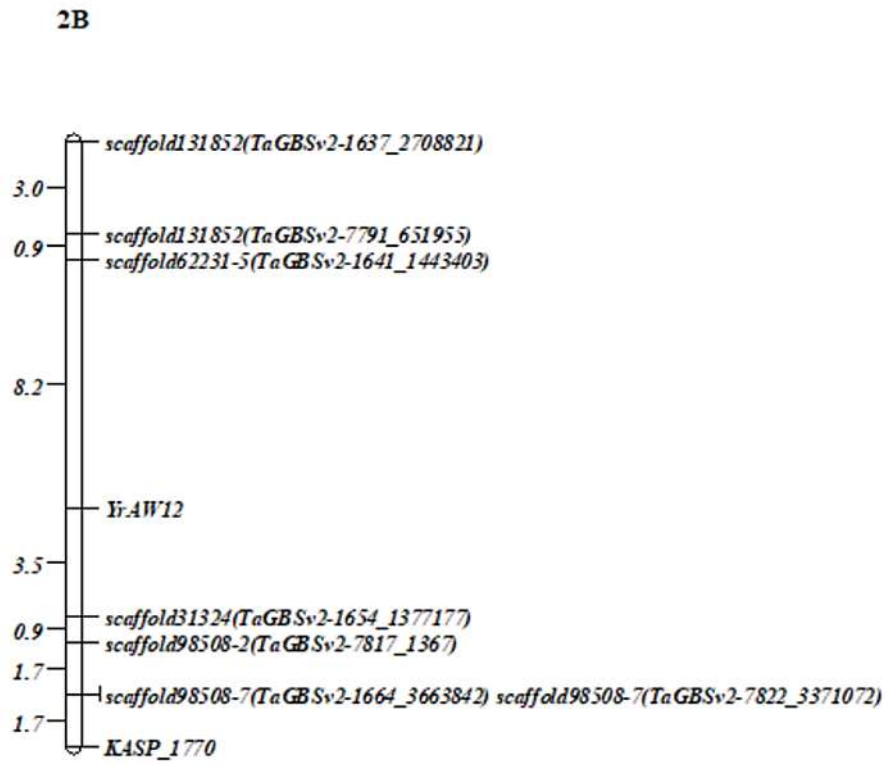

Fig. 5.3 Partial linkage map of Aus26670/AvS chromosome 2BL showing location of *YrAW12*

5.3.6 Quantitative trait loci (QTL) mapping

Composite interval mapping detected four QTL; *QYr.sun-1BL*, *QYr.sun-5AL*, *QYr.sun-5BL* and *QYr.sun-6DS* in the Aus26670/AvS RIL population (Table 5.1; Fig. 5.4). *QYr.sun-1BL* and *QYr.sun-5AL* were significant and consistent across three years. *QYr.sun-1BL* peaked at the *Yr29*-linked marker *SNP1Lr46G22* (206.8 cM; Table 5.1; Fig. 5.4). This QTL contributed 19.5-31.1% to stripe rust response variation across different data sets. *QYr.sun-5AL* spanned the 180.91-186.95 cM region and contributed 5.4-7.3% towards phenotypic variation. In 2019 and 2020, *QYr.sun*-5BL mapped in the 193.29 to 203.54 cM interval, whereas the position of this locus (159.7 cM) in 2018-TS was proximal (Fig. 5.4).

Table 5.1 Details of stripe rust resistance QTL detected in Aus26670/AvS RIL population

Environments	Chromosome	QTL	Peak marker	Genetic position (cM)	*Physical position (bp)	LOD	R^2 (%)
2018-TS	1B	*QYr.sun-1BL (Yr29)*	*SNP1Lr46G22*	206.80	670,274,064	10.62	31.1
	5A	*QYr.sun-5AL*	*scaffold6791(TaGBSv2-3828_19303153)*	184.13	654,562,705	3.35	7.3
	5B	*QYr.sun-5BL*	*scaffold58781(TaGBSv2-10179_2801517)*	159.70	537,708,940	3.49	7.7
	6D	*QYr.sun-6DS*	*scaffold47994(TaGBSv2-5067_305932)*	4.01	1,475,089	1.89^{ns}	3.8
2019-TS	1B	*QYr.sun-1BL (Yr29)*	*SNP1Lr46G22*	206.80	670,274,064	8.43	19.5
	5A	*QYr.sun-5AL*	*scaffold6791(TaGBSv2-3828_19303153)*	184.13	654,562,705	3.93	7.2
	5B	*QYr.sun-5BL*	*scaffold8785(TaGBSv2-4118_1393483)*	200.49	565,659,290	8.15	16.5
	6D	*QYr.sun-6DS*	*scaffold47994(TaGBSv2-5067_305932)*	4.01	1,475,089	2.9	5.3
2019-LS	1B	*QYr.sun-1BL (Yr29)*	*SNP1Lr46G22*	206.80	670,274,064	9.41	20.6
	5A	*QYr.sun-5AL*	*scaffold6791(TaGBSv2-3828_19303153)*	184.13	654,562,705	3.01	5.4
	5B	*QYr.sun-5BL*	*scaffold8785(TaGBSv2-4118_1393483)*	200.49	565,659,290	5.5	10.7
	6D	*QYr.sun-6DS*	*scaffold47994(TaGBSv2-5067_305932)*	4.01	1,475,089	3.75	7.1
2020-TS	1B	*QYr.sun-1BL (Yr29)*	*SNP1Lr46G22*	206.80	670,274,064	8.77	20.2
	5A	*QYr.sun-5AL*	*scaffold6791(TaGBSv2-3828_19303153)*	184.13	654,562,705	3	5.8
	5B	*QYr.sun-5BL*	*scaffold8785(TaGBSv2-4118_1393483)*	200.49	565,659,290	5.67	11.9
	6D	*QYr.sun-6DS*	*scaffold47994(TaGBSv2-5067_305932)*	4.01	1,475,089	2.62	4.5

*Physical position as per IWGSC RefSeq v1.0; **ns**: Non-significant. **TS**: Timely sown and **LS**: Late sown

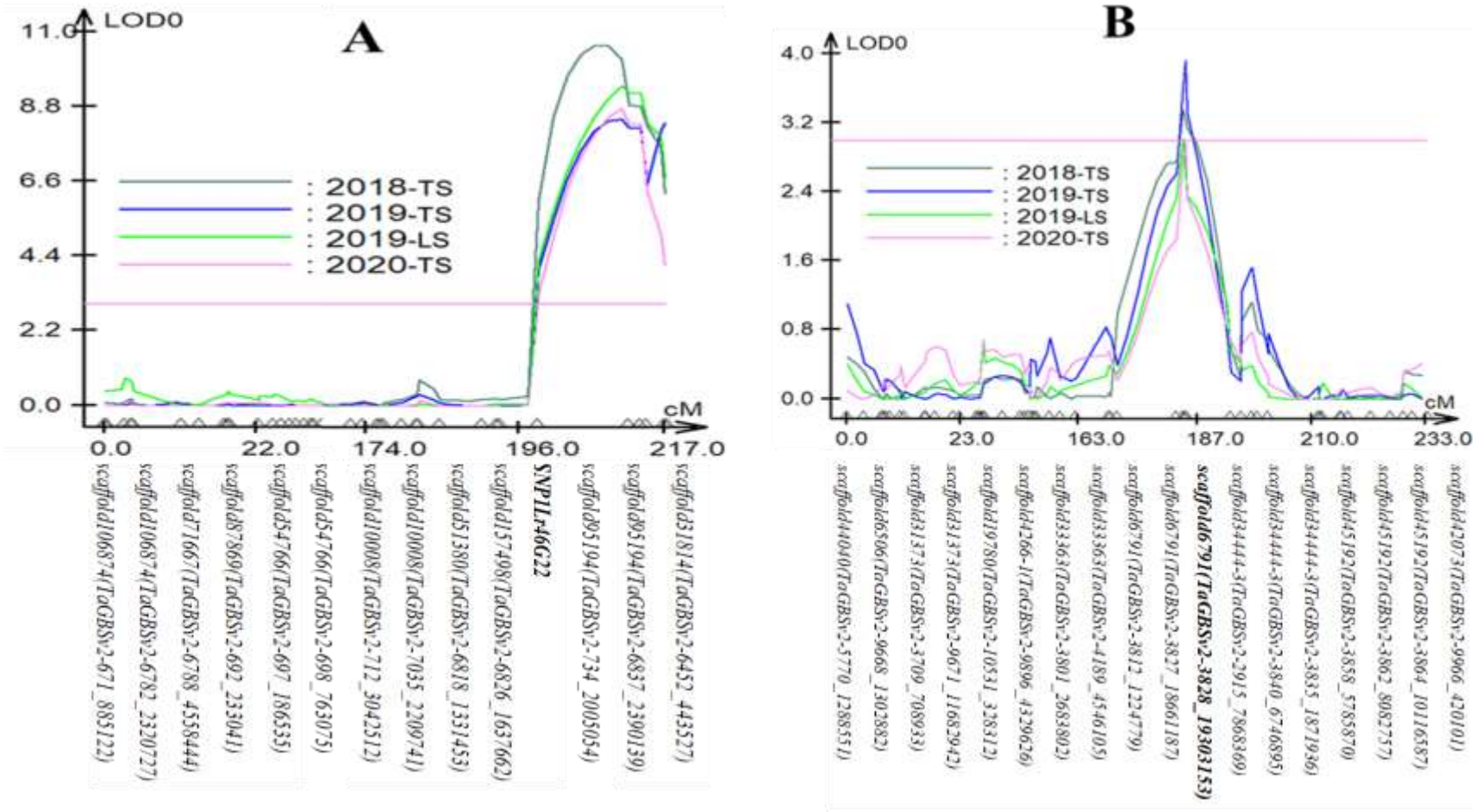
A
LOD0
11.0
8.8
6.6
4.4
2.2
0.0
: 2018-TS
: 2019-TS
: 2019-LS
: 2020-TS
cM
0.0
22.0
174.0
196.0
217.0
scaffold1006874(TaGBSv2-671_885122)
scaffold1006874(TaGBSv2-6782_2320727)
scaffold1006874(TaGBSv2-6788_4558444)
scaffold71667(TaGBSv2-692_233041)
scaffold87869(TaGBSv2-698_763075)
scaffold54766(TaGBSv2-697_186535)
scaffold54766(TaGBSv2-712_3042512)
scaffold10008(TaGBSv2-7035_2209741)
scaffold10008(TaGBSv2-6818_1331453)
scaffold51380(TaGBSv2-6826_1637662)
SNP1Lr46G22
scaffold157498(TaGBSv2-734_2005054)
scaffold95194(TaGBSv2-6837_2390139)
scaffold95194(TaGBSv2-6452_443527)
scaffold31814(TaGBSv2-5770_1288551)
B
LOD0
4.0
3.2
2.4
1.6
0.8
0.0
: 2018-TS
: 2019-TS
: 2019-LS
: 2020-TS
cM
0.0
23.0
163.0
187.0
210.0
233.0
scaffold44040(TaGBSv2-9668_1302882)
scaffold65506(TaGBSv2-9671_1168294)
scaffold31373(TaGBSv2-3709_708933)
scaffold19780(TaGBSv2-10531_328312)
scaffold42666-1(TaGBSv2-9896_4329626)
scaffold33363(TaGBSv2-3801_2683802)
scaffold33363(TaGBSv2-4189_4546105)
scaffold6791(TaGBSv2-3812_1224779)
scaffold6791(TaGBSv2-3827_1866187)
scaffold6791(TaGBSv2-3828_19303153)
scaffold34444-3(TaGBSv2-2915_7868369)
scaffold34444-3(TaGBSv2-3835_1871936)
scaffold34444-3(TaGBSv2-3840_6746895)
scaffold45192(TaGBSv2-3858_5755870)
scaffold45192(TaGBSv2-3862_8082757)
scaffold45192(TaGBSv2-3864_10116587)
scaffold44207-3(TaGBSv2-9966_420101)

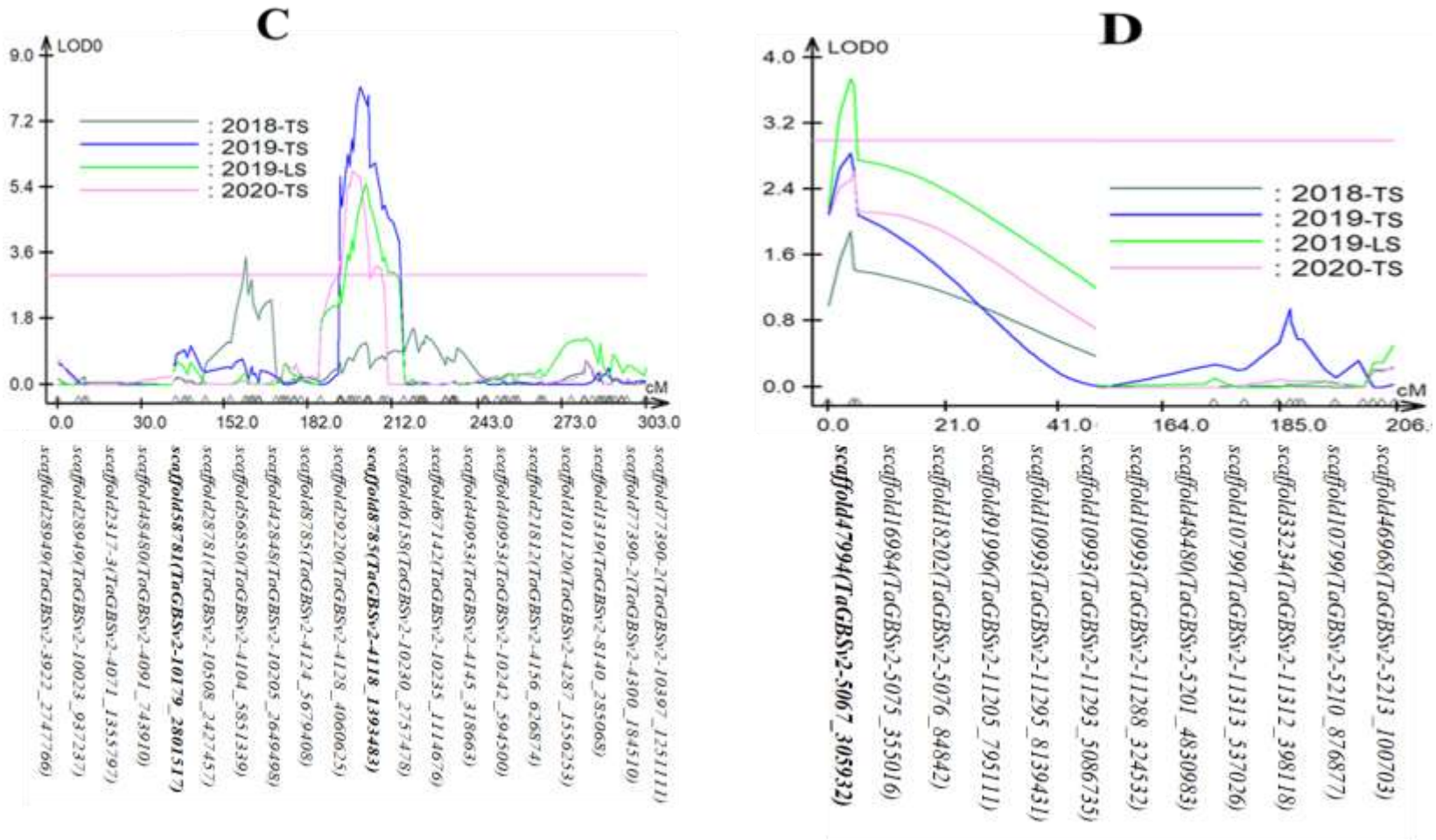

Fig. 5.4 Contours showing stripe rust resistance QTL on chromosome **A**) 1B (*QYr.sun-1BL/Yr29*), **B**) 5A (*QYr.sun-5AL*) **C**) 5B (*QYr.sun-5BL*) and **D**) 6D (*QYr.sun-6DS*) in Aus26670/AvS RIL population (TS: Timely sown and LS: Late sown) detected in present study

QYr.sun-5BL explained 7.7-16.5% variation in stripe rust response among Aus26670/AvS RILs. *QYr.sun-6DS* spanned across a 4.01-17.32 cM region and the LOD score was above 2.5 in the 2019 and 2020 crop seasons (Fig. 5.4). Contribution of *QYr.sun-6DS* in reducing disease severity (3.8-7.1%) was equivalent to *QYr.sun-5AL*. All QTL were contributed by Aus26670.

5.4 Discussion

Landraces have been a great source for genetic variation for disease resistance in crop plants and several new rust resistance loci were identified in the last decade (Bariana and Bansal 2017). Four QTL (*QYr.sun-1BL*, *QYr.sun-5AL*, *QYr.sun-5BL* and *QYr.sun-6DS*) for stripe rust resistance and one race-specific ASR gene *YrAW12* were identified in landrace Aus26670. Variations in stripe rust pressure across the studied environments resulted in a little skewness towards moderate susceptible and susceptible responses in 2019 and 2020.

YrAW12 is effective against Pst pathotypes 134 E16A+Yr17+Yr27+ and 110 E+143A+ and was mapped on the long arm of chromosome 2B in the 754.9–763.9 Mb region (IWGSC RefSeq v 1.0). A previously described ASR gene Yr72 was mapped in the 765.0–767.1 Mb region (Chhetri 2015). *YrAW12* and *Yr72* produce ITs of 23C to 3C and are ineffective against a recently detected Pst pathotype 239 E237A-Yr17+Yr33+. Based on the IT data and similar pathotypic specificity, we concluded *YrAW12* to be *Yr72*. Infection type 3C is difficult to score and hence slight variation in map locations of *YrAW12* and *Yr72* falls within limits of the standard error. A similar situation prevailed for the identities of *Yr34* and *Yr48* which was resolved by Qureshi et al. (2018). Failure to detect the *YrAW12* region in the QTL analysis in 2018 was surprising, when the *YrAW12*-avirulent pathotype was used. Development of an *YrAW12* near-isogenic line in an AvS background will allow better understanding of expression of resistance by this locus.

QYr.sun-1BL was concluded to be *Yr29* based on peaking of this QTL at the *Yr29*-linked marker *SNP1Lr46G22* (670.24 Mb). *QYr.sun-5AL* was detected on the long arm of chromosome 5A. Based on position of the peak marker *scaffold6791*(*TaGBSv2-3828_19303153*), it was placed at the 654.5 Mb position. Eight QTL namely: *QYr.ucw-5AL_PI610750/Yr48* (Lowe et al. 2011)*, QYr-5A_Opata85* (Boukhatem et al. 2002), *QYr.cim-5AL_Pastor* (Rosewarne et al. 2012)*, QYr.caas- 5AL.2_SHA3/CBRD* (Ren et al. 2012), *QYr.caas-5AL_Pingyuan 50* (Lan et al. 2010), *QYr.ucw-5A.1* (Maccaferri et al. 2015), *QYr.wsu-5A* (Bulli et al. 2016) and *QYr.hebau-5AL/QLr.hebau-5AL* (Zhang et al. 2019b) have been reported on this chromosome. Most of these QTL were detected among germplasm collections including worldwide collection, CIMMYT genetic stocks and synthetic-derived wheat or cultivars, except *QYr.caas-5AL_Pingyuan 50* (698.6 Mb), which was detected in a Chinese landrace and named *Yr48* (Lowe et al. 2011). *QYr.ucw-5A.1* (Maccaferri et al. 2015) and *QYr.wsu-5A,* (Bulli et al. 2016) overlap the *Yr48* region (Lan et al. 2010; Lowe et al. 2011; Ren et al. 2012). Qureshi et al. (2018) demonstrated that *Yr34* and *Yr48* are either allelic or the same and placed *Yr34/Yr48* at 697.9 Mb (*Excalibur_c46261_342*) on the physical map. QTL *QYr-5A_Opata85* and *QYr.cim-5AL_Pastor* were identified using RFLPs (Restricted fragment length polymorphisms; *Xfbb209* and *Xabg391*) by Boukhatem et al. (2002) and DArT markers (*wPt-0837* and *wPt-5231*) by Rosewarne et al. (2012), respectively. Information about the physical position of RFLP, SSR and DArT markers in the wheat genome is limited. To determine the uniqueness, an integrated map was developed by Maccaferri et al. (2015); in the current study, a software Pretzel was used to position the detected in this study and previously reported QTL in the physical map in order to demonstrate their uniqueness (Fig. 5.5). Four SNPs (*IWB35236, IWB6459, IWB59054* and *IWB9855*) and two SSRs (*wmc410* and *barc261*) covering 680.6-702.9Mb region were reported to be linked with *QYr.caas- 5AL.2_SHA3/CBRD* (Ren et al.

2012). A pleiotropic QTL, *QYr.hebau-5AL/QLr.hebau-5AL*, was mapped in the 578.2-580.4 Mb region (Zhang et al. 2019b). DArT markers *wPt-0837* and *wPt-5231*, and SSR markers *gwm179* and *wmc577* covered the *QYr-5A_Opata85* and *QYr.cim-5AL_Pastor* regions and are placed at the 664-671.3 Mb position. Comparison of the physical location of linked markers in the present study with published QTL, we concluded that *QYr.sun-5AL* is a new locus.

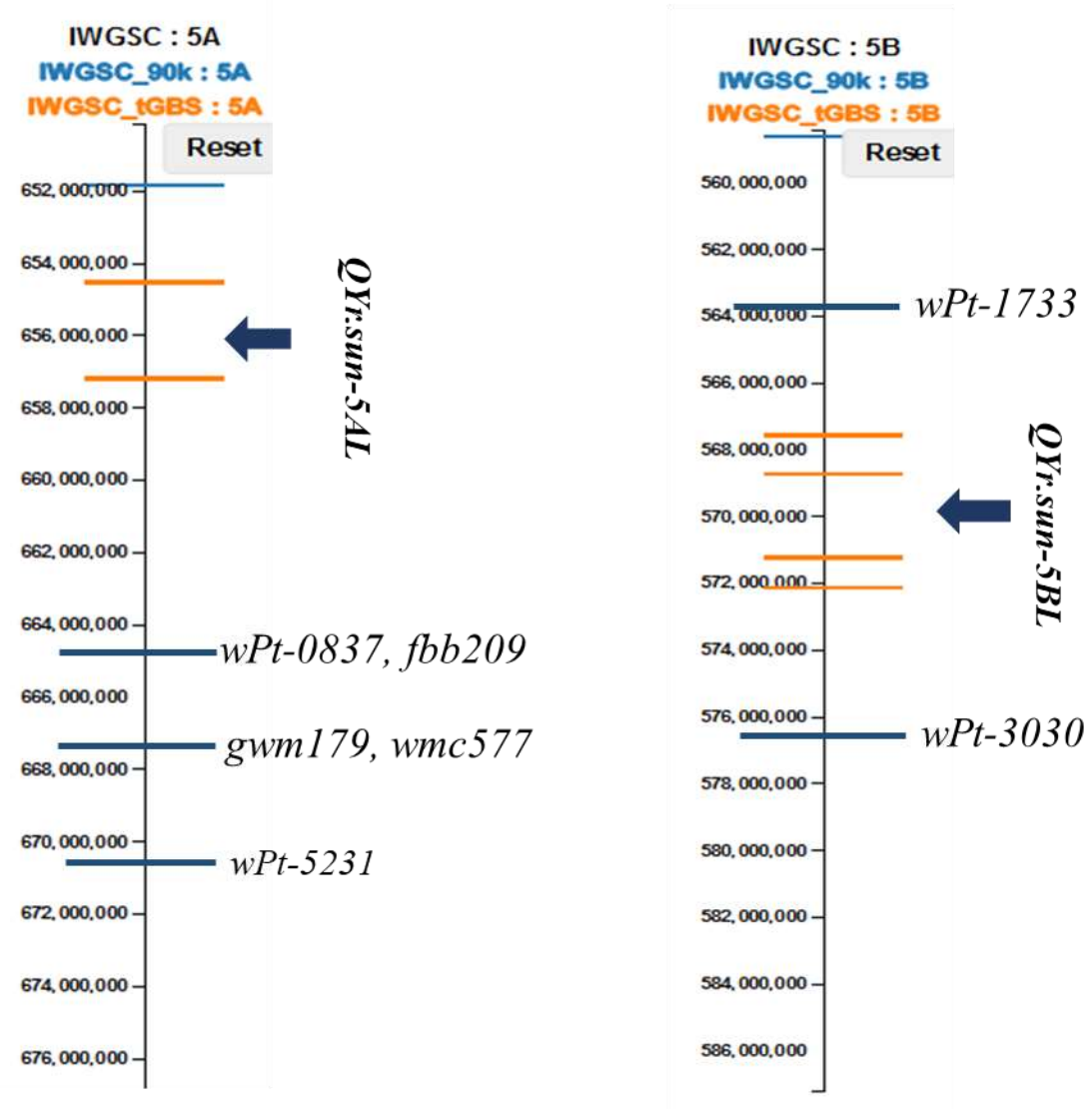

Fig. 5.5 Comparison of common SSR and DArT markers across genetic linkage maps in Pretzel; a genetic map viewing software (https://plantinformatics.io) showing positions of QTL **A)** *QYr.sun-5AL* (peak marker of this QTL was placed at 654.5 Mb and nearest known gene *Yr34/Yr48* was placed at 697.9-698.6 Mb; Qureshi et al. 2018) and **B)** *QYr.sun-5BL*

QYr.sun-5BL peak marker *scaffold8785 (TaGBSv2-4118_1393483)* was mapped at 565.6 Mb. Six QTL; *QYr.sun-5B_Janz* (Bariana et al. 2010), *QYr.tem-5B.2_Flinor* (Feng et al. 2011), *QYr.caas-5BL.2_Libellula* (Lu et al. 2009), *QYr.inra-5BL.2_CampRemy* (Mallard et al. 2005), *QYr.sun-5B_Wollaroi* (Bansal et al. 2014a) and *QYr.ui-5B_IDO444* (Chen et al. 2012) have been reported on the long arm of chromosome 5B. SSR and DArT markers linked with these QTL and their flanking SNPs adopted from the integrated map were assigned physical positions using Pretzel (Maccaferri et al. 2015). Marker *wPt-1733* (563.7 Mb) and *wPt-3030* (576.9 Mb) that flanked *QYr.sun-5B_Janz* mapped near the 565.5-574.2 Mb interval that carried *QYr.sun-5BL* identified in this study (Fig. 5.5). Therefore, *QYr.sun-5BL* and *QYr.sun-5B_Janz* could be the same QTL.

Two QTL namely *QYr.ufs-6D_Cappelle-Desprez* (42.4-56.1 cM; Agenbag et al. 2012), *QYr-6D_W-7984* (71.6-77.8 cM; Boukhatem et al. 2002) and an APR gene *Yr77* (SNP *IWA167*-105.53 Mb; McIntosh et al. 2017) have been reported on chromosome 6DS. *QYr.sun-6DS* was detected on chromosome 6DS through linked marker *scaffold47994 (TaGBSv2-5067_305932).* This marker was located at the 1.47 Mb position of the physical map and is distal to the previously located QTL on this chromosome, therefore, *QYr.sun-6DS* may represent a new locus. Less density of tGBS markers on D genome may have resulted in lower LOD score of this QTL.

Precise mapping of multiple QTL underpinning rust resistance has been fast-tracked through the availability of robust genotyping platforms. The deployment of these QTL in future wheat cultivars could act as a preventive measure to minimise losses incurred by the stripe rust pathogen (Bariana et al. 2016). QTL identified at significant levels consistently at least in two environments were considered stable and deserve further investigation (Agenbag et al. 2012). The present study demonstrated the utility of Pretzel and IWGSC

RefSeq v1.0 in aligning QTL detected in different studies. The tGBS assay demonstrated its scope in the detection of four stripe rust resistance QTL and an ASR gene in this investigation. The genomic regions carrying QTL *QYr.sun-5AL* and *QYr.sun-6DS* will be Mendelised and closely linked markers for these putatively new loci will be developed for marker assisted selection.

Chapter 6

Identification of genomic regions conferring rust resistance and mineral accumulation in a diverse wheat panel

6.1 Introduction

Three rust diseases of wheat include stripe rust caused by *Puccinia striiformis* f. sp. *tritici* (*Pst*), leaf rust caused by *P. triticina* (*Pt*) and stem rust caused by *P. graminis* f. sp. *tritici* (*Pgt*) (McIntosh et al. 1995). The rust pathogens can adapt to diverse environmental conditions and their virulence profiles may shift to cause rust epidemics worldwide (Singh et al. 2011). Breeding for rust resistance has been and remains a key criterion in wheat improvement programs in all nations and breeding for high concentrations of micronutrients was initiated in 1993 under the HarvestPlus program.

Wheat is an essential source of calories for one-fifth of the world's population. More than two billion people suffer from malnutrition due to inadequate intake of essential minerals, vitamins, and protein (WHO 2017). This problem is severe in pregnant women and children under the age of five (Stoecker et al. 2009). More than 400,000 children die from nutrient deficiencies annually (Black et al. 2013; Cakmak 2008). The biofortification project initiated by CIMMYT-HarvestPlus aimed to increase the Zn level in wheat grain (from 25 mg/kg to 37 mg/kg) particularly in South Asia (Velu et al. 2014). Landraces, wild emmer, spelt and synthetic wheats with the potential to accumulate more than 60 mg/kg of grain Zn and Fe were identified (Cakmak et al. 2004; Peleg et al. 2008; Velu et al. 2014) and these wheats were used to develop new cultivars. The recommended dietary allowance (RDA) of Zn for women and men is 8 mg/day and 11 mg/day, respectively (Trumbo et al. 2001). The RDA for men and postmenopausal women is 8 mg/day; the RDA for premenopausal women is 18 mg/day (Anonymous 2001).

There are concerns about possible negative associations between grain concentration of these nutrients and grain yield of wheat and similar issues were reported for negative effects of rust resistance gene *Sr26* on grain yield (The et al. 1988). Grain protein content was found positively associated with grain Zn and Fe content and negatively correlated with grain yield (Kumar et al. 2018). Some studies indicated a partial negative relationship between grain Zn concentration and yield in wheat (Peleg et al. 2009; Zhao et al. 2009; Gomez-Becerra et al. 2010) while other researchers have not observed this trend (Welch and Graham 2004; Velu et al. 2012). Micronutrient enriched wheat seeds show improved seedling viability and vigour as roots can penetrate deeper in nutrient-deficit soil to scavenge water and the required minerals (Welch and Graham 2004). This early seedling growth results in improved yield (Welch and Graham 2004) and improvement in stress tolerance and disease resistance (Welch 1999). Promoting micro-nutrient dense seed in wheat is a 'win-win' opportunity, especially in developing countries where availability of basic input for agriculture is a major challenge. Progress has been made and wheat cultivars Zincol-2016, Zinc Shakti, HPBW-01, WB-02 and BARI-Gom33 with 30% higher grain Zn and yield at least equivalent to local wheat cultivars have been released in South Asia (Velu et al. 2015; Gupta et al. 2017; Khondoker et al. 2019).

Genome-wide association study (GWAS) is the preferred method to detect novel alleles for complex traits among large numbers of unrelated materials through exploitation of historical recombination, enhanced resolution, and assessment of allelic diversity at a specific locus in a diversity panel (Yu and Buckler 2006). It utilises linkage disequilibrium (LD) to elucidate marker-trait associations (MTAs) and has been employed to evaluate rust resistance and nutrient accumulation in wheat (Yu et al. 2014; Maccaferri et al. 2015; Gao et al. 2016; Pasam et al. 2017; Kumar et al. 2018; Pinto da Silva et al. 2018; Velu et al. 2018;

Sapkota et al. 2019; Cu et al. 2020; Joukhadar et al. 2020) in worldwide germplasm collection.

A diverse CIMMYT-HarvestPlus association mapping panel (HPAMP) comprising landraces, synthetic hexaploids (durum and dicoccon-derived), spelt wheat and pre-breeding lines was characterised for rust resistance and mineral concentration in wheat grain. The aim of this study was to identify genomic regions favouring rust resistance and higher mineral accumulation as well as to validate previous findings.

6.2 Materials and methods

6.2.1 Plant materials

An HPAMP containing 293 wheat lines comprising of 1) landraces, 2) *T. dicoccon*-based synthetic derivatives, 3) *T. durum*-based synthetic derivatives, 4) *T. spelta* derivatives and 5) pre-breeding derivatives developed from diverse progenitors. The pedigree detail of these lines is given in Appendix III.

6.2.2 Rust response assessments under field conditions

The wheat diversity panel was evaluated in two field sites: Horse research unit (HRU) and Lansdowne research unit (LDN) of the University of Sydney Plant Breeding Institute in two replications during the first week of June in the 2018 and 2019 crop season. These field conditions offered natural rust infection. To build up the disease pressure at these sites, a mixture of four *Pst* pathotypes (134 E16A+Yr17+Yr27+, 150 E16A+, 134 E16A+YrJ +YrT+ and 239 E237A-Yr17+Yr33+), a mixture of four *Pt* pathotypes [104-2,3,6,(7); 104-1,2,3,(6),(7),(9),11,13+Lr24; 104-1,3,4,6,7,8,9,10,12+Lr37 and 76-1,3,5,7,9,10,12,13+Lr37] and a mixture of three *Pgt* pathotypes (34-1,2,7+Sr38; 98-

1,2,3,5,6,7 and 34-2,12,13) were artificially inoculated repeatedly at two-week intervals (Table 6.1) after a month of sowing.

Every sixth row included a mixture of rust susceptible spreaders in addition to an early sown rust spreader block. To prepare suspensions for inoculation, 8 g of urediniospores were dissolved in 300 ml of light mineral oil (Isopar-L, Univar) and applied using a hand-held sprayer (Micron Sprayers Ltd., Bromyard, Herefordshire, UK). The experimental area was irrigated twice a week to achieve optimised plant stand and to favour the development of rust epidemics. Rust response assessments were done at the Zadoks growth stage 69 (anthesis complete stage; Zadoks et al. 1974) on a 1-9 scale described in Bariana et al. (2007b), where 1 and 9 indicate very resistant and very susceptible responses, respectively.

6.2.3 Measurement of grain mineral concentration in 2018 and 2019

The HPAMP and additional varietal checks were sown in a completely randomised block design that accounted 21 ranges and 29 rows with two replications at the IA Watson Grains Research Centre, Plant Breeding Institute, Narrabri in the first week of June 2018. Plots comprised 6 rows of 6 m length and 2 m width. Plots were reduced to 8 m^2 (4 m x 2 m) at harvesting stage and grain yield was estimated plot-wise. The two replications hereafter were considered as 2018-Narr-I and 2018-Narr-II. The same panel was also sown in the second week of June 2019 in a completely randomised block design that accommodated 120 ranges and six rows in two replications at LDN and HRU sites of the University of Sydney Plant Breeding Institute, Cobbitty, NSW (New south wales) and these experiments were named 2019-LDN and 2019-HRU, respectively. Individual rows include 20 ranges, and five lines were fitted into each range. Each line of the panel was sown in a short row of 70 cm.

Table 6.1 Virulence and avirulence pattern of rust pathotypes used in present study based Australian differential set

Rust	#PBI culture	Pathotypes	Virulent on genes	Avirulent on genes
Stripe rust	**617***	134 E16A+Yr17+Yr27+	*Yr2,Yr6,Yr7,Yr8,Yr9,Yr17,Yr27*	*Yr1,Yr3,Yr4,Yr5,Yr10,YrSp*
	598*	150 E16A+	*Yr2,Yr6,Yr7,Yr8,Yr9,Yr10,Yr24*	*Yr1,Yr3,Yr4,Yr5,Yr17,YrSK,YrSp*
	444*	110 E143A+	*Yr2,Yr3,Yr4,Yr6,Yr7,YrA*	*Yr1,Yr5,Yr8,Yr9,Yr10,Yr17,YrSK,YrSp*
	674*	239 E237A-Yr17+Yr33+	*Yr1,Yr2,Yr3,Yr4,Yr6,Yr7,Yr9,Yr17,Yr25, Yr32,Yr33,YrND,YrS92/O,YrSP*	*Yr5,Yr8,Yr10,Yr15,Yr27,YrA,YrJ,YrT*
	615	134 E16A+YrJ +YrT+	*Yr2,Yr6,Yr7,Yr8,Yr9,YrJackie,YrToburuk*	*Yr1,Yr3,Yr4,Yr5,Yr8,Yr10,Yr17,YrSp*
Leaf rust	**231***	104-2,3,6,(7)	*Lr1,Lr2c,Lr3a,Lr10,Lr14a,(Lr17a),Lr23, Lr27+31*	*Lr13,Lr15,Lr16,Lr20,Lr24,Lr26,Lr28, Lr3ka+13*
	547*	104-1,2,3,(6),(7),(9),11,13+Lr24	*Lr1,Lr3a,Lr14a,(Lr17a),Lr20,Lr23,Lr24 ,(Lr26),(Lr27+31)*	*Lr13,Lr15,Lr17b,Lr28,Lr3ka+13*
	621*	76-1,3,5,7,9,10,12+Lr37	*Lr2c,Lr3a,Lr3ka,Lr10,Lr13,Lr14a,Lr17a ,Lr17b,Lr20,Lr26,Lr37*	*Lr15,Lr16,Lr17a,Lr23,Lr24,Lr26,Lr27 +31,Lr28*
	634*	104-1,3,4,6,7,8,9,10,12+Lr37	*Lr1,Lr3a,Lr13,Lr14a,Lr15,Lr17a,Lr17b, Lr20,Lr26,Lr27+31,Lr28,Lr37*	*Lr3a+13,Lr23*
	630	76-1,3,5,7,9,10,12,13+Lr37	*Lr3a,Lr3ka,Lr13,Lr14a,Lr17a,Lr17b,Lr 20,Lr24,Lr26,Lr37*	*Lr1,Lr2a,Lr15,Lr23,Lr27+31*
Stem rust	**103***	34-1,2,3,4,5,6,7	*Sr6,Sr11,Sr7b+9b,Sr7b+36,Sr7b+17,Sr 8a,Sr15*	*Sr30,Sr8b,SrAgi,SrEm,Sr27,SrSatu*
	205*	34-1,2,3,6,7,8,9	*Sr6,Sr11,Sr7b+9b,Sr8a,Sr15,Sr30,SrAgi*	*Sr7b+36,Sr7b+17,Sr8b,SrEm,Sr27,SrS atu*
	565*	34-1,2,7+Sr38 (VPM)	*Sr6,Sr11,Sr15,Sr38*	*Sr7b+9b,Sr7b+36,Sr7b+17,Sr8a,Sr8b, Sr30,SrAgi,SrEm,Sr27,SrSatu*
	580	98-1,2,3,5,6,7(Wyalkatchem)	*Sr6,Sr7b+9b,Sr7b+17,Sr8aSr11,Sr15*	*Sr7b+36,Sr8b,SrAgi,SrEm,Sr27,Sr30,S rSatu*
	427	34-2,12,13,(Satu)	*Sr11,Sr27,SrSatu*	*Sr6,Sr7b+9b,Sr7b+36,Sr7b+17,Sr8a,S r30,SrAgi,SrEm,Sr8b*

#PBI: Plant Breeding Institute; * Partial virulent against the gene(s) in parenthesis.

6.2.4 Sampling and nutrient analysis

Five random wheat spikes per accession were collected at physiological maturity in 2018 and 2019. These spikes were hand threshed and sub-sampled. One set containing 10 gm seed was oven-dried at 80°C for 4 hrs for nutrient analysis. Around 0.3 gm of each sub-sample was digested with solution of hydrogen peroxide and nitric acid in 50 ml polypropylene centrifuge tubes (covered to avoid any contamination) on a programable digestion system (Wheal et al. 2011). Each digested sample solution was analysed using inductively coupled plasma mass spectrometry (ICPMS 7500x; Agilent Santa Clara, CA) following the protocol described in Palmer et al. (2014). A certified reference material (CRM; NIST 1567a wheat flour) and a blank sample were also added in each digestion batch. Mineral concentrations on a dry weight basis, were estimated as mg/kg. Wheat seed of each individual plot was cleaned and 450 gm seed was used to measure grain protein content (%) at 11% moisture using near-infrared spectroscopy (FOSS, InfratecTM 1241, Sweden).

6.2.5 Statistical analysis

All variables assessed in the 2018 and 2019 field experiments were analysed using the linear mixed model function of Genstat 18th edition (VSN International, Hemel Hempstead, UK, 2015). Analyses were performed for each dataset considering genotype as a fixed effect and row and range coordinates within replicates as random effects. An analysis across years was also performed where genotype (G) and year (Y) were considered fixed effects and rows and ranges within replicates and years as random effects in the model. The adjusted means were used for subsequent analyses. Pearson's correlation coefficients were calculated between dataset of each environment of 2018 and 2019 for three rust diseases and across years for grain mineral concentration. The significance of mineral correlations was determined with a two-tailed test at $P< 0.001$ and $P< 0.05$. Means and standard deviations

were estimated using Genstat. The Shapiro-Wilk test was used to confirm the normal distribution (P>0.05) of the phenotypic datasets using the R program. The Box-cox transformation was performed to attain normal distribution of the original datasets using GenStat. The 'Boxplot' function was used to differentiate marker alleles and create boxplots for significant MTAs. Kruskal-Wallis H test (a rank-based nonparametric test) was performed to determine statistically significant differences between two groups carrying different alleles of associated DNA markers (R Core Team 2018).

6.2.6 Genotypic data, population structure and linkage disequilibrium

The iSelect 90K Infinium SNP array based genotypic data were available under the Australian Research Council project (Wang et al. 2014). Marker data were filtered for missing values, 0.05 minor allele frequency and heterozygosity greater than 10% resulting in 16,110 SNPs. The snpgdsLDpruning function in the SNPRelate package of R program was used to select SNPs with a high level of pairwise linkage disequilibrium (LD; LD threshold=0.9) (Calus and Vandenplas 2018) to produce a set of effective independent markers. The plot of the pairwise LD, measured as the squared correlation (r^2) between phased alleles, was designed within a 10 cM window. The SNPs derived principal components (PCs) determined population structure (Q) of the HPAMP panel. A kinship matrix (K) using centred - identity by state (IBS) was constructed using TASSEL 5.2.60. The HELIUM pedigree visualisation tool was used to demonstrate relationships among pedigrees in the panel to identify key progenitors (Shaw et al. 2014). A VanRaden heat plot was created to describe genetic relatedness (VanRaden 2007). The GAPIT package in R program was used to plot LD decay (Tang et al. 2016).

6.2.7 Identification of known rust resistance genes

The HPAMP panel was tested with markers linked with rust resistance genes *Yr15, Yr34, Lr34/Yr18/Sr57/Ltn1, Lr46/Yr29/Sr58/Ltn2, Lr67/Yr46/Sr55/Ltn3, Lr16/Sr23, Lr23, Sr31/Lr26/Yr9, Sr38/Lr37/Yr17, Sr24/Lr24, Sr2/Lr27/Yr30/Pbc1, Sr22* and *Sr15/Lr20.* Table 6.2 shows markers' name and types, and protocol for each marker were followed as per cited references. For non-KASP markers, PCR amplifications were performed in 10µl reaction volumes containing 60 ng genomic DNA, 0.5 µM of each marker (forward and reverse), 0.2 mM dNTPs, 1x PCR buffer containing 1.5mM MgCl2 and 0.2 U Immolase (Hotstart from Bioline Meridian Bioscience). For KASP assays, the protocol given in Nsabiyera et al. (2016) were followed. PCR amplifications were performed in 8µl reaction volumes containing 90 ng genomic DNA, 0.11 µl of KASP primer mix (12 µM each allele-specific A1 and A2 primers and 30 µM of reverse primer), 4 µl PACE mix (3CrBioscience) and 0.89 µl of milliQ water. The end-point fluorescent images were detected with the CFX96 Touch™ real-time PCR detection system and allelic discrimination was analysed using Bio-Rad CFX Manager Software (Bio-Rad Laboratories Pty. Ltd., USA). The presence of *Sr2/Lr27/Yr30* was also determined based on blackening of glumes and stem internodes referred to as pseudo-black chaff under field conditions (Hare and McIntosh 1979).

6.2.8 Genome-wide association study (GWAS)

Significant MTAs were identified from the mixed linear model (MLM) using TASSEL v 5.2.60 software. Days to heading was used as a covariate in this analysis. Manhattan plots were generated for 2018 and 2019 data. Each plot depicts a chromosome name on the x-axis and -log10 (p-value) on the y-axis (Bradbury et al. 2007; Buckler et al. 2007). Population

Table 6.2 List of gene-linked markers used in this study

Gene	Chr arm	Linked markers	Marker class	References
Yr15	1BS	*kinI*	KASP	Klymiuk et al. (2018)
Yr34	5AL	*sunKASP_112*	KASP	Qureshi et al. (2018)
Yr18/ Lr34/Sr57	7DS	*csLV34*	STS	Lagudah et al. (2006)
Lr46/Yr29/Sr58	1BL	*SNP1Lr46G22*	KASP	Lagudah unpublished
Lr67/Yr46/Sr55	4DL	*TM4*	KASP	Moore et al. (2015)
Lr16/Sr23	2BS	*2BS_5175914_kwm847*	KASP	Kassa et al. (2017)
Lr23	2BS	*sunKASP_16*	KASP	Chhetri et al. (2017)
Sr31/Lr26/Yr9	1BL:1RS	*iag95*	STS	Mago et al. (2002)
Sr38/Lr37/Yr17	2AS#2NS	*Ventrip* and *LN2*	STS	Helguera et al. (2003)
Sr24/Lr24	3DL	*Sr24#12-F* and *Sr24#12-R*	STS	Mago et al. (2005)
Sr2/Lr27/Yr30	3BS	*csSr2*	CAPS	Mago et al. (2011)
Sr22	7AL	*csIH81-BM*	STS	Periyannan et al. (2011)
Sr15/Lr20	7AL	*wri4*	STS	Jayatilake et al. (2013)

structure and relatedness among individuals in the panel can result in false positive associations (Falush et al. 2007). Therefore, population structure and total genetic effects of individuals were fitted as covariates in the MLM procedure (Yu et al. 2006).

The identification of significant MTAs ($P \leq 0.001$) was based on adult plant rust responses and mineral concentrations using the MLM; which included an optimum compression level and P3D (Population parameter previously determined) as a variance component. The threshold for significant MTAs was set to 1/n (n is the number of markers) which is -log10 (P-value) ≥ 3.7 ($P < 2\times10^{-}4$) (Yang et al. 2014b). The ensuing r^2 (%) explained the phenotypic variances and determined the magnitude of MTA effects.

6.3 Result

6.3.1 Adult plant rust response variation

Adult plant response variation for stripe rust, leaf rust and stem rust is presented in Fig. 6.1. A high proportion of lines were score 2 (resistant; R) and only a few lines were scored 6 (moderately susceptible; MS). Mean stripe rust responses ranged from 2.6±0.9 (HRU 2018) to 3.1±1.1 (LDN 2019). Leaf rust responses of 40% genotypes ranged from RMR (score 3) to moderately resistant to moderately susceptible (MRMS; score 5) with responses ranging from 2.2±0.7 (LDN 2018) to 4.7±1.4 (HRU 2018). Leaf rust scores of many lines varied from 6 (MS) to 8 (susceptible S) at the HRU sites in both years. More than 200 lines scored resistant (score 2) in all experiments and only a few lines were scored MRMS (score 5) at the HRU site in 2018 and 2019. Mean stem rust responses ranged from 2.1±0.5 (LDN 2018) to 2.4±0.8 (HRU 2019).

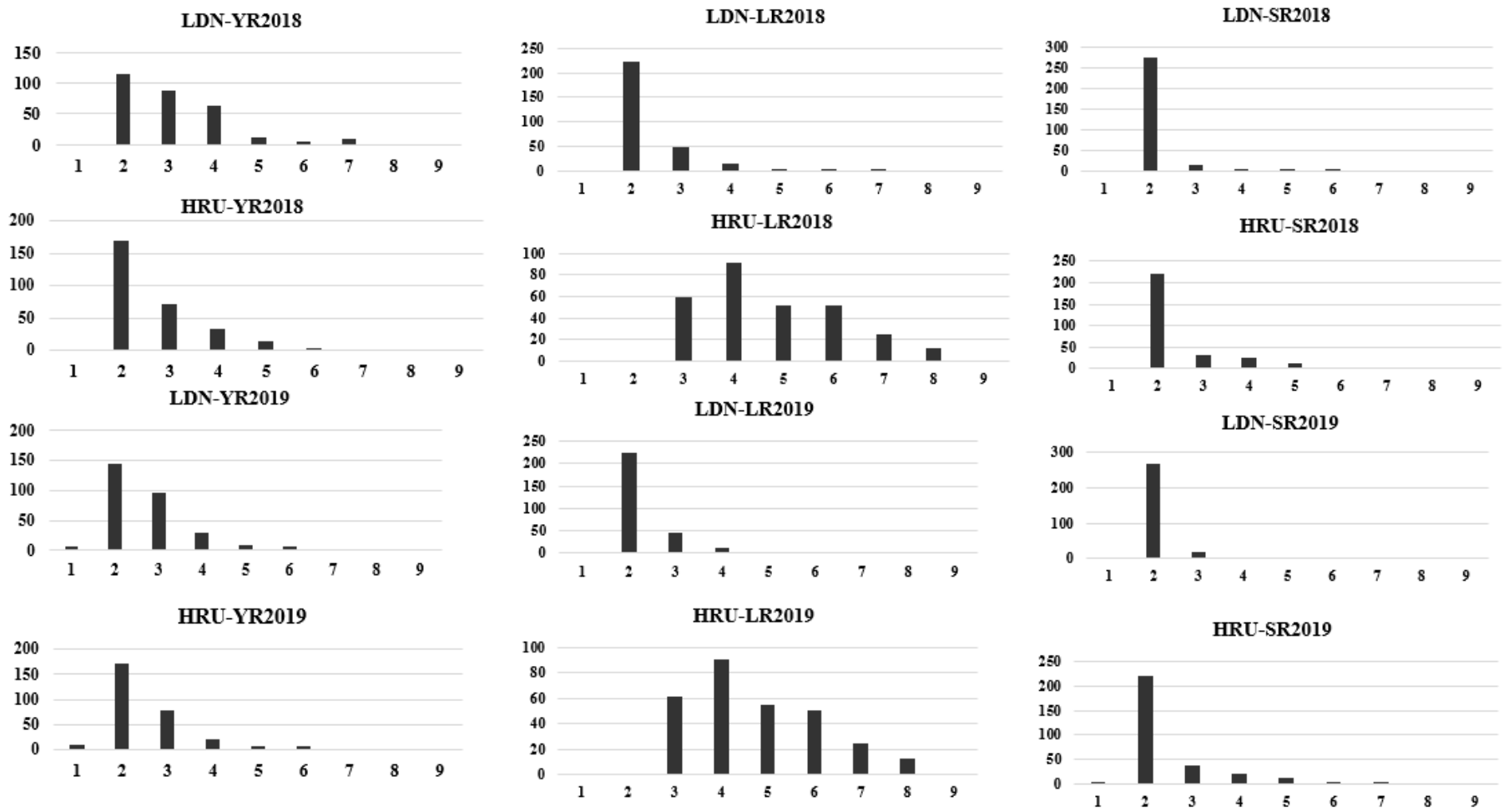

Fig. 6.1 Frequency distribution of the diversity panel against a mixture of pathotypes (field study). X-axis shows 1-9 disease scale and Y-axis shows number of accessions. LDN and HRU indicate Lansdowne and Horse research unit experimental site, respectively. Stripe rust (YR), Leaf rust (LR), Stem rust (SR), and experimental site and year of study are written together.

6.3.2 Detection of known rust resistance genes using linked markers

The mapping panel was genotyped with 13 markers linked to rust resistance genes listed in table 6.2 and results of genotypes carrying known genes are illustrated in Fig. 6.2. Ninety-two per cent and 15% lines carried the pleiotropic APR gene *Lr46/Yr29/Sr58* and *Lr34/Yr18/Sr57*, respectively. The *Lr34/Yr18/Sr57* and *Lr46/Yr29/Sr58* combination was present in 13% lines. Linked markers detected the presence of *Lr23*, *Sr38/Lr37/Yr17*, *Yr34*, *Lr16/Sr23*, *Sr24/Lr24*, *Sr31/Lr26/Yr9*, *Sr15/Lr20*, *Yr15* and *Lr67/Yr46/Sr55* in 19%, 15%, 11%, 10%, 7%, 5%, 4%, 3%, 1% lines respectively. *Sr2/Lr27/Yr30*-linked marker *csSr2* tested positive in one line. Ten percent lines expressed *Sr2*-linked pseudo-black chaff (linked with *Sr2/Lr27/Yr30)* on stem internodes and glumes.

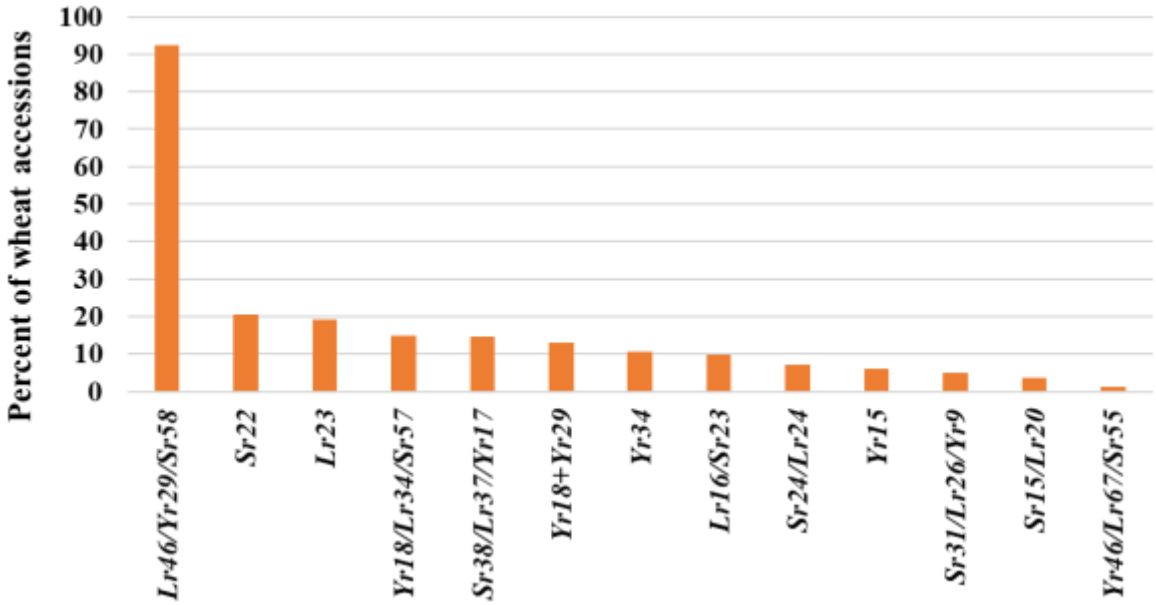

Fig. 6.2 Marker survey: Distribution of known rust resistance genes among the diversity panel

6.3.3 Phenotypic variation for grain mineral accumulation and agronomical traits

The wheat AM panel showed variation for grain concentration of five macronutrients (Ca, K, Mg, P and S) and five micronutrients (B, Fe, Cu, Mn and Zn) in four environments, namely 2018-Narr-I, 2018-Narr-II, 2019-LDN and 2019-HRU (Table 6.3). The accumulation of B and K was higher in 2019 at HRU and LDN sites compared to the Narrabri site in 2018. The concentrations of Ca, Cu, Fe, Mg, Mn and P were higher at Narrabri site in 2018. The accumulation of S and Zn was almost equal at all sites and across years.

Table 6.3 Nutrients profile (mg/kg) of association mapping (HPAMP) panel across 2018 and 2019

Micro and macro nutrient/	**2018**			Micronutrient/	**2019**		
location	**mean ± SD**	**Max**	**Min**	location	**mean ± S**	**Max**	**Min**
B-Narr-I	0.79±0.15	2.5	0.52	B-HRU	0.94±0.15	1.7	0.64
B-Narr-II	0.8±0.1	1.2	0.56	B-LDN	0.96±0.14	1.5	0.67
Ca-Narr-I	525.99±61.55	760	380	Ca-HRU	504.93±82.02	910	320
Ca-Narr-II	518.82±62.89	790	390	Ca-LDN	574.97±75.56	830	400
Cu-Narr-I	4.96±0.65	7.4	3.2	Cu-HRU	2.72±0.64	5.5	1.2
Cu-Narr-II	5.02±0.73	8.6	3.3	Cu-LDN	3.87±0.81	6.7	2.1
Fe-Narr-I	41.49±4.48	61	32	Fe-HRU	34.14±5.01	53	24
Fe-Narr-II	41.29±4.44	68	32	Fe-LDN	34.31±4.74	49	25
K-Narr-I	4005.82±347.2	5300	3300	K-HRU	4238.28±508.76	8600	3200
K-Narr-II	3907.61±324.7	5000	3200	K-LDN	3967.36±503.21	7100	3100
Mg-Narr-I	1401.88±93.55	1790	1180	Mg-HRU	1355.07±144.4	2100	1020
Mg-Narr-II	1412.04±96.65	1850	1190	Mg-LDN	1294.31±137.78	1870	1000
Mn-Narr-I	46.1±5.18	62	34	Mn-HRU	44.7±7.17	63	25
Mn-Narr-II	47.68±5.73	66	34	Mn-LDN	38.67±6.93	60	20
P-Narr-I	3591.78±296.37	4800	2900	P-HRU	3443.45±444.62	5600	2400
P-Narr-II	3500±291.07	4700	2800	P-LDN	3174.65±501.79	5300	2200
S-Narr-I	1749.38±135.83	2300	1380	S-HRU	1760.59±141.82	2400	1470
S-Narr-II	1734.39±122.12	2200	1380	S-LDN	1716.15±138.23	2400	1430
Zn-Narr-I	32.49±4.55	58	22	Zn-HRU	33.66±6.52	64	22
Zn-Narr-II	33.64±4.95	66	26	Zn-LDN	35.16±7.33	65	22
Protein (%)-Narr-I	13.9±0.84	17	12				
Protein (%)-Narr-II	13.5±0.9	17	12				

*Narr-I and Narr-II represent two replications at I. A. Watson Grain research centre Narrabri; HRU and LDN represent Horse research and Lansdowne research unit at Plant Breeding Institute Cobbitty. SD indicates standard deviation.

6.3.4 Marker distribution

SNP data were subjected to filtering and 5,099 independent SNPs were used in this study. Distribution of SNPs among the A, B, and D genomes is depicted in Fig. 6.3. The B genome had the highest number of SNPs (49.7%), followed by the A (39.4%) and D (10.8%) genomes. The average number of SNPs per chromosome was 242.8. Chromosome 7A was the longest (241.4 cM) and chromosome 4B was the shortest (119.4 cM; Fig. 6.3). Total map distance of the wheat genome was 3656.1 cM and average markers per cM interval was 1.39. The genotypic data of the 13 rust resistance gene-linked markers were incorporated into the genetic map.

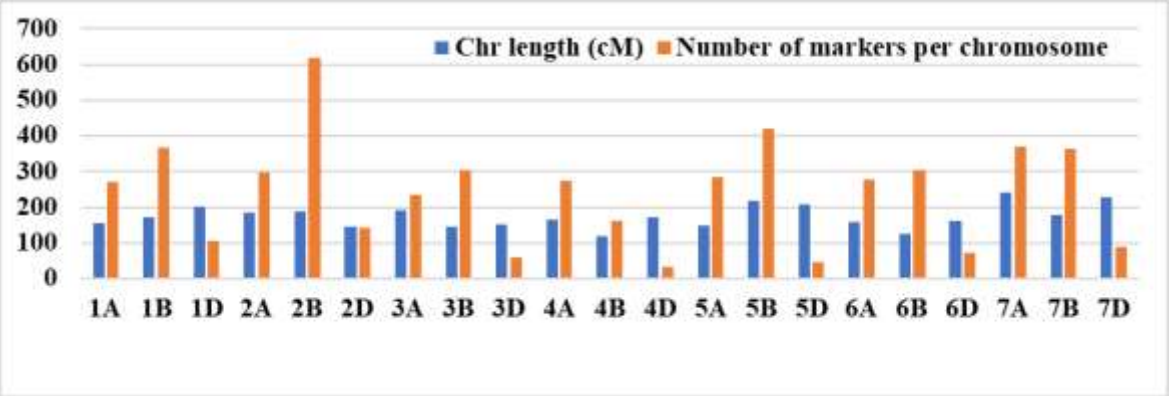

Fig. 6.3 Distribution of SNPs across chromosomes and length of individual chromosome

6.3.5 Population structure, kinship, and linkage disequilibrium

The first two principal components explained 11.9 and 7.5% of total genetic variance, respectively and revealed four subpopulations (I-IV) in HPAMP (Fig. 6.4). Thirty-nine lines were present in subpopulation I; this group included derivatives of CIMMYT's pre-breeding lines Quaiu, Tukuru and Kuruku. Subpopulation II (89 lines) was the second largest group and comprised derivatives of Chapio, Mutus, Babax, WBLL1 and Brambling. One hundred lines of the panel were grouped into subpopulation III. This subpopulation was primarily dominated by derivatives of Kachu, Kukuna, Chonte, Pastor, Danphe and *T. spelta*.

Subpopulation IV included 65 lines that share their parentage with Waxwing (ATTILA*2/STAR) and Francolin (Waxwing*2/Vivitsi). HELIUM was used to reveal parentage source and 632 parental lines were found depicting 929 relationships (Fig. 6.5.1). *T. dicoccon* PI94625, *T. dicoccon* CI9309, Kukuna, Francolin#1, Quaiu#2, Chonte, Brambling, Mutus, Solala and Waxwing*2/Tukuru*2 were the genotypes used as parents in the panel (Fig. 6.5.2 and 6.5.3).

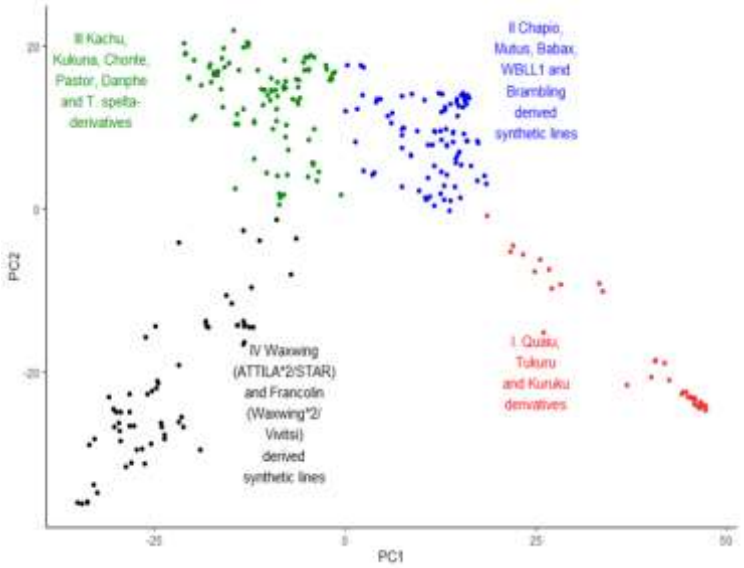

Fig. 6.4 Representation of population structure using first two major principal components

The heat map revealed the cryptic relatedness among genotypes and the magnitude of genetic relatedness indicated by the intensity of red colour (Fig. 6.6). LD was assessed (Appendix IV) and each dot in the decay plot represents a pair of distances between two SNPs on the window and their r (correlation coefficient) squared value. The red line indicates the moving average of the 10 adjacent markers. The decay plot showed that LD dropped at 3 cM that corresponds to an r^2 of 0.25. A confidence interval for QTL regions was considered ±3 cM.

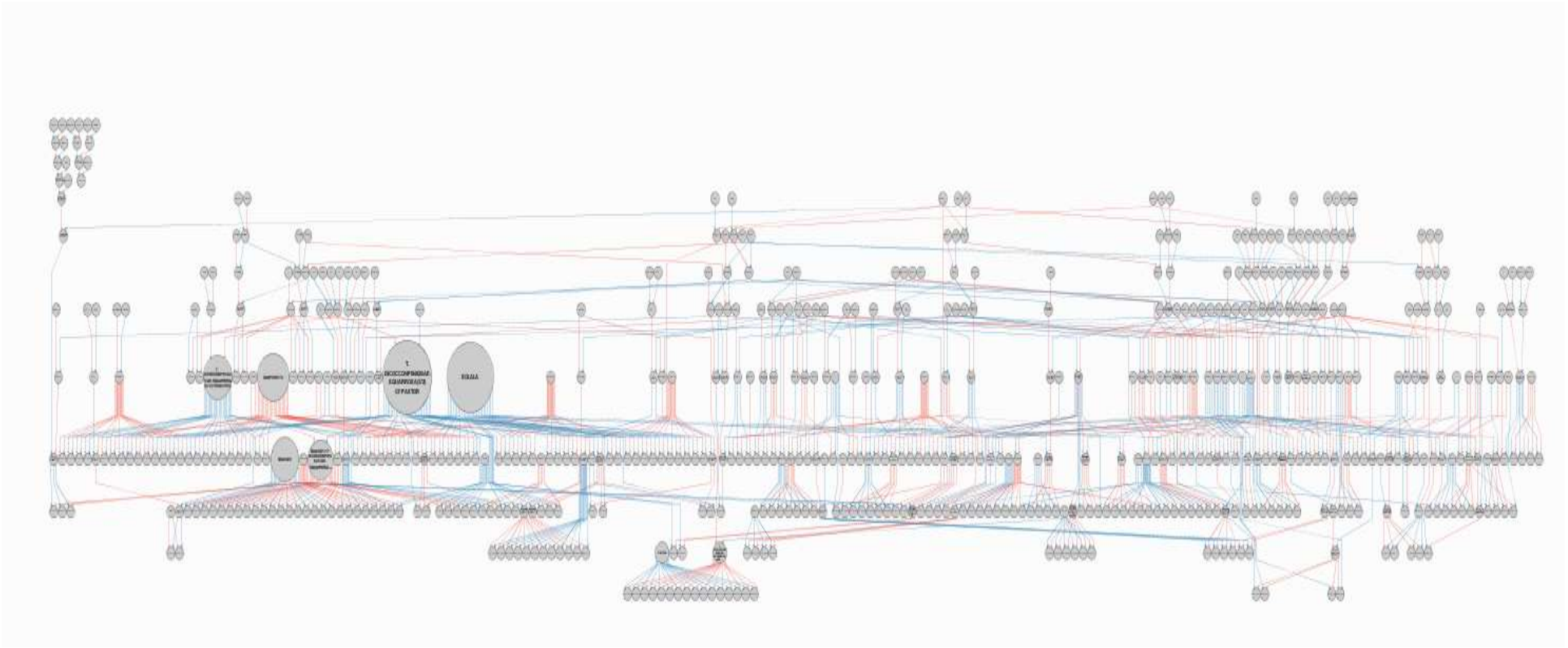

Fig. 6.5.1 Representation of 929 relationships among the association mapping panel (HPAMP) using pedigree visualisation tool HELIUM

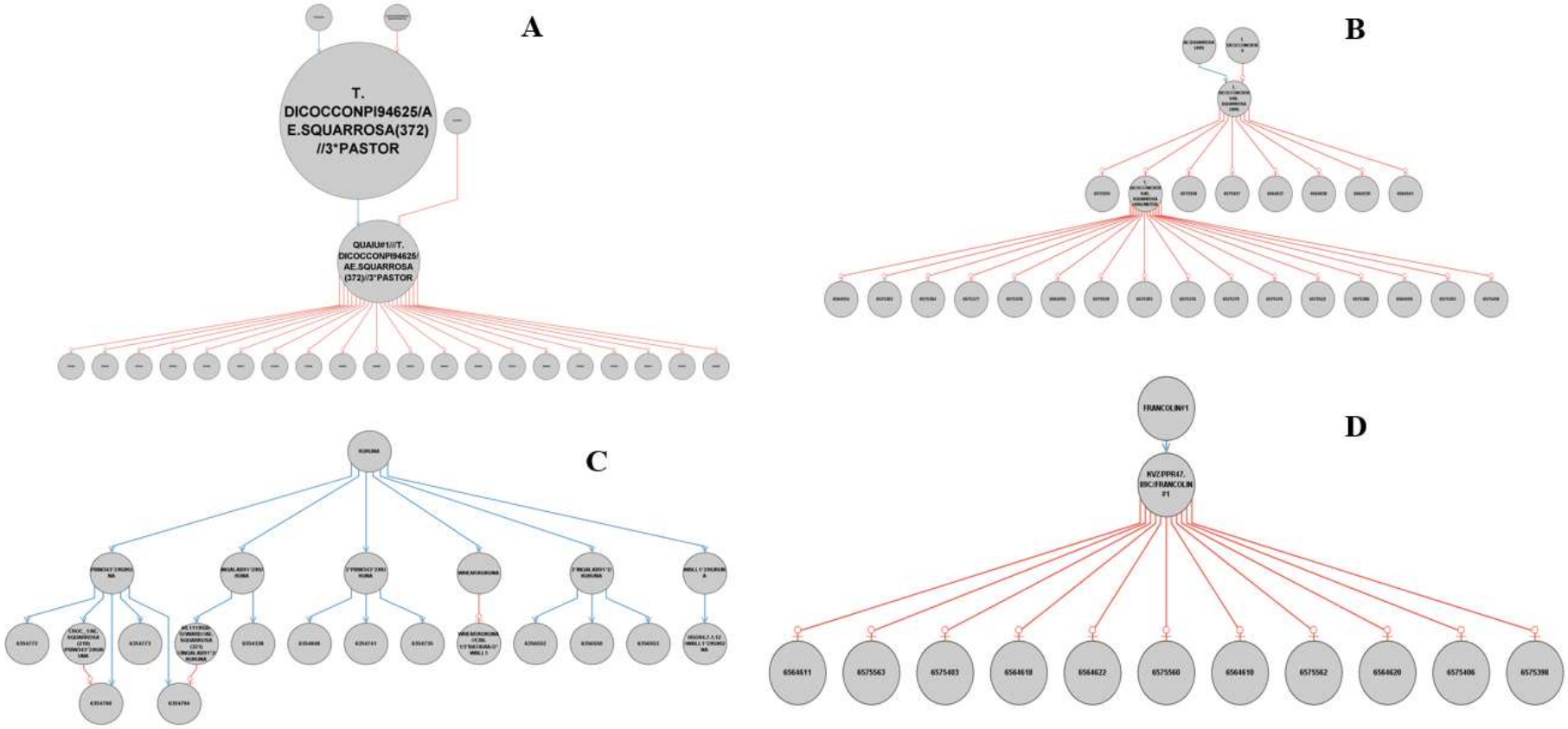

Fig. 6.5.2 Visualisation of wheat pedigrees derived using *T. dicoccon* PI94625 (A), *T. dicoccon* CI9309 (B), Kukuna (C) and Francolin#1 (D)

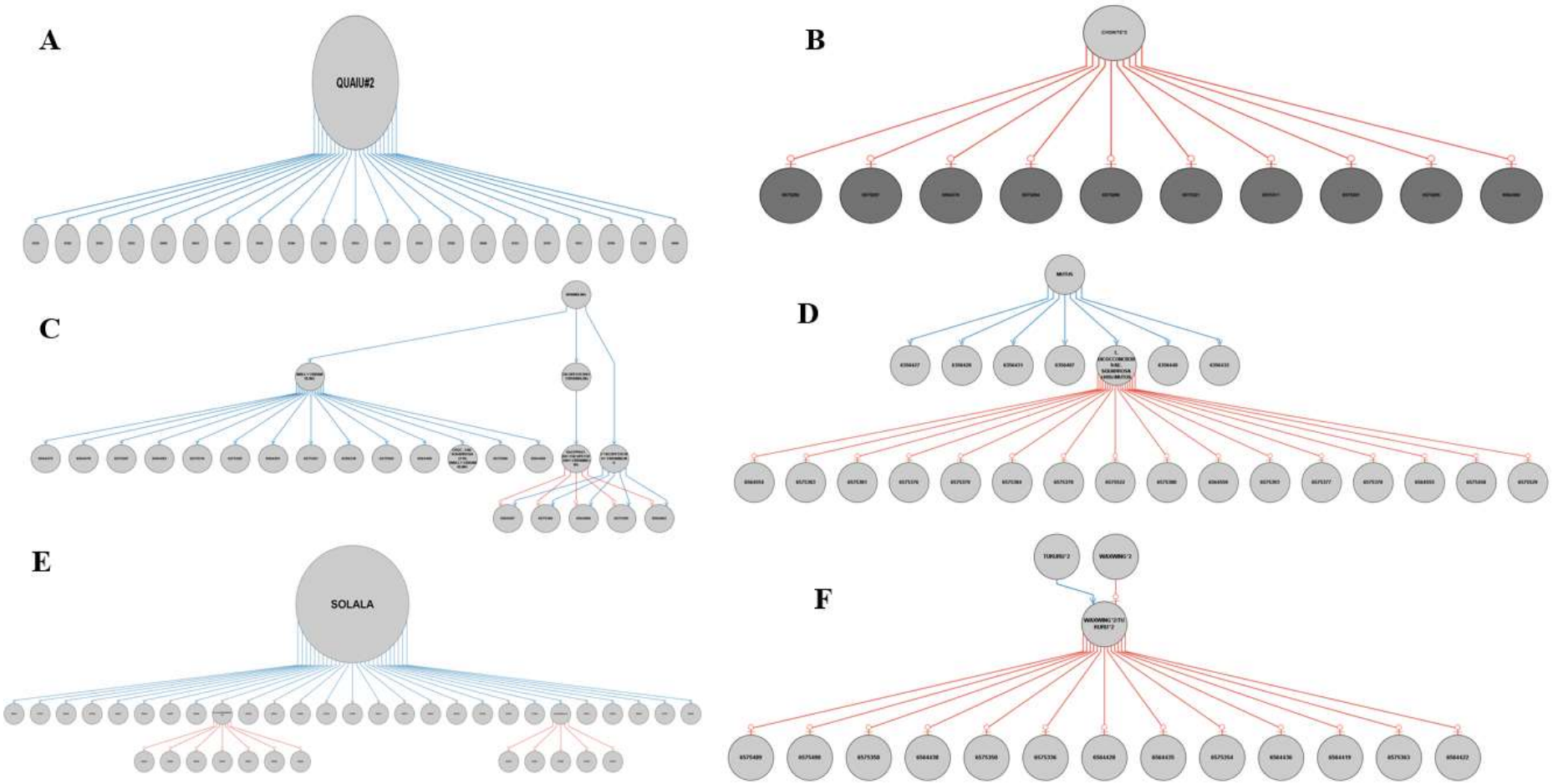

Fig. 6.5.3 Visualisation of wheat pedigrees derived using Quaiu#2(A), Chonte*2 (B), Brambling (C), Mutus (D), Solala (E) and Waxwing*2/Tukuru*2 (F)

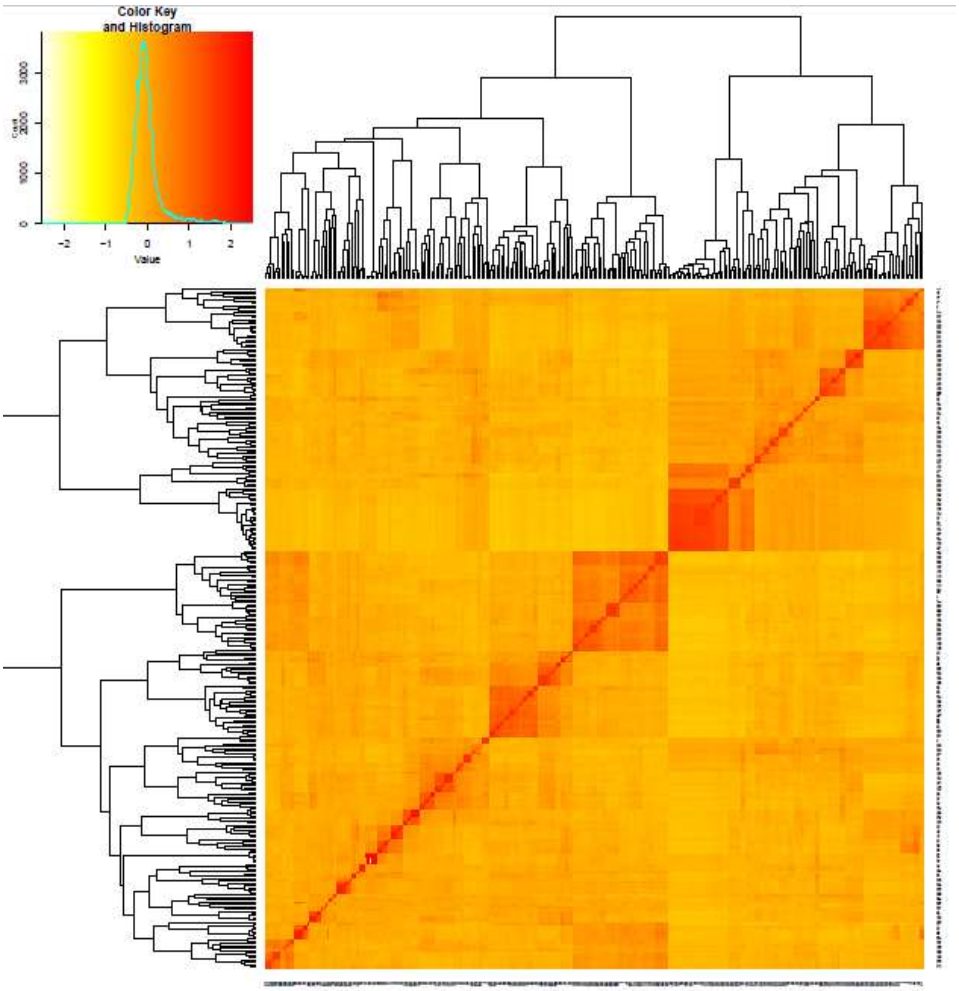

Fig. 6.6 Heat map presenting kinship among the diversity panel (red blocks indicate closely related accessions)

6.3.6 Genome wide association study for rust resistance

Significant marker-trait associations conferring rust resistance, their position, phenotypic variation explained, and underlying genes are listed in Table 6.4 and Appendices V-VII. In total 17 QTL were observed for stripe rust resistance in different environments. Unfortunately, results were not conclusive, presumably due the dominance of one or the other pathotype in each experiment. Phenotypic variation (R^2) of these MTA ranged from 4.17-11.06 % and LOD ranged from 3.15-7.08. The 2B-markers explained the highest portion of variation (R^2 = 7.87 and 11.06%) with LOD score (7.08 and 4.72), followed by the 5A-markers *IWA2947* (R^2 -7.65% and LOD- 4.84).

While nine and seven significant MTAs for leaf rust and stem rust resistance were detected, the presence of different pathotypes appears to have detected different MTAs in different environments. R^2 values of leaf rust MTAs ranged from 4.17-5.44% and LOD scores varied from 3.22-3.95. R^2 values of stem rust ranged from 4.03-5.1% and LOD scores varied from 3.08 to 3.86.

6.3.7 Genome wide association study for grain mineral concentration

The significant QTL conditioning enhanced mineral accumulation, their position, and phenotypic variation explained are given in Table 6.5 and Appendix VIII and IX. Sixteen QTL for B, 10 QTL for Ca, 8 QTL for Cu, 16 QTL for Fe, 9 QTL for K, 10 QTL for Mg, 9 QTL for Mn, 14 QTL for P, 10 QTL for S and 15 QTL for Zn concentration were detected (Table 6.5). None of these QTL were detected across years and locations, except the chromosome 1B QTL for S. SNP *IWB62537-1A* was associated with higher accumulation of P, Mn and Mg. Considering average mineral content data, 75 wheat lines carrying the favourable allele (T:T) of *IWB62537* showed increased mean concentration of P and Mn (3425 and 45.25 mg/kg, respectively) compared to 197 lines lacking this allele (3350 and 42.25 mg/kg, respectively; Fig. 6.7). Markers linked with *Sr31/Lr26/Yr9*, *Yr15*, *(Yr17*/*Lr37/Sr38)* and *Yr18/Lr34/Sr57* were also associated with accumulation of some minerals. Details of these linked markers are given in Fig. 6.8 and Appendices X-XII. Eight lines carrying the resistant allele of *Yr15* and 44 lines carrying *Lr34/Yr18/Sr57* showed improved Zn loading in wheat grain (Fig. 6.8). Sixteen wheat genotypes carrying the resistant allele of *Yr9/Lr26/Sr31* (1B:1R) linked to *iag95* showed a higher concentration of all minerals (Fig. 6.8; Appendices X-XII). Similarly, 43 wheat genotypes carrying positive allele of *Yr17/Lr37/Sr38* linked to *Ventrip* and *LN2* showed high accumulation of Cu and Fe (4.55 and 38.83 mg/kg, respectively) than other lines (4.08 and 37.66 mg/kg, respectively; Fig. 6.8; Appendices X-XI).

Table 6.4 List of significant marker-trait association (MTA) conferring triple rust resistance at field level

SN	Environments*	Marker (No. of SNPs)	Chromosome	Position (cM)	Position (Mb)	LOD	R^2 (%)	Postulation
Stripe rust resistance								
1	HRU 2018	*IWB9998* **(3)**	1B	64.95	298.1	4.34	6.35	*Yr24/Yr26* (308.1-336.2 Mb; Wu et al. 2018 and Cheng et al. 2020)
2	HRU 2019 and LDN 2019	*IWB43583* **(2)**	1B	79.77	557.3	3.64	5.05	*QYr-1B_Sachem* (562.3 Mb; Singh et al. 2013)
3	LDN 2018 and 2019	*IWB14343*	1D	37.82	12.3	3.15	4.17	*QYrst.orr-1DS* (16.7 Mb; Vazquez et al. 2012)
4	HRU 2019 and LDN 2019	*IWA4323* **(8)**	2B	91.1	133.3	4.72	7.87	*QYr.cim-2BS_Francolin#1* (165.5 Mb; Lan et al. 2014)
5	HRU 2019 and LDN 2019	*IWA5081* **(3)**	2B	130.62	751.2	7.08	11.06	*Yr5* (754.9 Mb; Marchal et al. 2018)
6	HRU 2019	*IWB19393*	2D	81.41	614.7	3.44	5.22	*Yr54* (639.09 Mb; Basnet et al. 2014); *Yr8*
7	HRU 2019 and LDN 2019	*IWB12194*	3B	11.56	6.5	3.53	5.79	*QYr-3B_Opata85* (Singh et al. 2000);
8	HRU 2019 and LDN 2019	*IWB57629*	4A	58.38	509.1	4.2	6.28	*QYr-3B.1-Pavon76* (William et al. 2006)
9	HRU 2019	*IWA6227*	5A	26.51	10.3	3.47	5.54	**New**
10	HRU 2019 and LDN 2019	*IWB43526* **(3)**	5A	86.31	570.1	3.19	4.46	**New**
11	HRU 2019 and LDN 2019	*IWA2947*	5A	131.42	688.3	4.84	7.65	*Yr34? QRYr5A.1_T. boeticum* (558.3 Mb; Chhuneja et al. 2008)? *QYr.cim-5AL_Francolin#1* (536.9 Mb; Lan et al. 2014)
12	LDN 2019	*IWB63643*	5B	28.35	26.2	4.37	6.39	*Yr48* (698.0 Mb; Lowe et al. 2011)
13	HRU 2019	*IWB5837***(2)**	5B	144.12	665.8	3.99	5.81	*QYr.uga-5B_AGS2000* (34.7 Mb; Hao et al. 2011)?
14	LDN 2019	*IWA4950* **(2)**	6A	100.12	581.7	3.26	4.35	*QYr.sun-5B_Wollaroi* (668.4 Mb; Bansal et al. 2014a)
15	LDN 2019	*IWA179* **(2)**	7A	219.59	724.1	3.76	6.08	*QYr.cim-6AL_Francolin#1* (593.0 Mb; Lan et al. 2014)
16	HRU 2019	*IWB14579*	7D	47.38	-	3.71	5.38	*Yr75* (717.0 Mb); *QYr.sgi-7A_Kariega* (Prins et al. 2011)

17	LDN 2019	*IWB15318*	7D	176.3	596.9	3.9	5.44	*Yr18/Lr34*
Leaf rust resistance								
1	HRU 2018 and 2019	*IWA3125* **(2)**	1D	3.4	0.4	3.95	5.44	*Lr42* (Gao et al. 2016)
2	HRU 2018 and 2019	*Lr23_sunKasp_16* **(4)**	2B	82.47	-	3.23	4.17	*Lr23* and *Lr13*
3	LDN 2018	*IWA2674***(3)**	2B	93.84	164	3.25	4.21	*Lr23*, *IWA4894* and *IWB37811* (158.0 Mb; Gao et al. 2016 and Turner et al. 2017),
4	LDN 2018	*IWB35521*	4A	100.38	641.5	3.29	4.76	**New**
5	HRU 2018 and 2019	*IWB60219*	6B	36.69	26.6	3.27	4.33	*Lr61*; *QLr.wpt-6BS.2*? (29.9 Mb; Gerard et al. 2018)
6	HRU 2018	*IWB25446*	6B	82.56	645.6	3.22	4.37	*Lr3a* (631-720.5 Mb; Gao et al. 2016 and Riaz et al. 2018)
7	LDN 2018	*IWA2196***(2)**	7A	42.08	12.1	3.49	4.58	*Lr47* (11.5 Mb; Helguera et al. 2000)
8	HRU 2018 and 2019	*IWB34640*	7A	216.36	711.8	3.88	5.21	*Lr20*? (733.8 Mb) *IWA4175* (717 Mb; Turner et al. 2017)
9	HRU 2018 and 2019	*IWA5837*	7B	136.26	701.1	3.22	4.24	*Lr14b Lr68* (740 Mb; Herrera-Foessel et al. 2012)
Stem rust resistance								
1	HRU 2018 and 2019	*IWB8040* **(2)**	1A	110.68	538.6	3.22	4.22	*QSr.cdl-1AL_Thatcher* (Rouse et al. 2014)
2	HRU 2018 and 2019	*IWB72463*	2A	77.91	42.4	3.21	4.52	*Sr32* (47.1 Mb; Mago et al. 2013 and Yu et al. 2014); *Sr32+Sr38*
3	HRU 2018 and 2019	*IWB29111* **(2)**	2A	106.86	534.9	3.55	5.1	*Sr32+Sr38*; unnamed CIMMYT QTL (Yu et al. 2014)
4	HRU 2018 and 2019	*IWB13993*	2D	76.57	600.9	3.68	4.94	**New**
5	HRU 2018 and 2019	*IWB5927*	3A	136.18	695.7	3.08	4.03	*Sr35* (691.5 Mb; Saintenac et al. 2013)
6	LDN 2018 and 2019	*IWA149*	3B	139.62	818.1	3.86	5.52	**New**
7	LDN 2018 and 2019	*IWB36370*	7A	117.61	85.4	3.22	4.2	*Sr22* (Periyannan et al. 2011)

* LDN and HRU indicate Lansdowne and Horse research unit experimental site, respectively. Experimental site and year of study are written together.

Table 6.5 List of significant marker-trait associations (MTA) conferring grain mineral concentration

SN	Trait-Environment*	Significant MTA	Chr	Position (cM)	Position (Mb)	LOD#	R^2 (%)	Postulation
Boron								
1	B-Narr-I	*IWA1955*	1B	59.86	319.1	3.11	7.62	**New**
2	B-Narr-I	*IWB1411*	2A	119.93	711.5	4.07	5.36	**New**
3	B-Narr-I	*IWB2479*	2A	123.11	709.6	4.27	5.46	**New**
4	B-Narr-I	*IWB58213*	2A	147.99	747.6	4.08	5.26	**New**
5	B-Narr-I	*IWB21976*	3A	26.01	-	5.03	6.74	**New**
6	B-HRU	*IWB32527*	3A	68.66	45.6	4.14	6.01	**New**
7	B-Narr-I	*IWB4872*	3B	14.1	7.6	3.93	4.94	**New**
8	B-Narr-I	*IWB23357*	3D	4.56	1.3	5.15	6.76	**New**
9	B-HRU	*IWB20649*	4A	47.53	56.5	3.82	5.5	**New**
10	B-Narr-I	*IWB67908*	4A	144.38	-	3.33	4.23	**New**
11	B-Narr-I	*IWB574*	4A	164.13	733.4	3.25	3.96	**New**
12	B-Narr-I	*IWA5214*	5B	69.19	-	3.92	4.93	**New**
13	B-HRU	*IWB4550*	5D	187.21	543.1	3.16	4.3	**New**
14	B-Narr-I	*IWB42415*	7A	35.31	4.9	4.11	5.37	**New**
15	B-LDN	*IWB57105*	7A	56.17	25.5	3.34	5.21	**New**
16	B-Narr-II	*IWB55488*	7B	160.43	732.4	3.24	4.26	**New**
Calcium								
1	Ca-LDN	*IWB72107*	1B	43.86	20.6	3.33	5.12	*S1B_6867825* (6.8 Mb; Bhatta et al. 2018)
2	Ca-LDN	*IWB14686*	1B	60.62	173.1	3.07	4.6	*QGCa.sun-1B* (143 Mb; Kapfuchira 2015)
3	Ca-Narr-I	*IWB11666*	3B	80.13	723.4	3.2	4.61	*QGCa.sun-3B* (742.4 Mb; Kapfuchira 2015); *S3B_655010350* (655.0 Mb; Bhatta et al. 2018)
4	Ca-LDN	*IWB63696*	6A	25.53	9.7	3.32	4.56	*S6A_50345873* (50.3 Mb; Bhatta et al. 2018)

5	Ca-LDN	*IWA7994*	6A	121.61	596.6	3.28	4.51	*S6A_592562315* (592.5 Mb; Bhatta et al. 2018)
6	Ca-Narr-I and Narr-II	*IWA2338*	6D	9.47	-	4.06	5.69	**New**
7	Ca-HRU	*IWB29043*	6D	117.58	453	3.78	5.18	**New**
8	Ca-Narr-II	*IWB10792*	7A	212.66	694.7	3.84	5.22	**New**
9	Ca-LDN	*IWB58295*	7B	133.59	700.6	3.2	4.27	**New**
10	Ca-HRU and Narr-I	*IWB4045*	7D	95.68	68.4	3.66	4.97	**New**
Copper								
1	Cu-HRU	*IWB8131*	1D	82.82	356.2	3.09	4.13	**New**
2	Cu-HRU	*IWB39800*	2B	142.54	777.5	3.3	4.36	**New**
3	Cu-Narr-II	*IWB21527*	3A	77.57	56.7	4.2	6.37	*S3A_23297031* (23.2 Mb; Bhatta et al. 2018)
4	Cu-Narr-II	*IWB57116*	3D	69.57	-	3.47	4.46	**New**
5	Cu-LDN	*IWB74227*	4B	15.91	4.9	3.21	4.19	*S4B_37424735* (37.4 Mb; Bhatta et al. 2018)
6	Cu-LDN	*IWA928*	6A	137.03	599.8	3.23	4.5	*S6A_613579920* (613.5 Mb; Bhatta et al. 2018)
7	Cu-LDN	*IWA3297*	6B	0.37	3.9	3.13	4.73	*S6B_6241996* (6.2 Mb; Bhatta et al. 2018)
8	Cu-HRU	*IWA2710*	7A	97.76	68	4.01	5.5	**New**
Iron								
1	Fe-HRU*	*IWB59323*	1A	30.99	11.6		3.2	*QGFe.sun-1A.1* (23.1 Mb; Kapfuchira 2015)
2	Fe-HRU	*IWA6610*	1B	43.86	109.7		3.41	**New**
3	Fe-HRU	*IWB7923*	1B	56.65	38.9		3.07	Fe and Protein content (57.7 Mb; Kumar et al. 2018)
4	Fe-HRU	*IWB39764*	1B	57.6	49.5		3.84	Fe and Protein content (57.7 Mb; Kumar et al. 2018)
5	Fe-Narr-II	*IWB45407*	1B	74.37	508.4		3.66	*QGFe.sun-1B.1*(438.1 Mb; Kapfuchira 2015)
6	Fe-LDN	*IWB3677*	1B	81.61	553.1		3.15	**New**

7	Fe-Narr-II	*IWA3151*	2A	108.46	558.5		3.91	Fe and Zn content (Cu et al. 2020)
8	Fe-HRU	*IWA6026*	2B	80.77	75.6		3.08	**New**
9	Fe-Narr-II	*IWB57730*	2B	80.77	-		3.32	**New**
10	Fe-Narr-II	*IWB27598*	3A	53.32	32.1		3.19	**New**
11	Fe-Narr-II	*IWB16311*	3A	80.07	-		3.43	*S3A_534535579* (534.5 Mb; Bhatta et al. 2018)
12	Fe-Narr-I	*IWB4872*	3B	14.1	7.6		3.21	Fe, Cu and Mn (Cu et al. 2020)
13	Fe-Narr-I	*IWB771*	3D	4	1.3		3.48	**New**
14	Fe-Narr-II	*IWB6702*	5A	74.76	552.1		3.08	**New**
15	Fe-LDN	*IWA1110*	7A	136.43	617.6		3.44	**New**
16	Fe-Narr-II	*IWA4873*	7B	64.59	111.9		3.29	**New**
Potassium								
17	K-Narr-I	*IWB27962*	1A	111.91	-		3.1	*QGK.sun-1A* (372.7 Mb; Kapfuchira 2015)
18	K-Narr-I	*IWB64556*	1A	113.81	549.4		4.23	**New**
19	K-Narr-I	*IWB9961*	1A	130.09	547.9		3.4	**New**
20	K-LDN	*IWB56774*	1B	53.35	8		3.52	**New**
21	K-Narr-I	*IWB63170*	2A	95.75	70.1		3.44	**New**
22	K-HRU	*IWB41295*	2D	49.59	146.3		3.91	**New**
23	K-LDN	*IWB53342*	4A	95.45	631.9		3.39	**New**
24	K-LDN	*IWB11035*	5B	150.93	679.4		3.78	**New**
25	K-LDN	*IWB23484*	6A	133.74	609.4		3.33	*QGK.sun-6A* (557.5 Mb; Kapfuchira 2015)
Magnesium								
1	Mg-LDN*	*IWB62537*	1A	113.19	-	4.8	6.95	**New**; Favours accumulation of Mn and P
2	Mg-LDN	*IWB58556*	1A	118.83	549.8	3.19	4.16	**New**
3	Mg-LDN	*IWA8135*	1A	133.15	553.1	5.09	7.16	**New;** Favours accumulation of Zn, Mn and P
4	Mg-Narr-I	*IWA6530*	1A	137.2	578.5	3.5	4.75	**New**

5	Mg-LDN	*IWB3934*	1B	109.7	637.4	3.23	4.26	*QGMg.sun-1B.2*(582.3 Mb; Kapfuchira 2015)
6	Mg-Narr-II	*IWB55767*	2B	99.73	477.4	4.31	7.03	**New**
7	Mg-HRU	*IWB60934*	4A	91.23	627.8	3.11	4.15	*QGMg.sun-4A* (Kapfuchira 2015)
8	Mg-Narr-I	*IWB23688*	4A	147.28	732.5	3.94	5.43	*S4A_740606543* (740.6 Mb; Bhatta et al. 2018)
9	Mg-HRU	*IWB71708*	6A	128.26	599.1	3.61	5.59	**New**
10	Mg-Narr-II	*IWA7005*	7A	226.07	730.4	3.31	4.79	**New**
Manganese								
1	Mn-LDN	*IWB62537*	1A	113.19	-	3.72	5.29	Cu et al. (2020); Favours accumulation of Mg and P
2	Mn-LDN	*IWA8135*	1A	133.15	553.1	4.24	5.9	*QGMn.sun-1A* (495.3 Mb; Kapfuchira 2015) Favours accumulation of P and Zn
3	Mn-Narr-II	*IWA7703*	1B	51.1	46.8	3.58	4.9	**New**
4	Mn-HRU	*IWB6730*	1B	81.61	562.9	3.16	4.43	*QGMn.sun-1B* (543.5 Mb); *QGMn.sun-1B* (570.8 Mb)- Kapfuchira (2015)
5	Mn-Narr-I	*IWB50475*	3A	15.05	8.7	3.88	6.16	**New**
6	Mn-HRU	*Sr24#12*	3Ag# 3DL	-	-	3.55	4.73	**New** *Sr24/Lr24*
7	Mn-Narr-I	*IWB67390*	3D	4.56	-	3.43	4.78	**New**
8	Mn-Narr-I	*IWB42628*	6D	77.53	61.1	3.07	4.07	Cu et al. (2020)
9	Mn-Narr-I	*IWB71691*	7B	118.09	680.2	3.29	4.9	**New**
Phosphorous								
1	P-LDN*	*IWB62537*	1A	113.19	-	3.16	4.34	**New**
2	P-LDN	*IWA8135*	1A	133.15	553.1	3.59	4.85	**New;** Favours accumulation of Zn and Mn
3	P-Narr-II	*IWB45937*	1B	76.09	461.3	4.14	5.78	*QGP.sun-1B* (512.6 Mb) Kapfuchira (2015)
4	P-Narr-I	*IWB9653*	2A	124.5	717.8	3.21	4.2	*Ku_c25175_1248* (722.1 Mb; Cu et al. 2020)
5	P-Narr-I	*IWB3052*	2D	76.39	722.2	3.35	4.67	**New**

6	P-HRU	*IWB8780*	3B	144.74	-	3.11	4.11	*QGP.sun-3B.2* (648.9 Mb; Kapfuchira 2015)
7	P-Narr-I	*IWB56874*	3D	84.38	-	3.36	4.52	**New**
8	P-LDN	*IWB22009*	4A	103.04	679.3	3.3	4.48	**New**
9	P-HRU	*IWB26650*	5B	30.56	35.9	3.49	4.68	*QGP.sun-5B.2* (Kapfuchira 2015)
10	P-LDN	*IWB64255*	6A	136.7	604.9	3.17	4.43	**New**
11	P-Narr-I	*IWB50824*	6D	82.14	310	3.76	5.23	**New**
12	P-Narr-I	*IWB25416*	7A	33.45	1.4	3.08	4.19	**New**
13	P-LDN	*IWA7942*	7A	126.4	118.2	3.19	4.31	**New**
14	P-Narr-I	*IWB12233*	7A	212.66	712.8	3.66	4.96	**New**
Sulphur								
1	S-Narr-II	*IWB44655*	1A	26.6	8.2	3.48	4.65	**New**
2	S-HRU and LDN	*IWB46598*	1B	43.86	670.2	3.37	4.64	*Yr9/Lr26/Sr31*; *QGS.sun-1B* (582.3 Mb; Kapfuchira 2015)
3	S-Narr-I and Narr-II	*IWB20686*	1B	108.41	632.4	4.63	6.98	*Yr9/Lr26/Sr31*; *QGS.sun-1B* (582.3 Mb; Kapfuchira 2015)
4	S-LDN	*IWA6076*	2B	107.49	632.9	3.11	4.2	**New**
5	S-Narr-I	*IWB48388*	2B	153.49	785.9	3.29	4.37	**New**
6	S-Narr-II	*IWB8792*	5B	37.18	41.6	3.84	5.36	**New**
7	S-Narr-II	*IWB71672*	5B	45.4	396.5	3.21	4.29	**New**
8	S-Narr-I	*IWB56335*	5B	49.01	395.6	3.2	4.26	**New**
9	S-LDN	*IWA5670*	5B	69.19	514.9	4.69	6.62	*QGS.sun-5B* (501.4 Mb; Kapfuchira 2015)
10	S-LDN	*IWB71785*	7A	58.82	22.9	3.11	4.28	**New**
Zinc								
1	Zn-LDN*	*IWA8135*	1A	133.15	553.1	3.05	3.98	Favour's accumulation of Mn and P; *AX-158539950* (553.6 Mb; Alomari et al. 2018)
2	Zn-Narr-I	*IWB8918*	1A	144.41	585.8	4.07	6.04	**New**
3	Zn-Narr-I	*IWB35116*	1B	60.62	-	4.48	6.24	**New**

4	Zn-Narr-II	*IWB10413*	1B	70.08	456.3	3.12	4.1	**New**
5	Zn-LDN	*IWB3934*	1B	109.7	637.4	3.45	4.89	Zn, Fe and protein content (626.2 Mb; Kumar et al. 2018)
6	Zn-Narr-II	*IWB8907*	2A	143.22	747.1	3.12	4.02	*S2A_742969119* (742.9 Mb) and S2A_750621751 (750.6 Mb; Bhatta et al. 2018)
7	Zn-HRU and Narr-II	*IWB64607*	3B	107.15	772.4	3.73	5.68	*S3B_813450132* (813.4 Mb; Bhatta et al. 2018)
8	Zn-LDN	*IWB22009*	4A	103.04	679.3	4.04	5.86	*BobWhite_c3656_1155* (631.9 Mb; Cu et al. 2020); *S4A_681683160* (681.6 Mb; Bhatta et al. 2018)
9	Zn-Narr-I	*IWA2365*	5A	73.97	547.6	3.33	5.47	*S5A_552354940* (552.3 Mb; Bhatta et al. 2018)
10	Zn-HRU	*IWB29170*	5A	117.67	666.9	3.4	4.55	*AX-94416605* (673.7 Mb; Alomari et al. 2018)
11	Zn-Narr-I	*IWB10135*	5B	100.64	571.6	3.99	5.46	*BS00073015_51* (555.1 Mb; Cu et al. 2020)
12	Zn-HRU	*IWB24648*	5D	198.19	546.9	3.6	4.9	**New**
13	Zn-Narr-II	*IWA5704*	6A	136.85	602.7	4.47	6	**New**
14	Zn-Narr-II	*IWB57103*	7A	145.1	651	3.24	4.11	**New**
15	Zn-Narr-I	*IWB8586*	7B	158.11	730.9	3.12	4.2	*QGZn.sun-7B* (678.7 Mb; Kapfuchira 2015)

#LOD: Logarithm of odds; *Narr-I and Narr-II represent I. A. Watson Grain research centre Narrabri and year 2018. LDN and HRU indicate Lansdowne and Horse research unit experimental site, respectively and year 2019.

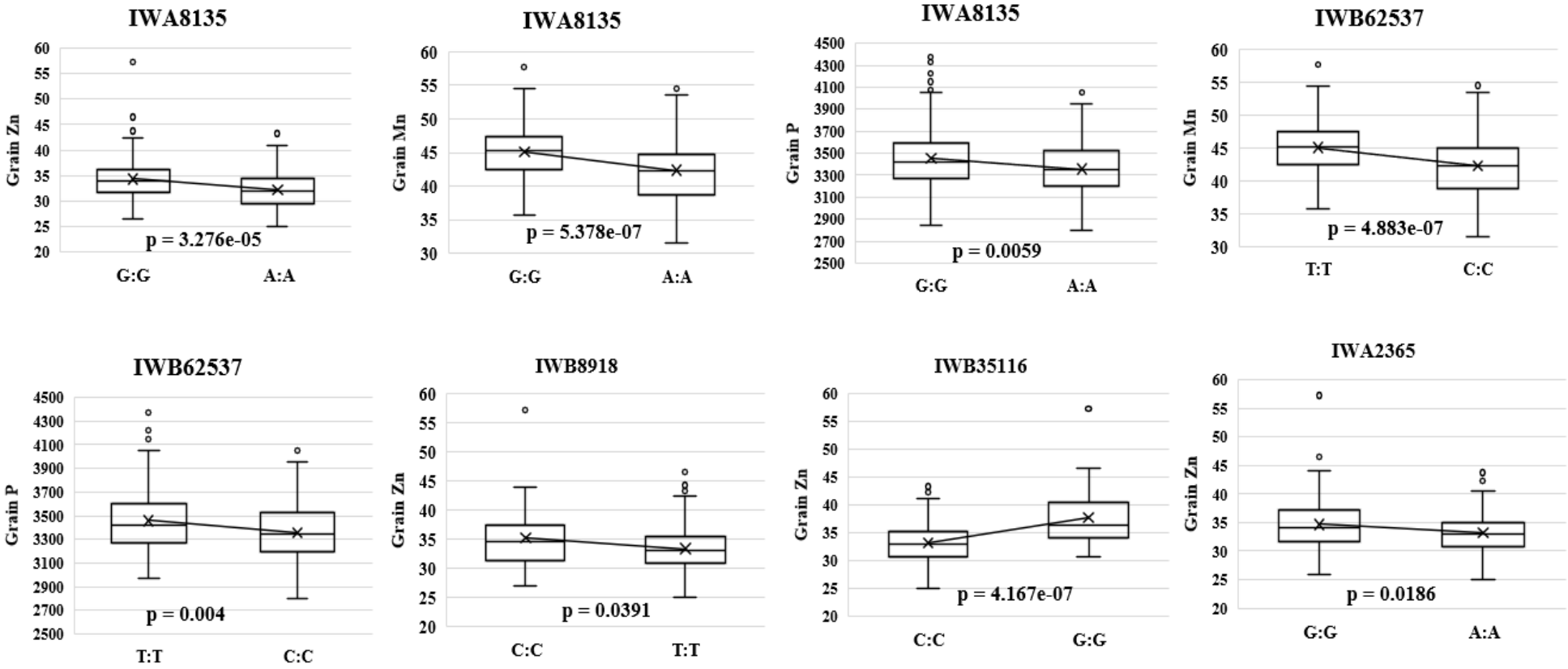

Fig. 6.7 Boxplot analysis depicting contribution of significant markers in grain mineral accumulation. X- and Y-axis represent alleles and mineral concentration (mg/kg) in wheat grain, respectively.

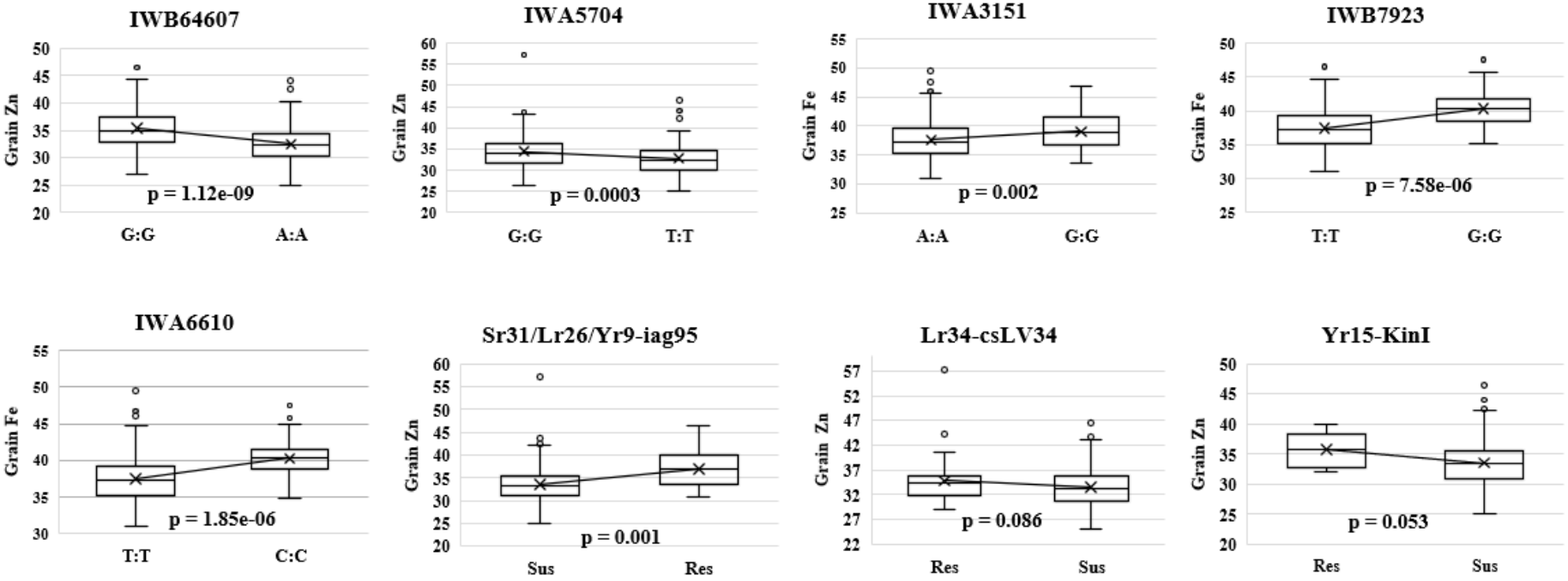

Fig. 6.8 Boxplot analysis depicting contribution of significant markers including markers linked with rust resistance in grain mineral accumulation. X- and Y-axis represent alleles and mineral concentration (mg/kg) in wheat grain, respectively.

6.3.8 Identification of biofortified rust resistance donor sources

Fifteen biofortified lines had resistant to moderately resistant (R-MR) rust responses (Table 6.6). Of 31 QTL for grain Zn and Fe concentration, 28 were found in these lines (Table 6.6). Line number 45 tested positive for rust resistance genes (*Lr46, Sr24, Sr31, Sr38*) and carried 25 favourable alleles. This line demonstrated good yield (5.11 t/ha), higher protein content (15.8%), and high grain Zn (39 mg/kg) and Fe content (46 mg/kg). Line number 271 with resistance genes (*Lr46, Sr22, Sr38)* carried 17 favourable alleles and had better yield (6.45 t/ha), higher micronutrient content (>40 mg/kg) and protein content (14%). Line number 56 demonstrated increased Zn and Fe loading (>46 mg/kg) and grain protein content (16%) but was inferior for grain yield (4.11 t/ha).

6.4 Discussion

The discovery of QTL conferring rust resistance and higher mineral accumulation is a constant challenge in wheat breeding programs. In this study, the HarvestPlus association mapping wheat panel was selected and grouped into four subpopulations using principal component analysis. Derivatives of the pre-breeding lines Quaiu, Tukuru and Kuruku clustered into the first subpopulation and these lines have been identified as sources of stem rust and stripe rust resistance against the race TTKST and Mexican pathotypes, respectively (Singh et al. 2000; Kosgey et al. 2015). Quaiu3, a high-yielding CIMMYT spring wheat line, was released as cultivars Koshan09 and Gambo in Afghanistan and Ethiopia, respectively. Rust resistance genes *Lr42*, *Yr29*, *Yr30* and *Yr54* were present in Quaiu3 (Basnet et al. 2013; Basnet et al. 2014). The second and fourth subpopulations included half of the panel and were dominated by derivatives of synthetic hexaploid wheats (SHW). Subpopulation III comprised derivatives of Kachu, Kukuna, Chonte, Pastor, Danphe and *T. spelta.* These parental sources

Table 6.6 List of rust resistance and biofortified lines for stripe (YR), leaf (LR) and stem (SR) rust resistance on 1-9 disease scale and corresponding favourable alleles

ID	YR	LR	SR	#CID	SID	GID	Cross	Fe (mg/kg)	Zn (mg/kg)	Yield (t/ha)	Protein (%)	Favourable alleles (33 MTAs for Rust + 31 MTAs for grain Zn and Fe + known genes)
7	1.7	4.5	2.5	533510	73	6356390	REH/HARE//2*BCN/3/CROC_1/AE.SQUARROSA (213)//PGO/4/HUITES/5/T.SPELTA PI348599/6/REH/HARE//2*BCN/3/CROC_1/AE.SQUARROSA (213)//PGO/4/HUITES/7/QUAIU	40.25	38.75	6.11	13.8	9+15+*Lr46*+*Sr38*
25	3	3	2	521101	139	6354150	NAC/TH.AC//3*PVN/3/MIRLO/BUC/4/2*PASTOR/5/T.DICOCCON PI94624/AE.SQUARROSA (409)//BCN/6/WBLL4//BABAX.1B.1B*2/PRL/3/PASTOR	37.25	30.75	5.83	13.3	3+17+*Lr46*+*Lr23*
35	2.1	3.5	2	522517	110	6354806	GARZA/BOY//AE.SQUARROSA (467)/3/T.DICOCCON PI94625/AE.SQUARROSA (372)//3*PASTOR/4/T.DICOCCON PI94625/AE.SQUARROSA (372)//3*PASTOR	36.25	32.5	5.68	13.5	8+11+*Lr46*
36	2.1	2.5	2	522517	112	6354808	GARZA/BOY//AE.SQUARROSA (467)/3/T.DICOCCON PI94625/AE.SQUARROSA (372)//3*PASTOR/4/T.DICOCCON PI94625/AE.SQUARROSA (372)//3*PASTOR	39.25	36.5	5.23	14.2	8+10+*Lr46*
45	2.8	3	2.5	533511	194	6356407	REH/HARE//2*BCN/3/CROC_1/AE.SQUARROSA (213)//PGO/4/HUITES/5/T.DICOCCON PI94624/AE.SQUARROSA (409)//BCN/6/REH/HARE//2*BCN/3/CROC_1/AE.SQUARROSA (213)//PGO/4/HUITES/7/MUTUS	46	39	5.11	15.8	9+16+*Lr46*+*Sr31*+*Sr38*+*Sr24*
56	3.3	4	2	521104	235	6354171	REH/HARE//2*BCN/3/CROC_1/AE.SQUARROSA (213)//PGO/4/HUITES/5/T.SPELTA PI348599/6/REH/HARE//2*BCN/3/CROC_1/AE.SQUARROSA (213)//PGO/4/HUITES	47.5	46.5	4.11	16.0	10+6+*Lr46*+*Sr31*+*Sr22*
58	2	4.5	2	521105	331	6354171	REH/HARE//2*BCN/3/CROC_1/AE.SQUARROSA (213)//PGO/4/HUITES/5/T.DICOCCON PI94624/AE.SQUARROSA (409)//BCN/6/REH/HARE//2*BCN/3/CROC_1/AE.SQUARROSA (213)//PGO/4/HUITES	43	34	5.24	14.3	8+5+*Lr34*+*Lr46*+*Yr34*+*Sr31*
62	2.3	2.5	2	522490	52	6354364	GTO95.1.20/HUW468/5/SITE/MO/4/NAC/TH.AC//3*PVN/3/MIRLO/BUC	40.75	40.25	5.21	14.0	12+5+*Lr34*+*Lr46*+*Lr23*+*Yr34*

73	2.5	2.5	2	522522	253	6354828	CROC_1/AE.SQUARROSA (444)/3/T.DICOCCON PI94625/AE.SQUARROSA (372)//3*PASTOR/4/T.DICOCCON PI94625/AE.SQUARROSA (372)//3*PASTOR	39.25	32.75	4.55	15.6	8+3+*Lr46+Lr23*
215*	2.9	5	2	537254	302	6575370	T.DICOCCON CI9309/AE.SQUARROSA (409)//MUTUS/3/2*MUTUS	38.25	33	5.50	14.4	6+4+*Lr46+Sr38*
236	2.3	2.5	2.5	537267	115	6575426	COAH90.26.31/4/3*BL2064//SW89-5124*2/FASAN/3/TILHI	38.75	33.5	4.92	13.5	5+14+*Lr46+Yr34*
242	3.2	3	2.5	533466	83	6575441	COAH90.26.31/4/2*BL2064//SW89-5124*2/FASAN/3/TILHI	43	44.25	5.37	14.8	7+15+*Lr34+Lr46+Yr34*
265	2.2	3	2.5	537144	111	6575508	VILLA JUAREZ F2009/3/T.DICOCCON PI94625/AE.SQUARROSA (372)//3*PASTOR/4/WBLL1*2/BRAMBLING	37.25	31.5	5.86	13.4	4+6+*Lr46+Lr23*
271*	3.4	5	2	537254	339	6575529	T.DICOCCON CI9309/AE.SQUARROSA (409)//MUTUS/3/2*MUTUS	40.25	42.25	6.45	14.0	10+7+*Lr46+Sr38+Sr22*
286^	3.3	3.5	2.8	546234	54	6575660	KACHU/SOLALA	38.25	32	5.97	13.5	7+5+*Lr46+Sr38+Lr23*

#CID: Cross identifier; SID: Selection identifier; GID: Genotype identifier. *Released as wheat varieties HPBW01, WB2 (India) and ^BARI Gom33 (Bangladesh).

have been reported for enhanced rust resistance and grain minerals (Kosgey et al. 2015; Velu et al. 2018). This panel has 20 *T. spelta* derivatives that have not been explored for rust resistance.

Confounding phenotypic variation attributable to population structure and genetic relatedness can increase the probability of false negatives (Atwell et al. 2010). MLM approach is widely accepted in the majority of GWAS (Yang et al. 2014a). Population structure and total genetic effects of individuals were fitted as covariates in the MLM approach to minimise false positives (Yu et al. 2006). MTAs identified for rust resistance and grain mineral accumulation in this study were compared with previously published literature to confirm their uniqueness (McIntosh et al. 1995; Yu et al. 2014; Kapfuchira 2015; Maccaferri et al. 2015; Gao et al. 2016; Turner et al. 2017; Wang and Chen 2017; Alomari et al. 2018; Bhatta et al. 2018; Kumar et al. 2018; Pinto da Silva et al. 2018; Velu et al. 2018; Cu et al. 2020).

Previous studies postulated presence of *Yr3, Yr4, Yr6, Yr9/Lr26/Sr31, Yr17/Lr37/Sr38, Yr27, Yr34, Lr1, Lr3a, Lr10, Lr13, Lr16, Lr23, Sr8a, Sr8b, Sr12, Sr24/Lr24* and *Sr30* in CIMMYT wheat germplasms (Singh 1993; Dadkhodaie et al. 2012; Chemayek 2016; Saffdar 2019). Findings of these phenotypic assays and gene-linked markers were used in validation of identified MTAs representing field rust resistance. The outcome of the GWAS and physical position of linked markers (IWGSC RefSeq v 1.0; Appels et al. 2018) were used to align significant MTAs and underlying genes/QTL using Pretzel, a physical map viewing software (https://plantinformatics.io; Keeble-Gagnère et al. 2019) and Wheat@URGI portal (Alaux et al. 2018).

Measurement of mineral content, especially micronutrients is a highly sensitive process. This investigation provided initial information and assessment of contrasting

genotypes for each mineral under different geographical conditions, but more replications will be required to select high yielding genotypes with high mineral loading across diverse environments. The use of rust resistant and high mineral loading genotypes in this study will be useful in tackling malnutrition issues in developing nations.

Three new QTL for stripe rust resistance were observed on chromosome arms 4AS, 5AS and 7DL. The short arm of chromosome arm 4A does not harbour any reported genes/QTL while *Yr51* and *Yr60* were reported on chromosome 4AL (Maccaferri et al. 2015; McIntosh et al. 2017; Wang and Chen 2017). QTL *IWB57629* (4A-58.38 cM) was mapped at 509.1 Mb on chromosome 4A while *Yr51* (715.5-744.3 Mb; Randhawa et al. 2014) and *Yr60* (739.5Mb; Herrera-Foessel et al. 2015) were mapped beyond 715 Mb. Therefore, *IWB57629* was considered a new locus. The short arm of chromosome 5A carries only one QTL *QYr.cau-5AS_AQ24788-53* (325.9 Mb; Quan et al. 2013). QTL *IWA6227* was located at 10.3Mb (5A) and represents a new locus. Chromosome 7DL carried known gene *Yr33* (450.5 Mb; Zahravi et al. 2003; Gebrewahid et al. 2020) that is ineffective in field due to prevalence of *Yr33*-virulent *Pst* pathotype 239 E237A-Yr17+Yr33+. Therefore, *IWB15318* (7DL-596.9 Mb) was considered a new QTL (Table 6.4). All nine QTL for leaf rust resistance were previously reported.

Two new QTL for stem rust resistance were detected. The 2DL-QTL associated with marker *IWB13993* (600.9 Mb) was considered new as no other gene/QTL was previously reported on this arm. *Sr2, Sr12* (500.5 Mb; Hiebert et al. 2016) and other unnamed QTL were reported on chromosome 3B (Rouse et al. 2014 and Yu et al. 2014). However, these were mapped on the short arm or near the centromere on chromosome 3B. A new MTA involving *IWA149* (818.1 Mb) was detected and placed at the telomeric position of chromosome 3BL. To confirm the uniqueness of potential new rust resistance genes, allelism test and additional

marker surveys of underlying QTL/genes are needed. Utilization of diverse sources of the disease resistance in wheat breeding program will enhance the durability of these genes.

Sixteen QTL on chromosomes 1B, 2A, 3A, 3B, 3D, 4A, 5B, 5D, 7A and 7B for B concentration were detected (Table 6.5). None of the previous studies focussed on identifying QTL for B content in wheat. Therefore, all QTL were considered new. Five QTL for Ca accumulation were found on chromosomes 1B, 3B and 6A that coincide well with two previous studies by Kapfuchira (2015) and Bhatta et al. (2018). Five new QTL on chromosomes 6D, 7A, 7B and 7D were identified for Ca accumulation. Four detected QTL on chromosomes 3A, 4B, 6A and 6B for Cu content was aligned well with findings of Bhatta et al. (2018). Four new QTL for Cu accumulation were detected on chromosome 1D, 2B, 3D and 7A. Seven Fe-QTL on chromosomes 1A, 1B, 2B, 2A, 3A and 3B were previously reported. Nine new genomic regions on chromosomes 1B (2), 2B (2), 3A, 3D, 5A, 7A and 7B were detected for Fe content. The new MTAs associated with *IWA6610* (1B-109.7 Mb) and reported QTL *IWB7923* (1B-38.9 Mb) and *IWA3151* (2A-108.46 cM) had major effects on Fe accumulation. Cu et al. (2020) reported that Fe-QTL *IWA3151*-2A can accumulate Zn, and *IWB4872*-3B can favour accumulation of Cu and Mn. Two QTL on chromosomes 1A (*IWB27962*) and 6A (*IWB23484*) for K accumulation represented already known QTL (Kapfuchira 2015). Additional seven QTL for K accumulation were observed on chromosomes 1A, 1B, 2A, 2D, 4A and 5B, and considered new. One of them associated with *IWB41295* (2D-146.3 Mb) had a major effect on the accumulation of K.

Three QTL on chromosome 1B and 4A for Mg concentration were reported QTL by Kapfuchira (2015) and (Bhatta et al. 2018). Seven additional QTL on chromosomes 1A, 2B, 6A and 7A including major effect MTAs *IWB62537* (1A-113.19 cM) and *IWA8135* (1A-133.15 cM) were considered new. Beside Mg accumulation, the MTA involving *IWB62537* also

enhanced loading of Mn and P concentration, and *IWA8135* governed Zn, Mn and P loading in wheat grain. Cu et al. (2020) also reported that QTL spanning the 113.2-113.8 cM region on chromosome 1A that governed Mn, Zn and Fe accumulation in wheat grain.

Three QTL on chromosome 1A, 1B and 6D for Mn content represented known QTL (Kapfuchira 2015; Cu et al. 2020). The remaining six QTL for Mn content was placed on chromosomes 1A, 1B, 3A, 3D and 7B and considered new. *Sr24/Lr24* linked marker *Sr24#12* was associated with Mn accumulation in one environment only. Four QTL on chromosomes 1B, 2A, 3B and 5B for P accumulation were found to be known QTL (Kapfuchira 2015; Cu et al. 2020). Ten new QTL for P accumulation were found on chromosomes 1A, 2D, 3D, 4A, 6A, 6D and 7A. Three QTL for S concentration on chromosome 1B and 5B represented *Sr31/Lr26/Yr9* and known QTL (Kapfuchira 2015; Table 6.5). Seven new QTL for S concentration were detected on chromosomes 1A, 2B, 5B and 7A. One QTL linked with marker *IWB46598* expressed consistent and major effect for S content. Nine QTL on chromosomes 1A, 1B, 2A, 3B, 4A, 5A, 5B and 7B for Zn concentration represented known QTL/MTAs (Kapfuchira 2015; Alomari et al. 2018; Bhatta et al. 2018; Kumar et al. 2018; Cu et al. 2020; Table 6.5). Six new QTL for Zn concentration were found on chromosomes 1A, 1B, 5D, 6A and 7A (Table 6). Of these, markers *IWA8135* (1A-553.1Mb), *IWB8918* (1A-585.8 Mb), *IWB35116* (1B-60.6 cM), *IWB64607* (3B-772.4 Mb), *IWA2365* (5A-547.6 Mb) and *IWA5704* (6A-602.7 Mb) had major effects in Zn accumulation.

Genotypes carrying rust resistance genes *Yr15* and *Lr34/Yr18/Sr57* had a major effect on Zn accumulation, and this is likely the first report of this dual effect. *Sr31/Lr26/Yr9* (1B:1R) linked marker *iag95* expressed a major effect for the accumulation of all ten minerals. Velu et al. (2019) reported association between the 1B:1R segment and higher Zn concentration. Enhanced Cu and Fe accumulation was found in lines carrying *Yr17/Lr37/Sr38*. This study

demonstrated the importance of 1B:1R and the 2NS translocations for enhanced mineral accumulation. There is unlikely to be linkage drag associated with these rust resistance genes as they have been used widely in wheat breeding (Bariana et al. 2007b). Two sister lines of this panel namely, *T. dicoccon* CI9309/*Ae. squarrosa* (409) //Mutus/3/2*Mutus (Line number 215 and 271; GID 6575370 and 6575529) and another line Kachu/Solala (Line number 286; GID: 6575660) are rust resistant, high yielding (≥5.5 t/ha), medium plant height (85.5-93 cm), medium bold seed type (average 1000-seed weight: ~44.2 gm), rich in micronutrients and protein content. These lines have been released as wheat varieties in India (Line number 215 and 271 as varieties HPBW01 and WB2, respectively; Gupta et al. 2017) and Bangladesh (Line number 286 as variety BARI Gom33) (Khondoker et al. 2019; Table 6.6). These cultivars carried the 2NS segment and demonstrated high yield potential. This is a confirmation of the positive association between 2NS and yield as well as multiple disease resistance and higher accumulation of Cu and Fe.

In summary, 33 significant QTL for rust resistance and 117 QTL for ten grain mineral accumulation were identified in this panel. Of the 33 rust resistance QTL, six QTL linked markers namely *IWB57629* (Yr), *IWA6227* (Yr), *IWB15318* (Yr), *IWB35521* (Lr), *IWB13993* (Sr) and *IWA149* (Sr) located on chromosomes 2D, 3B, 4A, 5A and 7D were considered new. Of the 117 MTAs linked to grain mineral concentration, 41 were previously reported and 76 are new. These new QTL valuable sources of rust resistance and mineral accumulation. Deployment of these QTL in future wheat varieties will provide rust resistance and biofortification of minerals. Fifteen elite donors carrying rust resistance, higher micronutrient concentrations and grain protein content were identified in this study for use in wheat improvement programs.

Chapter 7

Conclusions

The worldwide avoidance of yield losses due to rust diseases through resistance breeding is an important endeavour to sustain global food supply. It can also restrict fungicide application to combat environmental pollution. Selection of higher mineral content in future wheat cultivars is also important to alleviate malnutrition in developing nations. Wheat breeding programs rely on genetically diverse sources for economic traits such as disease resistance and end-use quality. The present investigation included high-resolution mapping of *Lr49*, characterisation of two bi-parental RIL populations for stripe rust resistance and association mapping targeting triple rust resistance and grain mineral concentration. This study identified diverse sources of rust resistance and higher micronutrient accumulating marker-trait associations for use in breeding programs.

The development non-gel based kompetitive allele specific PCR markers *sunKASP_21* (0.4 cM proximal) and *sunKASP_24* (0.6 cM distal) linked with *Lr49* will enable pyramiding of this gene with other marker tagged sources of rust resistance. Fine mapping of rust resistance gene *Sr45* (Periyannan et al. 2014), *Sr56* (Bansal et al. 2014b), *Yr47* and *Lr52* (Qureshi et al. 2017) and *Yr34* (Qureshi et al. 2018) using currently available genomic resources including 9K and 90K SNP arrays, sequencing of flow sorted chromosome and genome sequence of Chinese Spring has been performed and closely linked markers were developed. Similarly, Bansal et al. (2020) fine mapped rust resistance genes *Yr70* and *Lr76* through sequencing of flow sorted chromosome 5D. Deployment of these genes in future wheat cultivars in different combinations through marker-assisted selection will facilitate release of tripe rust resistant cultivars.

To provide breeders with genetically diverse sources of rust resistance; a putatively new ASR gene, *YrVL*, was mapped on the long arm of chromosome 2B in 769.1-779.3 Mb region of the physical map of Chinese Spring (IWGSC RefSeq v1.0). In addition to the discovery of this ASR in VL404, two new adult plant resistance loci *QYr.sun-5AL* and *QYr.sun-6DS* were also identified in a Tunisian landrace Aus26670. Of the total 83 catalogued stripe rust resistance genes, 37 have been designated in the last decade. This strong discovery record highlights the advancements in genomic resources and their implementation in research programs. Rosewarne et al. (2013) and Maccaferri et al. (2015) compiled QTL analysis results from various studies. Many QTL have been identified in more than one study indicating the presence of those loci at a higher frequency. The named APR loci *Yr18* and *Yr29* represented this class. A bi-parental mapping population segregating for a single new QTL can be used for detailed mapping. Bariana et al. (2016) isolated one of the QTL identified on chromosome 3D of Australian cultivar Sunco and reported markers linked closely with this locus. This locus was formally named *Yr71*. The transfer of genetically diverse sources of resistance into well adapted modern wheat backgrounds is important for achieving durable control. For example, stripe rust resistance genes *Yr51* and *Yr57* were transferred into stripe rust susceptible Australian and Indian cultivars under the Indo-Australian collaboration and material was distributed to wheat breeders (Randhawa et al. 2019).

While disease resistance is an important objective in wheat improvement programs worldwide, breeding for nutritional quality has also attracted attention in the last couple of decades. Genome-wide association study of a HarvestPlus Association Mapping panel identified three new QTL for stripe rust (*IWB57629*-4A, *IWA6227*-5A, *IWB15318*-7D), one for leaf rust (*IWB35521*-4A), two for stem rust resistance (*IWB13993*-2D, *IWA149*-3B) and 76 for accumulation of 10 minerals. Accessions carrying 1B:1R translocation displayed higher accumulation of all the minerals. The 2NS segment from *Aegilops ventricosa* showed higher

accumulation of Cu and Fe compared to non-2NS lines. In addition to these alien translocations, some association for mineral accumulation were observed in the spelt and common wheat accessions. Enhanced Zn accumulation was observed in accessions carrying *Yr15* and *Yr18*. A new pleiotropic locus accumulating Zn, Mg, Mn and P was identified on chromosome 1AL. Fifteen biofortified accessions expressing acceptable levels of rust resistance under field conditions were selected as donor sources. Various studies have identified genomic regions that control mineral accumulation in wheat grain using bi-parental populations or limited number of entries. These include QTL for Mn and P content (Kapfuchira 2015; Cu et al. 2020), Zn content (Kapfuchira 2015; Alomari et al. 2018; Bhatta et al. 2018; Kumar et al. 2018; Cu et al. 2020), Mg content (Kapfuchira 2015; Bhatta et al. 2018), K content (Kapfuchira 2015) and Cu content (Bhatta et al. 2018). A careful comparison of results across different studies is essential to identify genotypes accumulating the target mineral in diverse geographical regions.

Overall, this investigation delivered selection technology (markers closely linked with adult plant leaf rust resistance gene *Lr49*), new sources of rust (*YrVL*, *QYr.sun-5AL* and *QYr.sun-6DS*) and genotypes carrying combination of higher mineral content with triple rust resistance. The results of this study will enable breeders to release rust resistant and better nutritional quality wheat cultivars.

Future directions

The continuation of research on aspects studied in this project will enable:

1. Cloning of *Lr49* and development of a perfect marker.
2. High resolution mapping of *YrVL*.
3. Detailed mapping of *QYr.sun-5AL* and *QYr.sun-6DS*.

4. Incorporation of reported QTL/genomic loci in genomic selection of elite wheat lines.
5. Development of donors carrying new loci for higher accumulation of micronutrients.

References

Aciksoz SB, Ozturk L, Gokmen OO, Römheld V, Cakmak I (2011) Effect of nitrogen on root release of phytosiderophores and root uptake of Fe (III)-phytosiderophore in Fe-deficient wheat plants. Physiol Plant 142:287-296

Acquaah G (2009) Principles of Plant Genetics and Breeding. John Wiley & Sons pp.1-540

Admassu B, Friedt W, Ordon F (2012) Stem rust seedling resistance genes in Ethiopian wheat cultivars and breeding lines. Afric Crop Sci J 20:149-162

Agenbag G, Pretorius Z, Boyd L, Bender C, Prins R (2012) Identification of adult plant resistance to stripe rust in the wheat cultivar Cappelle-Desprez. Theor Appl Genet 125:109-120

Ahmed NU, Trethowan RM (2020) A Rapid Breeding Technology of Wheat. Science and Technology Innovation for a Sustainable Economy. Springer, pp 109-119

Alaux M, Rogers J, Letellier T, Flores R, Alfama F, Pommier C, Mohellibi N, Durand S, Kimmel E, Michotey C (2018) Linking the International Wheat Genome Sequencing Consortium bread wheat reference genome sequence to wheat genetic and phenomic data. Genom Biol 19:111-115

Ali S, Rodriguez-Algaba J, Thach T, Sørensen CK, Hansen JG, Lassen P, Nazari K, Hodson DP, Justesen AF, Hovmøller MS (2017) Yellow rust epidemics worldwide were caused by pathogen races from divergent genetic lineages. Front Plan Sci 8:1057

Allard RW (1999) Principles of Plant Breeding. John Wiley & Sons pp. 1-264

Allen AM, Winfield MO, Burridge AJ, Downie RC, Benbow HR, Barker GL and Davassi A (2017). Characterization of a Wheat Breeders' Array suitable for high-throughput SNP genotyping of global accessions of hexaploid bread wheat (*Triticum aestivum*). Plant Biotechnol J 15:390-401

Alomari DZ, Eggert K, Von Wirén N, Alqudah AM, Polley A, Plieske J, Ganal MW, Pillen K, Röder MS (2018) Identifying candidate genes for enhancing grain Zn concentration in wheat. Front Plant Sci 9:1313-1318

Anderson LK, Lai A, Stack SM, Rizzon C, Gaut BS (2006) Uneven distribution of expressed sequence tag loci on maize pachytene chromosomes. Genome Res 16:115-122

Anonymous (2001). Institute of Medicine (US) panel on micronutrients. Dietary reference intakes for Vitamin A, Vitamin K, Arsenic, Boron, Chromium, Copper, Iodine, Iron, Manganese, Molybdenum, Nickel, Silicon, Vanadium, and Zinc. Washington (DC): National Academies Press (US) pp. 260-266 Available from: https://www.ncbi.nlm.nih.gov/books/NBK222309/

Appels R, Eversole K, Stein N, Feuillet C, Keller B, Rogers J, Pozniak CJ, Choulet F, Distelfeld A, Poland J, Ronen G, Sharpe AG, Barad O, Baruch K, Keeble-Gagnère G, Mascher M, Ben-Zvi G, Josselin A-A, Himmelbach A, Balfourier F, Gutierrez-Gonzalez J, Hayden M, Koh C, Muehlbauer G, Pasam RK, Paux E, Rigault P, Tibbits J, Tiwari V, Spannagl M, Lang D, Gundlach H, Haberer G, Mayer KFX, Ormanbekova D, Prade V, Šimková H, Wicker T, Swarbreck D, Rimbert H, Felder M, Guilhot N, Kaithakottil G, Keilwagen J, Leroy P, Lux T, Twardziok S, Venturini L, Juhász A, Abrouk M, Fischer I, Uauy C, Borrill P, Ramirez-Gonzalez RH, Arnaud D, Chalabi S, Chalhoub B, Cory A, Datla R, Davey MW, Jacobs J, Robinson SJ, Steuernagel B, van Ex F, Wulff BBH, Benhamed M, Bendahmane A, Concia L, Latrasse D, Bartoš J, Bellec A, Berges H, Doležel J, Frenkel Z, Gill B, Korol A, Letellier T, Olsen O-A, Singh K, Valárik M, van der Vossen E, Vautrin S, Weining S, Fahima T, Glikson V, Raats D, Číhalíková J, Toegelová H, Vrána J, Sourdille P, Darrier B, Barabaschi D, Cattivelli L, Hernandez P, Galvez S, Budak H, Jones JDG, Witek K, Yu G, Small I, Melonek J, Zhou R, Belova T, Kanyuka K, King R, Nilsen

K, Walkowiak S, Cuthbert R, Knox R, Wiebe K, Xiang D, Rohde A, Golds T, Čížková J, Akpinar BA, Biyiklioglu S, Gao L, N'Daiye A, Kubaláková M, Šafář J, Alfama F, Adam-Blondon A-F, Flores R, Guerche C, Loaec M, Quesneville H, Condie J, Ens J, Maclachlan R, Tan Y, Alberti A, Aury J-M, Barbe V, Couloux A, Cruaud C, Labadie K, Mangenot S, Wincker P, Kaur G, Luo M, Sehgal S, Chhuneja P, Gupta OP, Jindal S, Kaur P, Malik P, Sharma P, Yadav B, Singh NK, Khurana JP, Chaudhary C, Khurana P, Kumar V, Mahato A, Mathur S, Sevanthi A, Sharma N, Tomar RS, Holušová K, Plíhal O, Clark MD, Heavens D, Kettleborough G, Wright J, Balcárková B, Hu Y, Salina E, Ravin N, Skryabin K, Beletsky A, Kadnikov V, Mardanov A, Nesterov M, Rakitin A, Sergeeva E, Handa H, Kanamori H, Katagiri S, Kobayashi F, Nasuda S, Tanaka T, Wu J, Cattonaro F, Jiumeng M, Kugler K, Pfeifer M, Sandve S, Xun X, Zhan B, Batley J, Bayer PE, Edwards D, Hayashi S, Tulpová Z, Visendi P, Cui L, Du X, Feng K, Nie X, Tong W, Wang L (2018) Shifting the limits in wheat research and breeding using a fully annotated reference genome. Science 361:eaar7191:1-13Arora S, Steuernagel B, Gaurav K, Chandramohan S, Long Y, Matny O, Johnson R, Enk J, Periyannan S, Singh N (2019a) Resistance gene cloning from a wild crop relative by sequence capture and association genetics. Nature Biotech 37:139-142

Arora S, Steuernagel B, Gaurav K, Chandramohan S, Long Y, Matny O, Johnson R, Enk J, Periyannan S, Singh N (2019a) Resistance gene cloning from a wild crop relative by sequence capture and association genetics. Nature Biotech 37:139-143

Arora S, Cheema J, Poland J, Uauy C, Chhuneja P (2019b) Genome-Wide Association Mapping of Grain Micronutrients Concentration in Aegilops tauschii. Front Plant Sci 10:1-8

Ashburner M (1989) Drosophila. A laboratory handbook. Cold Spring Harbor Laboratory Press pp.1-1409

Atwell S, Huang YS, Vilhjálmsson BJ, Willems G, Horton M, Li Y, Meng D, Platt A, Tarone AM, Hu TT (2010) Genome-wide association study of 107 phenotypes in *Arabidopsis thaliana* inbred lines. Nature 465:627-631

Avni R, Nave M, Barad O, Baruch K, Twardziok SO, Gundlach H, Hale I, Mascher M, Spannagl M, Wiebe K (2017) Wild emmer genome architecture and diversity elucidate wheat evolution and domestication. Sci 357:93-97

Ayliffe M, Singh R, Lagudah E (2008) Durable resistance to wheat stem rust needed. Current opinion in plant biology 11:187-192

Bansal U, Forrest K, Hayden M, Miah H, Singh D, Bariana H (2011) Characterisation of a new stripe rust resistance gene *Yr47* and its genetic association with the leaf rust resistance gene *Lr52*. Theor Appl Genet 122:1461-1466

Bansal UK, Arief V, Miah H, DeLacy IH, Bariana, HS. (2010). Association mapping of rust resistance in pre-green revolution wheat accessions. Borlaug Global Rust Initiative 2010 Technical Workshops. St. Petersburg Russia. 30-31 May 2010 pp.45

Bansal UK, Arief VN, DeLacy IH, Bariana HS (2013) Exploring wheat landraces for rust resistance using a single marker scan. Euphytica 194:219-233

Bansal UK, Kazi AG, Singh B, Hare RA, Bariana HS (2014a) Mapping of durable stripe rust resistance in a durum wheat cultivar Wollaroi. Mole Breed 33:51-59

Bansal U, Bariana H, Wong D, Randhawa M, Wicker T, Hayden M, Keller B (2014b) Molecular mapping of an adult plant stem rust resistance gene *Sr56* in winter wheat cultivar Arina. Theor Appl Genet 127:1441-1448

Bansal UK, Muhammad S, Forrest KL, Hayden MJ, Bariana HS (2015) Mapping of a new stem rust resistance gene *Sr49* in chromosome 5B of wheat. Theor Appl Genet 128:2113-2119

Bansal M, Adamski NM, Toor PI, Kaur S, Molnár I, Holušová K, Vrána J, Doležel J, Valárik M, Uauy C, Chhuneja P (2020) *Aegilops umbellulata* introgression carrying leaf rust and stripe rust resistance genes *Lr76* and *Yr70* located to 9.47-Mb region on 5DS telomeric end through a combination of chromosome sorting and sequencing. Theor Appl Genet 133:903-915

Bariana HS, Hayden MJ, Ahmed N, Bell J, Sharp P, McIntosh R (2001) Mapping of durable adult plant and seedling resistances to stripe rust and stem rust diseases in wheat. Crop Past Sci 52:1247-1255

Bariana HS (2003) Breeding for disease resistance. In:Thomas B, Murphy DJ, Murray BG (eds) Encyclopedia of Applied Plant Sciences. Harcourt, Academic Press, UK, pp 244–253

Bariana H, Brown G, Bansal U, Miah H, Standen G, Lu M (2007a) Breeding triple rust resistant wheat cultivars for Australia using conventional and marker-assisted selection technologies. Crop Past Sci 58:576-587

Bariana HS, Miah H, Brown GN, Willey N, Lehmensiek A (2007b) Molecular mapping of durable rust resistance in wheat and its implication in breeding. In: Wheat production in stressed environments. Developments in Plant Breeding. Springer Publ 12:723-728

Bariana HS, Bansal UK, Schmidt A, Lehmensiek A, Kaur J, Miah H, Howes N, McIntyre CL (2010) Molecular mapping of adult plant stripe rust resistance in wheat and identification of pyramided QTL genotypes. Euphytica 176:251-260

Bariana H, Forrest K, Qureshi N, Miah H, Hayden M, Bansal U (2016) Adult plant stripe rust resistance gene *Yr71*. Mol Breed 36:1-10

Bariana HS, Bansal UK (2017) Breeding for rust resistance. In: Encyclopedia of Applied Plant Sciences, 2nd edition Elsevier, Amsterdam. pp 69–76

Basnet B, Singh R, Herrera-Foessel S, Ibrahim A, Huerta-Espino J, Calvo-Salazar V, Rudd J (2013) Genetic analysis of adult plant resistance to yellow rust and leaf rust in common spring wheat Quaiu 3. Plant Dis 97:728-736

Basnet B, Singh R, Ibrahim A, Herrera-Foessel S, Huerta-Espino J, Lan C, Rudd J (2014) Characterization of *Yr54* and other genes associated with adult plant resistance to yellow rust and leaf rust in common wheat Quaiu 3. Mole Breed 33:385-399

Beddow JM, Pardey PG, Chai Y, Hurley TM, Kriticos DJ, Braun H-J, Park RF, Cuddy WS, Yonow T (2015) Research investment implications of shifts in the global geography of wheat stripe rust. Nat Plant 1:1-5

Benjamini Y, Hochberg Y (1995) Controlling the false discovery rate: a practical and powerful approach to multiple testing. J Royal Statis Soci: series B (Methodological) 57:289-300

Bernardo R (2020) Breeding for Quantitative Traits in Plants, Third edn. Stemma press Woodbury MN pp.1-411

Bhatta M, Baenziger P, Waters B, Poudel R, Belamkar V, Poland J, Morgounov A (2018) Genome-wide association study reveals novel genomic regions Associated with 10 grain minerals in synthetic hexaploid wheat. Intl J Mol Sci 19:3237-3241

Biffen RH (1905) Mendel's laws of inheritance and wheat breeding. J Agri Sci 1:4-48

Bipinraj A, Honrao B, Prashar M, Bhardwaj S, Rao S, Tamhankar S (2011) Validation and identification of molecular markers linked to the leaf rust resistance gene *Lr28* in wheat. J Appl Genet 52:171-175

Black RE, Victora CG, Walker SP, Bhutta ZA, Christian P, De Onis M, Ezzati M, Grantham-McGregor S, Katz J, Martorell R (2013) Maternal and child undernutrition and overweight in low-income and middle-income countries. Lanc 382:427-451

Borrill P, Adamski N, Uauy C (2015) Genomics as the key to unlocking the polyploid potential of wheat. New Phyt 208:1008-1022

Bouis HE (2003) Micronutrient fortification of plants through plant breeding: can it improve nutrition in man at low cost? Proc Nutri Soci 62:403-411

Bouis HE, Hotz C, McClafferty B, Meenakshi J, Pfeiffer WH (2011) Biofortification: a new tool to reduce micronutrient malnutrition. Food Nutri Bull 32:31-40

Boukhatem N, Baret P, Mingeot D, Jacquemin J (2002) Quantitative trait loci for resistance against yellow rust in two wheat-derived recombinant inbred line populations. Theor Appl Genet 104:111-118

Bradbury PJ, Zhang Z, Kroon DE, Casstevens TM, Ramdoss Y, Buckler ES (2007) TASSEL:software for association mapping of complex traits in diverse samples. Bioinfor 23:2633-2635

Brenchley R, Spannagl M, Pfeifer M, Barker GL, D'Amore R, Allen AM, McKenzie N, Kramer M, Kerhornou A, Bolser D (2012) Analysis of the bread wheat genome using whole-genome shotgun sequencing. Nature 491:705-710

Broadley SA, Hartl FU (2009) The role of molecular chaperones in human misfolding diseases. FEBS Letter 583:2647-2653

Brown JK, Hovmøller MS (2002) Aerial dispersal of pathogens on the global and continental scales and its impact on plant disease. Sci 297:537-541

Buckler E, Bradbury P, Kroon D (2007) TASSEL: Trait Association, Evolution, and Linkage Analysis software package. Buckler Lab for Maize Genetics and Diversity

Bulli P, Zhang J, Chao S, Chen X, Pumphrey M (2016) Genetic architecture of resistance to stripe rust in a global winter wheat germplasm collection. G3: Gen Genom Genet 6:2237-2253

Cakmak I, Ozkan H, Braun H, Welch R, Romheld V (2000) Zinc and iron concentrations in seeds of wild, primitive, and modern wheats. Food Nutri Bullet 21:401-403

Çakmak İ, Torun A, Millet E, Feldman M, Fahima T, Korol A, Nevo E, Braun H, Özkan H (2004) *Triticum dicoccoides*: an important genetic resource for increasing zinc and iron concentration in modern cultivated wheat. Soil Sci Plan Nutri 50:1047-1054

Cakmak I (2008) Enrichment of cereal grains with zinc: agronomic or genetic biofortification? Plan Soil 302:1-17

Cakmak I, Pfeiffer WH, McClafferty B (2010) Biofortification of durum wheat with zinc and iron. Cer Chemis 87:10-20

Calderini DF, Ortiz-Monasterio I (2003) Are synthetic hexaploids a means of increasing grain element concentrations in wheat? Euphytica 134:169-178

Calus MP, Vandenplas J (2018) SNPrune: an efficient algorithm to prune large SNP array and sequence datasets based on high linkage disequilibrium. Genet Selec Evol 50:34-37

Cavanagh CR, Chao S, Wang S, Huang BE, Stephen S, Kiani S, Forrest K, Saintenac C, Brown-Guedira GL, Akhunova A (2013) Genome-wide comparative diversity uncovers multiple targets of selection for improvement in hexaploid wheat landraces and cultivars. Proc Natl Acad Sci 110:8057-8062

Chapman JA, Mascher M, Buluç A, Barry K, Georganas E, Session A, Strnadova V, Jenkins J, Sehgal S, Oliker L (2015) A whole-genome shotgun approach for assembling and anchoring the hexaploid bread wheat genome. Genom Biol 16:26-32

Chemayek B (2016) Studies on Resistance to Biotic and Abiotic Stresses in Wheat. PhD thesis The University of Sydney pp. 1-186

Chen J, Chu C, Souza EJ, Guttieri MJ, Chen X, Xu S, Zemetra R (2012) Genome-wide identification of QTL conferring high-temperature adult-plant (HTAP) resistance to stripe rust (*Puccinia striiformis* f. sp. *tritici*) in wheat. Mol Breed 29:791-800

Chen X (2014). Integration of cultivar resistance and fungicide application for control of wheat stripe rust. Canad J Plant Pathol 36:311-326

Chen S, Rouse MN, Zhang W, Zhang X, Guo Y, Briggs J, Dubcovsky J (2020) Wheat gene *Sr60* encodes a protein with two putative kinase domains that confers resistance to stem rust. New Phytologist 225:948-959

Cheng P, Chen XM (2010). Molecular mapping of a gene for stripe rust resistance in spring wheat cultivar IDO377s. Theor Appl Genet 121:195-204

Cheng B, Gao X, Cao N, Ding Y, Gao Y, Chen T, Xin Z, Zhang L (2020) Genome-wide association analysis of stripe rust resistance loci in wheat accessions from southwestern China. J Appl Genetics:1-14

Chhetri M (2015) Molecular Mapping and Genetic Characterization of Rust Resistance in Wheat. PhD thesis University of Sydney Australia pp.1-96

Chhetri M, Bariana H, Wong D, Sohail Y, Hayden M, Bansal U (2017) Development of robust molecular markers for marker-assisted selection of leaf rust resistance gene *Lr23* in common and durum wheat breeding programs. Mol Breed 37:21

Chhuneja P, Kaur S, Garg T, Ghai M, Kaur S, Prashar M, Bains N, Goel R, Keller B, Dhaliwal H (2008) Mapping of adult plant stripe rust resistance genes in diploid A genome wheat species and their transfer to bread wheat. Theor Appl Genet 116:313-324

Cu ST, Guild G, Nicolson A, Velu G, Singh R, Stangoulis J (2020) Genetic dissection of zinc, iron, copper, manganese and phosphorus in wheat (*Triticum aestivum* L.) grain and rachis at two developmental stages. Plant Sci 291:110338

Cuddy W, Hollaway G (2018) Detection of a new wheat stripe rust pathotype in Victoria. Cereal Rust Rep 16:1

Cui F, Zhang N, Fan X, Zhang W, Zhao C, Yang L, Zhao X (2017). Utilization of a wheat 660K SNP array-derived high-density genetic map for high-resolution mapping of a major QTL for kernel number. Scient Rep 7:1-12

Dadkhodaie N, Singh D, Park R (2011) Characterisation of resistance to leaf rust in an international bread wheat nursery. J Plan Pathol 93:627-641

Daetwyler HD, Bansal UK, Bariana HS, Hayden MJ, Hayes BJ (2014) Genomic prediction for rust resistance in diverse wheat landraces. Theor Appl Genet 127:1795-1803

Dean R, Van Kan JA, Pretorius ZA, Hammond-Kosack KE, Di Pietro A, Spanu PD, Rudd JJ, Dickman M, Kahmann R, Ellis J (2012). The top 10 fungal pathogens in molecular plant pathology. Molec Plan Pathol 13: 414-430

Distelfeld A, Cakmak I, Peleg Z, Ozturk L, Yazici AM, Budak H, Saranga Y, Fahima T (2007) Multiple QTL-effects of wheat *Gpc-B1* locus on grain protein and micronutrient concentrations. Physiol Plant 129:635-643

Doyle JJ, Doyle JL (1987) A rapid DNA isolation procedure for small quantities of fresh leaf tissue. Phytochem Bullet 19:11-15

Elshire R J, Glaubitz JC, Sun Q, Poland JA, Kawamoto K, Buckler ES, Mitchell SE (2011) A robust, simple genotyping-by-sequencing (GBS) approach for high diversity species. PloS One 6:19379-19383

Endelman JB (2011) Ridge regression and other kernels for genomic selection with R package rrBLUP. Plant Genome 4:250-255

Erenoglu EB, Kutman UB, Ceylan Y, Yildiz B, Cakmak I (2011) Improved nitrogen nutrition enhances root uptake, root-to-shoot translocation and remobilization of zinc (65^{Zn}) in wheat. New Phytol 189:438-448

Falush D, Stephens M, Pritchard JK (2007) Inference of population structure using multilocus genotype data: dominant markers and null alleles. Mol Ecol Not 7:574-578

Feng J, Zuo L, Zhang Z, Lin R, Cao Y, Xu S (2011) Quantitative trait loci for temperature-sensitive resistance to *Puccinia striiformis f. sp. tritici* in wheat cultivar Flinor. Euphytica 178:321-329

Feuillet C, Travella S, Stein N, Albar L, Nublat A, Keller B (2003) Map-based isolation of the leaf rust disease resistance gene *Lr10* from the hexaploid wheat (*Triticum aestivum* L.) genome. Proc Natl Acad Sci 100:15253-15258

Fu D, Uauy C, Distelfeld A, Blechl A, Epstein L, Chen X, Sela H, Fahima T, Dubcovsky J (2009) A *kinase-START* gene confers temperature-dependent resistance to wheat stripe rust. Sci 323:1357-1360

Gao L, Turner MK, Chao S, Kolmer J, Anderson JA (2016) Genome wide association study of seedling and adult plant leaf rust resistance in elite spring wheat breeding lines. PLoS One 11:e0148671:1-7

Gebrewahid TW, Zhang P, Zhou Y, Yan X, Xia X, He Z, Liu D, Li Z (2020) QTL mapping of adult plant resistance to stripe rust and leaf rust in a Fuyu 3/Zhengzhou 5389 wheat population. Crop J 8:655-665

Genc Y, Verbyla A, Torun A, Cakmak I, Willsmore K, Wallwork H, McDonald G (2009) Quantitative trait loci analysis of zinc efficiency and grain zinc concentration in wheat using whole genome average interval mapping. Plan Soil 314:49-52

Gessese M, Bariana H, Wong D, Hayden M, Bansal U (2019) Molecular mapping of stripe rust resistance gene *Yr81* in a common wheat landrace Aus27430. Plant Dis 103:1166-1171

Gerard GS, Kobiljski B, Lohwasser U, Börner A, Simon MR (2018) Genetic architecture of adult plant resistance to leaf rust in a wheat association mapping panel. Plant Pathology 67:584-594

Giorgi D, Farina A, Grosso V, Gennaro A, Ceoloni C, Lucretti S (2013) FISHIS: fluorescence in situ hybridization in suspension and chromosome flow sorting made easy. PLoS One 8:e57994:1-4

Gomez-Becerra HF, Erdem H, Yazici A, Tutus Y, Torun B, Ozturk L, Cakmak I (2010) Grain concentrations of protein and mineral nutrients in a large collection of spelt wheat grown under different environments. J Cere Sci 52:342-349

Gupta A, Kumar V, Singh C, Tiwari V (2017) Development and release of new wheat and barley varieties for different zones and states J Wheat Res 9:68-71

Gupta PK, Balyan HS, Sharma S, Kumar R (2020) Genetics of yield, abiotic stress tolerance and biofortification in wheat (*Triticum aestivum* L.). Theor Appl Genet 133:1569–1602

Haldane J (1919) The probable errors of calculated linkage values, and the most accurate method of determining gametic from certain zygotic series. J Genetics 8:291-297

Hao Y, Chen Z, Wang Y, Bland D, Buck J, Brown-Guedira G, Johnson J (2011) Characterization of a major QTL for adult plant resistance to stripe rust in US soft red winter wheat. Theor Appl genetics 123:1401-1411

Hare R, McIntosh R (1979) Genetic and cytogenetic studies of durable adult-plant resistances in 'Hope' and related cultivars to wheat rusts. Zeitsch Pflanz J Plan Breed 83:350-367

Helguera M, Khan IA, Dubcovsky J (2000) Development of PCR markers for wheat leaf rust resistance gene *Lr47*. Theor Appl Genet 101:625-631

Helguera M, Khan I, Kolmer J, Lijavetzky D, Zhong-Qi L, Dubcovsky J (2003) PCR assays for the *Lr37-Yr17-Sr38* cluster of rust resistance genes and their use to develop isogenic hard red spring wheat lines. Crop Sci 43:1839-1847

Herrera-Foessel SA, Singh RP, Huerta-Espino J, Rosewarne GM, Periyannan SK, Viccars L, Calvo-Salazar V, Lan C, Lagudah ES (2012) *Lr68*: a new gene conferring slow rusting resistance to leaf rust in wheat. Theor Appl Genet 124:1475-1486

Herrera-Foessel S, Singh R, Lan C, Huerta-Espino J, Calvo-Salazar V, Bansal U, Bariana H, Lagudah E (2015) *Yr60*, a gene conferring moderate resistance to stripe rust in wheat. Plant Dis 99:508-511

Hiebert CW, Kolmer JA, McCartney CA, Briggs J, Fetch T, Bariana H, Choulet F, Rouse MN, Spielmeyer W (2016) Major gene for field stem rust resistance co-locates with resistance gene *Sr12* in 'Thatcher'wheat. PloS One 11:e0157029:1-8

Hovmøller MS, Justesen AF (2007) Rates of evolution of avirulence phenotypes and DNA markers in a northwest European population of *Puccinia striiformis* f. sp. *tritici*. Mol Ecol 16:4637-4647

Huang L, Brooks SA, Li W, Fellers JP, Trick HN, Gill BS (2003) Map-based cloning of leaf rust resistance gene *Lr21* from the large and polyploid genome of bread wheat. Genet 164:655-664

Jayatilake DV, Tucker EJ, Bariana H, Kuchel H, Edwards J, McKay AC, Chalmers K, Mather DE (2013) Genetic mapping and marker development for resistance of wheat against the root lesion nematode *Pratylenchus neglectus*. BMC Plant Biol 13:230-234

Jighly A, Alagu M, Makdis F, Singh M, Singh S, Emebiri LC, Ogbonnaya FC (2016) Genomic regions conferring resistance to multiple fungal pathogens in synthetic hexaploid wheat. Mol Breed 36:127-131

Jordan KW, Wang S, Lun Y, Gardiner L-J, MacLachlan R, Hucl P, Wiebe K, Wong D, Forrest KL, Sharpe AG (2015) A haplotype map of allohexaploid wheat reveals distinct patterns of selection on homoeologous genomes. Genom Biol 16:48-52

Joukhadar R, Hollaway G, Shi F, Kant S, Forrest K, Wong D, Petkowski J, Pasam R, Tibbits J, Bariana H, Bansal U, Spangenberg G, Daetwyler H, Gendall T, Hayden M (2020) Genome-wide association reveals a complex architecture for rust resistance in 2300 worldwide bread wheat accessions screened under various Australian conditions. Theor Appl Genet 133:2695–2712

Juliana P, Rutkoski JE, Poland JA, Singh RP, Murugasamy S, Natesan S, Barbier H, Sorrells ME (2015) Genome-wide association mapping for leaf tip necrosis and pseudo-black chaff in relation to durable rust resistance in wheat. Plan Genom 8:1-12

Juliana P, Singh RP, Singh PK, Poland JA, Bergstrom GC, Huerta-Espino J, Sorrells ME (2018) Genome-wide association mapping for resistance to leaf rust, stripe rust and tan spot in wheat reveals potential candidate genes. Theor Appl Genet 131:1405-1422

Kandiah P, Bariana H, Qureshi N, Wong D, Hayden M, Bansal U (2019) Identification of a new source of stripe rust resistance *Yr82* in wheat. Theor Appl Genet 132:3169–3176

Kankwatsa P, Singh D, Thomson PC, Babiker EM, Bonman JM, Newcomb M, Park RF (2017) Characterization and genome-wide association mapping of resistance to leaf rust, stem rust and stripe rust in a geographically diverse collection of spring wheat landraces. Molec Breed 37:113-117

Kapfuchira T (2015) Genetics of Biofortified Wheat. PhD thesis The University of Sydney:1-308

Kassa MT, You FM, Hiebert CW, Pozniak CJ, Fobert PR, Sharpe AG, Menzies JG, Humphreys DG, Harrison NR, Fellers JP (2017) Highly predictive SNP markers for efficient selection of the wheat leaf rust resistance gene *Lr16*. BMC Plant Biol 17:45-49

Keeble-Gagnère G, Isdale D, Suchecki R, Kruger A, Lomas K, Carroll D, Tibbits J (2019) Integrating past, present and future wheat research with Pretzel. BioRxiv 517953: doi: 10.1101/517953:1-3

Keller B, Wicker T, Krattinger SG (2018) Advances in wheat and pathogen genomics: implications for disease control. Ann Rev Phytopath 56:67-87

Khondoker A, Mottaleb VG, Singh PK, Kai S, Xinyao H, Singh RP, Joshi AK, Naresh CD B, Gideon K, Olaf E (2019) Economic benefits of blast-resistant biofortified wheat in Bangladesh: The case of BARI Gom 33. Crop Protec 123:45-58

Klymiuk V, Yaniv E, Huang L, Raats D, Fatiukha A, Chen S, Feng L, Frenkel Z, Krugman T, Lidzbarsky G (2018) Cloning of the wheat *Yr15* resistance gene sheds light on the plant tandem kinase-pseudokinase family. Natur Comm 9:3735-3740 doi: 10.1038/s41467-018-06138-9

Kolmer JA, Singh RP, Garvin DF, Viccars L, William HM, Huerta-Espino J, Ogbonnaya FC, Raman H, Orford S, Bariana HS (2008) Analysis of the rust resistance region in wheat germplasm. Cro Sci 48:1841-1852

Korte A, Farlow A (2013) The advantages and limitations of trait analysis with GWAS: a review. Plant Method 9:1-9

Kosambi D (1943) The estimation of map distances from recombination values. Ann Hum Genet 12:172-175

Kosgey Z, Owuoche JO, Kiror M, Njau PN (2015) Inheritance of stem rust (*Puccinia graminis* Pers. f. sp. *tritici* ericks and E. Hen) resistance in bread wheat (*Triticum aestivum*) lines to TTKST races. IJAAR 7:1-13

Krattinger SG, Lagudah ES, Spielmeyer W, Singh RP, Huerta-Espino J, McFadden H, Bossolini E, Selter LL, Keller B (2009) A putative ABC transporter confers durable resistance to multiple fungal pathogens in wheat. Sci 323:1360-1363

Kumar J, Saripalli G, Gahlaut V, Goel N, Meher PK, Mishra KK, Mishra PC, Sehgal D, Vikram P, Sansaloni C, Singh S, Sharma PK, Gupta PK (2018) Genetics of Fe, Zn, β-carotene, GPC and yield traits in bread wheat (*Triticum aestivum* L.) using multi-locus and multi-traits GWAS. Euphytica 214:1-17

Kumar S, Palve A, Joshi C, Srivastava RK, Rukhsar (2019) Crop biofortification for iron (Fe), zinc (Zn) and vitamin A with transgenic approaches. Heliyon 5:e01914:1-8

Kutman UB, Yildiz B, Cakmak I (2011) Improved nitrogen status enhances zinc and iron concentrations both in the whole grain and the endosperm fraction of wheat. J Cere Sci 53:118-125

Lagudah E, McFadden H, Singh R, Huerta-Espino J, Bariana, H, Spielmeyer, W (2006). Molecular genetic characterization of the *Lr34/Yr18* slow rusting resistance gene region in wheat. Theor Appl Genet 114:21-30

Lan C, Liang S, Zhou X, Zhou G, Lu Q, Xia X, He Z (2010) Identification of genomic regions controlling adult-plant stripe rust resistance in Chinese landrace Pingyuan 50 through bulked segregant analysis. Phytopathol 100:313-318

Lan C, Rosewarne GM, Singh RP, Herrera-Foessel SA, Huerta-Espino J, Basnet BR, Zhang Y, Yang E (2014) QTL characterization of resistance to leaf rust and stripe rust in the spring wheat line Francolin#1. Mol Breeding 34:789-803

Lebowitz R, Soller M, Beckmann J (1987). Trait-based analyses for the detection of linkage between marker loci and quantitative trait loci in crosses between inbred lines. Theor Appl Genet 73:556-562

Li Z, Xia X, Zhou X, Niu Y, He Z, Zhang Y, Li G, Wan A, Wang D, Chen X (2006) Seedling and slow rusting resistance to stripe rust in Chinese common wheats. Plan Dis 90:1302-1312

Li Z, Lan C, He Z, Singh RP, Rosewarne GM, Chen X, Xia X (2014) Overview and application of QTL for adult plant resistance to leaf rust and powdery mildew in wheat. Crop Sci 54:1907-1925

Li J, Dundas I, Dong C, Li G, Trethowan R, Yang Z, Zhang P (2020) Identification and characterization of a new stripe rust resistance gene *Yr83* on rye chromosome 6R in wheat. Theor Appl Genet 133:1095-1107

Liu W, Frick M, Huel R, Nykiforuk CL, Wang X, Gaudet DA, Eudes F, Conner RL, Kuzyk A, Chen Q (2014) The stripe rust resistance gene *Yr10* encodes an evolutionary-conserved and unique CC–NBS–LRR sequence in wheat. Mol Plant 7:1740-1755

Lowe I, Jankuloski L, Chao S, Chen X, See D, Dubcovsky J (2011) Mapping and validation of QTL which confer partial resistance to broadly virulent post-2000 North American races of stripe rust in hexaploid wheat. Theor App Genet 123:143-157

Lu Y, Lan C, Liang S, Zhou X, Liu D, Zhou G, Xia X (2009) QTL mapping for adult-plant resistance to stripe rust in Italian common wheat cultivars Libellula and Strampelli. Theor Appl Genet 119:1349-1359

Maccaferri M, Zhang J, Bulli P, Abate Z, Chao S, Cantu D, Bossolini E, Chen X, Pumphrey M, Dubcovsky J (2015) A genome-wide association study of resistance to stripe rust (*Puccinia striiformis* f. sp. *tritici*) in a worldwide collection of hexaploid spring wheat (*Triticum aestivum* L.). G3: Gen Genome Genet 5:449-465

Mago R, Spielmeyer W, Lawrence G, Lagudah E, Ellis J, Pryor A (2002) Identification and mapping of molecular markers linked to rust resistance genes located on chromosome 1RS of rye using wheat-rye translocation lines. Theor Appl Genet 104:1317-1324

Mago R, Bariana H, Dundas I, Spielmeyer W, Lawrence G, Pryor A, Ellis J (2005) Development of PCR markers for the selection of wheat stem rust resistance genes *Sr24* and *Sr26* in diverse wheat germplasm. Theor Appl Genet 111:496-504

Mago R, Tabe L, McIntosh RA, Pretorius Z, Kota R, Paux E, Wicker T, Breen J, Lagudah ES, Ellis JG, Spielmeyer W (2011) A multiple resistance locus on chromosome arm 3BS in wheat confers resistance to stem rust (*Sr2*), leaf rust (*Lr27*) and powdery mildew. Theor Appl Genet 123:615-623

Mago R, Verlin D, Zhang P, Bansal U, Bariana H, Jin Y, Ellis J, Hoxha S, Dundas I (2013) Development of wheat–*Aegilops speltoides* recombinants and simple PCR-based markers for *Sr32* and a new stem rust resistance gene on the 2S# 1 chromosome. Theor Appl Genet 126:2943-2955

Mago R, Zhang P, Vautrin S, Šimková H, Bansal U, Luo M-C, Rouse M, Karaoglu H, Periyannan S, Kolmer J (2015) The wheat *Sr50* gene reveals rich diversity at a cereal disease resistance locus. Nat Plant 1:1-6

Mago R, Till B, Periyannan S, Yu G, Wulff BB, Lagudah E (2017) Generation of loss-of-function mutants for wheat rust disease resistance gene cloning. Wheat Rust Diseases. Springer, pp 199-205

Mallard S, Gaudet D, Aldeia A, Abelard C, Besnard AL, Sourdille P, Dedryver F (2005) Genetic analysis of durable resistance to yellow rust in bread wheat. Theor Appl Genet 110:1401-1409

Manly KF, Cudmore JRH, Meer JM (2001) Map Manager QTX cross-platform software for genetic mapping. Mammal Geno 12:930-932

Marchal C, Zhang J, Zhang P, Fenwick P, Steuernagel B, Adamski N, Boyd L, McIntosh R, Wulff B, Berry S (2018) BED-domain containing immune receptors confer 2 diverse resistance spectra to yellow rust. Nat Plant 4:662-668

Mascher M, Richmond TA, Gerhardt DJ, Himmelbach A, Clissold L, Sampath D, Ayling S, Steuernagel B, Pfeifer M, D'Ascenzo M (2013) Barley whole exome capture: a tool for genomic research in the genus *Hordeum* and beyond. Plant J 76:494-505

McAlpine D (1906) The Rusts of Australia: Their Structure, Nature, and Classification. RS Brain, government printer. Pp. 1-76

McIntosh R (2007) From Farrer to the Australian cereal rust control program. Aust J Agri Res 58:550-557

McDonald GK, Mousavvi NM (2009) Increasing the supply of sulphur increases the grain zinc concentration in bread and durum wheat. Proc Intl Plant Nutri Colloq XVI- 1-5

McIntosh R, Wellings C, Park R (1995) Wheat Rusts: An Atlas of Resistance Genes. CSIRO Publishing, Melbourne. pp.1-204

McIntosh R, Dubcovsky J, Rogers WJ, Morris C, Appels R, Xia XC (2017) Catalogue of gene symbols for wheat:2017 supplementary 10-140

Meng L, Li H, Zhang L, Wang J (2015) QTL IciMapping: integrated software for genetic linkage map construction and quantitative trait locus mapping in biparental populations. Crop J 3:269-283

Michelmore RW, Paran I, Kesseli RV (1991) Identification of markers linked to disease-resistance genes by bulked segregant analysis: a rapid method to detect markers in specific genomic regions by using segregating populations. Proc Nat Acad Sci 21:9828-9832

Milus EA, Kristensen K, Hovmøller MS (2009) Evidence for increased aggressiveness in a recent widespread strain of *Puccinia striiformis* f. sp. *tritici* causing stripe rust of wheat. Phytopath 99:89-94

Monasterio I, Graham RD (2000) Breeding for trace minerals in wheat. Food and Nutrition Bulletin 21:392-396

Moore JW, Herrera-Foessel S, Lan C, Schnippenkoetter W, Ayliffe M, Huerta-Espino J, Lillemo M, Viccars L, Milne R, Periyannan S (2015) A recently evolved hexose transporter variant confers resistance to multiple pathogens in wheat. Nature Genet 47:1494–1498

Morgounov A, Gómez-Becerra HF, Abugalieva A, Dzhunusova M, Yessimbekova M, Muminjanov H, Zelenskiy Y, Ozturk L, Cakmak I (2007) Iron and zinc grain density in common wheat grown in Central Asia. Euphytica 155:193-203

Morris ER, Ellis R (1976) Isolation of monoferric phytate from wheat bran and its biological value as an iron source to the rat. J Nutrit 106:753-760

Murray GM, Brennan JP (2009) Estimating disease losses to the Australian wheat industry. Austral Plant Pathol 38:558-570

Nadeem M, Anjum FM, Amir RM, Khan MR, Hussain S, Javed MS (2010) An overview of anti-nutritional factors in cereal grains with special reference to wheat-A review. Pak J Food Sci 20:54-61

Nevo E, Korol AB, Beiles A, Fahima T (2013) Evolution of wild emmer and wheat improvement: population genetics, genetic resources, and genome organization of wheat's progenitor, *Triticum dicoccoides*. Springer Science & Business Media doi 10.1007/978-3-662-07140-3 10:364-368

Nsabiyera V, Baranwal D, Qureshi N, Kay P, Forrest K, Valárik M, Doležel J, Hayden MJ, Bariana HS, Bansal UK (2020) Fine mapping of *Lr49* using 90K SNP chip array and flow-sorted chromosome sequencing in wheat. Front Plant Sci 10:1-10

Nsabiyera V, Bariana HS, Qureshi N, Wong D, Hayden MJ, Bansal UK (2018) Characterisation and mapping of adult plant stripe rust resistance in wheat accession Aus27284. Theor App Gene 131:1459–1467

Nsabiyera V, Qureshi N, Bariana HS, Wong D, Forrest KL, Hayden MJ, Bansal UK (2016) Molecular markers for adult plant leaf rust resistance gene *Lr48* in wheat. Molec Breed 36:1-9

O'Brien L, Brown J, Young R, Pascoe I (1980) Occurrence and distribution of wheat stripe rust in Victoria and susceptibility of commercial wheat cultivars. Austral Plan Pathol 9:14-14

Oury F-X, Leenhardt F, Remesy C, Chanliaud E, Duperrier B, Balfourier F, Charmet G (2006) Genetic variability and stability of grain magnesium, zinc and iron concentrations in bread wheat. Euro J Agro 25:177-185

Ozkan H, Brandolini A, Torun A, Altintas S, Eker S, Kilian B, Braun H, Salamini F, Cakmak I (2007) Natural variation and identification of microelements content in seeds of einkorn wheat (*Triticum monococcum*). Wheat Production in Stressed Environments. Springer, pp 455-462

Pallauf J, Pietsch M, Rimbach G (1998) Dietary phytate reduces magnesium bioavailability in growing rats. Nutri Res 18:1029-1037

Palmer LJ, Palmer LT, Rutzke MA, Graham RD, Stangoulis JC (2014) Nutrient variability in phloem: examining changes in K, Mg, Zn and Fe concentration during grain loading in common wheat (*Triticum aestivum*). Physio Plantar 152:729-737

Pardey PG, Beddow J, Kriticos D, Hurley T, Park R, Duveiller E, Sutherst R, Burdon J, Hodson D (2013) Right-sizing stem-rust research. Sci 340:147-148

Park R, Bansal U, Bariana H, Singh D (2020). Rust resistance genotypes and expected rust responses of Australian common wheat, durum wheat and triticale varieties. Cereal Rust Rep 1-10.

Pathan AK, Park RF (2007) Evaluation of seedling and adult plant resistance to stem rust in European wheat cultivars. Euphytica 155:87-105

Pasam RK, Bansal U, Daetwyler HD, Forrest KL, Wong D, Petkowski J, Willey N, Randhawa M, Chhetri M, Miah H (2017) Detection and validation of genomic regions associated with resistance to rust diseases in a worldwide hexaploid wheat landrace collection using BayesR and mixed linear model approaches. Theor Appl Genet 130:777-793

Peleg Z, Cakmak I, Ozturk L, Yazici A, Jun Y, Budak H, Korol AB, Fahima T, Saranga Y (2009) Quantitative trait loci conferring grain mineral nutrient concentrations in durum wheat× wild emmer wheat RIL population. Theor Appl Genet 119:353-369

Peleg Z, Saranga Y, Yazici A, Fahima T, Ozturk L, Cakmak I (2008) Grain zinc, iron and protein concentrations and zinc-efficiency in wild emmer wheat under contrasting irrigation regimes. Plan Soil 306:57-67

Periyannan S, Moore J, Ayliffe M, Bansal U, Wang X, Huang L, Deal K, Luo M, Kong X, Bariana H (2013) The gene *Sr33*, an ortholog of barley *Mla* genes, encodes resistance to wheat stem rust race Ug99. Sci 341:786-788

Periyannan SK, Bansal UK, Bariana HS, Pumphrey M, Lagudah ES (2011) A robust molecular marker for the detection of shortened introgressed segment carrying the stem rust resistance gene *Sr22* in common wheat. Theor Appl Genet 122:1-7

Pinto da Silva GB, Zanella CM, Martinelli JA, Chaves MS, Hiebert CW, McCallum BD, Boyd LA (2018) Quantitative trait loci conferring leaf rust resistance in hexaploid wheat. Phytopath 108:1344-1354

Poland JA, Rife TW (2012) Genotyping-by-sequencing for plant breeding and genetics. Plant Genome 5:92-102

Preece C, Livarda A, Christin PA, Wallace M, Martin G, Charles M, Jones G, Rees M, Osborne CP (2017) How did the domestication of Fertile Crescent grain crops increase their yields? Funct Ecol 31:387-397

Prins R, Pretorius Z, Bender C, Lehmensiek A (2011) QTL mapping of stripe, leaf and stem rust resistance genes in a Kariega× Avocet S doubled haploid wheat population. Mol Breed 27:259-270

Qiu J-W, Schürch AC, Yahiaoui N, Dong L-L, Fan H-J, Zhang Z-J, Keller B, Ling H-Q (2007) Physical mapping and identification of a candidate for the leaf rust resistance gene *Lr1* of wheat. Theor Appl Genet 115:159-168

Quan W, Hou G, Chen J, Du Z, Lin F, Guo Y, Liu S, Zhang Z (2013) Mapping of QTL lengthening the latent period of *Puccinia striiformis* in winter wheat at the tillering growth stage. Euro J Plant Path 136:715-727

Qureshi N, Bariana H, Forrest K, Hayden M, Keller B, Wicker T, Faris J, Salina E, Bansal U (2017) Fine mapping of the chromosome 5B region carrying closely linked rust resistance genes *Yr47* and *Lr52* in wheat. Theor Appl Genet 130:495-504

Qureshi N, Bariana H, Zhang P, McIntosh R, Bansal U, Wong D, Hayden MJ, Dubcovsky J, Shankar M (2018) Genetic relationship of stripe rust resistance genes *Yr34* and *Yr48* in wheat and identification of linked KASP markers. Plant Dis 102:413-420

R Core Team (2018) R: A language and environment for statistical computing: R Foundation for Statistical Computing, Vienna, Austria

Randhawa M, Bansal U, Lillemo M, Miah H, Bariana H (2016) Postulation of rust resistance genes in Nordic spring wheat genotypes and identification of widely effective sources of resistance against the Australian rust flora. J Appl Genet 57:453-465

Randhawa M, Bansal U, Valarik M, Klocova B, Dolezel J, Bariana H (2014) Molecular mapping of stripe rust resistance gene *Yr51* in chromosome 4AL of wheat. Theor Appl Genet 127:317-324

Randhawa MS, Bariana HS, Mago R, Bansal UK (2015) Mapping of a new stripe rust resistance locus *Yr57* on chromosome 3BS of wheat. Mole Breed 35:65-70

Randhawa MS, Bains NS, Sohu VS, Chhuneja P, Trethowan RM, Bariana HS, Bansal U (2019) Marker assisted transfer of stripe rust and stem rust resistance genes into four wheat cultivars. Agronomy 9:497-503

Ranganathan J, Waite, R, Searchinger T, Hanson C (2019) How to Sustainably Feed 10 Billion People by 2050, in 21 Charts. World Resources Institute Retrieved on January 26, 2021. https://www.wri.org/blog/2018/12/how-sustainably-feed-10-billion-people-2050-21-charts

Rawat N, Tiwari VK, Neelam K, Randhawa GS, Chhuneja P, Singh K, Dhaliwal HS (2009) Development and characterization of *Triticum aestivum–Aegilops kotschyi* amphiploids with high grain iron and zinc contents. Plan Genet Resour 7:271-280

Ray DK, Mueller ND, West PC, Foley JA (2013) Yield trends are insufficient to double global crop production by 2050. PloS One 8:e66428:1-6

Ren Y, He Z, Li J, Lillemo M, Wu L, Bai B, Du J (2012) QTL mapping of adult-plant resistance to stripe rust in a population derived from common wheat cultivars Naxos and Shanghai 3/Catbird. Theor Appl Genet 125:1211-1221

Riaz A, Athiyannan N, Periyannan SK, Afanasenko O, Mitrofanova OP, Platz GJ, Aitken EA, Snowdon RJ, Lagudah ES, Hickey LT (2018) Unlocking new alleles for leaf rust resistance in the Vavilov wheat collection. Theor Appl Genet 131:127-144

Rosewarne GM, Singh RP, Huerta-Espino J, Herrera-Foessel SA, Forrest KL, Hayden MJ, Rebetzke GJ (2012) Analysis of leaf and stripe rust severities reveals pathotype changes and multiple minor QTLs associated with resistance in an Avocet x Pastor wheat population. Theor Appl Genet 124:1283-1294

Rosewarne G, Herrera-Foessel S, Singh R, Huerta-Espino J, Lan C, He Z (2013) Quantitative trait loci of stripe rust resistance in wheat. Theor Appl Genet 126:2427-2449

Rouse MN, Talbert LE, Singh D, Sherman JD (2014) Complementary epistasis involving *Sr12* explains adult plant resistance to stem rust in Thatcher wheat (*Triticum aestivum* L.). Theor Appl Genet 127:1549-1559

Rude RK, Singer FR, Gruber HE (2009) Skeletal and hormonal effects of magnesium deficiency. J Amer Col Nutr 28:131-141

Ruibal-Mendieta NL, Delacroix DL, Mignolet E, Pycke J-M, Marques C, Rozenberg R, Petitjean G, Habib-Jiwan J-L, Meurens M, Quetin-Leclercq J (2005) Spelt (*Triticum aestivum* ssp. *spelta*) as a source of breadmaking flours and bran naturally enriched in oleic acid and minerals but not phytic acid. J Agri Food Chem 53:2751-2759

Saffdar H (2019) Rust Resistance in Wheat: Genetic Analysis and Molecular Mapping. PhD thesis The University of Sydney. pp. 1-93

Saintenac C, Falque M, Martin OC, Paux E, Feuillet C, Sourdille P (2009) Detailed recombination studies along chromosome 3B provide new insights on crossover distribution in wheat (*Triticum aestivum* L.). Genet 181:393-403

Saintenac C, Zhang W, Salcedo A, Rouse MN, Trick HN, Akhunov E, Dubcovsky J (2013) Identification of wheat gene *Sr35* that confers resistance to Ug99 stem rust race group. Sci 341:783-786

Salamini F, Özkan H, Brandolini A, Schäfer-Pregl R, Martin W (2002) Genetics and geography of wild cereal domestication in the Near East. Natur Rev Genet 3:429-434

Samtiya M, Aluko RE, Dhewa T (2020) Plant food anti-nutritional factors and their reduction strategies: an overview. Food Prod Process Nutrit 2:6-10

Sánchez-Martín J, Steuernagel B, Ghosh S, Herren G, Hurni S, Adamski N, Vrána J, Kubaláková M, Krattinger SG, Wicker T (2016) Rapid gene isolation in barley and wheat by mutant chromosome sequencing. Genome Biol 17:221-226

Sapkota S, Hao Y, Johnson J, Buck J, Aoun M, Mergoum M (2019) Genome-wide association study of a worldwide collection of wheat genotypes reveals novel quantitative trait loci for leaf rust resistance. Plant Genome 12:1-14

Shatalina M, Wicker T, Buchmann JP, Oberhaensli S, Šimková H, Doležel J, Keller B (2013) Genotype-specific SNP map based on whole chromosome 3B sequence information from wheat cultivars Arina and Forno. Plant Biotech J 11:23-32

Shaw PD, Graham M, Kennedy J, Milne I, Marshall DF (2014) Helium: visualization of large scale plant pedigrees. BMC Bioinfor 15:1-15

Silme RS, Cagirgan MI (2007) TILLING (Targetting induced local lesions in genomes) technology for plant functional genomics. J Appl Bio Sci: 1:77-80

Singh R, Rajaram S (1992) Genetics of adult-plant resistance of leaf rust in'Frontana'and three CIMMYT wheats. Genome 35:24-31

Singh R (1993) Resistance to leaf rust in 26 Mexican wheat cultivars. Crop Sci 33:633-637

Singh R, Nelson J, Sorrells M (2000) Mapping *Yr28* and other genes for resistance to stripe rust in wheat. Crop Sci 40:1148-1155

Singh D, Park R, McIntosh R, Bariana H (2008) Characterisation of stem rust and stripe rust seedling resistance genes in selected wheat cultivars from the United Kingdom. J Plan Pathol 90:553-562

Singh K, Chhuneja P, Tiwari V, Rawat N, Neelam K, Aggarwal R, Malik S, Keller B, Dhaliwal H (2010) Mapping of QTL for grain iron and zinc content in diploid A genome wheat and validation of these loci in U and S genomes. Plant and Animal Genomes XVIII Conference, pp 9-13

Singh R, Hodson DP, Huerta-Espino J, Jin Y, Bhavani S, Njau P, Herrera-Foessel S, Singh PK, Singh S, Velu G (2011) The emergence of Ug99 races of the stem rust fungus is a threat to world wheat production. Ann Rev Phytopath 49:465-481

Singh A, Pandey M, Singh A, Knox R, Ammar K, Clarke J, Clarke F, Singh R, Pozniak C, DePauw R (2013) Identification and mapping of leaf, stem and stripe rust resistance quantitative trait loci and their interactions in durum wheat. Mol Breed 31:405-418

Singh B, Bansal UK, Muhammad HM, Gill B, Bariana HS (2014) Postulation of resistance genes and assessment of adult plant response variation for stripe rust in three international wheat nurseries. Ind J Genet Plan Breed 74:1-9

Singh B, Singh AK (2015) Marker-assisted plant breeding: principles and practices. Springer pp.10-56

Sohail Y, Bansal U, Bariana H, Chhuneja P, Mumtaz A, Rattu A, Trethowan R (2014) Identification of a co-dominant eSTS marker linked with leaf rust resistance gene *Lr28* in wheat (*Triticum aestivum* L.). Austr J Crop Sci 8:1210-1216

Sorrells ME, Gustafson JP, Somers D, Chao S, Benscher D, Guedira-Brown G, Huttner E, Kilian A, McGuire PE, Ross K (2011) Reconstruction of the Synthetic W7984× Opata M85 wheat reference population. Genome 54:875-882

Srinivasa J, Arun B, Mishra VK, Singh GP, Velu G, Babu R, Vasistha NK, Joshi AK (2014) Zinc and iron concentration QTL mapped in a *Triticum spelta* × *T. aestivum* cross. Theor Appl Genet 127:1643-1651

Steuernagel B, Periyannan SK, Hernández-Pinzón I, Witek K, Rouse MN, Yu G, Hatta A, Ayliffe M, Bariana H, Jones JD (2016) Rapid cloning of disease-resistance genes in plants using mutagenesis and sequence capture. Nat Biotech 34:652-655

Steuernagel B, Witek K, Krattinger SG, Ramirez-Gonzalez RH, Schoonbeek H-j, Yu G, Baggs E, Witek A, Yadav I, Krasileva KV (2020) The NLR-Annotator tool enables annotation of the intracellular immune receptor repertoire. Plan Physiol 183: 468-482

Stoecker B, Abebe Y, Hubbs-Tait L, Kennedy T, Gibson R, Arbide I, Teshome A, Westcott J, Krebs N, Hambidge K (2009) Zinc status and cognitive function of pregnant women in Southern Ethiopia. Europ J Clin Nutri 63:916-918

Takahashi M, Terada Y, Nakai I, Nakanishi H, Yoshimura E, Mori S, Nishizawa NK (2003) Role of nicotianamine in the intracellular delivery of metals and plant reproductive development. Plant Cell 15:1263-1280

Tang Y, Liu X, Wang J, Li M, Wang Q, Tian F, Su Z, Pan Y, Liu D, Lipka AE (2016) GAPIT version 2: an enhanced integrated tool for genomic association and prediction. Plant Genome 9:1-9

Taylor J, Butler D (2017) R package ASMap: efficient genetic linkage map construction and diagnosis. Jour Statist Soft 79:1-29

The TT, Latter BDH, McIntosh RA, Ellison FW, Brennan PS, Fisher J, Hollamby GJ, Rathjen AJ, Wilson RE (1988) Grain yields of near isogenic lines with added genes for stem rust resistance. In 'Proceedings of the 7th International Wheat Genetics Symposium'. Cambridge, England. (Eds TE Miller, RMD Koebner) Institute of Plant Science: Cambridge, UK pp. 901–906

Thind AK, Wicker T, Simkova H, Fossati D, Moullet O, Brabant C, Vrana J, Dolezel J, Krattinger SG (2017) Rapid cloning of genes in hexaploid wheat using cultivar-specific long-range chromosome assembly. Nat Biotechnol 35:793-796

Tiwari C, Wallwork H, Arun B, Mishra VK, Velu G, Stangoulis J, Kumar U, Joshi AK (2016) Molecular mapping of quantitative trait loci for zinc, iron and protein content in the grains of hexaploid wheat. Euphyt 207:563-570

Tiwari VK, Rawat N, Chhuneja P, Neelam K, Aggarwal R, Randhawa GS, Dhaliwal HS, Keller B, Singh K (2009) Mapping of quantitative trait loci for grain iron and zinc concentration in diploid A genome wheat. J Hered 100:771-776

Troccoli A, Codianni P (2005) Appropriate seeding rate for einkorn, emmer, and spelt grown under rainfed condition in southern Italy. Europ J Agr 22:293-300

Trumbo P, Yates AA, Schlicker S, Poos M (2001) Dietary reference intakes: vitamin A, vitamin K, arsenic, boron, chromium, copper, iodine, iron, manganese, molybdenum, nickel, silicon, vanadium, and zinc. Journal of the American Dietetic Association 101:294-301

Turner MK, Kolmer JA, Pumphrey MO, Bulli P, Chao S, Anderson JA (2017) Association mapping of leaf rust resistance loci in a spring wheat core collection. Theor Appl Genet 130:345-361

Uauy C, Distelfeld A, Fahima T, Blechl A, Dubcovsky J (2006) A NAC gene regulating senescence improves grain protein, zinc, and iron content in wheat. Science 314:1298-1301

USDA (2020) First Look at 2019/20 by United State Department of Agriculture (USDA) Sees Another Record World Wheat Crop. Accessed on May 30, 2020 from https://www.uswheat.org/wheatletter/first-look-at-2019-20-by-usda-sees-another-record-world-wheat-crop/

VanRaden P (2007) Efficient estimation of breeding values from dense genomic data. J Dairy Sci 90:374-375

Vazquez MD, Peterson CJ, Riera-Lizarazu O, Chen X, Heesacker A, Ammar K, Crossa J, Mundt CC (2012) Genetic analysis of adult plant, quantitative resistance to stripe rust in wheat cultivar 'Stephens' in multi-environment trials. Theor Appl Genet 124:1-11

Velu G, Singh R, Huerta-Espino J, Peña R, Arun B, Mahendru-Singh A, Mujahid MY, Sohu V, Mavi G, Crossa J (2012) Performance of biofortified spring wheat genotypes in target environments for grain zinc and iron concentrations. Field Crop Res 137:261-267

Velu G, Ortiz-Monasterio I, Cakmak I, Hao Y, Singh R (2014) Biofortification strategies to increase grain zinc and iron concentrations in wheat. J Cer Sci 59:365-372

Velu G, Singh R, Balasubramaniam A, Mishra VK, Chand R, Tiwari C, Joshi A, Virk P, Cherian B, Pfeiffer W (2015) Reaching out to farmers with high zinc wheat varieties through public-private partnerships: an experience from eastern-gangetic plains of India. Adv Food Tech Nut Sci 1:73-75

Velu G, Singh RP, Crespo-Herrera L, Juliana P, Dreisigacker S, Valluru R, Stangoulis J, Sohu VS, Mavi GS, Mishra VK (2018) Genetic dissection of grain zinc concentration in

spring wheat for mainstreaming biofortification in CIMMYT wheat breeding. Scient Rep 8:13526

Velu G, Crespo Herrera L, Guzman C, Huerta J, Payne T, Singh RP (2019) Assessing genetic diversity to breed competitive biofortified wheat with enhanced grain Zn and Fe concentrations. Front Plan Sci 9:1971-1976

Voorrips R (2002) MapChart: software for the graphical presentation of linkage maps and QTLs. J Her 93:77-78

Vrána J, Šimková H, Kubaláková M, Číhalíková J, Doležel J (2012) Flow cytometric chromosome sorting in plants: the next generation. Methods 57:331-337

Wan A, Chen X (2014). Virulence characterization of *Puccinia striiformis f. sp. tritici* using a new set of *Yr* single-gene line differentials in the United States in 2010. Plant Dis 98:1534-1542.

Wang M, Chen X (2017) Stripe rust resistance In Chen X and Kang Z (eds) Stripe Rust. Springer, pp 353-558

Wang S, Basten C, Zeng Z (2012) Windows QTL Cartographer 2.5. Department of Statistics, North Carolina State University. Raleigh NC https://statgen. ncsu. edu/qtlcart. WQTLCart. htm

Wang S, Wong D, Forrest K, Allen A, Chao S, Huang BE, Maccaferri M, Salvi S, Milner SG, Cattivelli L (2014) Characterization of polyploid wheat genomic diversity using a high-density 90000 single nucleotide polymorphism array. Plant Biotech J 12:787-796

Welch RM (1999) Importance of seed mineral nutrient reserves in crop growth. In Mineral nutrition of crops. Fundamental mechanisms and implications. Edited by Z. Rengel. Food Products Press New York. pp. 205-226

Welch RM, Graham RD (2004) Breeding for micronutrients in staple food crops from a human nutrition perspective. J Exp Bot 55:353-364

Wellings C (2007) *Puccinia striiformis* in Australia: a review of the incursion, evolution, and adaptation of stripe rust in the period 1979–2006. Crop Past Scien 58:567-575

Wellings C, Wright D, Keiper F, Loughman R (2003) First detection of wheat stripe rust in Western Australia: evidence for a foreign incursion. Austral Plant Path 32:321-322

Wheal MS, Fowles TO, Palmer LT (2011) A cost-effective acid digestion method using closed polypropylene tubes for inductively coupled plasma optical emission spectrometry (ICP-OES) analysis of plant essential elements. Analyt Method 3:2854-2863

White PJ, Broadley MR (2005) Biofortifying crops with essential mineral elements. Trends Plants Sci 10:586-593

WHO (2002) The world health report 2002: reducing risks, promoting healthy life. World Health Organization 52-156. Accessed on 26 January 2021. https://www.who.int/whr/2002/en/

WHO (2008) Worldwide Prevalence of Anaemia 1993–2005. In World Health Organization Global Database on Anaemia (eds) Benoist B, McLean E, Egli I and Cogswell M. World Health Organization Press, Geneva pp 1-9

WHO (2017) The double burden of malnutrition: policy brief. https://www.who.int/nutrition/publications/doubleburdenmalnutrition-policybrief/en/ accessed on 26th January 2021. World Health Organization, Geneva, pp 1-10

Wicker T, Gundlach H, Spannagl M, Uauy C, Borrill P, Ramirez-Gonzalez RH, De Oliveira R, Mayer KF, Paux E, Choulet F (2018) Impact of transposable elements on genome structure and evolution in bread wheat. Genom Biol 19:103-110

William H, Singh R, Huerta-Espino J, Palacios G, Suenaga K (2006) Characterization of genetic loci conferring adult plant resistance to leaf rust and stripe rust in spring wheat. Genome 49:977-990

Winfield MO, Allen AM, Burridge AJ, Barker GL, Benbow HR, Wilkinson PA, Coghill J, Waterfall C, Davassi A, Scopes G (2015) High-density SNP genotyping array for hexaploid wheat and its secondary and tertiary gene pool. Plant Biotech J 14:1195-1206

Winzeler M, Mesterházy Á, Park R (2000) Resistance of European winter wheat germplasm to leaf rust. Agron 20:783-792

Wright S (1968) Evolution and The Genetics of Populations. In Genetic and Biometric Foundations Vol 1 The University of Chicago Press, Chicago. pp. 1-48

Wu J, Zeng Q, Wang Q, Liu S, Yu S, Mu J, Huang S, Sela H, Distelfeld A, Huang L (2018) SNP-based pool genotyping and haplotype analysis accelerate fine-mapping of the wheat genomic region containing stripe rust resistance gene *Yr26*. Theor Appl Genet 131:1481-1496

Xu LS, Wang MN, Cheng P, Kang Z, Hulbert S, Chen X (2013). Molecular mapping of *Yr53*, a new gene for stripe rust resistance in durum wheat accession PI 480148 and its transfer to common wheat. Theor Appl Genet 126:523-533

Yang J, Zaitlen NA, Goddard ME, Visscher PM, Price AL (2014a) Advantages and pitfalls in the application of mixed-model association methods. Nat Genet 46:100-102

Yang N, Lu Y, Yang X, Huang J, Zhou Y, Ali F, Wen W, Liu J, Li J, Yan J (2014b) Genome wide association studies using a new nonparametric model reveal the genetic architecture of 17 agronomic traits in an enlarged maize association panel. PLoS Genet 10:1-14

Yu J, Buckler ES (2006) Genetic association mapping and genome organization of maize. Curr Opin Biotech 17:155-160

Yu J, Pressoir G, Briggs WH, Bi IV, Yamasaki M, Doebley JF, McMullen MD, Gaut BS, Nielsen DM, Holland JB (2006) A unified mixed-model method for association mapping that accounts for multiple levels of relatedness. Nat Genet 38:203-208

Yu L-X, Barbier H, Rouse MN, Singh S, Singh RP, Bhavani S, Huerta-Espino J, Sorrells ME (2014) A consensus map for Ug99 stem rust resistance loci in wheat. Theor Appl Genet 127:1561-1581

Yu L-X, Lorenz A, Rutkoski J, Singh RP, Bhavani S, Huerta-Espino J, Sorrells ME (2011) Association mapping and gene–gene interaction for stem rust resistance in CIMMYT spring wheat germplasm. Theor Appl Genet 123:1257-1268

Yuan C, Singh RP, Liu D, Randhawa MS, Huerta-Espino J, Lan C (2020) Genome-wide mapping of adult plant resistance to leaf rust and stripe rust in CIMMYT wheat line Arableu# 1. Plant Dis 104:1455-1464

Zadoks JC, Chang TT, Konzak CF (1974) A decimal code for the growth stages of cereals. Weed Res 14:415-421

Zahravi M, Bariana H, Shariflou M, Balakrishna P, Banks P, Ghannadha M, Pogna N (2003) Bulk segregant analysis of stripe rust resistance in wheat (Triticum aestivum) using microsatellite markers. Proceedings 10th International Wheat Genetics Symposium, Instituto Sperimentale per Cerealcoltura, Rome (Pogna NE, Romano M, Pogna EA & Galterio, eds), pp 861-863

Zhang D, Bowden RL, Yu J, Carver BF, Bai G (2014) Association analysis of stem rust resistance in US winter wheat. PLoS One 9:e103747:1-12

Zhang C, Huang L, Zhang H, Hao Q, Lyu B, Wang M, Epstein L, Liu M, Kou C, Qi J (2019a) An ancestral NB-LRR with duplicated 3′ UTRs confers stripe rust resistance in wheat and barley. Natur Comm 10:1-8

Zhang P, Li X, Gebrewahid TW, Liu H, Xia X, He, Li Z, Liu D (2019b) QTL Mapping of Adult-Plant Resistance to Leaf and Stripe Rust in Wheat Cross SW 8588/Thatcher using the Wheat 55K SNP Array. Plan Dis 103:3041-3049

Zhang W, Chen S, Abate Z, Nirmala J, Rouse MN, Dubcovsky J (2017) Identification and characterization of *Sr13*, a tetraploid wheat gene that confers resistance to the Ug99 stem rust race group. Proceed Nation Acad Scien:20170627:1-6

Zhang Z, Ersoz E, Lai C-Q, Todhunter RJ, Tiwari HK, Gore MA, Bradbury PJ, Yu J, Arnett DK, Ordovas JM (2010) Mixed linear model approach adapted for genome-wide association studies. Natur Genet 42:355-360

Zhao F, Su Y, Dunham S, Rakszegi M, Bedo Z, McGrath S, Shewry P (2009) Variation in mineral micronutrient concentrations in grain of wheat lines of diverse origin. J Cer Scien 49:290-295

Appendix I Supplementary Figure 1 of Chapter 3

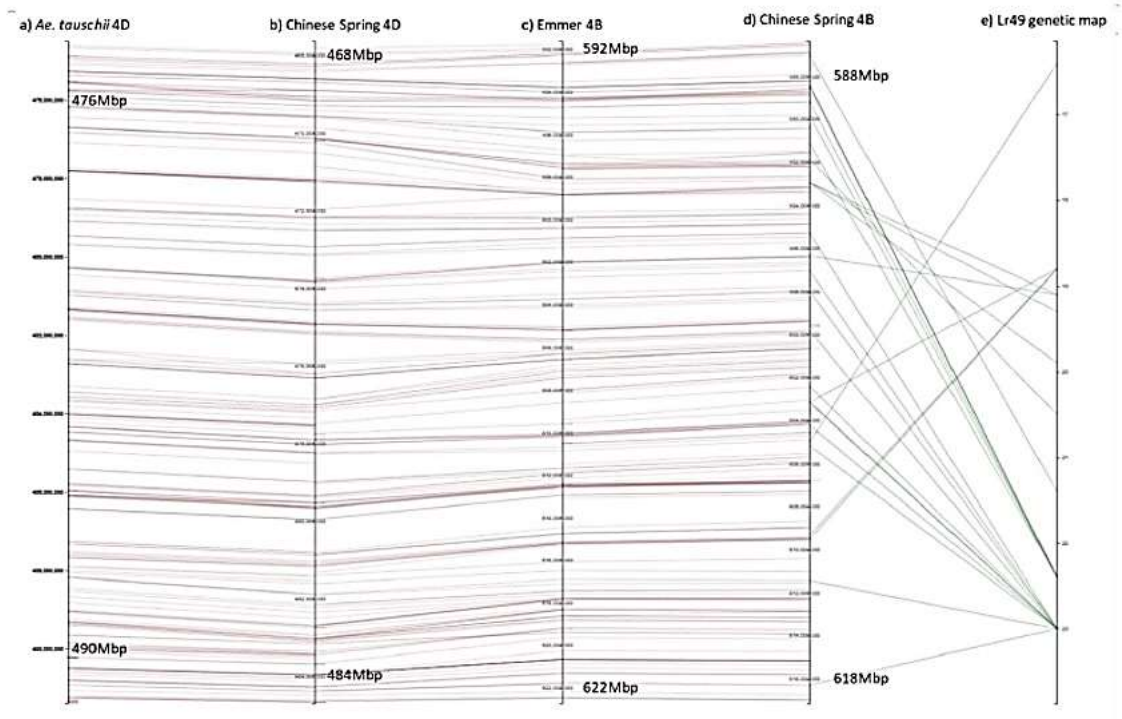

Supplementary Figure 1. Pretzel (http://plantinformatics.io) visualisation of synteny between (a) *Ae. tauschii* chromosome 4D, (b) Chinese Spring chromosome 4D, (c) emmer chromosome 4B, (d) Chinese Spring chromosome 4B, and (e) the *Lr49* genetic map, based on physical mapping of high confidence genes across the *Lr49* region (a to d) and corresponding physical map position (d) and genetic map position (e) of markers across the *Lr49* region. Red lines link high confidence genes. Green lines link markers. High confidence genes in all chromosomes are colinear, while the genetic map order of markers across the *Lr49* region show rearrangement relative to their physical mapping order in Chinese Spring.

Appendix II Supplementary Figure 2 of Chapter 3

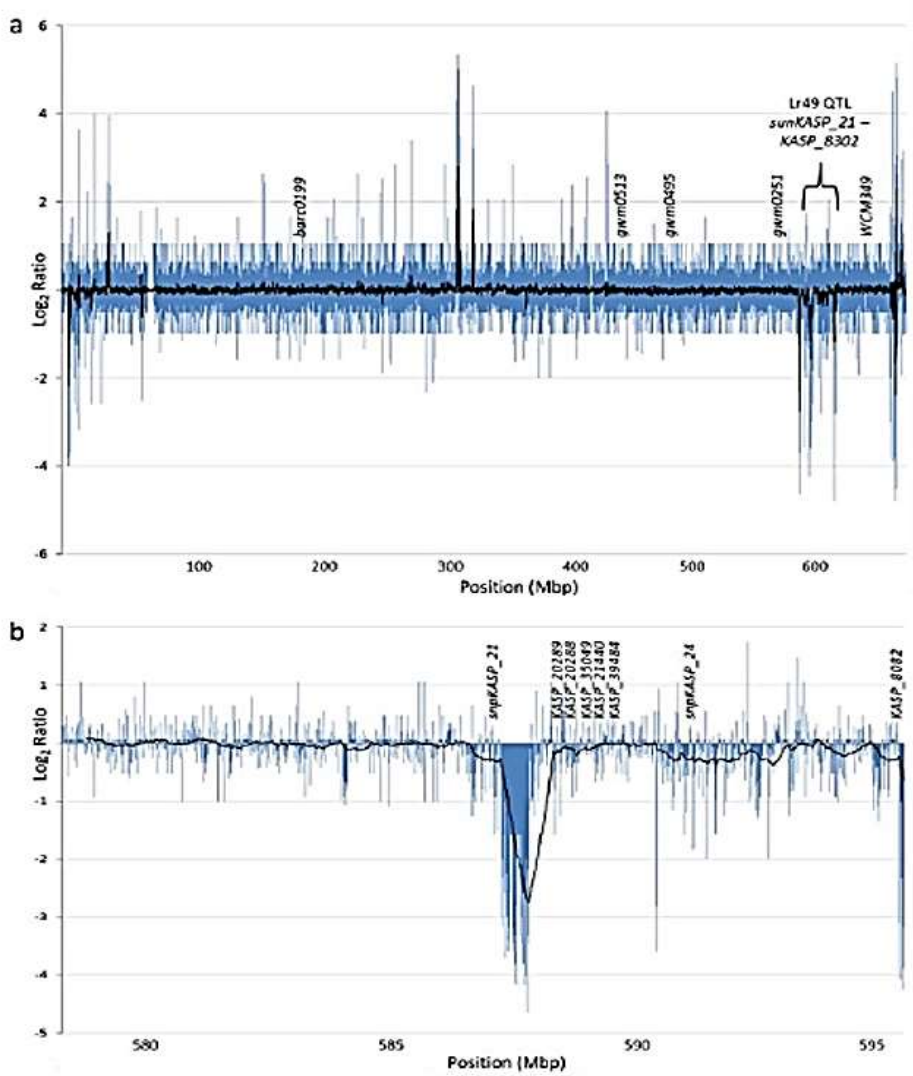

Supplementary Figure 2. Log_2 ratio plot (VL404:WL711) of average paired-end sequence read coverage across (a) chromosome 4B, and (b) *Lr49* region. Blue and black lines represent sequence coverage based on 10 and 500 kb sliding windows, respectively. Physical mapping position of microsatellite markers and the *Lr49* interval in chromosome 4B are shown in (a). The position of the putative deletion in VL404, relative to WL711, along with physical mapping position for markers that validated (*sunKASP_21* and *KASP_8082*) and did not validate (*KASP_20289*, *KASP_20288*, *KASP_35049*, *KASP_21440*, *KASP_39484* and *sunKASP_24*) are shown in (b).

Appendix III List of genotypes of HarvestPlus AM panel (HPAMP) and their pedigree

Line number	#GID	CID	SID	Cross
1	6356229	533487	164	PICUS/3/KAUZ*2/BOW//KAUZ/4/KKTS/5/T.SPELTA PI348530/6/2*FRANCOLIN #1
2	6356239	533487	174	PICUS/3/KAUZ*2/BOW//KAUZ/4/KKTS/5/T.SPELTA PI348530/6/2*FRANCOLIN #1
3	6356248	533487	183	PICUS/3/KAUZ*2/BOW//KAUZ/4/KKTS/5/T.SPELTA PI348530/6/2*FRANCOLIN #1
4	6356378	533508	53	OASIS/SKAUZ//4*BCN/3/2*PASTOR/4/T.SPELTA PI348449/5/BACEU #1/6/WBLL1*2/CHAPIO
5	6356380	533508	55	OASIS/SKAUZ//4*BCN/3/2*PASTOR/4/T.SPELTA PI348449/5/BACEU #1/6/WBLL1*2/CHAPIO
6	6356384	533508	59	OASIS/SKAUZ//4*BCN/3/2*PASTOR/4/T.SPELTA PI348449/5/BACEU #1/6/WBLL1*2/CHAPIO
7	6356390	533510	73	REH/HARE//2*BCN/3/CROC_1/AE.SQUARROSA (213)//PGO/4/HUITES/5/T.SPELTA PI348599/6/REH/HARE//2*BCN/3/CROC_1/AE.SQUARROSA (213)//PGO/4/HUITES/7/QUAIU
8	6356391	533510	74	REH/HARE//2*BCN/3/CROC_1/AE.SQUARROSA (213)//PGO/4/HUITES/5/T.SPELTA PI348599/6/REH/HARE//2*BCN/3/CROC_1/AE.SQUARROSA (213)//PGO/4/HUITES/7/QUAIU
9	6356427	533511	214	REH/HARE//2*BCN/3/CROC_1/AE.SQUARROSA (213)//PGO/4/HUITES/5/T.DICOCCON PI94624/AE.SQUARROSA (409)//BCN/6/REH/HARE//2*BCN/3/CROC_1/AE.SQUARROSA (213)//PGO/4/HUITES/7/MUTUS
10	6356431	533511	218	REH/HARE//2*BCN/3/CROC_1/AE.SQUARROSA (213)//PGO/4/HUITES/5/T.DICOCCON PI94624/AE.SQUARROSA (409)//BCN/6/REH/HARE//2*BCN/3/CROC_1/AE.SQUARROSA (213)//PGO/4/HUITES/7/MUTUS
11	6356432	533511	219	REH/HARE//2*BCN/3/CROC_1/AE.SQUARROSA (213)//PGO/4/HUITES/5/T.DICOCCON PI94624/AE.SQUARROSA (409)//BCN/6/REH/HARE//2*BCN/3/CROC_1/AE.SQUARROSA (213)//PGO/4/HUITES/7/MUTUS
12	6356440	533511	227	REH/HARE//2*BCN/3/CROC_1/AE.SQUARROSA (213)//PGO/4/HUITES/5/T.DICOCCON PI94624/AE.SQUARROSA (409)//BCN/6/REH/HARE//2*BCN/3/CROC_1/AE.SQUARROSA (213)//PGO/4/HUITES/7/MUTUS
13	6356465	533512	185	KACHU #1/T.SPELTA PI348764//2*KACHU
14	6356486	533513	230	KACHU #1/3/T.DICOCCON PI94624/AE.SQUARROSA (409)//BCN/4/2*KACHU
15	6356488	533513	232	KACHU #1/3/T.DICOCCON PI94624/AE.SQUARROSA (409)//BCN/4/2*KACHU
16	6356550	533519	43	INQALAB 91*2/TUKURU//T.SPELTA PI348599/3/2*INQALAB 91*2/KUKUNA
17	6356552	533519	45	INQALAB 91*2/TUKURU//T.SPELTA PI348599/3/2*INQALAB 91*2/KUKUNA
18	6353851	521088	98	FRET2/TUKURU//FRET2*2/3/T.SPELTA PI348530
19	6353852	521088	99	FRET2/TUKURU//FRET2*2/3/T.SPELTA PI348530
20	6353862	521091	217	FRET2/WBLL1//TACUPETO F2001*2/3/T.DICOCCON PI94624/AE.SQUARROSA (409)//BCN……..**continue**

#GID: Genotype identifier; CID: Cross identifier; SID: Selection identifier

21	6353863	521091	218	FRET2/WBLL1//TACUPETO F2001*2/3/T.DICOCCON PI94624/AE.SQUARROSA (409)//BCN
22	6354109	521095	109	WBLL1*2/TUKURU/3/T.DICOCCON PI94624/AE.SQUARROSA (409)//BCN/4/WBLL1*2/TUKURU
23	6354131	521101	120	NAC/TH.AC//3*PVN/3/MIRLO/BUC/4/2*PASTOR/5/T.DICOCCON PI94624/AE.SQUARROSA (409)//BCN/6/WBLL4//BABAX.1B.1B*2/PRL/3/PASTOR
24	6354138	521101	127	NAC/TH.AC//3*PVN/3/MIRLO/BUC/4/2*PASTOR/5/T.DICOCCON PI94624/AE.SQUARROSA (409)//BCN/6/WBLL4//BABAX.1B.1B*2/PRL/3/PASTOR
25	6354150	521101	139	NAC/TH.AC//3*PVN/3/MIRLO/BUC/4/2*PASTOR/5/T.DICOCCON PI94624/AE.SQUARROSA (409)//BCN/6/WBLL4//BABAX.1B.1B*2/PRL/3/PASTOR
26	6354283	521112	576	BL 1724*2/3/T.DICOCCON PI272533/AE.SQUARROSA (458)//CMH81A.1261/VEE#10
27	6354312	521112	605	BL 1724*2/3/T.DICOCCON PI272533/AE.SQUARROSA (458)//CMH81A.1261/VEE#10
28	6354328	521112	621	BL 1724*2/3/T.DICOCCON PI272533/AE.SQUARROSA (458)//CMH81A.1261/VEE#10
29	6354338	521113	121	INQALAB 91*2/TUKURU//T.SPELTA PI348599/3/INQALAB 91*2/KUKUNA
30	6354373	522492	91	GTO95.1.20/KIRITATI//MUU
31	6354760	522503	106	CROC_1/AE.SQUARROSA (210)//PBW343*2/KUKUNA/3/PBW343*2/KUKUNA
32	6354772	522506	114	CROC_1/AE.SQUARROSA (210)//PBW343*2/KHVAKI/3/PBW343*2/KUKUNA
33	6354773	522506	115	CROC_1/AE.SQUARROSA (210)//PBW343*2/KHVAKI/3/PBW343*2/KUKUNA
34	6354794	522508	66	68.111/RGB-U//WARD/3/AE.SQUARROSA (321)/4/INQALAB 91*2/KUKUNA/5/PBW343*2/KUKUNA
35	6354806	522517	110	GARZA/BOY//AE.SQUARROSA (467)/3/T.DICOCCON PI94625/AE.SQUARROSA (372)//3*PASTOR/4/T.DICOCCON PI94625/AE.SQUARROSA (372)//3*PASTOR
36	6354808	522517	112	GARZA/BOY//AE.SQUARROSA (467)/3/T.DICOCCON PI94625/AE.SQUARROSA (372)//3*PASTOR/4/T.DICOCCON PI94625/AE.SQUARROSA (372)//3*PASTOR
37	6354820	522522	245	CROC_1/AE.SQUARROSA (444)/3/T.DICOCCON PI94625/AE.SQUARROSA (372)//3*PASTOR/4/T.DICOCCON PI94625/AE.SQUARROSA (372)//3*PASTOR
38	6354821	522522	246	CROC_1/AE.SQUARROSA (444)/3/T.DICOCCON PI94625/AE.SQUARROSA (372)//3*PASTOR/4/T.DICOCCON PI94625/AE.SQUARROSA (372)//3*PASTOR
39	6354824	522522	249	CROC_1/AE.SQUARROSA (444)/3/T.DICOCCON PI94625/AE.SQUARROSA (372)//3*PASTOR/4/T.DICOCCON PI94625/AE.SQUARROSA (372)//3*PASTOR
40	6356234	533487	169	PICUS/3/KAUZ*2/BOW//KAUZ/4/KKTS/5/T.SPELTA PI348530/6/2*FRANCOLIN #1
41	6356298	533493	97	BAV92//IRENA/KAUZ/3/HUITES/4/T.SPELTA PI348764/5/2*BAV92//IRENA/KAUZ/3/HUITES
42	6356339	533503	216	WBLL1*2/VIVITSI/3/T.DICOCCON PI94624/AE.SQUARROSA (409)//BCN/4/WBLL1*2/VIVITSI/5/WBLL1*2/BRAMBLING
43	6356366	533504	176	PRL/2*PASTOR*3//T.SPELTA PI348530
44	6356377	533508	52	OASIS/SKAUZ//4*BCN/3/2*PASTOR/4/T.SPELTA PI348449/5/BACEU #1/6/WBLL1*2/CHAPIO……..continue

45	6356407	533511	194	REH/HARE//2*BCN/3/CROC_1/AE.SQUARROSA (213)//PGO/4/HUITES/5/T.DICOCCON PI94624/AE.SQUARROSA (409)//BCN/6/REH/HARE//2*BCN/3/CROC_1/AE.SQUARROSA (213)//PGO/4/HUITES/7/MUTUS
46	6356420	533511	207	REH/HARE//2*BCN/3/CROC_1/AE.SQUARROSA (213)//PGO/4/HUITES/5/T.DICOCCON PI94624/AE.SQUARROSA (409)//BCN/6/REH/HARE//2*BCN/3/CROC_1/AE.SQUARROSA (213)//PGO/4/HUITES/7/MUTUS
47	6356478	533513	222	KACHU #1/3/T.DICOCCON PI94624/AE.SQUARROSA (409)//BCN/4/2*KACHU
48	6356487	533513	231	KACHU #1/3/T.DICOCCON PI94624/AE.SQUARROSA (409)//BCN/4/2*KACHU
49	6356553	533519	46	INQALAB 91*2/TUKURU//T.SPELTA PI348599/3/2*INQALAB 91*2/KUKUNA
50	6353841	521088	88	FRET2/TUKURU//FRET2*2/3/T.SPELTA PI348530
51	6353871	521091	226	FRET2/WBLL1//TACUPETO F2001*2/3/T.DICOCCON PI94624/AE.SQUARROSA (409)//BCN
52	6353875	521092	63	WBLL1*2/KKTS*2//T.SPELTA PI348449
53	6353971	521093	112	WBLL1*2/KKTS*2/3/T.DICOCCON PI272533/AE.SQUARROSA (458)//CMH81A.1261/VEE#10
54	6354118	521096	100	WBLL1*2/VIVITSI//T.SPELTA PI348764/3/WBLL1*2/VIVITSI
55	6354143	521101	132	NAC/TH.AC//3*PVN/3/MIRLO/BUC/4/2*PASTOR/5/T.DICOCCON PI94624/AE.SQUARROSA (409)//BCN/6/WBLL4//BABAX.1B.1B*2/PRL/3/PASTOR
56	6354171	521104	235	REH/HARE//2*BCN/3/CROC_1/AE.SQUARROSA (213)//PGO/4/HUITES/5/T.SPELTA PI348599/6/REH/HARE//2*BCN/3/CROC_1/AE.SQUARROSA (213)//PGO/4/HUITES
57	6354173	521104	237	REH/HARE//2*BCN/3/CROC_1/AE.SQUARROSA (213)//PGO/4/HUITES/5/T.SPELTA PI348599/6/REH/HARE//2*BCN/3/CROC_1/AE.SQUARROSA (213)//PGO/4/HUITES
58	6354200	521105	331	REH/HARE//2*BCN/3/CROC_1/AE.SQUARROSA (213)//PGO/4/HUITES/5/T.DICOCCON PI94624/AE.SQUARROSA (409)//BCN/6/REH/HARE//2*BCN/3/CROC_1/AE.SQUARROSA (213)//PGO/4/HUITES
59	6354202	521105	333	REH/HARE//2*BCN/3/CROC_1/AE.SQUARROSA (213)//PGO/4/HUITES/5/T.DICOCCON PI94624/AE.SQUARROSA (409)//BCN/6/REH/HARE//2*BCN/3/CROC_1/AE.SQUARROSA (213)//PGO/4/HUITES
60	6354210	521105	341	REH/HARE//2*BCN/3/CROC_1/AE.SQUARROSA (213)//PGO/4/HUITES/5/T.DICOCCON PI94624/AE.SQUARROSA (409)//BCN/6/REH/HARE//2*BCN/3/CROC_1/AE.SQUARROSA (213)//PGO/4/HUITES
61	6354291	521112	584	BL 1724*2/3/T.DICOCCON PI272533/AE.SQUARROSA (458)//CMH81A.1261/VEE#10
62	6354364	522490	52	GTO95.1.20/HUW468/5/SITE/MO/4/NAC/TH.AC//3*PVN/3/MIRLO/BUC
63	6354368	522490	56	GTO95.1.20/HUW468/5/SITE/MO/4/NAC/TH.AC//3*PVN/3/MIRLO/BUC
64	6354380	522493	54	MICH95.3.1.4/4/ALTAR 84/AEGILOPS SQUARROSA (TAUS)//OCI/3/VEE/MJI//2*TUI/5/SOKOLL ……..continue

65	6354383	522493	57	MICH95.3.1.4/4/ALTAR 84/AEGILOPS SQUARROSA (TAUS)//OCI/3/VEE/MJI//2*TUI/5/SOKOLL
66	6354407	522494	264	DGO95.1.24/TUKURU//MONARCA F2007
67	6354431	522494	288	DGO95.1.24/TUKURU//MONARCA F2007
68	6354486	522496	588	MICH95.3.1.4/HUW468/5/SITE/MO/4/NAC/TH.AC//3*PVN/3/MIRLO/BUC
69	6354506	522496	608	MICH95.3.1.4/HUW468/5/SITE/MO/4/NAC/TH.AC//3*PVN/3/MIRLO/BUC
70	6354735	522501	346	CROC_1/AE.SQUARROSA (210)//2*PBW343*2/KUKUNA
71	6354741	522501	352	CROC_1/AE.SQUARROSA (210)//2*PBW343*2/KUKUNA
72	6354813	522517	117	GARZA/BOY//AE.SQUARROSA (467)/3/T.DICOCCON PI94625/AE.SQUARROSA (372)//3*PASTOR/4/T.DICOCCON PI94625/AE.SQUARROSA (372)//3*PASTOR
73	6354828	522522	253	CROC_1/AE.SQUARROSA (444)/3/T.DICOCCON PI94625/AE.SQUARROSA (372)//3*PASTOR/4/T.DICOCCON PI94625/AE.SQUARROSA (372)//3*PASTOR
74	6354848	522524	81	IWA 8600211//2*PBW343*2/KUKUNA
75	6354231	521107	299	KACHU #1/3/T.DICOCCON PI94624/AE.SQUARROSA (409)//BCN/4/KACHU
76	6564264	537121	186	QUAIU #1/3/T.DICOCCON PI94625/AE.SQUARROSA (372)//3*PASTOR/4/QUAIU
77	6564268	537121	190	QUAIU #1/3/T.DICOCCON PI94625/AE.SQUARROSA (372)//3*PASTOR/4/QUAIU
78	6564270	537121	192	QUAIU #1/3/T.DICOCCON PI94625/AE.SQUARROSA (372)//3*PASTOR/4/QUAIU
79	6564271	537121	193	QUAIU #1/3/T.DICOCCON PI94625/AE.SQUARROSA (372)//3*PASTOR/4/QUAIU
80	6564274	537123	182	QUAIU #1/3/T.DICOCCON PI94625/AE.SQUARROSA (372)//3*PASTOR/4/QUAIU #2
81	6564286	537123	194	QUAIU #1/3/T.DICOCCON PI94625/AE.SQUARROSA (372)//3*PASTOR/4/QUAIU #2
82	6564290	537123	198	QUAIU #1/3/T.DICOCCON PI94625/AE.SQUARROSA (372)//3*PASTOR/4/QUAIU #2
83	6564293	537123	201	QUAIU #1/3/T.DICOCCON PI94625/AE.SQUARROSA (372)//3*PASTOR/4/QUAIU #2
84	6564298	537123	206	QUAIU #1/3/T.DICOCCON PI94625/AE.SQUARROSA (372)//3*PASTOR/4/QUAIU #2
85	6564313	537124	59	DANPHE #1*2/3/T.DICOCCON PI94625/AE.SQUARROSA (372)//3*PASTOR
86	6564321	537124	67	DANPHE #1*2/3/T.DICOCCON PI94625/AE.SQUARROSA (372)//3*PASTOR
87	6564326	537125	103	DANPHE #1*2/SOLALA
88	6564329	537125	106	DANPHE #1*2/SOLALA
89	6564332	537125	109	DANPHE #1*2/SOLALA
90	6564337	537125	114	DANPHE #1*2/SOLALA
91	6564345	537125	122	DANPHE #1*2/SOLALA
92	6564347	537125	124	DANPHE #1*2/SOLALA

……..continue

93	6564351	537126	201	DANPHE #1*2/3/T.DICOCCON PI94625/AE.SQUARROSA (372)//SHA4/CHIL
94	6564355	537126	205	DANPHE #1*2/3/T.DICOCCON PI94625/AE.SQUARROSA (372)//SHA4/CHIL
95	6564358	537126	208	DANPHE #1*2/3/T.DICOCCON PI94625/AE.SQUARROSA (372)//SHA4/CHIL
96	6564371	537131	122	KINDE*2/SOLALA
97	6564376	537131	127	KINDE*2/SOLALA
98	6564378	537134	126	CHONTE*2/SOLALA
99	6564380	537134	128	CHONTE*2/SOLALA
100	6564387	537137	157	PAURAQ*2/SOLALA
101	6564395	537137	165	PAURAQ*2/SOLALA
102	6564397	537137	167	PAURAQ*2/SOLALA
103	6564404	537137	174	PAURAQ*2/SOLALA
104	6564410	537137	180	PAURAQ*2/SOLALA
105	6564419	537139	245	WAXWING*2/TUKURU*2/3/T.DICOCCON PI94625/AE.SQUARROSA (372)//3*PASTOR
106	6564422	537139	248	WAXWING*2/TUKURU*2/3/T.DICOCCON PI94625/AE.SQUARROSA (372)//3*PASTOR
107	6564428	537139	254	WAXWING*2/TUKURU*2/3/T.DICOCCON PI94625/AE.SQUARROSA (372)//3*PASTOR
108	6564435	537141	204	WAXWING*2/TUKURU*2/3/T.DICOCCON PI94625/AE.SQUARROSA (372)//SHA4/CHIL
109	6564436	537141	205	WAXWING*2/TUKURU*2/3/T.DICOCCON PI94625/AE.SQUARROSA (372)//SHA4/CHIL
110	6564438	537141	207	WAXWING*2/TUKURU*2/3/T.DICOCCON PI94625/AE.SQUARROSA (372)//SHA4/CHIL
111	6564440	537142	117	FRNCLN*2/4/T.DICOCCON PI94625/AE.SQUARROSA (372)//TUI/CLMS/3/2*PASTOR
112	6564442	537142	119	FRNCLN*2/4/T.DICOCCON PI94625/AE.SQUARROSA (372)//TUI/CLMS/3/2*PASTOR
113	6564463	537143	127	FRNCLN*2/7/CMH83.1020/HUITES/6/CMH79A.955/4/AGA/3/4*SN64/CNO67//INIA66/5/NAC
114	6564468	537143	132	FRNCLN*2/7/CMH83.1020/HUITES/6/CMH79A.955/4/AGA/3/4*SN64/CNO67//INIA66/5/NAC
115	6564470	537143	134	FRNCLN*2/7/CMH83.1020/HUITES/6/CMH79A.955/4/AGA/3/4*SN64/CNO67//INIA66/5/NAC
116	6564478	537145	95	VILLA JUAREZ F2009/SOLALA//WBLL1*2/BRAMBLING
117	6564479	537145	96	VILLA JUAREZ F2009/SOLALA//WBLL1*2/BRAMBLING
118	6564483	537145	100	VILLA JUAREZ F2009/SOLALA//WBLL1*2/BRAMBLING
119	6564489	537145	106	VILLA JUAREZ F2009/SOLALA//WBLL1*2/BRAMBLING
120	6564490	537145	107	VILLA JUAREZ F2009/SOLALA//WBLL1*2/BRAMBLING
121	6564491	537145	108	VILLA JUAREZ F2009/SOLALA//WBLL1*2/BRAMBLING

……..continue

122	6564497	537147	95	WHEAR/KUKUNA/3/C80.1/3*BATAVIA//2*WBLL1/4/T.DICOCCON PI94625/AE.SQUARROSA (372)//3*PASTOR/5/WHEAR/KUKUNA/3/C80.1/3*BATAVIA//2*WBLL1
123	6564498	537147	96	WHEAR/KUKUNA/3/C80.1/3*BATAVIA//2*WBLL1/4/T.DICOCCON PI94625/AE.SQUARROSA (372)//3*PASTOR/5/WHEAR/KUKUNA/3/C80.1/3*BATAVIA//2*WBLL1
124	6564501	537147	99	WHEAR/KUKUNA/3/C80.1/3*BATAVIA//2*WBLL1/4/T.DICOCCON PI94625/AE.SQUARROSA (372)//3*PASTOR/5/WHEAR/KUKUNA/3/C80.1/3*BATAVIA//2*WBLL1
125	6564511	537149	114	WHEAR/KUKUNA/3/C80.1/3*BATAVIA//2*WBLL1/4/T.DICOCCON PI94625/AE.SQUARROSA (372)//SHA4/CHIL/5/WHEAR/KUKUNA/3/C80.1/3*BATAVIA//2*WBLL1
126	6564513	537149	116	WHEAR/KUKUNA/3/C80.1/3*BATAVIA//2*WBLL1/4/T.DICOCCON PI94625/AE.SQUARROSA (372)//SHA4/CHIL/5/WHEAR/KUKUNA/3/C80.1/3*BATAVIA//2*WBLL1
127	6564514	537149	117	WHEAR/KUKUNA/3/C80.1/3*BATAVIA//2*WBLL1/4/T.DICOCCON PI94625/AE.SQUARROSA (372)//SHA4/CHIL/5/WHEAR/KUKUNA/3/C80.1/3*BATAVIA//2*WBLL1
128	6564518	537149	121	WHEAR/KUKUNA/3/C80.1/3*BATAVIA//2*WBLL1/4/T.DICOCCON PI94625/AE.SQUARROSA (372)//SHA4/CHIL/5/WHEAR/KUKUNA/3/C80.1/3*BATAVIA//2*WBLL1
129	6564523	537149	126	WHEAR/KUKUNA/3/C80.1/3*BATAVIA//2*WBLL1/4/T.DICOCCON PI94625/AE.SQUARROSA (372)//SHA4/CHIL/5/WHEAR/KUKUNA/3/C80.1/3*BATAVIA//2*WBLL1
130	6564528	537149	131	WHEAR/KUKUNA/3/C80.1/3*BATAVIA//2*WBLL1/4/T.DICOCCON PI94625/AE.SQUARROSA (372)//SHA4/CHIL/5/WHEAR/KUKUNA/3/C80.1/3*BATAVIA//2*WBLL1
131	6564539	537253	156	T.DICOCCON CI9309/AE.SQUARROSA (409)/4/3*CHIBIA//PRLII/CM65531/3/SKAUZ/BAV92
132	6564541	537253	158	T.DICOCCON CI9309/AE.SQUARROSA (409)/4/3*CHIBIA//PRLII/CM65531/3/SKAUZ/BAV92
133	6564554	537254	267	T.DICOCCON CI9309/AE.SQUARROSA (409)//MUTUS/3/2*MUTUS
134	6564555	537254	268	T.DICOCCON CI9309/AE.SQUARROSA (409)//MUTUS/3/2*MUTUS
135	6564559	537254	272	T.DICOCCON CI9309/AE.SQUARROSA (409)//MUTUS/3/2*MUTUS
136	6564569	537256	99	T.DICOCCON PI94624/AE.SQUARROSA (409)//BCN/3/WAXWING/4/2*FRNCLN
137	6564570	537256	100	T.DICOCCON PI94624/AE.SQUARROSA (409)//BCN/3/WAXWING/4/2*FRNCLN
138	6564572	537256	102	T.DICOCCON PI94624/AE.SQUARROSA (409)//BCN/3/WAXWING/4/2*FRNCLN
139	6564577	537257	56	KVZ/PPR47.89C//3*PBW65/2*PASTOR
140	6564582	537257	61	KVZ/PPR47.89C//3*PBW65/2*PASTOR
141	6564589	537257	68	KVZ/PPR47.89C//3*PBW65/2*PASTOR
142	6564590	537257	69	KVZ/PPR47.89C//3*PBW65/2*PASTOR
143	6564597	537258	89	KVZ/PPR47.89C//TACUPETO F2001*2/BRAMBLING/3/2*TACUPETO F2001*2/BRAMBLING
144	6564600	537258	92	KVZ/PPR47.89C//TACUPETO F2001*2/BRAMBLING/3/2*TACUPETO F2001*2/BRAMBLING……continue

145	6564602	537258	94	KVZ/PPR47.89C//TACUPETO F2001*2/BRAMBLING/3/2*TACUPETO F2001*2/BRAMBLING
146	6564610	537259	95	KVZ/PPR47.89C//FRANCOLIN #1/3/2*PAURAQ
147	6564611	537259	96	KVZ/PPR47.89C//FRANCOLIN #1/3/2*PAURAQ
148	6564618	537259	103	KVZ/PPR47.89C//FRANCOLIN #1/3/2*PAURAQ
149	6564620	537259	105	KVZ/PPR47.89C//FRANCOLIN #1/3/2*PAURAQ
150	6564622	537259	107	KVZ/PPR47.89C//FRANCOLIN #1/3/2*PAURAQ
151	6564625	537262	37	HGO94.7.1.12/3/KIRITATI//PRL/2*PASTOR/4/KIRITATI//2*PRL/2*PASTOR/5/PRL/2*PASTOR
152	6564626	537262	38	HGO94.7.1.12/3/KIRITATI//PRL/2*PASTOR/4/KIRITATI//2*PRL/2*PASTOR/5/PRL/2*PASTOR
153	6564629	537262	41	HGO94.7.1.12/3/KIRITATI//PRL/2*PASTOR/4/KIRITATI//2*PRL/2*PASTOR/5/PRL/2*PASTOR
154	6564631	537262	43	HGO94.7.1.12/3/KIRITATI//PRL/2*PASTOR/4/KIRITATI//2*PRL/2*PASTOR/5/PRL/2*PASTOR
155	6564633	537266	74	CHIH95.2.6//WBLL1*2/KURUKU/3/WBLL1*2/KKTS/4/ND643/2*WBLL1
156	6564634	537266	75	CHIH95.2.6//WBLL1*2/KURUKU/3/WBLL1*2/KKTS/4/ND643/2*WBLL1
157	6564637	533453	65	T.DICOCCON CI9309/AE.SQUARROSA (409)//2*PANDORA
158	6564638	533453	66	T.DICOCCON CI9309/AE.SQUARROSA (409)//2*PANDORA
159	6564639	533455	22	KVZ/PPR47.89C//2*PBW65/2*PASTOR
160	6564646	533460	32	HGO94.7.1.12/2*QUAIU #1
161	6564647	533460	33	HGO94.7.1.12/2*QUAIU #1
162	6564653	533462	18	HGO94.7.1.12//WBLL1*2/KUKUNA/3/WBLL1*2/KURUKU
163	6564655	533462	20	HGO94.7.1.12//WBLL1*2/KUKUNA/3/WBLL1*2/KURUKU
164	6564658	533462	23	HGO94.7.1.12//WBLL1*2/KUKUNA/3/WBLL1*2/KURUKU
165	6564661	533467	55	COAH90.26.31//KIRITATI/WBLL1/3/KIRITATI/2*WBLL1
166	6564662	533467	56	COAH90.26.31//KIRITATI/WBLL1/3/KIRITATI/2*WBLL1
167	6564664	533467	58	COAH90.26.31//KIRITATI/WBLL1/3/KIRITATI/2*WBLL1
168	6564666	533467	60	COAH90.26.31//KIRITATI/WBLL1/3/KIRITATI/2*WBLL1
169	6575207	537121	224	QUAIU #1/3/T.DICOCCON PI94625/AE.SQUARROSA (372)//3*PASTOR/4/QUAIU
170	6575208	537121	225	QUAIU #1/3/T.DICOCCON PI94625/AE.SQUARROSA (372)//3*PASTOR/4/QUAIU
171	6575210	537121	227	QUAIU #1/3/T.DICOCCON PI94625/AE.SQUARROSA (372)//3*PASTOR/4/QUAIU
172	6575214	537122	58	QUAIU #1/SOLALA//QUAIU #2
173	6575215	537122	59	QUAIU #1/SOLALA//QUAIU #2
174	6575216	537122	60	QUAIU #1/SOLALA//QUAIU #2

…….. ……..continue

175	6575220	537122	64	QUAIU #1/SOLALA//QUAIU #2
176	6575224	537123	260	QUAIU #1/3/T.DICOCCON PI94625/AE.SQUARROSA (372)//3*PASTOR/4/QUAIU #2
177	6575225	537123	261	QUAIU #1/3/T.DICOCCON PI94625/AE.SQUARROSA (372)//3*PASTOR/4/QUAIU #2
178	6575226	537123	262	QUAIU #1/3/T.DICOCCON PI94625/AE.SQUARROSA (372)//3*PASTOR/4/QUAIU #2
179	6575228	537123	264	QUAIU #1/3/T.DICOCCON PI94625/AE.SQUARROSA (372)//3*PASTOR/4/QUAIU #2
180	6575229	537123	265	QUAIU #1/3/T.DICOCCON PI94625/AE.SQUARROSA (372)//3*PASTOR/4/QUAIU #2
181	6575231	537123	267	QUAIU #1/3/T.DICOCCON PI94625/AE.SQUARROSA (372)//3*PASTOR/4/QUAIU #2
182	6575233	537123	269	QUAIU #1/3/T.DICOCCON PI94625/AE.SQUARROSA (372)//3*PASTOR/4/QUAIU #2
183	6575234	537123	270	QUAIU #1/3/T.DICOCCON PI94625/AE.SQUARROSA (372)//3*PASTOR/4/QUAIU #2
184	6575241	537126	244	DANPHE #1*2/3/T.DICOCCON PI94625/AE.SQUARROSA (372)//SHA4/CHIL
185	6575242	537126	245	DANPHE #1*2/3/T.DICOCCON PI94625/AE.SQUARROSA (372)//SHA4/CHIL
186	6575246	537126	249	DANPHE #1*2/3/T.DICOCCON PI94625/AE.SQUARROSA (372)//SHA4/CHIL
187	6575261	537126	264	DANPHE #1*2/3/T.DICOCCON PI94625/AE.SQUARROSA (372)//SHA4/CHIL
188	6575266	537126	269	DANPHE #1*2/3/T.DICOCCON PI94625/AE.SQUARROSA (372)//SHA4/CHIL
189	6575273	537126	276	DANPHE #1*2/3/T.DICOCCON PI94625/AE.SQUARROSA (372)//SHA4/CHIL
190	6575274	537126	277	DANPHE #1*2/3/T.DICOCCON PI94625/AE.SQUARROSA (372)//SHA4/CHIL
191	6575275	537126	278	DANPHE #1*2/3/T.DICOCCON PI94625/AE.SQUARROSA (372)//SHA4/CHIL
192	6575276	537130	219	KINDE*2/4/T.DICOCCON PI94625/AE.SQUARROSA (372)//TUI/CLMS/3/2*PASTOR
193	6575280	537130	223	KINDE*2/4/T.DICOCCON PI94625/AE.SQUARROSA (372)//TUI/CLMS/3/2*PASTOR
194	6575283	537130	226	KINDE*2/4/T.DICOCCON PI94625/AE.SQUARROSA (372)//TUI/CLMS/3/2*PASTOR
195	6575292	537135	165	CHONTE*2/3/T.DICOCCON PI94625/AE.SQUARROSA (372)//3*PASTOR
196	6575294	537135	167	CHONTE*2/3/T.DICOCCON PI94625/AE.SQUARROSA (372)//3*PASTOR
197	6575295	537135	168	CHONTE*2/3/T.DICOCCON PI94625/AE.SQUARROSA (372)//3*PASTOR
198	6575296	537135	169	CHONTE*2/3/T.DICOCCON PI94625/AE.SQUARROSA (372)//3*PASTOR
199	6575297	537135	170	CHONTE*2/3/T.DICOCCON PI94625/AE.SQUARROSA (372)//3*PASTOR
200	6575301	537135	174	CHONTE*2/3/T.DICOCCON PI94625/AE.SQUARROSA (372)//3*PASTOR
201	6575311	537135	184	CHONTE*2/3/T.DICOCCON PI94625/AE.SQUARROSA (372)//3*PASTOR
202	6575321	537135	194	CHONTE*2/3/T.DICOCCON PI94625/AE.SQUARROSA (372)//3*PASTOR
203	6575326	537137	218	PAURAQ*2/SOLALA
204	6575327	537137	219	PAURAQ*2/SOLALA

…….. …….. ……..continue

205	6575328	537137	220	PAURAQ*2/SOLALA
206	6575331	537137	223	PAURAQ*2/SOLALA
207	6575332	537137	224	PAURAQ*2/SOLALA
208	6575336	537139	272	WAXWING*2/TUKURU*2/3/T.DICOCCON PI94625/AE.SQUARROSA (372)//3*PASTOR
209	6575350	537141	224	WAXWING*2/TUKURU*2/3/T.DICOCCON PI94625/AE.SQUARROSA (372)//SHA4/CHIL
210	6575354	537141	228	WAXWING*2/TUKURU*2/3/T.DICOCCON PI94625/AE.SQUARROSA (372)//SHA4/CHIL
211	6575358	537141	232	WAXWING*2/TUKURU*2/3/T.DICOCCON PI94625/AE.SQUARROSA (372)//SHA4/CHIL
212	6575363	537141	237	WAXWING*2/TUKURU*2/3/T.DICOCCON PI94625/AE.SQUARROSA (372)//SHA4/CHIL
213	6575365	537146	48	VILLA JUAREZ F2009/3/T.DICOCCON PI94625/AE.SQUARROSA (372)//3*PASTOR/4/WBLL1*2/BRAMBLING
214	6575367	537146	50	VILLA JUAREZ F2009/3/T.DICOCCON PI94625/AE.SQUARROSA (372)//3*PASTOR/4/WBLL1*2/BRAMBLING
215	6575370	537254	302	T.DICOCCON CI9309/AE.SQUARROSA (409)//MUTUS/3/2*MUTUS
216	6575376	537254	308	T.DICOCCON CI9309/AE.SQUARROSA (409)//MUTUS/3/2*MUTUS
217	6575377	537254	309	T.DICOCCON CI9309/AE.SQUARROSA (409)//MUTUS/3/2*MUTUS
218	6575378	537254	310	T.DICOCCON CI9309/AE.SQUARROSA (409)//MUTUS/3/2*MUTUS
219	6575379	537254	311	T.DICOCCON CI9309/AE.SQUARROSA (409)//MUTUS/3/2*MUTUS
220	6575380	537254	312	T.DICOCCON CI9309/AE.SQUARROSA (409)//MUTUS/3/2*MUTUS
221	6575381	537254	313	T.DICOCCON CI9309/AE.SQUARROSA (409)//MUTUS/3/2*MUTUS
222	6575383	537254	315	T.DICOCCON CI9309/AE.SQUARROSA (409)//MUTUS/3/2*MUTUS
223	6575384	537254	316	T.DICOCCON CI9309/AE.SQUARROSA (409)//MUTUS/3/2*MUTUS
224	6575393	537254	325	T.DICOCCON CI9309/AE.SQUARROSA (409)//MUTUS/3/2*MUTUS
225	6575395	537258	112	KVZ/PPR47.89C//TACUPETO F2001*2/BRAMBLING/3/2*TACUPETO F2001*2/BRAMBLING
226	6575396	537258	113	KVZ/PPR47.89C//TACUPETO F2001*2/BRAMBLING/3/2*TACUPETO F2001*2/BRAMBLING
227	6575398	537259	127	KVZ/PPR47.89C//FRANCOLIN #1/3/2*PAURAQ
228	6575403	537259	132	KVZ/PPR47.89C//FRANCOLIN #1/3/2*PAURAQ
229	6575406	537259	135	KVZ/PPR47.89C//FRANCOLIN #1/3/2*PAURAQ
230	6575408	537261	27	HGO94.7.1.12/2*QUAIU #1//QUAIU #2
231	6575409	537261	28	HGO94.7.1.12/2*QUAIU #1//QUAIU #2
232	6575411	537261	30	HGO94.7.1.12/2*QUAIU #1//QUAIU #2 …….. …….. ……..continue

233	6575417	537264	127	CHIH95.2.6/5/BABAX/LR42//BABAX*2/4/SNI/TRAP#1/3/KAUZ*2/TRAP//KAUZ/6/2*BABAX/LR42//BABAX*2/3/TUKURU
234	6575420	537264	130	CHIH95.2.6/5/BABAX/LR42//BABAX*2/4/SNI/TRAP#1/3/KAUZ*2/TRAP//KAUZ/6/2*BABAX/LR42//BABAX*2/3/TUKURU
235	6575421	537264	131	CHIH95.2.6/5/BABAX/LR42//BABAX*2/4/SNI/TRAP#1/3/KAUZ*2/TRAP//KAUZ/6/2*BABAX/LR42//BABAX*2/3/TUKURU
236	6575426	537267	115	COAH90.26.31/4/3*BL2064//SW89-5124*2/FASAN/3/TILHI
237	6575427	537267	116	COAH90.26.31/4/3*BL2064//SW89-5124*2/FASAN/3/TILHI
238	6575428	537267	117	COAH90.26.31/4/3*BL2064//SW89-5124*2/FASAN/3/TILHI
239	6575430	537267	119	COAH90.26.31/4/3*BL2064//SW89-5124*2/FASAN/3/TILHI
240	6575435	533460	50	HGO94.7.1.12/2*QUAIU #1
241	6575437	533466	79	COAH90.26.31/4/2*BL2064//SW89-5124*2/FASAN/3/TILHI
242	6575441	533466	83	COAH90.26.31/4/2*BL2064//SW89-5124*2/FASAN/3/TILHI
243	6575442	533466	84	COAH90.26.31/4/2*BL2064//SW89-5124*2/FASAN/3/TILHI
244	6575444	533466	86	COAH90.26.31/4/2*BL2064//SW89-5124*2/FASAN/3/TILHI
245	6575446	533466	88	COAH90.26.31/4/2*BL2064//SW89-5124*2/FASAN/3/TILHI
246	6575451	533467	75	COAH90.26.31//KIRITATI/WBLL1/3/KIRITATI/2*WBLL1
247	6575453	533467	77	COAH90.26.31//KIRITATI/WBLL1/3/KIRITATI/2*WBLL1
248	6575454	533467	78	COAH90.26.31//KIRITATI/WBLL1/3/KIRITATI/2*WBLL1
249	6575457	537253	176	T.DICOCCON CI9309/AE.SQUARROSA (409)/4/3*CHIBIA//PRLII/CM65531/3/SKAUZ/BAV92
250	6575458	537254	327	T.DICOCCON CI9309/AE.SQUARROSA (409)//MUTUS/3/2*MUTUS
251	6575460	537122	66	QUAIU #1/SOLALA//QUAIU #2
252	6575462	537125	153	DANPHE #1*2/SOLALA
253	6575463	537125	154	DANPHE #1*2/SOLALA
254	6575471	537125	162	DANPHE #1*2/SOLALA
255	6575480	537137	225	PAURAQ*2/SOLALA
256	6575484	537138	181	PAURAQ*2/3/T.DICOCCON PI94625/AE.SQUARROSA (372)//SHA4/CHIL
257	6575486	537138	183	PAURAQ*2/3/T.DICOCCON PI94625/AE.SQUARROSA (372)//SHA4/CHIL
258	6575489	537139	280	WAXWING*2/TUKURU*2/3/T.DICOCCON PI94625/AE.SQUARROSA (372)//3*PASTOR
259	6575490	537139	281	WAXWING*2/TUKURU*2/3/T.DICOCCON PI94625/AE.SQUARROSA (372)//3*PASTOR ……..continue

260	6575494	537142	126	FRNCLN*2/4/T.DICOCCON PI94625/AE.SQUARROSA (372)//TUI/CLMS/3/2*PASTOR
261	6575502	537142	134	FRNCLN*2/4/T.DICOCCON PI94625/AE.SQUARROSA (372)//TUI/CLMS/3/2*PASTOR
262	6575503	537142	135	FRNCLN*2/4/T.DICOCCON PI94625/AE.SQUARROSA (372)//TUI/CLMS/3/2*PASTOR
263	6575505	537142	137	FRNCLN*2/4/T.DICOCCON PI94625/AE.SQUARROSA (372)//TUI/CLMS/3/2*PASTOR
264	6575507	537144	110	VILLA JUAREZ F2009/3/T.DICOCCON PI94625/AE.SQUARROSA (372)//3*PASTOR/4/WBLL1*2/BRAMBLING
265	6575508	537144	111	VILLA JUAREZ F2009/3/T.DICOCCON PI94625/AE.SQUARROSA (372)//3*PASTOR/4/WBLL1*2/BRAMBLING
266	6575510	537145	130	VILLA JUAREZ F2009/SOLALA//WBLL1*2/BRAMBLING
267	6575513	537147	123	WHEAR/KUKUNA/3/C80.1/3*BATAVIA//2*WBLL1/4/T.DICOCCON PI94625/AE.SQUARROSA (372)//3*PASTOR/5/WHEAR/KUKUNA/3/C80.1/3*BATAVIA//2*WBLL1
268	6575514	537149	171	WHEAR/KUKUNA/3/C80.1/3*BATAVIA//2*WBLL1/4/T.DICOCCON PI94625/AE.SQUARROSA (372)//SHA4/CHIL/5/WHEAR/KUKUNA/3/C80.1/3*BATAVIA//2*WBLL1
269	6575518	537149	175	WHEAR/KUKUNA/3/C80.1/3*BATAVIA//2*WBLL1/4/T.DICOCCON PI94625/AE.SQUARROSA (372)//SHA4/CHIL/5/WHEAR/KUKUNA/3/C80.1/3*BATAVIA//2*WBLL1
270	6575522	537254	332	T.DICOCCON CI9309/AE.SQUARROSA (409)//MUTUS/3/2*MUTUS
271	6575529	537254	339	T.DICOCCON CI9309/AE.SQUARROSA (409)//MUTUS/3/2*MUTUS
272	6575531	537267	120	COAH90.26.31/4/3*BL2064//SW89-5124*2/FASAN/3/TILHI
273	6575533	537260	60	CROC_1/AE.SQUARROSA (210)//WBLL1*2/BRAMBLING/3/2*VILLA JUAREZ F2009
274	6575536	537260	63	CROC_1/AE.SQUARROSA (210)//WBLL1*2/BRAMBLING/3/2*VILLA JUAREZ F2009
275	6575538	537260	65	CROC_1/AE.SQUARROSA (210)//WBLL1*2/BRAMBLING/3/2*VILLA JUAREZ F2009
276	6575540	537260	67	CROC_1/AE.SQUARROSA (210)//WBLL1*2/BRAMBLING/3/2*VILLA JUAREZ F2009
277	6575736	546257	79	KINDE/4/CMH75A.66//H567.71/5*PVN/3/SERI
278	6575553	537264	137	CHIH95.2.6/5/BABAX/LR42//BABAX*2/4/SNI/TRAP#1/3/KAUZ*2/TRAP//KAUZ/6/2*BABAX/LR42//BABAX*2/3/TUKURU
279	6575554	537264	138	CHIH95.2.6/5/BABAX/LR42//BABAX*2/4/SNI/TRAP#1/3/KAUZ*2/TRAP//KAUZ/6/2*BABAX/LR42//BABAX*2/3/TUKURU
280	6575555	533451	58	T.DICOCCON CI9309/AE.SQUARROSA (409)/4/2*CHIBIA//PRLII/CM65531/3/SKAUZ/BAV92
281	6575558	533451	61	T.DICOCCON CI9309/AE.SQUARROSA (409)/4/2*CHIBIA//PRLII/CM65531/3/SKAUZ/BAV92
282	6575560	533457	21	KVZ/PPR47.89C//FRANCOLIN #1/3/PAURAQ
283	6575562	533457	23	KVZ/PPR47.89C//FRANCOLIN #1/3/PAURAQ
284	6575563	533457	24	KVZ/PPR47.89C//FRANCOLIN #1/3/PAURAQ …….. …….. ……..continue

285	6575565	537144	113	VILLA JUAREZ F2009/3/T.DICOCCON PI94625/AE.SQUARROSA (372)//3*PASTOR/4/WBLL1*2/BRAMBLING
286	6575660	546234	54	KACHU/SOLALA
287	6575681	546248	40	KIRITATI/4/2*SERI.1B*2/3/KAUZ*2/BOW//KAUZ/5/CMH81.530
288	6575708	546253	41	WHEAR/KIRITATI/3/C80.1/3*BATAVIA//2*WBLL1/4/CMH75A.66/SERI
289	6575715	546253	48	WHEAR/KIRITATI/3/C80.1/3*BATAVIA//2*WBLL1/4/CMH75A.66/SERI
290	6575720	546254	30	HUW234+LR34/PRINIA//PFAU/WEAVER/3/CMH83.30
291	6575725	546257	68	KINDE/4/CMH75A.66//H567.71/5*PVN/3/SERI
292	2430154	8890	1549	PBW343
293	2673706	313209	45	WAXWING

#GID: Genotype identifier; CID: Cross identifier; SID: Selection identifier

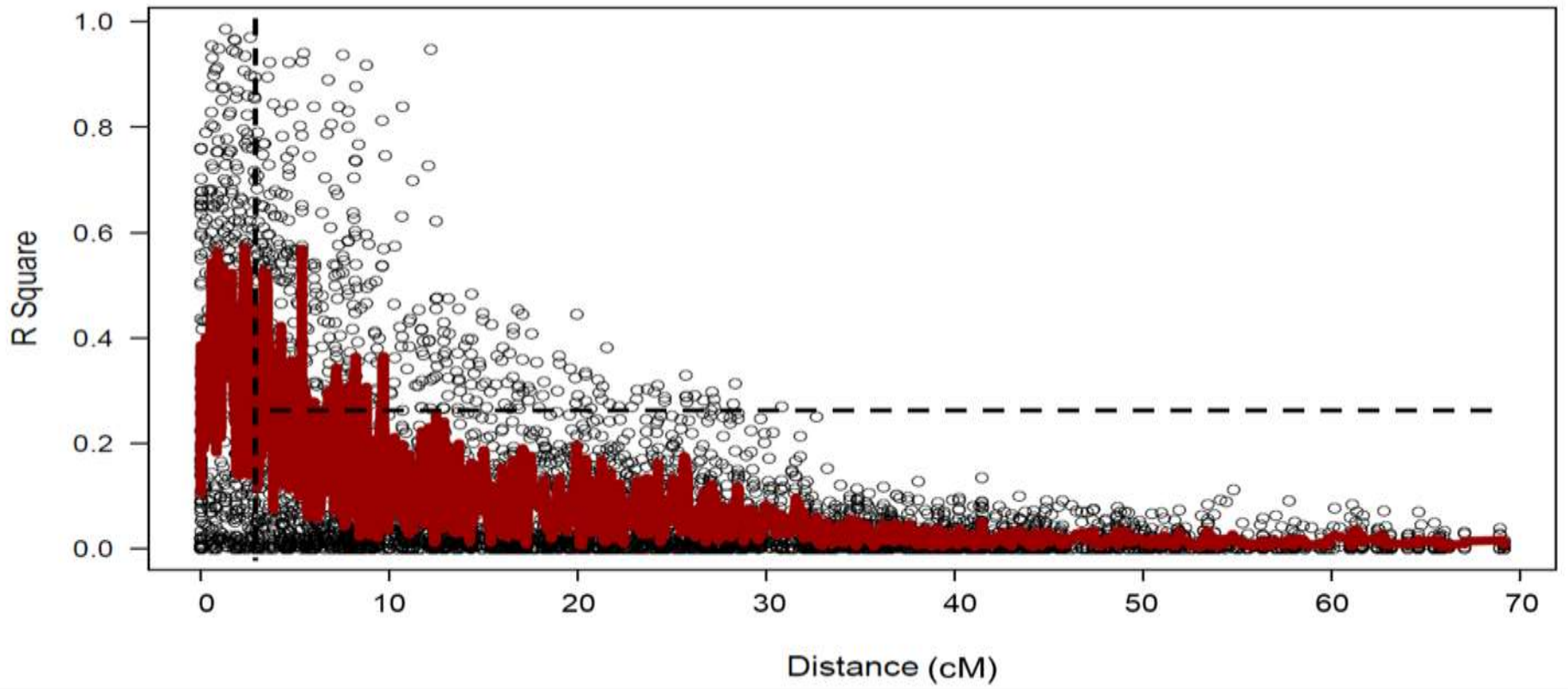

Appendix IV Representation of decay of linkage disequilibrium over distance. Each dot shows a pair of distances between two markers and their squared correlation coefficient (r^2). The red line indicates the moving average of the 10 adjacent markers.

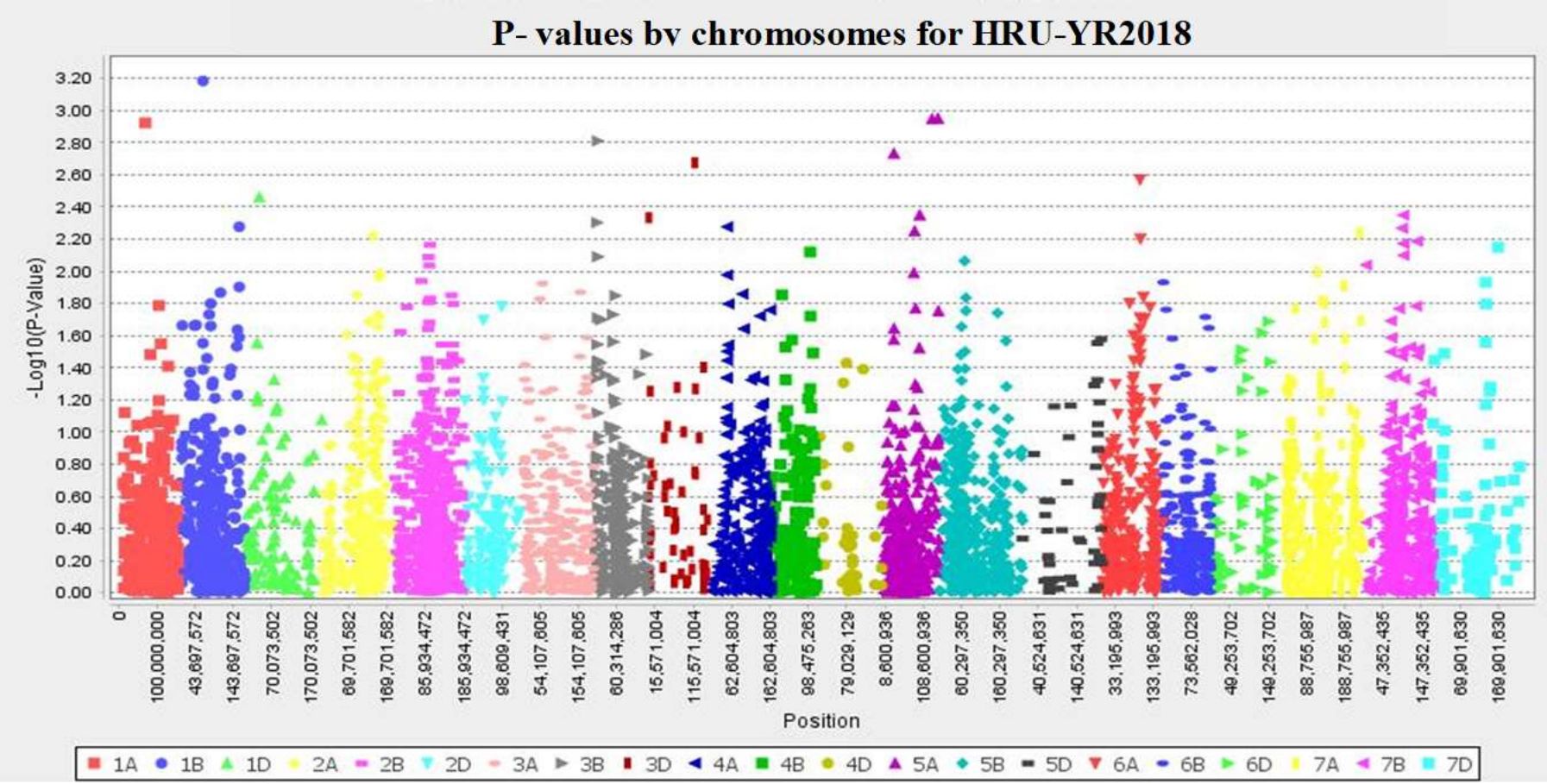

Appendix V Manhattan plots depicts significant SNPs detected against mixture of stripe rust (YR) pathotypes in field environments. Chromosome name on x-axis and the -log10 (p-value) on the y-axis have been plotted. Site (Horse research unit- HRU and Lansdowne research unit-LDN) is suffixed with the rust type and year e.g. HRU-YR2018. **Continue.**

P-values by Chromosomes for LDN-YR2018

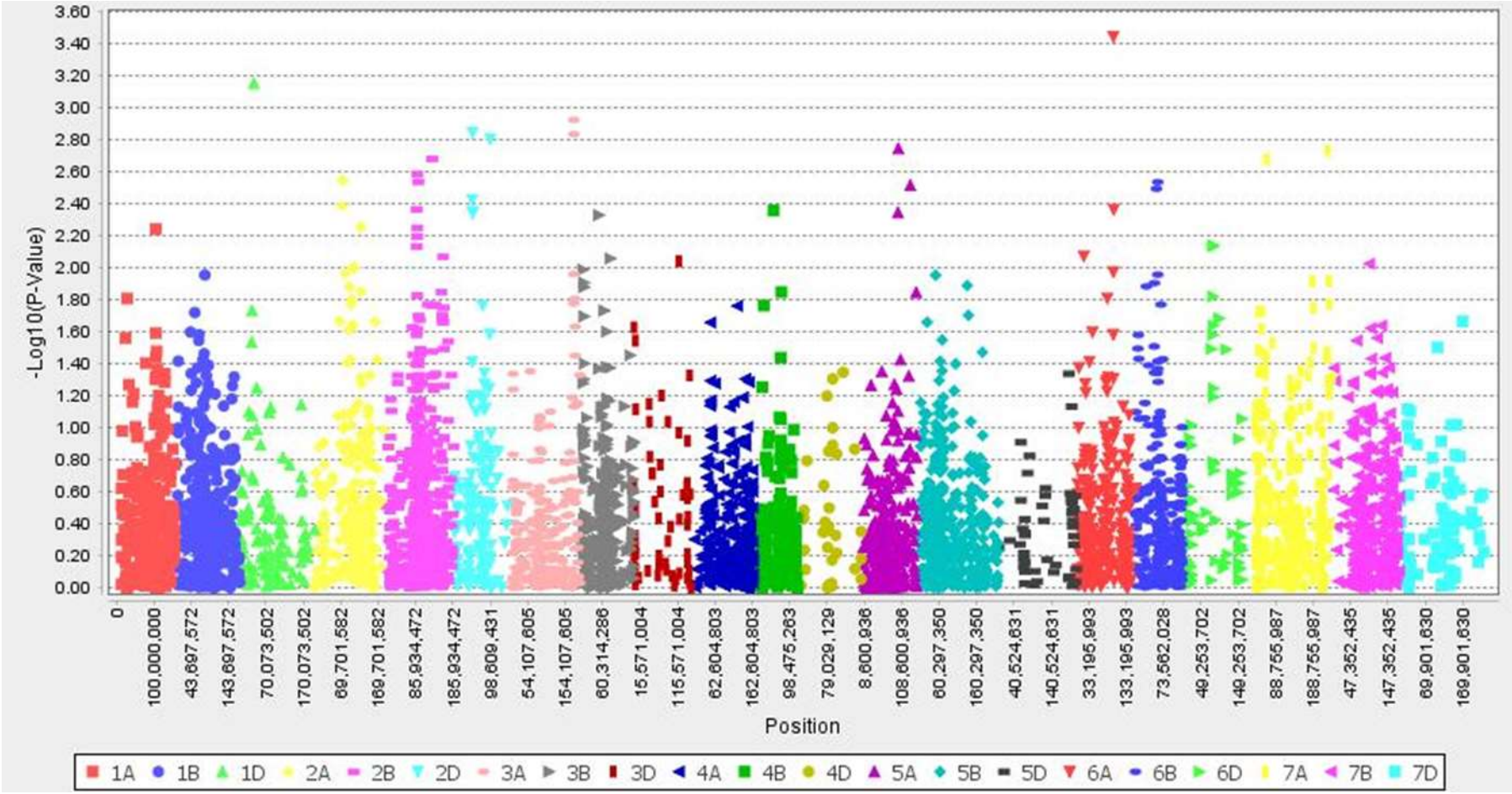

Continue.

P-values by Chromosomes for HRU-YR2019

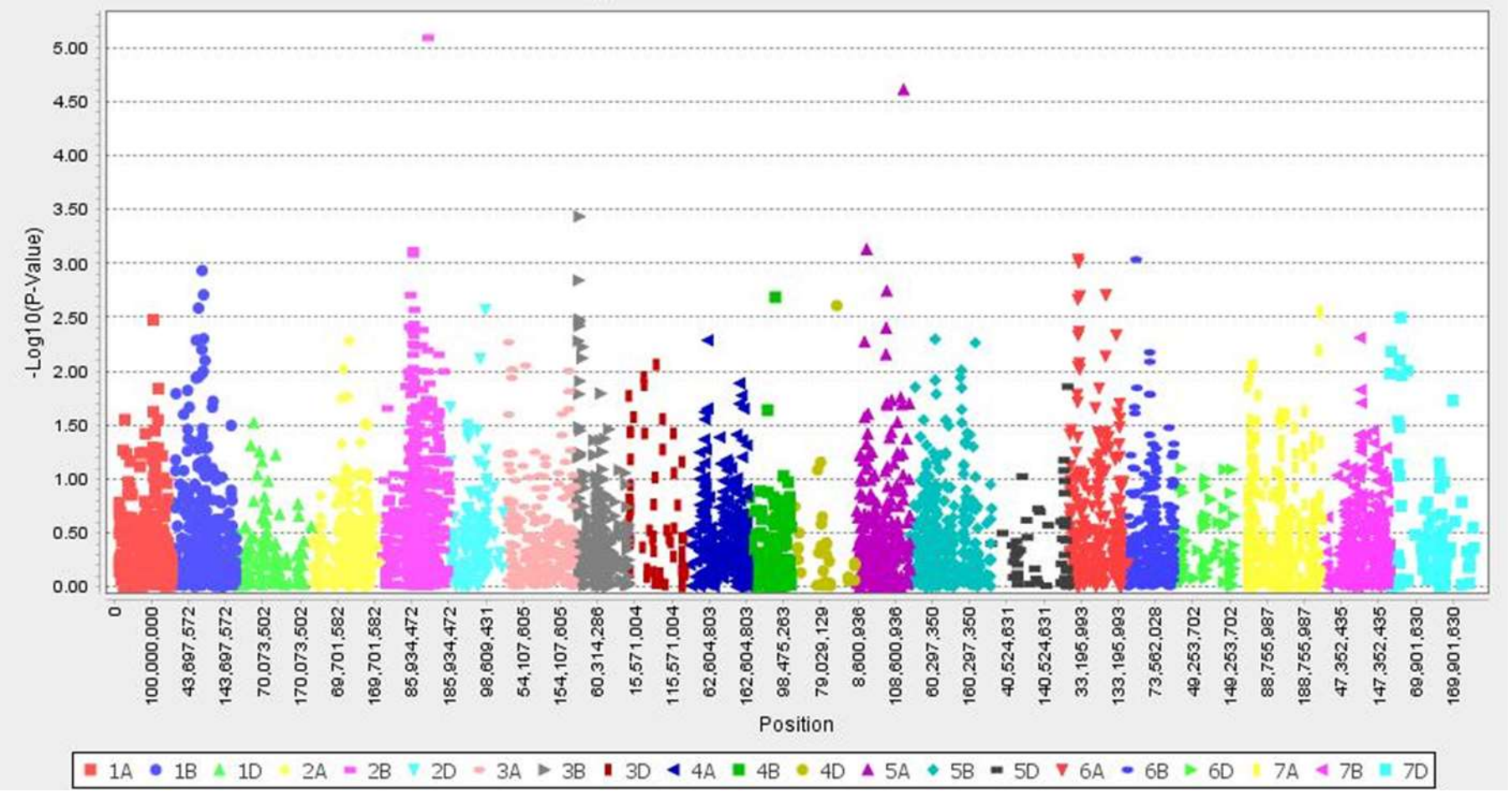

Continue.

P-values by Chromosomes for LDN-YR2019

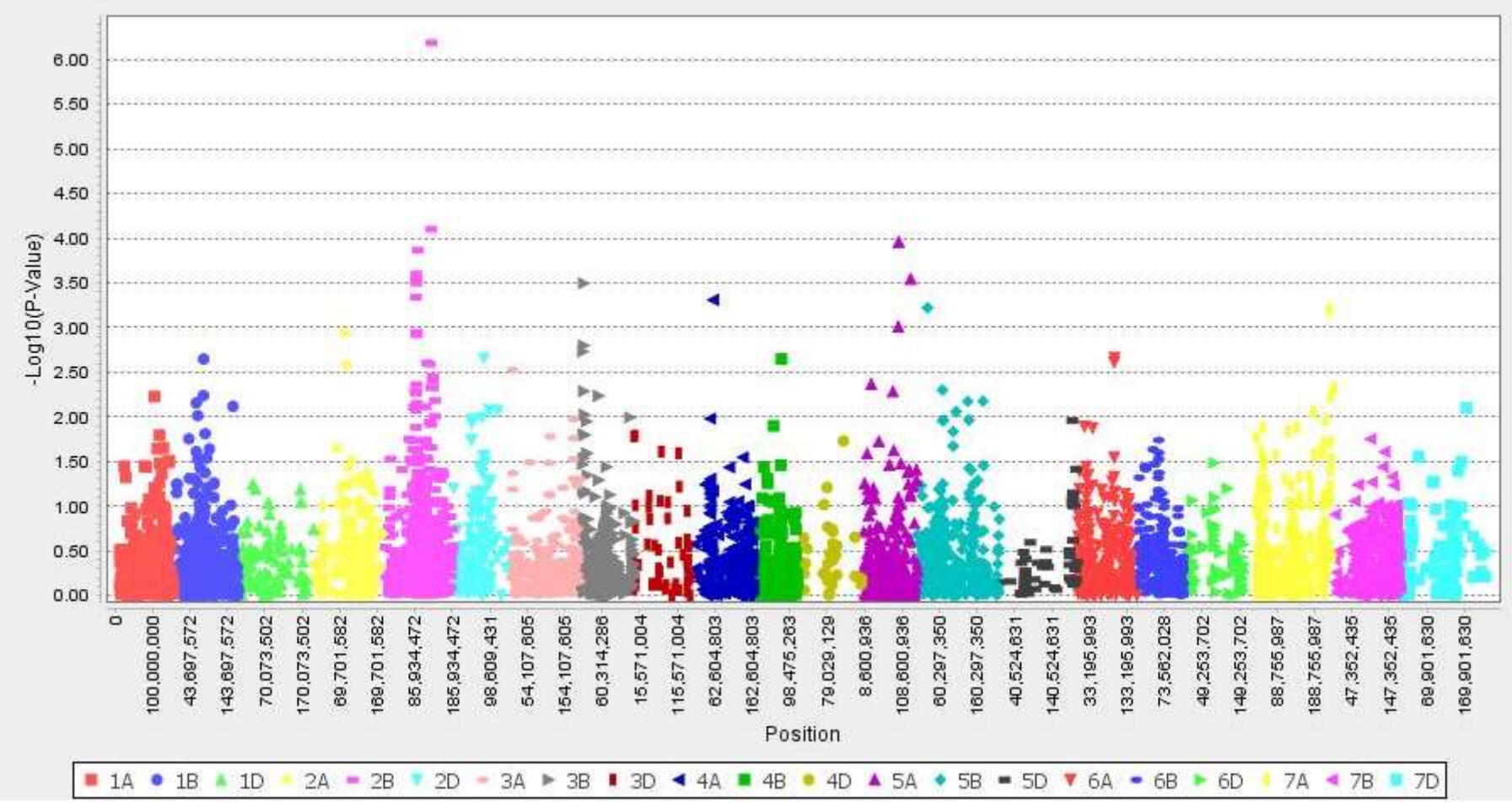

P-values by Chromosomes for HRU-LR2018

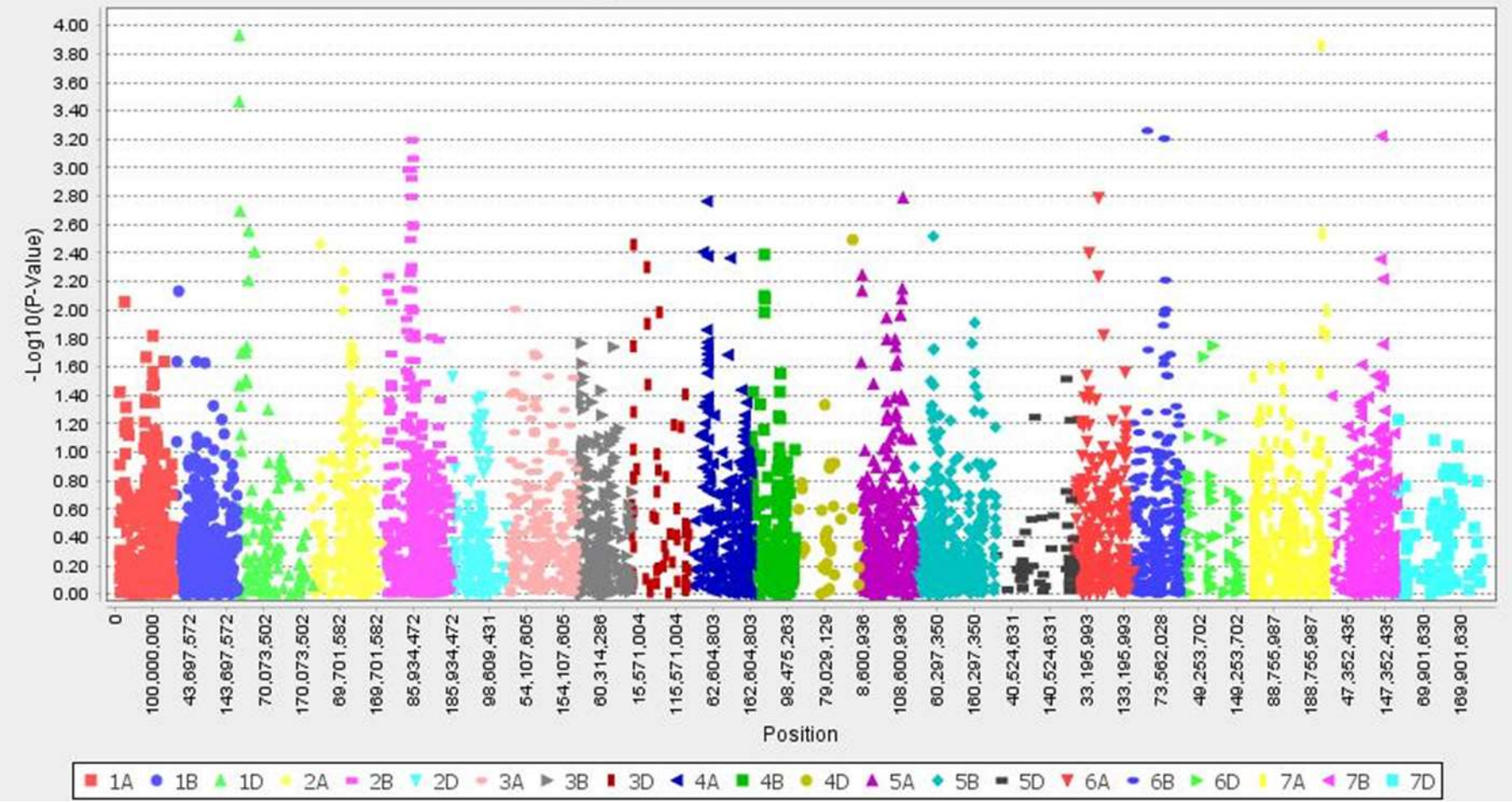

Appendix VI Manhattan plots depicts significant SNPs detected against mixture of leaf rust (LR) pathotypes in field environments. Chromosome name on x-axis and the -log10 (p-value) on the y-axis have been plotted. Site (Horse research unit- HRU and Lansdowne research unit-LDN) is suffixed with the rust type and year e.g. HRU-LR2018. **Continue.**

P-values by Chromosomes for LDN-LR2018

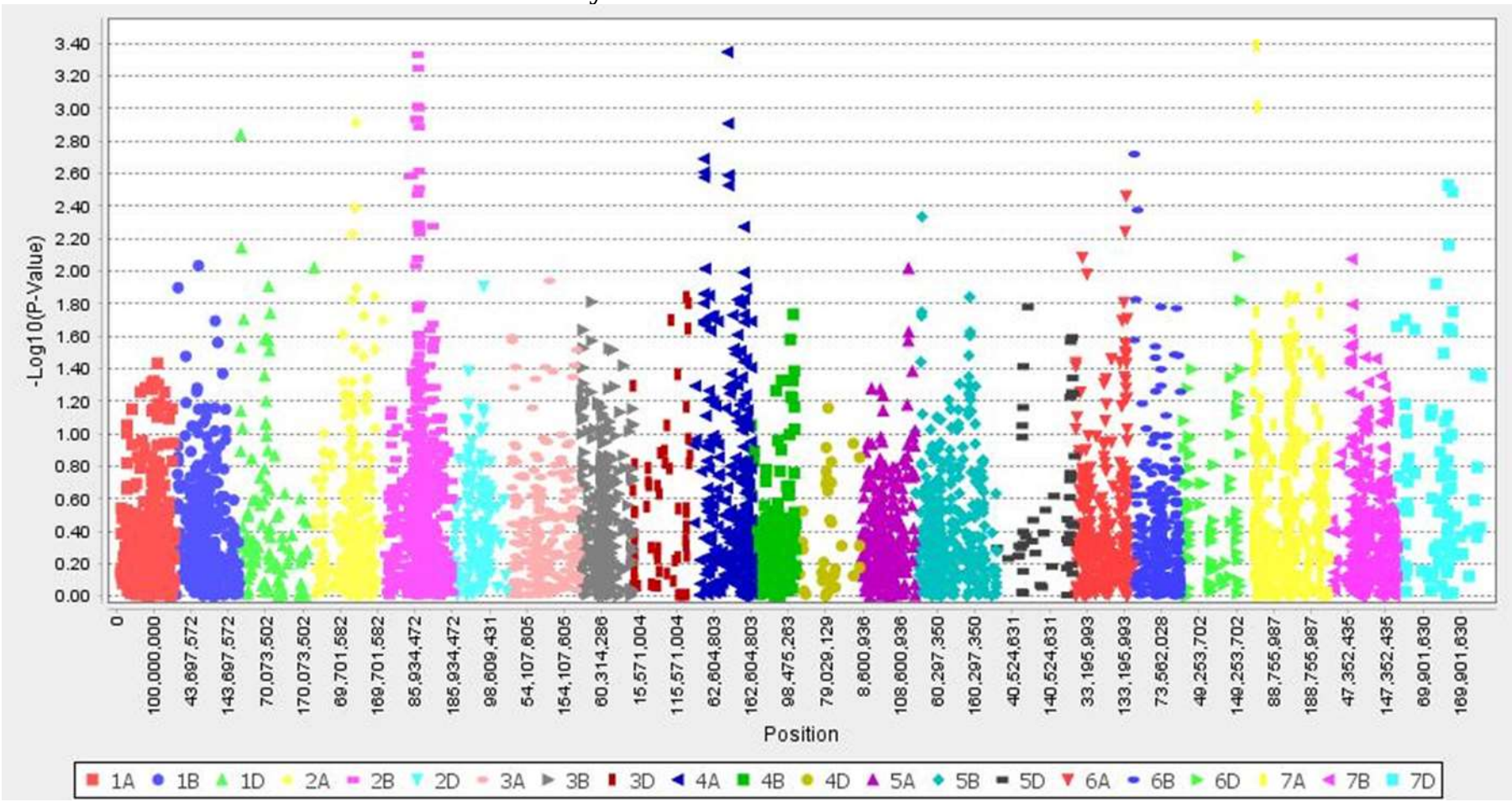

Continue.

P-values by Chromosomes for HRU-LR2019

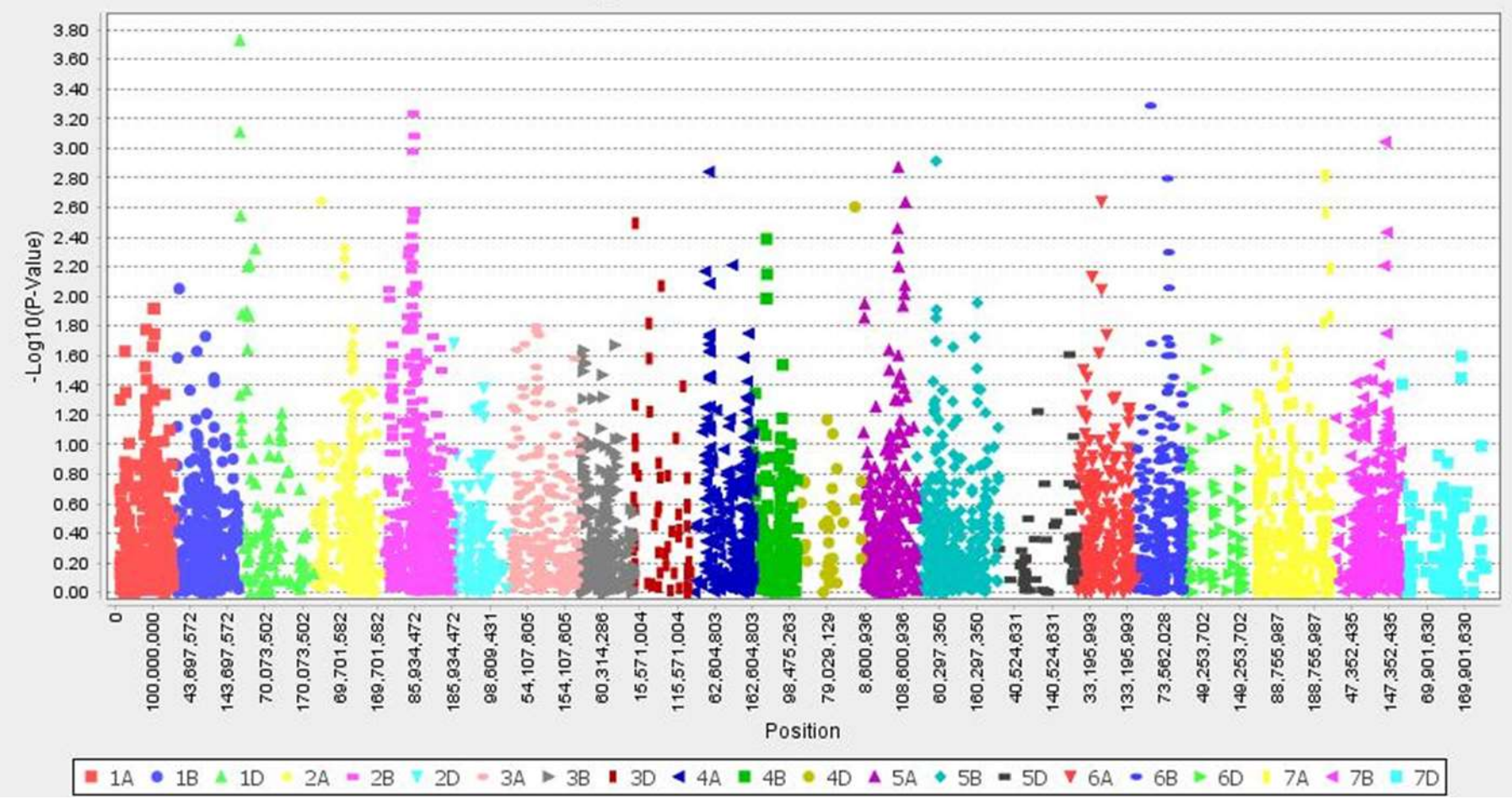

Continue.

P-values by Chromosomes for LDN-LR2019

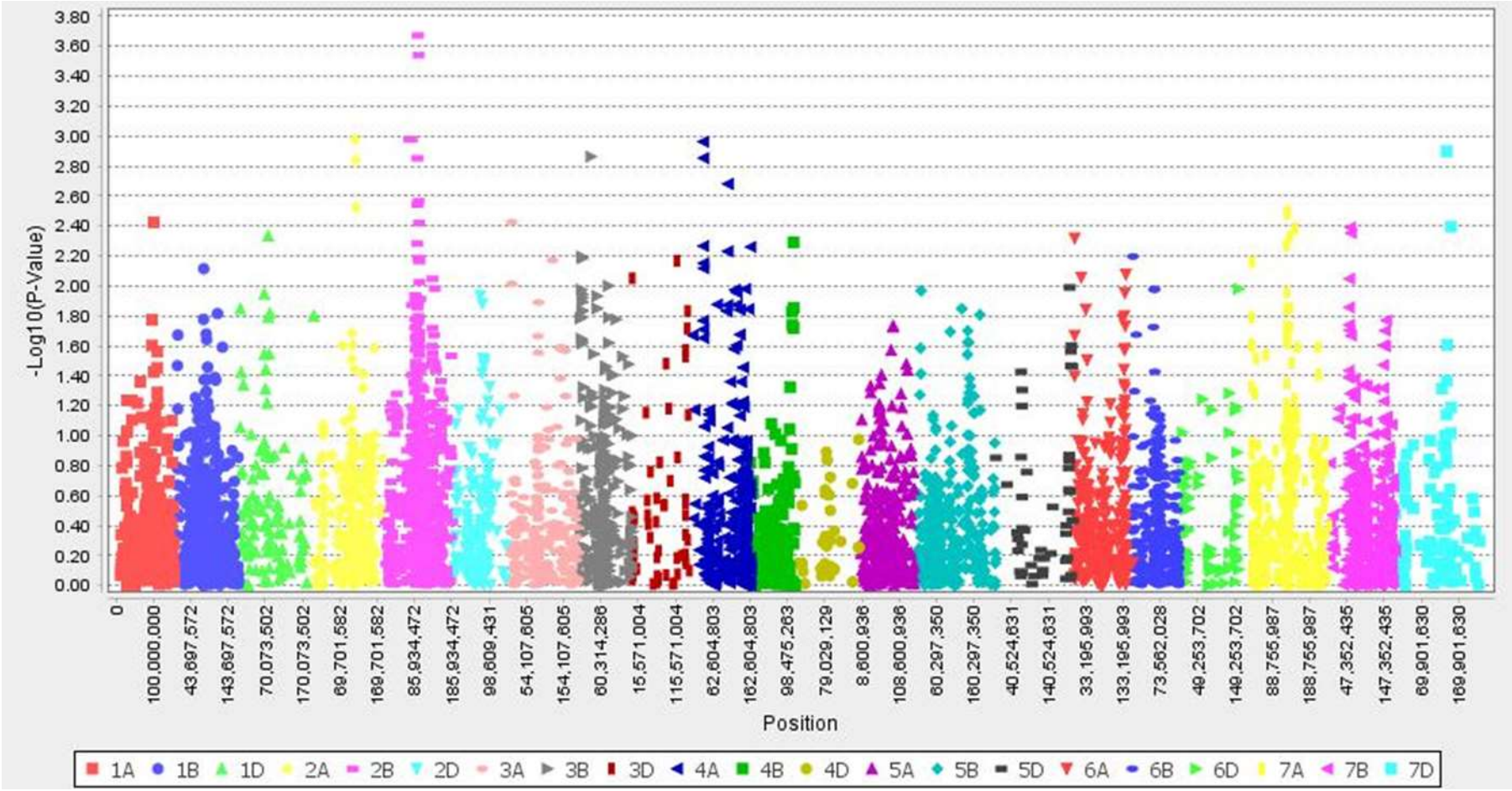

P-values by Chromosomes for HRU-SR2018

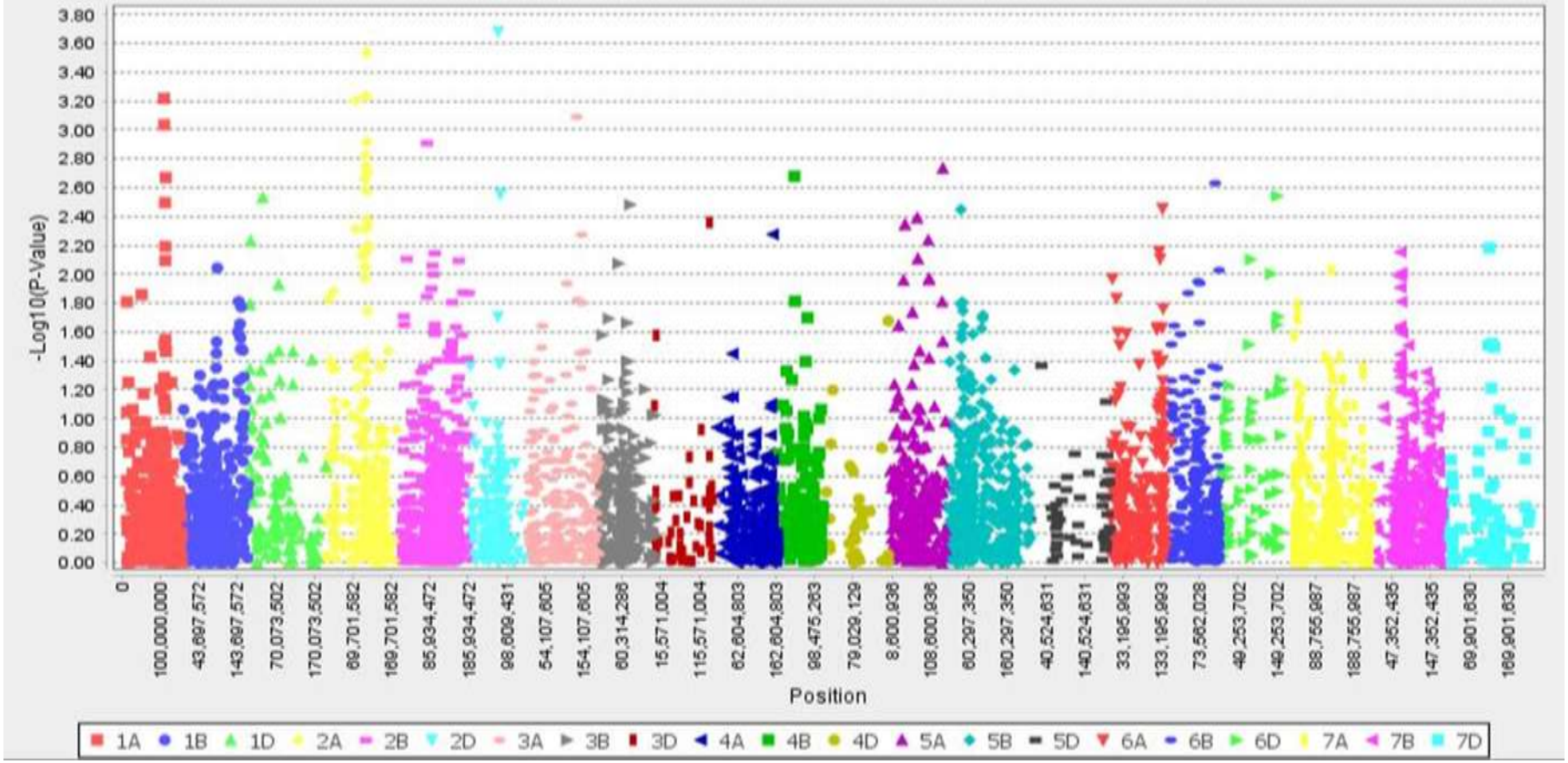

Appendix VII Manhattan plots depicts significant SNPs detected against mixture of stem rust (SR) pathotypes in field environments. Chromosome name on x-axis and the -log10 (p-value) on the y-axis have been plotted. Site (Horse research unit- HRU and Lansdowne experimental unit-LDN) is suffixed with the rust type and year e.g. HRU-SR2018 **Continue**.

P-values by Chromosomes for LDN-SR2018

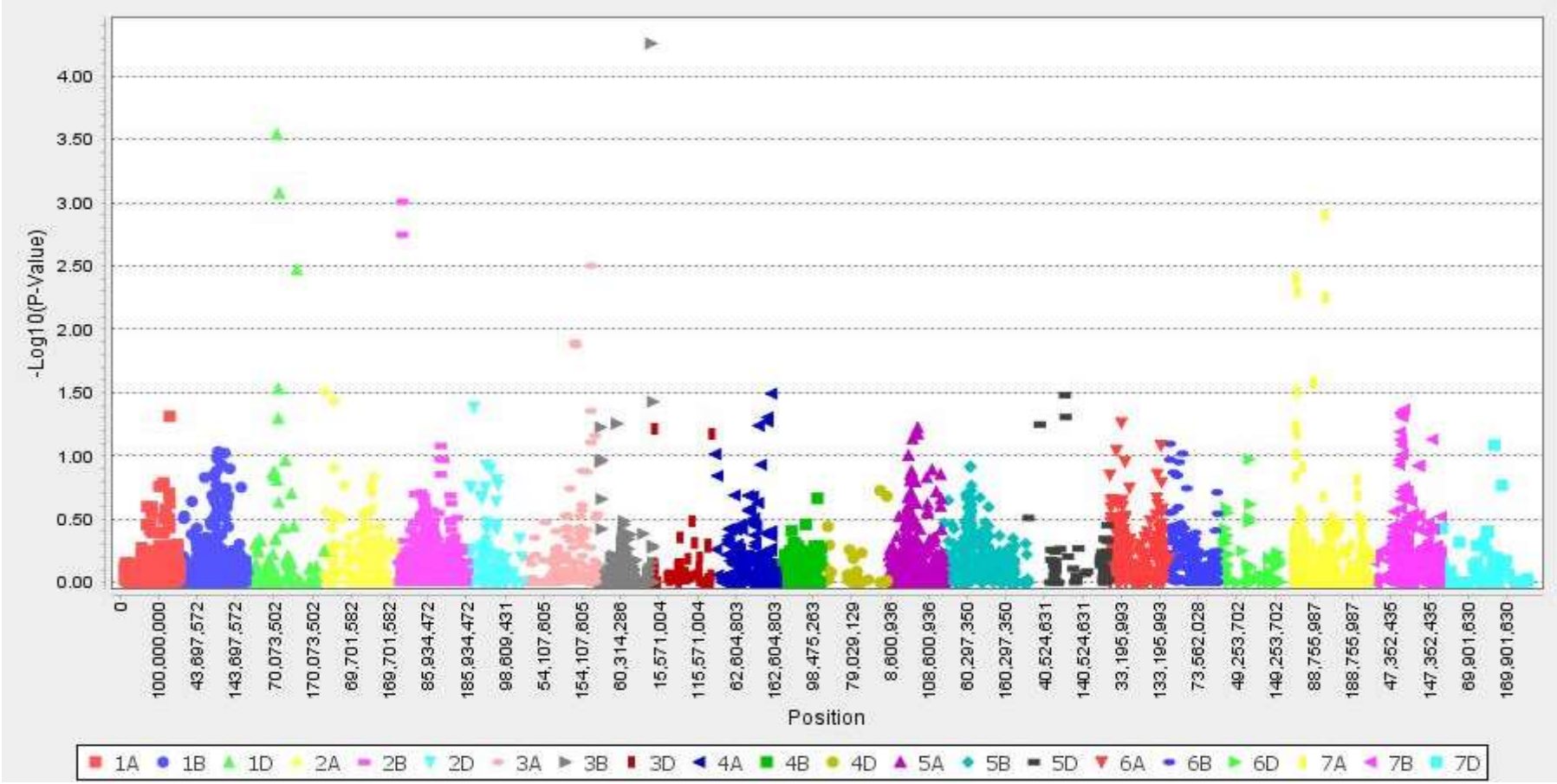

Continue.

P-values by Chromosomes for HRU-SR2019

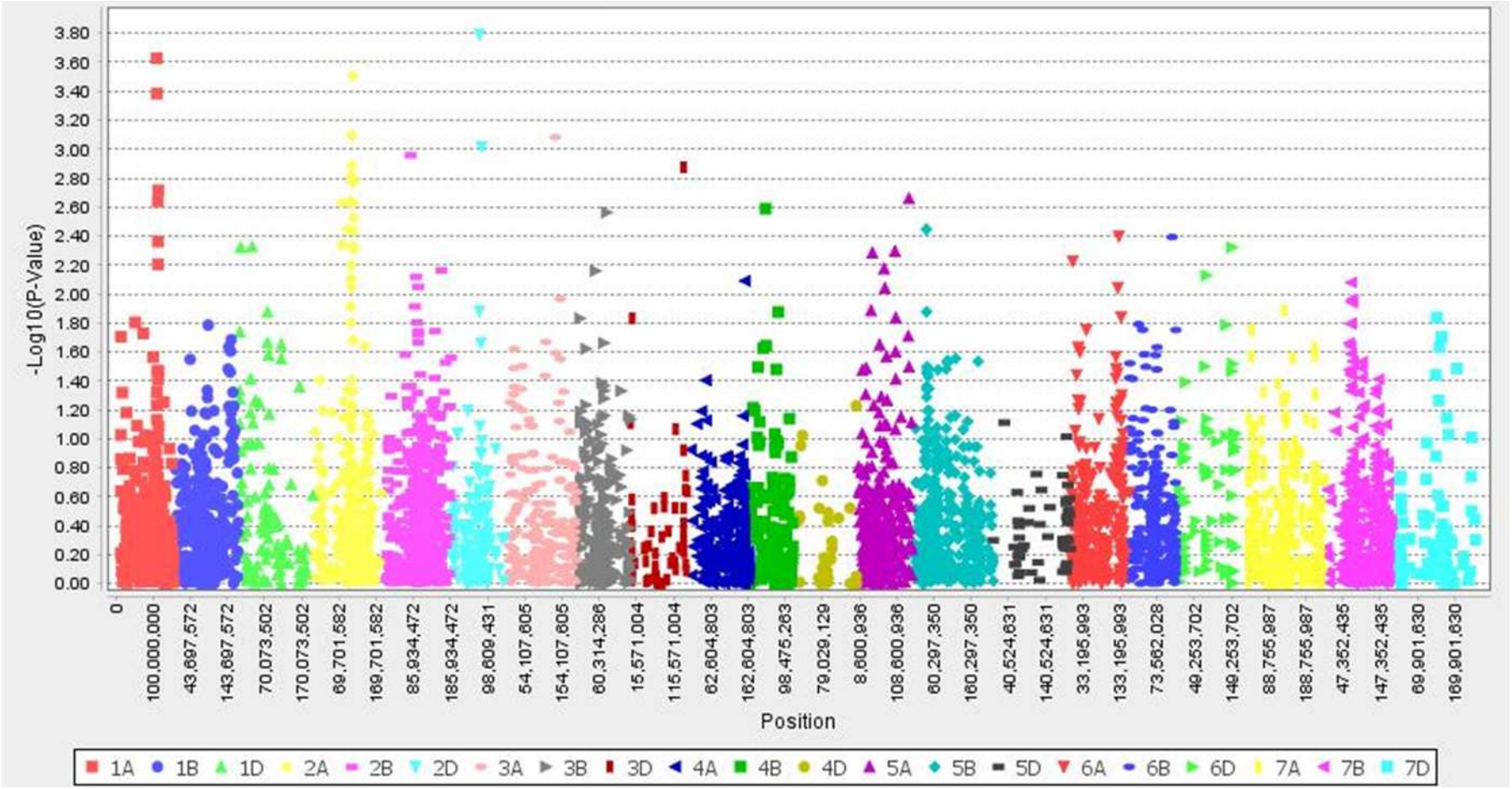

Continue.

P-values by Chromosomes for LDN-SR2019

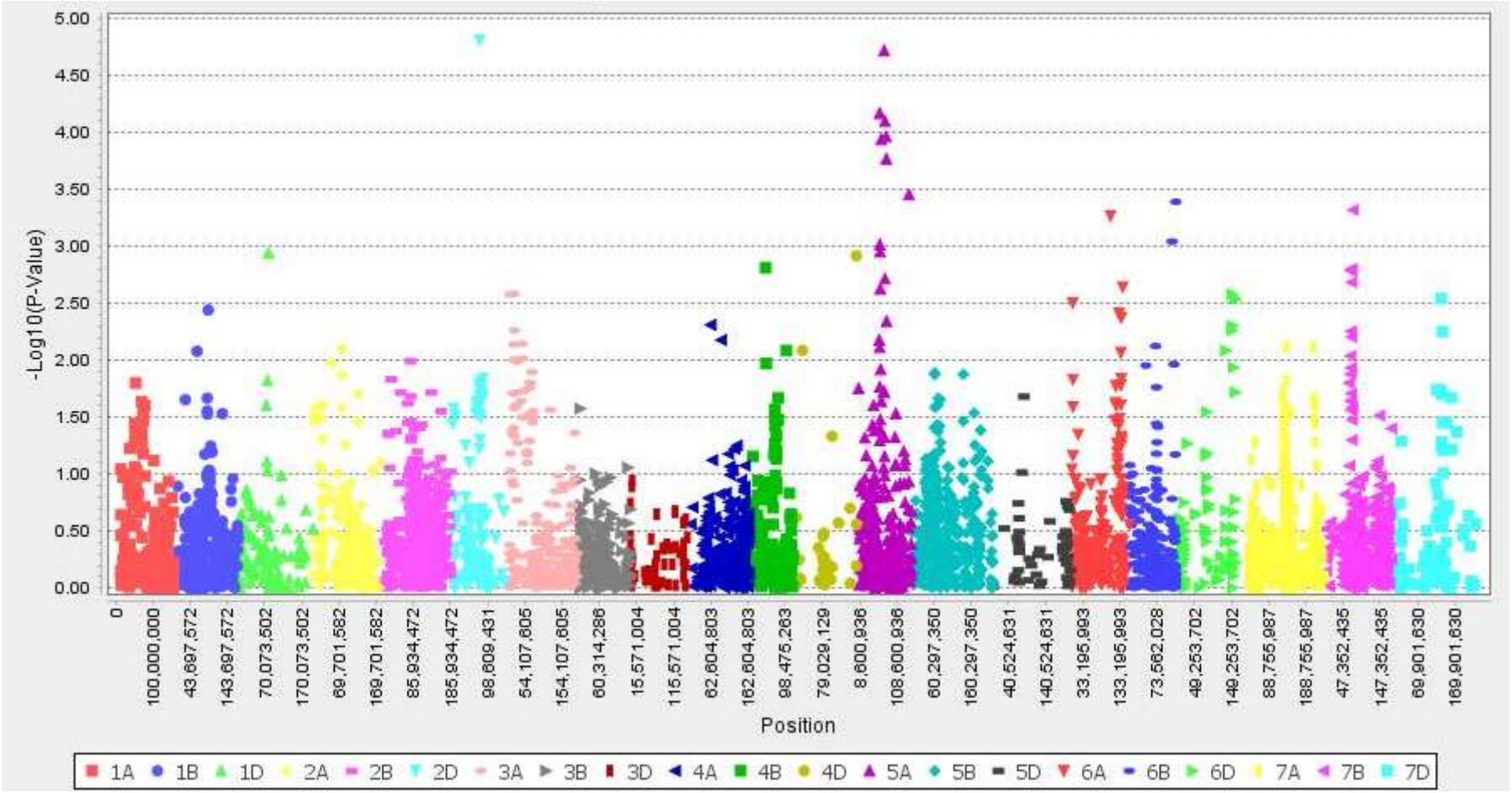

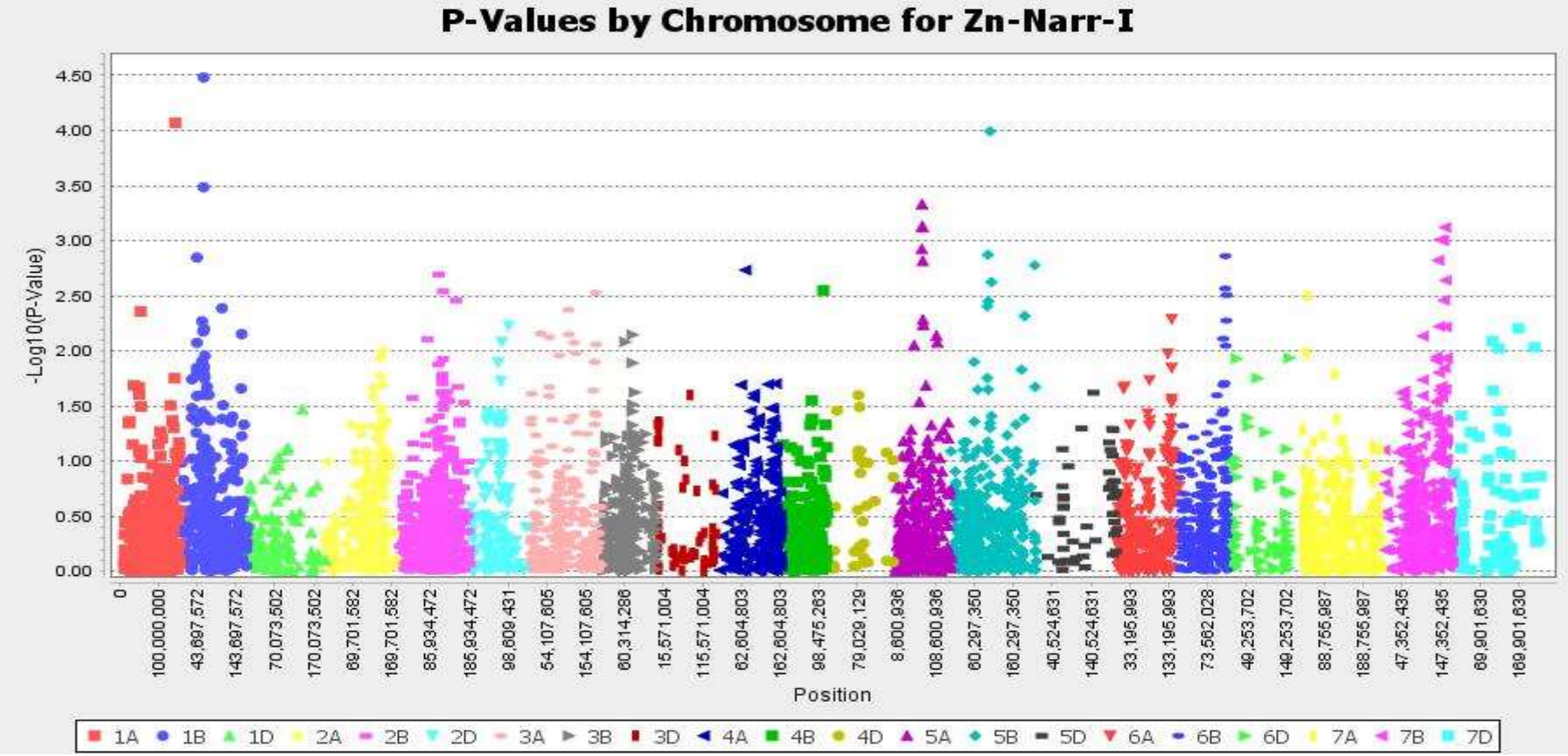

Appendix VIII Manhattan plots depicts significant grain Zn MTAs detected in field environments. Chromosome name on x axis and the -log10 (p-value) on the y-axis have been plotted. Narr-I, Narr-II, HRU and LDN represent 2018-Narr-I, 2018-Narr-II, 2019-Horse research unit and 2019-Lansdowne experimental unit, respectively. **Continue.**

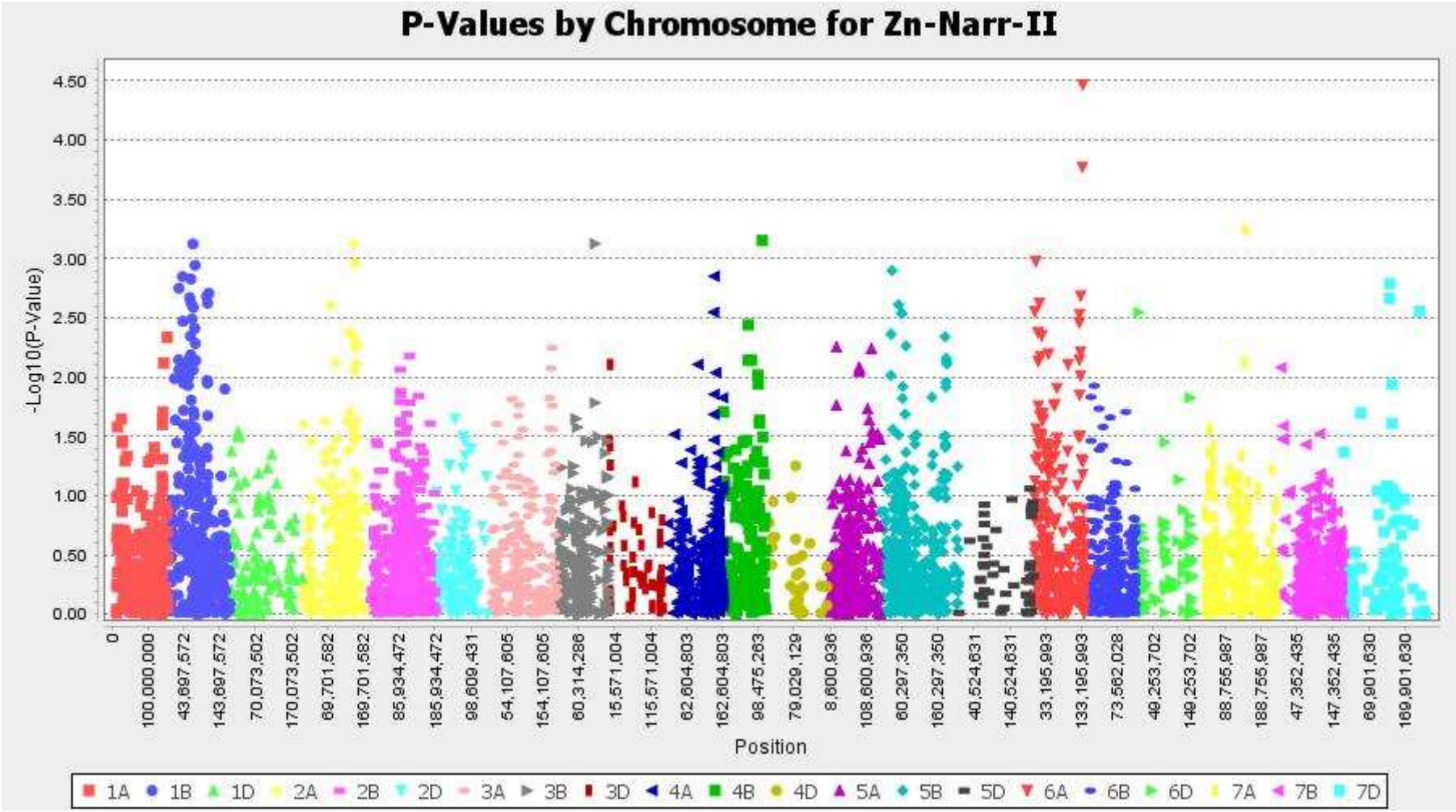
P-Values by Chromosome for Zn-Narr-II
-Log10(P-Value)
4.50
4.00
3.50
3.00
2.50
2.00
1.50
1.00
0.50
0.00
0
100,000,000
43,697,572
143,697,572
70,073,502
170,073,502
69,701,582
169,701,582
85,934,472
185,934,472
98,609,431
54,107,605
154,107,605
60,314,286
15,571,004
115,571,004
62,604,803
162,604,803
98,475,263
79,029,129
8,600,936
108,600,936
60,297,350
160,297,350
40,524,631
140,524,631
33,195,993
133,195,993
73,562,028
49,253,702
149,253,702
88,755,987
188,755,987
47,352,435
147,352,435
69,901,630
169,901,630
Position
1A
1B
1D
2A
2B
2D
3A
3B
3D
4A
4B
4D
5A
5B
5D
6A
6B
6D
7A
7B
7D

Continue.

P-values by Chromosomes for Zn-HRU

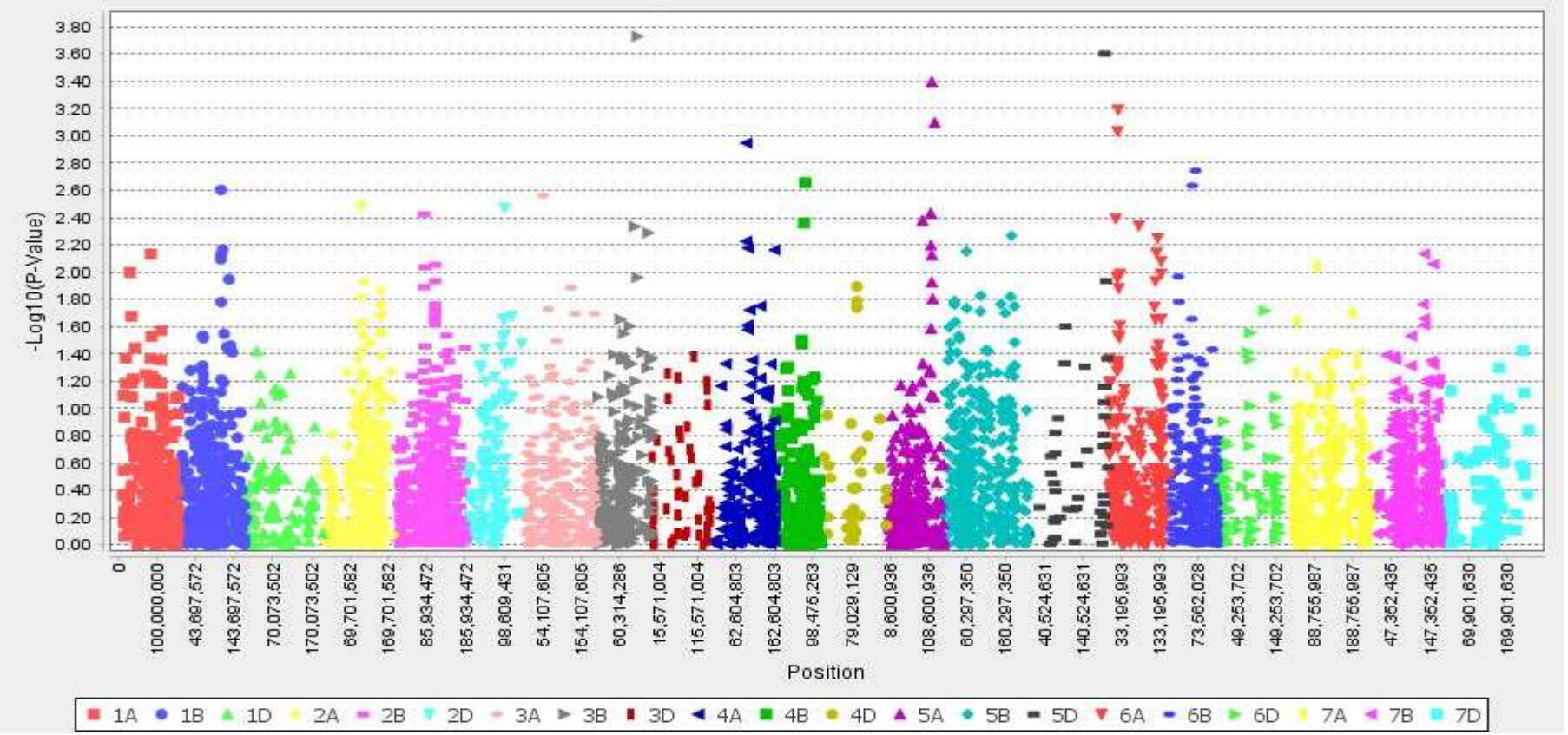

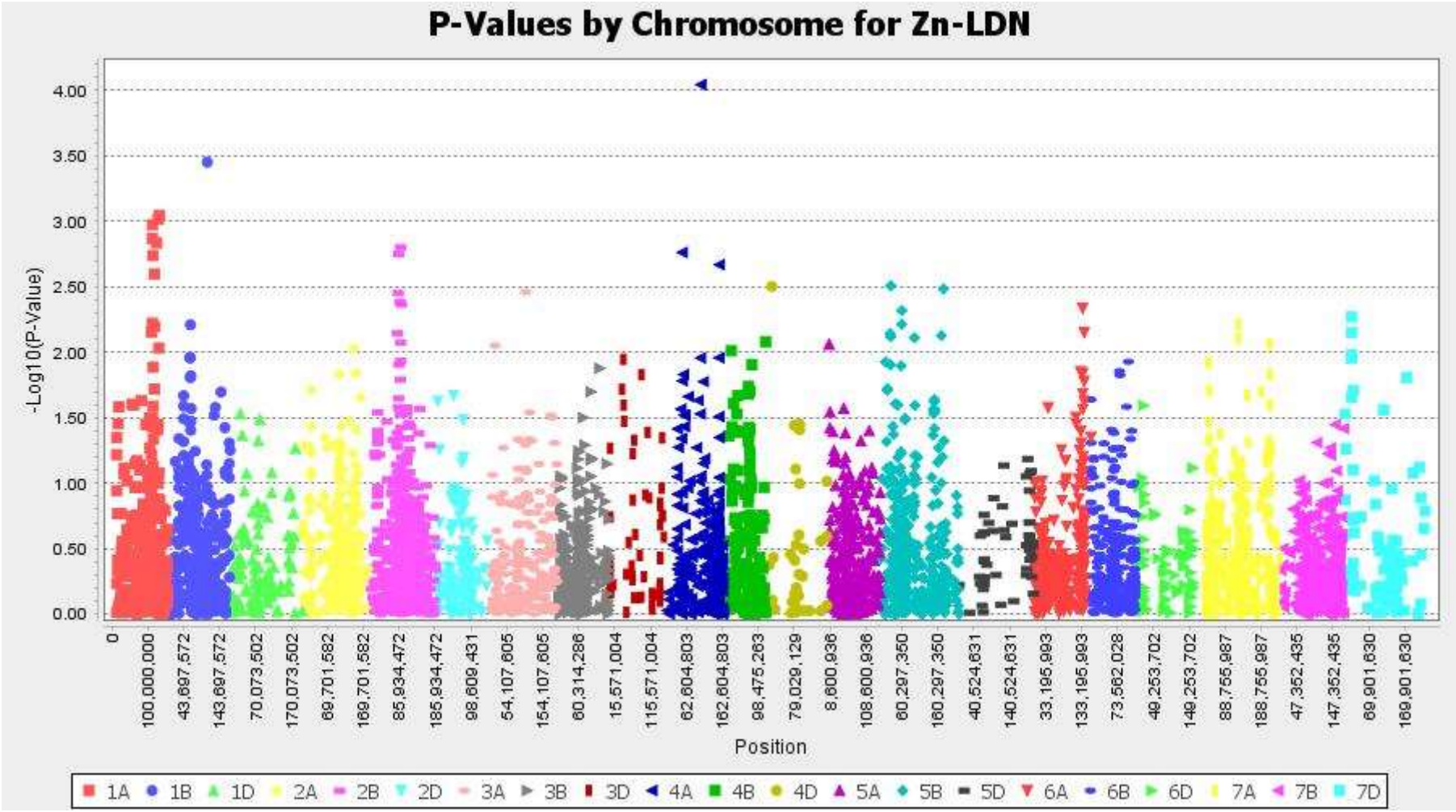
P-Values by Chromosome for Zn-LDN
-Log10(P-Value)
4.00
3.50
3.00
2.50
2.00
1.50
1.00
0.50
0.00
0
100,000,000
43,697,572
143,697,572
70,073,502
170,073,502
69,701,582
169,701,582
85,934,472
185,934,472
98,609,431
54,107,605
154,107,605
60,314,286
15,571,004
115,571,004
62,604,803
162,604,803
98,475,263
79,029,129
8,600,936
108,600,936
60,297,350
160,297,350
40,524,631
140,524,631
33,195,993
133,195,993
73,562,028
49,253,702
149,253,702
88,755,987
188,755,987
47,352,435
147,352,435
69,901,630
169,901,630
Position
1A
1B
1D
2A
2B
2D
3A
3B
3D
4A
4B
4D
5A
5B
5D
6A
6B
6D
7A
7B
7D

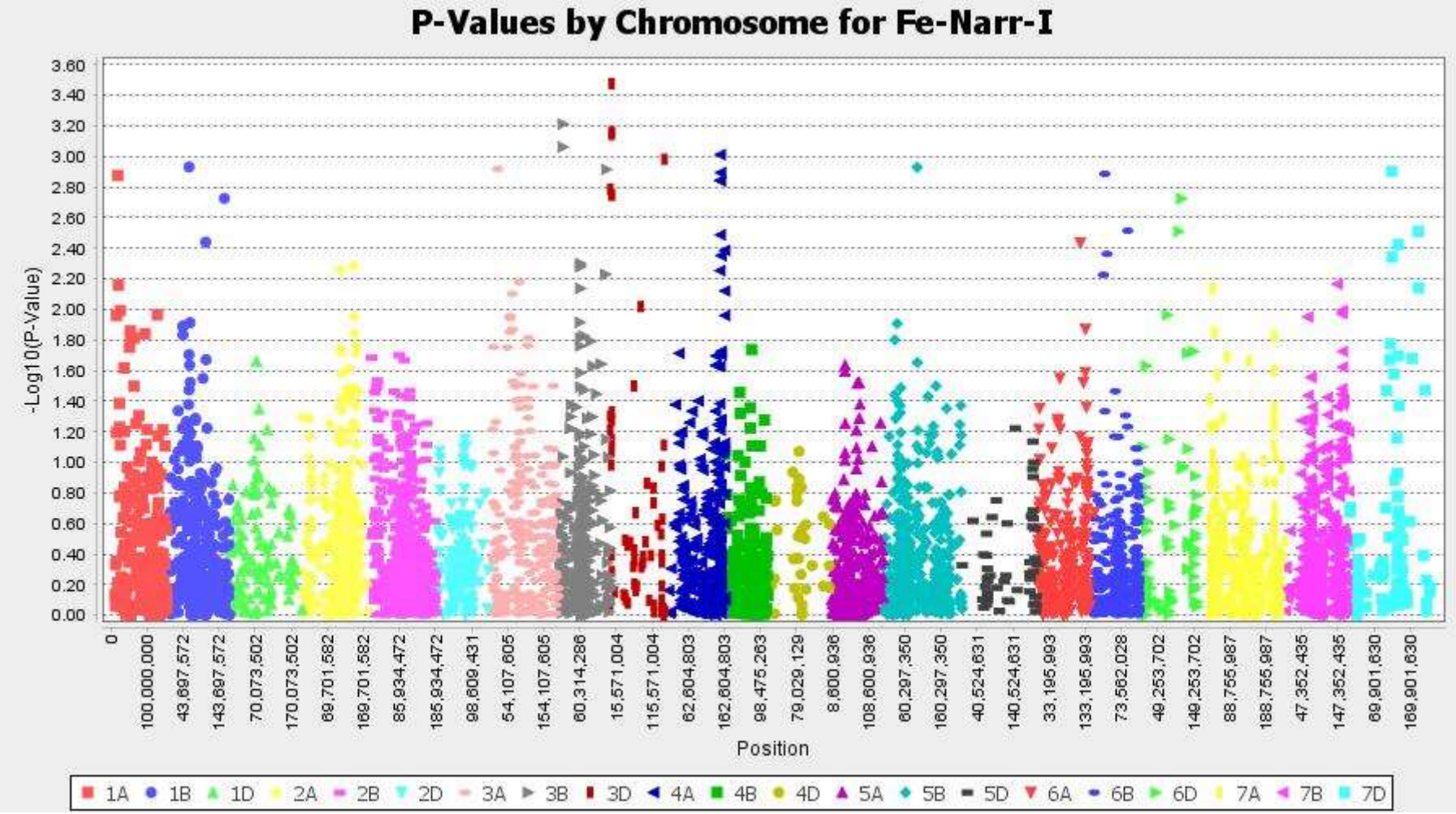

Appendix IX Manhattan plots depicts significant grain Fe MTAs detected in field environments. Chromosome name on x axis and the -log10 (p-value) on the y-axis have been plotted. Narr-I, Narr-II, HRU and LDN represent 2018-Narr-I, 2018-Narr-II, 2019-Horse research unit and 2019-Lansdowne research unit, respectively. **Continue.**

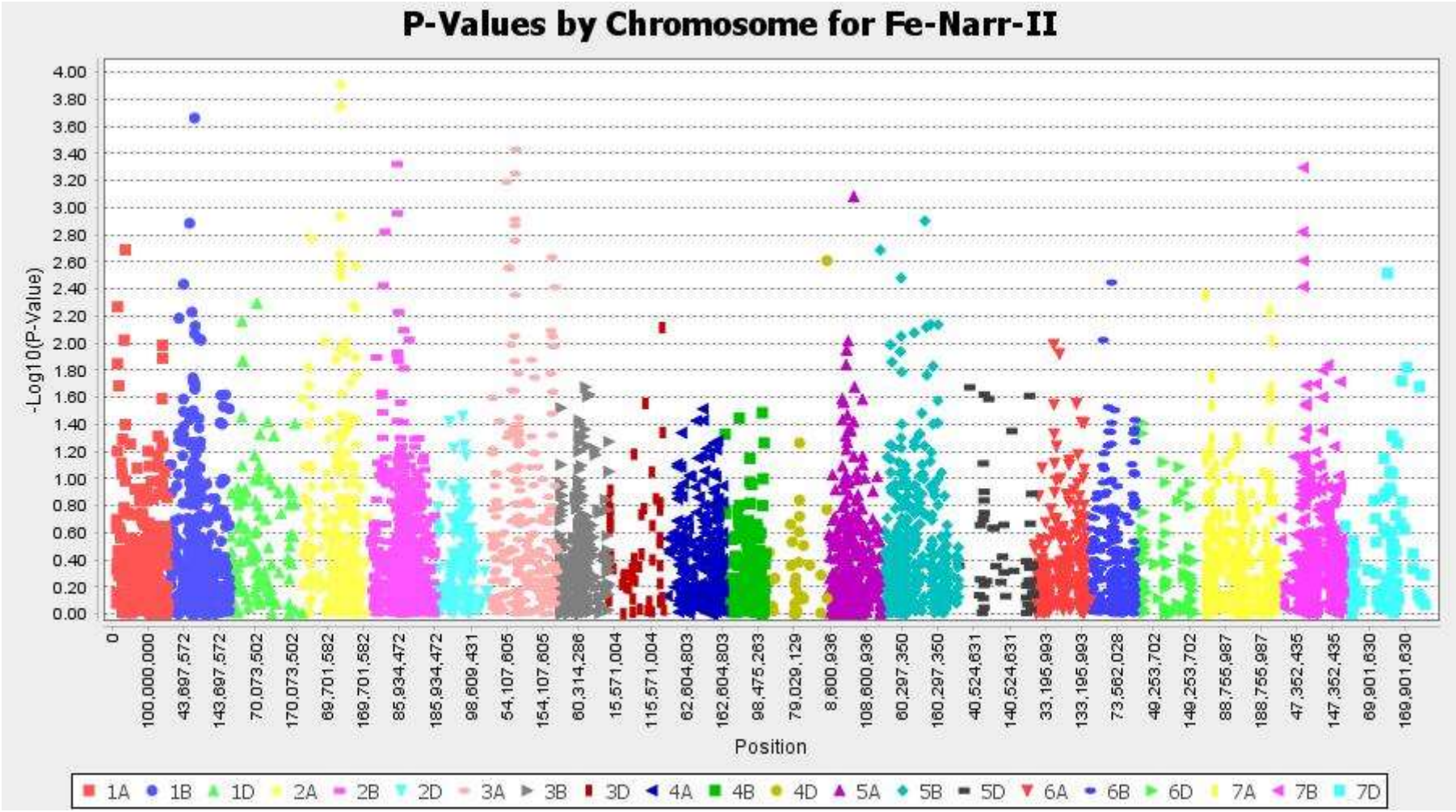
P-Values by Chromosome for Fe-Narr-II
-Log10(P-Value)
4.00
3.80
3.60
3.40
3.20
3.00
2.80
2.60
2.40
2.20
2.00
1.80
1.60
1.40
1.20
1.00
0.80
0.60
0.40
0.20
0.00
0
100,000,000
43,697,572
143,697,572
70,073,502
170,073,502
69,701,582
169,701,582
85,934,472
185,934,472
98,609,431
54,107,605
154,107,605
60,314,286
15,571,004
115,571,004
62,604,803
162,604,803
98,475,263
79,029,129
8,600,936
108,600,936
60,297,350
160,297,350
40,524,631
140,524,631
33,195,993
133,195,993
73,562,028
49,253,702
149,253,702
88,755,987
188,755,987
47,352,435
147,352,435
69,901,630
169,901,630
Position
1A
1B
1D
2A
2B
2D
3A
3B
3D
4A
4B
4D
5A
5B
5D
6A
6B
6D
7A
7B
7D

Continue.

P-values by Chromosomes for Fe-HRU

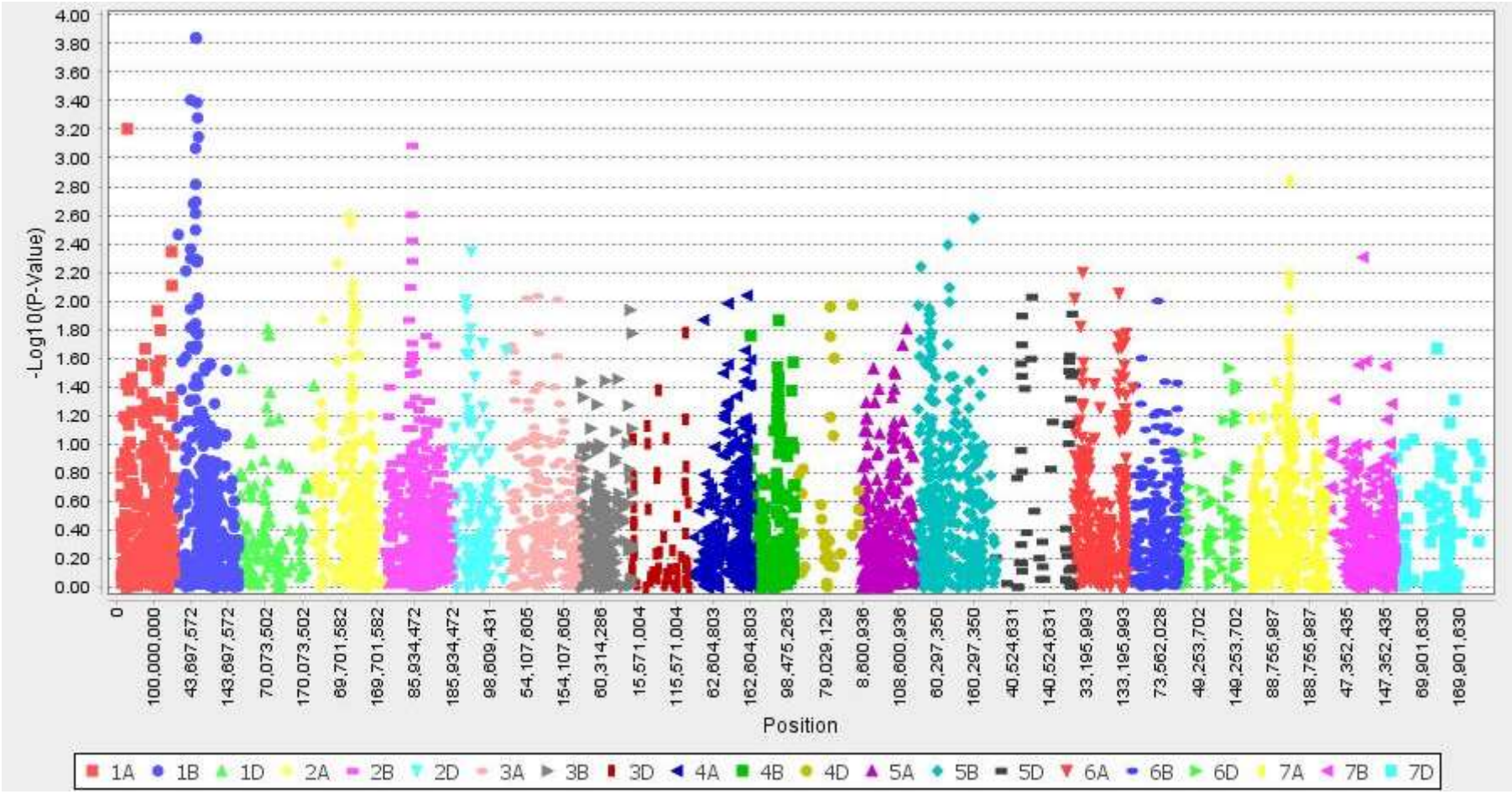

Continue.

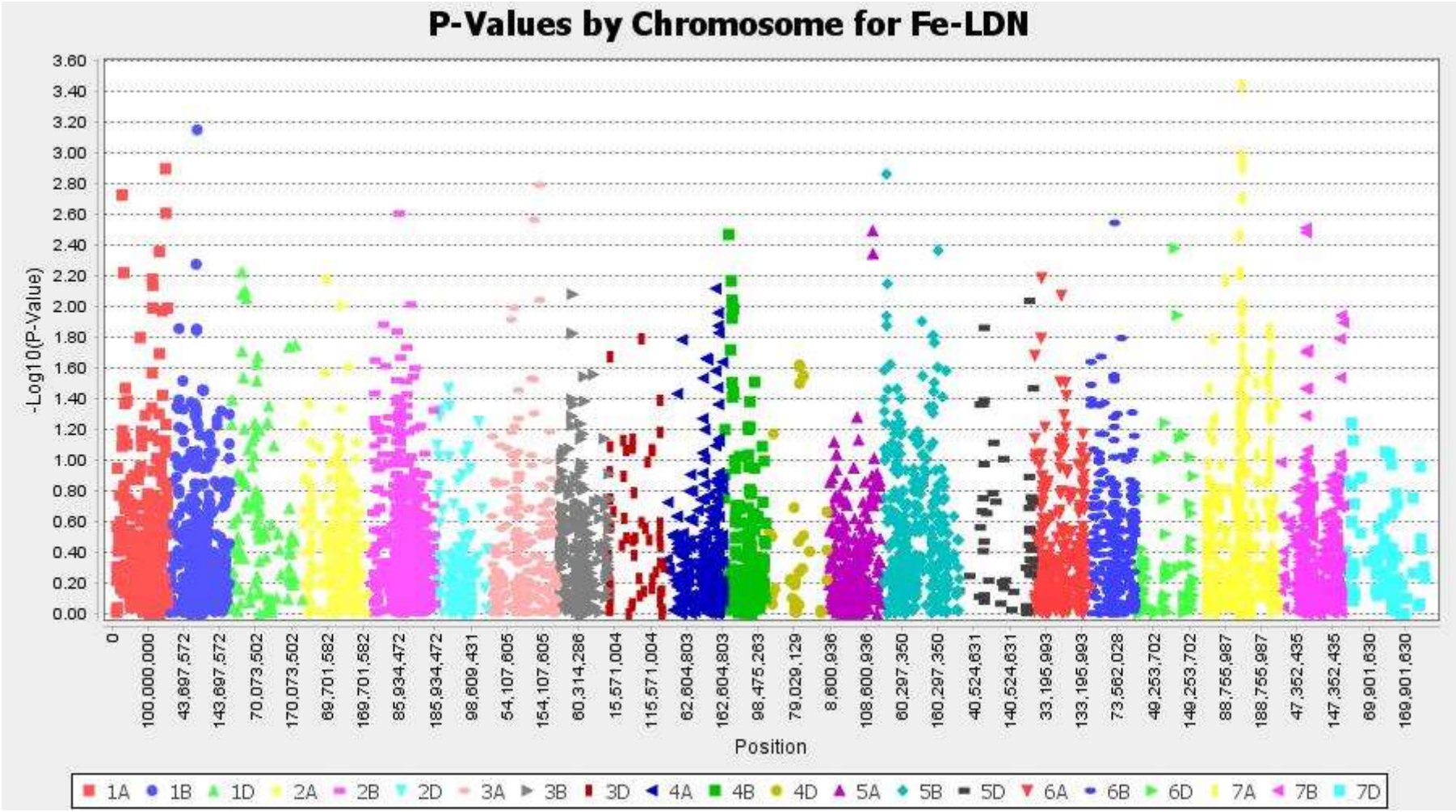
P-Values by Chromosome for Fe-LDN
-Log10(P-Value)
3.60
3.40
3.20
3.00
2.80
2.60
2.40
2.20
2.00
1.80
1.60
1.40
1.20
1.00
0.80
0.60
0.40
0.20
0.00
0
100,000,000
43,697,572
143,697,572
70,073,502
170,073,502
69,701,582
169,701,582
85,934,472
185,934,472
98,609,431
54,107,605
154,107,605
60,314,286
15,571,004
115,571,004
62,604,803
162,604,803
98,475,263
79,029,129
8,600,936
108,600,936
60,297,350
160,297,350
40,524,631
140,524,631
33,195,993
133,195,993
73,562,028
49,253,702
149,253,702
88,755,987
188,755,987
47,352,435
147,352,435
69,901,630
169,901,630
Position
1A
1B
1D
2A
2B
2D
3A
3B
3D
4A
4B
4D
5A
5B
5D
6A
6B
6D
7A
7B
7D

Appendix X List of significant markers and their alleles displaying their effects in accumulating higher grain minerals

SN	Trait	Major effect marker	Chr	Genetic position (cM)	Favourable allele	Alternate allele	Average mineral concentration (mg/kg) of lines carrying favourable allele	Average mineral concentration (mg/kg) of lines carrying alternate allele	
1	P	*IWB62537*	1A	113.19	75 C:C	197 T:T	3425	3350	
2	Mn	*IWB62537*	1A	113.19	75 C:C	197 T:T	45.25	42.25	
3	P	*IWA8135*	1A	133.15	212 G:G	76 A:A	3425	3350	
4	Mn	*IWA8135*	1A	133.15	212 G:G	76 A:A	45.25	42.25	
5	Zn	*IWA8135*	1A	133.15	212 G:G	76 A:A	33.88	32	
6	S	*IWB46598*	1B	43.86	30 C:C	256 A:A	1888	1717.5	
7	Zn	*IWB64607*	3B	107.15	90 G:G	174 A:A	35	32.25	
8	Zn	*IWA5704*	6A	136.85	158 G:G	126 T:T	34.12	32.25	
9	K	*IWB41295*	2D	49.59	54 A:A	235 G:G	4200	3950	
10	Ca	*IWB72107*	1B	43.86	130 C:C	119 T:T	538.75	502.5	
11	Fe	*IWA6610*	1B	43.86	34 C:C	253 T:T	40.25	37.49	
12	Fe	*IWB7923*	1B	56.65	30 G:G	252 T:T	40.3	37.25	
13	Zn	*IWA2365*	5A	73.97	74 G:G	158 A:A	34.13	33	
14	Fe	*IWA3151*	2A	108.46	50 G:G	239 A:A	38.87	37.25	
15	Zn	*IWB35116*	1B	60.62	32 G:G	260 C:C	36.25	33	
16	Zn	*IWB8918*	1A	144.41	45 C:C	219 T:T	34.5	33	
17	Cu	*Yr15-KinI*	1BS		8 Res	271 Sus	4.39	4.14	**Continue.**
18	Zn	*Yr15-KinI*	1BS		8 Res	271 Sus	35.78	33.62	

19	Ca	*Yr15-KinI*	1BS	8 Res	271 Sus	567.8	530.8
20	Zn	*Lr34-csLV34*	7DS	44 Res	242 Sus	34.8	33.5
21	B	*Sr31/Lr26/Yr9-iag95*	1BL:1RS	16 Res	277 Sus	0.95	0.87
22	Cu	*Sr31/Lr26/Yr9-iag95*	1BL:1RS	16 Res	277 Sus	4.81	4.11
23	Fe	*Sr31/Lr26/Yr9-iag95*	1BL:1RS	16 Res	277 Sus	40.6	37.67
24	Zn	*Sr31/Lr26/Yr9-iag95*	1BL:1RS	16 Res	277 Sus	36.96	33.53
25	Mn	*Sr31/Lr26/Yr9-iag95*	1BL:1RS	16 Res	277 Sus	46.5	44.2
26	Ca	*Sr31/Lr26/Yr9-iag95*	1BL:1RS	16 Res	277 Sus	559.5	529.5
27	Mg	*Sr31/Lr26/Yr9-iag95*	1BL:1RS	16 Res	277 Sus	1421.2	1362.9
28	S	*Sr31/Lr26/Yr9-iag95*	1BL:1RS	16 Res	277 Sus	1860.4	1732.8
29	P	*Sr31/Lr26/Yr9-iag95*	1BL:1RS	16 Res	277 Sus	3526.5	3423.4
30	K	*Sr31/Lr26/Yr9-iag95*	1BL:1RS	16 Res	277 Sus	4204.6	4019.4
31	Cu	*Sr38/Lr37/Yr17- Ventrip* and *LN2*	2AS:2NS	43 Res	250 Sus	4.55	4.08
32	Fe	*Sr38/Lr37/Yr17- Ventrip* and *LN2*	2AS:2NS	43 Res	250 Sus	38.83	37.66

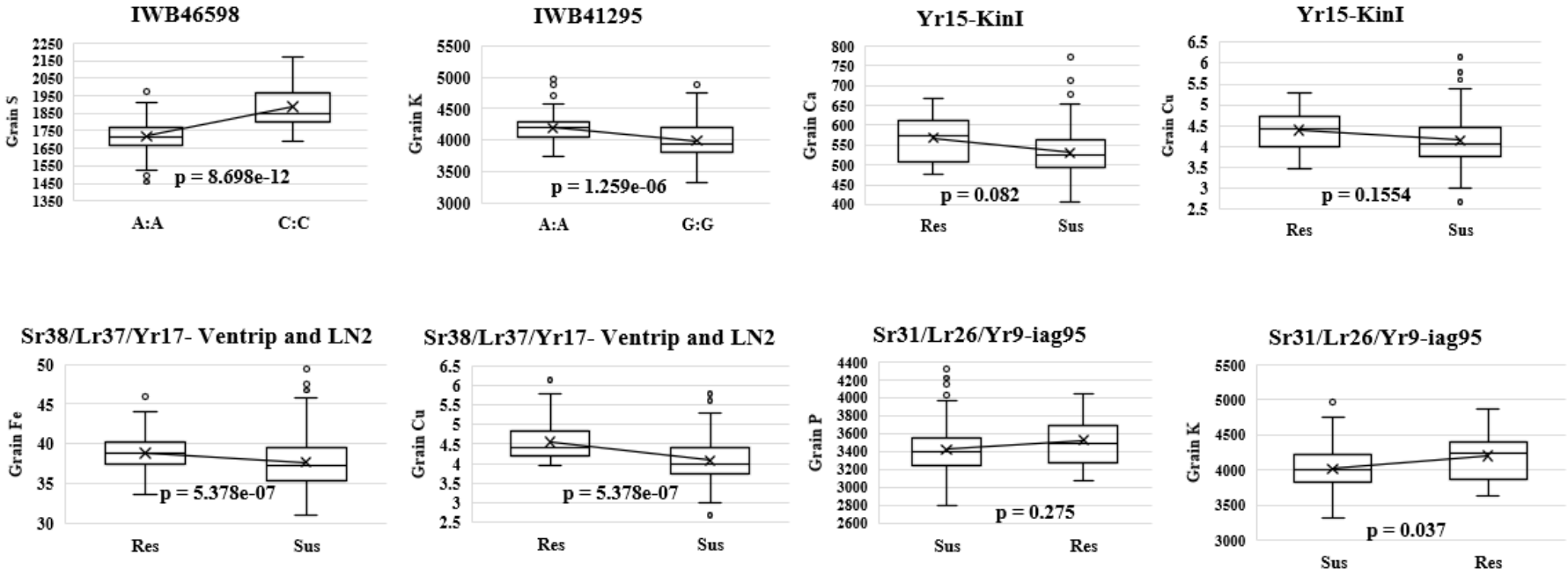

Appendix XI Boxplot analysis depicting contribution of significant markers in grain S, K, Ca, Cu, Fe and P accumulation. X- and Y-axis represent alleles and mineral concentration (mg/kg) in wheat grain, respectively.

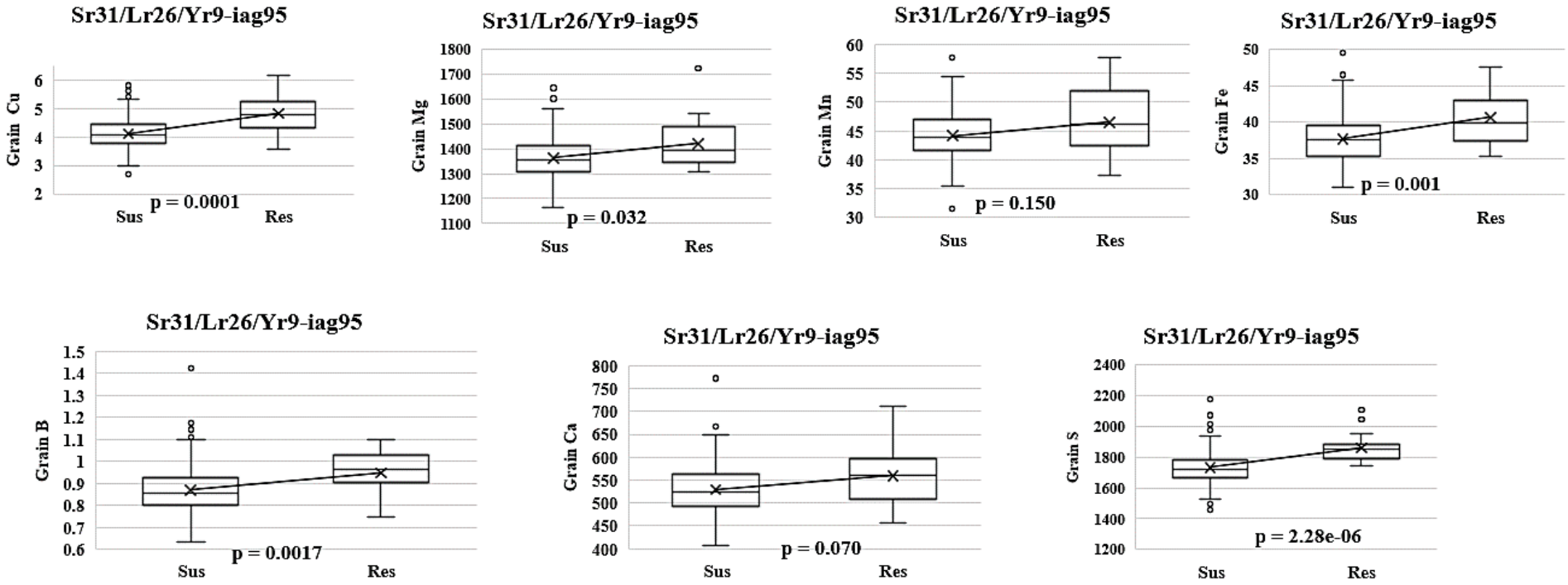

Appendix XII Boxplot analysis depicting contribution of *Sr31/Lr26/Y9* linked marker *iag95* in grain mineral accumulation. X- and Y-axis represent alleles and mineral concentration (mg/kg) in wheat grain, respectively